GEMS & GEMOLOGY

Featuring:

Yellow Diamonds
Emeralds from Zambia
Mt. Mica Tourmaline

EDITORIAL _____

FEATURE ARTICLES _____

pg. 89

pg. 146

REGULAR FEATURES _____

pg. 172

pg. 183

The Experts behind *Gems & Gemology:*
Our Editorial Review Board

What sets a peer-reviewed journal apart from other publications is its editorial review board. And what makes *Gems & Gemology* unique as a professional journal is the intellect that our reviewers bring to the task. Our review board members, who represent many different aspects of gemological research, independently evaluate submitted manuscripts for accuracy, research methodology, and usefulness to the journal's readership. Every manuscript that makes it to the pages of *G&G* has been improved by their comments and suggestions.

The members of this panel are dedicated to the advancement of gemology, working long hours with no remuneration. It is with great pride and gratitude that I take this opportunity to profile the *Gems & Gemology* Editorial Review Board.

- **Shigeru Akamatsu** is a leading authority on cultured pearls. A former manager of the Pearl Research Laboratory at K. Mikimoto & Co. and currently senior manager of its business administration department, Mr. Akamatsu is also vice-president of the CIBJO Pearl Commission.
- **Alan T. Collins** is an expert in the study of color centers and point defects in natural, synthetic, and treated diamonds. A widely published author and frequent lecturer, Dr. Collins is professor of physics at King's College London.
- **G. Robert Crowningshield**, a former vice president of the GIA Gem Trade Laboratory, is a legend in gemology (see profile in the Fall 2003 *G&G*, pp. 184–199). Mr. Crowningshield began writing for *G&G* in 1949 and was the longtime editor of the Lab Notes section.
- **John L. Emmett** is a leading authority on laser applications and heat treatment of gem materials. Formerly associate director of the Lawrence Livermore National Laboratory, Dr. Emmett is co-founder and president of Crystal Chemistry, a company specializing in the heat treatment of corundum.
- **Emmanuel Fritsch** has written numerous research articles, most related to the application of spectroscopy to gemology, the origin of color in gem materials, and treated and synthetic gems. Formerly with GIA Research, Dr. Fritsch is professor of physics at the University of Nantes, France.
- **Henry A. Hänni** is a prolific author and lecturer. His research interests include advanced analytical techniques, pearl formation, and corundum treatments. Dr. Hänni is director of the SSEF Swiss Gemmological Institute in Basel and professor of gemology at the University of Basel.
- **C. S. Hurlbut Jr.** is professor emeritus of mineralogy at Harvard University. A 1955 Guggenheim fellow, he has written several books on gemology and mineralogy. Dr. Hurlbut is a past president of the Mineralogical Society of America.
- **A. J. A. (Bram) Janse**, a well-known expert on diamond and kimberlite occurrences, has been involved in diamond exploration worldwide for nearly 50 years. Dr. Janse is managing director of Archon Exploration Pty Ltd. in Perth, Australia.
- **Alan Jobbins** has more than 50 years of experience as a gemologist. A former editor of *Journal of Gemmology*, he was the longtime curator of gems and minerals at the Geological Museum in London. Mr. Jobbins is president of Gem-A, London.
- **Mary L. Johnson** is a frequent contributor to *G&G*. As manager of research and development at GIA Research in Carlsbad, Dr. Johnson has helped lead the Institute's groundbreaking studies on emerald fillers and diamond cut proportions.
- **Anthony R. Kampf** conducts research in the areas of descriptive mineralogy, crystal chemistry, and structural crystallography. Dr. Kampf is curator and section head of mineral sciences at the Natural History Museum of Los Angeles County.
- **Robert E. Kane** is a former manager of identification at the GIA Gem Trade Laboratory and former director of the Gübelin Gem Lab in Lucerne, Switzerland. He continues to write on various gemological topics as president of Fine Gems International in Helena, Montana.
- **Alfred A. Levinson** is an authority on diamond deposits. A former editor of *Geochimica et Cosmochimica Acta*, Dr. Levinson is professor emeritus of geology at the University of Calgary.
- **Thomas M. Moses** has written a number of important research articles dealing with gem identification and the characteristics of natural and synthetic diamonds. Mr. Moses is vice president of identification and research services at the GIA Gem Laboratory in New York.
- **George R. Rossman** is professor of mineralogy at the California Institute of Technology, where he received the 2003–2004 Richard P. Feynman Prize for Excellence in Teaching. Among Dr. Rossman's research interests is the study of how electromagnetic radiation interacts with minerals.
- **Kenneth Scarratt** has more than 30 years of laboratory experience and is one of the world's leading authorities on natural and cultured pearls. Formerly head of the AGTA Gemological Testing Center, Mr. Scarratt is director of the new GIA research facility in Bangkok.
- **James E. Shigley**, an important contributor to *G&G* and many other journals, is also the editor of the new volume *Gems & Gemology in Review: Synthetic Diamonds*. Dr. Shigley has been director of GIA Research since 1986.
- **Christopher P. Smith** is a widely published gemologist who has performed research on HPHT-treated diamonds, rubies and sapphires, and gem treatments. Formerly head of the Gübelin Gem Lab, Mr. Smith is director of identification services at the GIA Gem Laboratory in New York.

G&G appreciates the selfless contributions of our reviewers. These are truly the experts behind *Gems & Gemology*.

Alice S. Keller
Editor-in-Chief

CHARACTERIZATION AND GRADING OF NATURAL-COLOR YELLOW DIAMONDS

John M. King, James E. Shigley, Thomas H. Gelb, Scott S. Guhin, Matthew Hall, and Wuyi Wang

To better understand the yellow diamonds currently in the marketplace, as well as identify possible changes in their trends seen over a five-year period, researchers at the GIA Gem Laboratory analyzed gemological data collected on more than 24,000 natural-color yellow diamonds examined in the calendar years 1998 and 2003. These data included color grade, type of cut, clarity grade, weight, ultraviolet fluorescence, and UV-visible and infrared spectra. Among natural-color colored diamonds, those with a yellow hue are some of the most abundant; even so, they are much less common than the colorless to light yellow diamonds associated with GIA's D-to-Z color grading scale. Since the yellow color is a continuation of the gradation of color associated with the D-to-Z scale, there can be misconceptions about the color grading, which involves different procedures from those used for D-to-Z grading. The grading and appearance aspects, as well as other characteristics of yellow diamonds, are discussed to clarify these differences. The authors have also identified five subgroups of type I yellow diamonds, which (with some overlap) are characterized by representative spectra and color appearances.

Today, yellow diamonds are among the most widely encountered of the "fancy color" diamonds (figure 1). From 1998 to the present, GIA has issued grading reports on more than 100,000 yellow diamonds, by far the most common of the fancy-color diamonds submitted to our laboratory. In 2003, for example, 58% of the diamonds submitted for GIA Colored Diamond Grading Reports or Colored Diamond Identification and Origin of Color Reports were in the yellow hue. Nevertheless, these represented only 2.4% of all diamonds submitted for various grading reports that year. The dichotomy between being common among colored diamonds yet relatively rare overall has created a mix of information and sometimes erroneous assumptions about yellow diamonds. In addition, although information about their "origin of color" or unusual characteristics (see below) has been documented over the years, little has been published about their color appearance and its relationship to color grading (one exception being Hofer, 1998).

This article presents data on more than 24,000 fancy-color yellow diamonds that were examined by the GIA Gem Laboratory during the years 1998 and 2003. While our main concern in this study was gathering information to characterize the gemological and spectroscopic properties of the entire population of samples, we were also interested in identifying any trends in size, color grade, or clarity grade among the yellow diamonds submitted to us that might be revealed over time. To that end, we selected a sample population from these two years separated by a five-year span.

Following a brief review of the literature on the geographic sources, cause of color, and other physical properties of fancy-color yellow diamonds, this article will focus on expanding the published information about these diamonds by documenting and

Figure 1. While abundant compared to other colored diamonds, fancy-color yellow diamonds represent a small portion of overall diamond production. Their beauty and the depths of color in which they occur offer a wide range of possibilities to the jeweler. The bracelet and the 4.13 ct oval and 6.20 ct emerald cut in the rings are courtesy of Harry Winston Inc.; the 8.70 ct (total weight) StarBurst cuts in the earrings are courtesy of Jonathan Doppelt Inc.; the yellow gradation eternity band is courtesy of N. Smid; and the two unmounted diamonds and the crystal are courtesy of the Scarselli family. Photo by Harold & Erica Van Pelt.

reporting on their range of color, color grading, clarity grading, and other gemological properties, as well as their spectroscopic characteristics.

We will also look at a number of aspects of color observation and appearance (as they apply to these diamonds) that are known and commonly addressed by vision scientists but may not be recognized by the layperson or even the experienced diamond dealer or retailer. As with the previous GIA studies of blue and pink diamonds (King et al., 1998, 2002), this article describes and illustrates some of these aspects to aid in understanding how they apply to color grading yellow diamonds.

BACKGROUND

History and Geographic Origin. Yellow diamonds have long been recognized and prized among collectors (Mawe, 1813; Bauer, 1904; Copeland and Martin, 1974; Gleason, 1985). For example, in his description of several famous diamonds he encountered while in India, the French traveler and gem dealer Jean-Baptiste Tavernier (1676) mentioned seeing a 137.27 ct yellow diamond that he referred to variously as the "Florentine," the "Austrian Yellow," and the "Grand Duke of Tuscany." As with other colors, yellow diamonds have come to the public's attention through the interest generated by a number of special stones, such as the historical 128.54 ct Tiffany (figure 2; see Balfour, 2000)

and 101.29 ct Allnat (see King and Shigley, 2003) diamonds, or the extraordinary 407.48 ct Incomparable (illustrated in King et al., 1994, p. 227). Indeed, the first reportedly authenticated diamond found in Africa, which was cut into the 10.73 ct Eureka, is a distinct yellow (Balfour, 2000; shown in Janse, 1995, p. 231). Its discovery in late 1866/early 1867 helped start the ensuing African diamond mining rush.

Although there were occasional finds over the centuries in India, Brazil (Cassedanne, 1989), and perhaps elsewhere, the first major discovery of quantities of what today would be considered fancy-color yellow diamonds occurred at several locations in South Africa in the late 1860s (Janse, 1995; figure 3). The early preponderance of light yellow diamonds from the Cape Province in South Africa led to their description in the jewelry trade as "cape stones," a usage that continues today (see, e.g., *GIA Diamond Dictionary*, 1993). While these light yellow diamonds are not now considered colored diamonds (rather, they fall toward the lower end of GIA's D-to-Z color scale), their noticeable color distinguished them from those of other deposits that yielded near-colorless or brown diamonds. Also found, however, were numerous diamonds that ultimately *would* be considered yellow. The earliest recorded find along the banks of the Orange River was, as noted above, a 21.25 ct (old carat weight) yellow crystal that was subsequently cut into the

Figure 2. The Tiffany yellow diamond is one of the best-known diamonds in the world. The 128.54 ct diamond has been in the Tiffany collection since 1879, and today it is displayed in its own case (as part of Jean Schlumberger's jewel, "Bird on a Rock") at Tiffany & Co. in New York City. It was graded by GIA in 1984. Photo courtesy of Tiffany & Co.

Eureka (Janse, 1995). In 1878, a 287.42 ct piece of rough recovered from a claim on the Kimberley mine was later fashioned into the Tiffany diamond (again, see figure 2). In 1964, the Dutoitspan mine yielded a spectacular 253.70 ct transparent yellow octahedral crystal known as the Oppenheimer diamond, which now resides in the Smithsonian Institution.

Today, yellow diamonds are found in the productions of mining operations throughout the world (Field, 1992, p. 353). The occurrence of fancy-color yellow diamonds is so widespread that no particular deposit stands out as an important source (though many of the larger pieces of yellow rough continue to originate from South Africa). Some data correlating diamond color and size has been published for certain deposits (in particular, the kimberlites in South Africa; see, e.g., Harris et al., 1979), but the literature contains no such information on yellow diamond abundances for other occurrences.

Noted Auction Sales and Other Publicity. As with other colored diamonds, yellow diamonds can command high prices and generate much public attention. At its 1988 auction, the Fancy brownish yellow* Internally Flawless Incomparable diamond reached a bid of $12 million before it was withdrawn without having met its reserve (Balfour, 1997). An 18.49 ct Fancy Intense* yellow known as the "Golden Drop" sold at auction for $203,461 per carat in 1990 (Hofer, 1998), while a 13.83 ct Fancy Vivid yellow sold for $238,792 per carat in 1997. In February 2005, a 10.02 ct Fancy Vivid yellow diamond sold for $772,848 (more than $77,131 per carat) at Sotheby's St. Moritz. Recently, a 101.28 ct Fancy Vivid yellow cushion modified brilliant known as the "Golden Star" was unveiled to the public in Palm Beach, Florida, by jeweler Laurence Graff, who reported that this diamond had been cut from a large crystal found at the Finsch mine in South Africa.

Past Studies. Differences noted in crystal form and physical and spectroscopic properties between (what were discovered to be) nitrogen-containing diamonds and those much rarer diamonds with virtually no nitrogen led early in the 20th century to the recognition by scientists of the type I and type II categories, respectively (Robertson et al., 1934; also see Anderson, 1963). At the atomic level in type I diamonds, nitrogen substitutes for carbon as either multiple atoms (aggregates) that occupy adjacent positions in the lattice (type Ia) or as single isolated atoms (type Ib).

There have been several recent reviews of the physical properties of diamond, including Field (1992), Davies (1994), and Wilks and Wilks (1994). A number of articles have discussed the visible and infrared spectra of yellow diamonds as they relate to the discrimination of natural-color diamonds from those that have been treated to change their color (Clark et al., 1956a,b; Crowningshield, 1957–8; Scarratt, 1979, 1982; Collins, 1978, 1982a,b, 2001; Woods and Collins, 1982, 1986; Woods, 1984; Collins et al., 1986; Mita, 1996; Fritsch, 1998; Haske, 2000; Kaminsky and Khachatryan, 2001; De Weerdt and Van Royen, 2001; Zaitsev, 2001). Additional articles have discussed the potential use of spectral measurements to quantitatively evaluate the color of faceted yellow diamonds (Vendrell-Saz et al., 1980; Sato and Sunagawa, 1982; Collins, 1984).

---

* Graded prior to modifications to GIA's colored diamond color grading system in 1995.

Gemologists have also recognized that certain inclusions are characteristic of particular gemstones and, as such, help provide information on their geologic history and diamond type. For example, Crowningshield (1959) reported that needle-like inclusions, as well as oriented plate-like inclusions, are found on occasion in some yellow diamonds. Such inclusions were later associated with type Ib yellow diamonds (Crowningshield, 1994).

Color and Color Origin. In general, the presence of nitrogen atoms gives rise to two kinds of absorption in the blue region of the visible spectrum; the remainder of the spectrum is transmitted, leading to an observed yellow color. In type Ia diamond, aggregates of nitrogen atoms in the form of the N3 center cause absorption as a sharp line at 415 nm. The N3 center is believed to consist of three nearest-neighbor substitutional nitrogen atoms all bonded around a common lattice site of a missing carbon atom (a *vacancy*). This absorption produces the lighter yellow coloration typical of "cape" diamonds.

The same N3 center is also responsible for blue long-wave ultraviolet fluorescence when seen in type Ia diamonds (Nayar, 1941; Mani, 1944; Dyer and Matthews, 1957). Based largely on observations with the prism spectroscope, Anderson (1943a,b, 1962) noted the general correlation between the intensity of the 415 nm absorption band and the strength of the diamond's yellow color (also see Anderson and Payne, 1956). Occasionally, the N3 center is accompanied by additional broader but weaker lines at 452, 465, and 478 nm (the N2 center; see Clark et al., 1956a; Davies et al., 1978; Davies, 1981), which also contribute to the yellow color. These lines are superimposed over a region of absorption that increases gradually toward the blue end of the spectrum.

Collins (1980) gave nitrogen concentration values of up to 3000 ppm for type Ia diamonds. Two additional nitrogen aggregates—designated *A* (a pair of nearest-neighbor nitrogen atoms) and *B* (four N atoms surrounding a vacancy)—are usually present in type Ia diamonds, but neither gives rise to absorption in the visible region (thus, they do not produce any coloration, but they do produce characteristic absorption features in the infrared spectrum).

In the much-less-common type Ib diamond, single-substitutional nitrogen atoms cause a broad region of absorption that increases below about 560 nm (but no sharp 415 nm absorption band), which in turn produces a more saturated yellow color. In some cases, type Ib diamonds exhibit a very weak to weak yellow or orange short-wave UV fluorescence (see Dyer et al., 1965; Fritsch, 1998, pp. 26–30 and 36–37; Hofer, 1998, pp. 354–359). Such diamonds have often been described as having a "canary" color (Wade, 1920; Anderson, 1943a; Liddicoat, 1976). In contrast to type Ia yellow diamonds, those that are type Ib contain much smaller amounts of nitrogen, normally well under 100 ppm (Collins, 1980; Field, 1992).

These subcategories of type I diamonds can be distinguished on the basis of characteristic features in their visible and infrared absorption spectra. It should be mentioned that these subcategories are not mutually exclusive, since at the atomic level the diamond lattice can contain different ratios of aggregated and isolated nitrogen atoms from one diamond to the next. In addition, infrared spectral features associated with both isolated and aggregated forms of nitrogen can be recorded from different portions within the same diamond. For example,

Figure 3. The late 1860s saw the first major discovery of diamonds in South Africa, and with that came an influx of yellow rough into the market. The Kimberley and Dutoitspan mines, between the Orange and Vaal Rivers, were some of the significant early (and continuous) sources of production. In 1964, the latter mine yielded the spectacular 253.70 ct yellow octahedral crystal known as the Oppenheimer diamond. Modified from Janse (1995).

Collins (1980) suggested that many type Ib diamonds also contain A-aggregates (type IaA) of nitrogen. For additional information on diamond types and optical centers, see Davies (1972); Davies and Summersgill (1973); Collins (1982a,b, 2001); Bursill and Glaisher (1985); Fritsch and Scarratt (1992, pp. 38–39); Briddon and Jones (1993); Wilks and Wilks (1994); and De Weerdt and Van Royen (2001).

GIA Color Descriptions for "Yellow" Diamonds. A hue has different color appearances depending on its tone and saturation (King et al., 1994, 2002). The color description that GIA gives diamonds on grading reports is based on the hue, and on the tone and saturation of that hue. For example, when a yellow hue becomes darker in tone and weaker in saturation, it appears increasingly brown, and this is reflected in the color description (i.e., brownish yellow). In certain darker/weaker areas of the yellow hue range, the color appears to have both brown and green components (as compared to similar tones and saturations of adjacent hues), which results in descriptions such as brownish greenish yellow and brown–greenish yellow. Figure 4 illustrates these appearance relationships within and surrounding "yellow" on the hue circle. (For a more detailed discussion of the GIA color description system for colored diamonds, please see King et al., 1994.)

MATERIALS AND METHODS

Samples. The 24,668 diamonds reported on in this article were examined in 1998 (7,213) and 2003 (17,455) at our laboratories in New York and Carlsbad. The color of each was identified as being of natural origin (using standard and, where appropriate, advanced gemological testing) and was described on the grading report as being yellow, brownish yellow, brownish greenish yellow, or brown–greenish yellow (again, see figure 4). The diamonds ranged in weight from 0.30 to 219.35 ct.

For the purposes of this study, we did not include diamonds in the narrower greenish yellow, green-yellow, orangy yellow, or orange-yellow hues. Not only did these samples represent less than 13% of the diamonds given "predominantly yellow" hues for the two years in which we retrieved data for this study—with no single hue representing more than 4%—but they are also approached differently in their trading and valuation (K. Ayvazian, pers. comm., 2004).

Because of time constraints or the type of laboratory service requested by the client (e.g., a less comprehensive "identification and origin" report), the database does not include the same gemological observations for all the diamonds. For these reasons, we have indicated in the Results if the data being discussed originate from some smaller subset of these 24,668 diamonds.

Grading and Testing Methods. We used the GIA Gem Laboratory standard methodology for color grading colored diamonds to describe all of the study samples (see King et al., 1994). Screened and trained laboratory staff evaluated each of the diamonds using a standardized D65 "daylight-equivalent" lighting environment (as provided by the Macbeth Judge II illumination box). Typically, from three to six staff members independently compared the overall face-up characteristic color of each diamond to GIA colored diamond color references in order to determine the appropriate color description and location in GIA's color space.

Equipment used for the gemological examination included a standard gemological microscope, a GIA Gem Instruments ultraviolet unit with long-wave (365 nm) and short-wave (254 nm) lamps, and a desk-model prism spectroscope.

Absorption spectra in the ultraviolet to visible (UV-Vis) range were recorded with a Thermo-Spectronic Unicam UV500 spectrophotometer over the range 250–850 nm with a sampling interval of 0.1 nm. The samples were mounted in a cryogenic cell and cooled using liquid nitrogen (–196°C). Infrared absorption spectra were recorded in the mid-infrared (6000–400 cm^{-1}, 1.0 cm^{-1} resolution) range at room temperature with a Thermo-Nicolet Nexus 670 Fourier-transform infrared (FTIR) spectrometer, equipped with a KBr beam splitter. A 6x beam condenser focused the incident beam on the sample, and a total of 1,024 scans (per spectrum) were collected to improve the signal-to-noise ratio. Diamond type was determined by infrared and visible spectroscopy. We selected a subset of 10,399 samples in order to study spectral differences within the two categories (Ia and Ib) of type I yellow diamonds, and to see if there were any relationships between spectra and color appearance or observations with the microscope.

Absorption coefficients for all spectra were calculated assuming a straight light path through the faceted gemstone. Using absorption coefficients, we were able to calculate approximate nitrogen concentrations (Field, 1992).
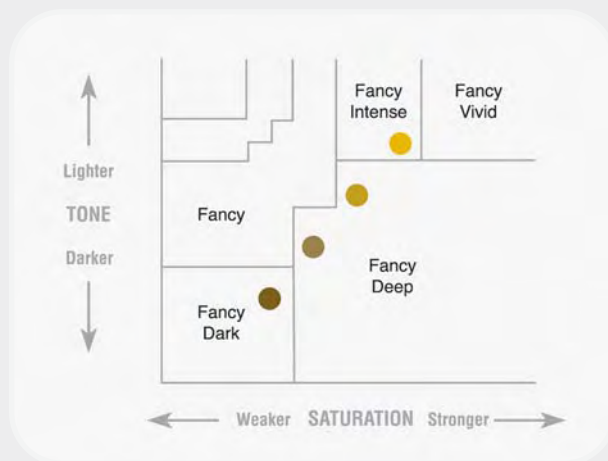
Figure 4. The diamonds within the bold lines of this chart illustrate some of the color appearances seen among the samples in the study and the terms associated with them, which are based on hue, tone, and saturation. As shown here, diamonds in the yellow hue range often appear to have brown and green components as they become weaker and/or darker. For the purposes of this illustration, the transition in color seen from the outer ring (at the top) to the inner ring (at the bottom) is of weakening saturation and increasing darkness (as illustrated on the tone/saturation chart to the left). Examples from the adjacent hues of orangy yellow and greenish yellow are included here for comparison. Note that brown-yellow (and, if the full range was shown, yellow-brown and yellowish brown) is in the orangy yellow hue range, not the yellow range.

DATA ANALYSIS AND RESULTS

Weight. A significant portion of our samples—30%—weighed 3 ct or more, while 17% weighed 5 ct or more and 5% weighed more than 10 ct. Of the latter, 23 were larger than 50 ct, and three were larger than 100 ct. In general, there are slight (statistically insignificant) differences in these percentages for 1998 and 2003 (figure 5).

Cut. Yellow diamonds in the modern marketplace are most often fashioned as fancy shapes. This trend was apparent in our data, where 94% of the yellow diamonds examined were shapes other than round brilliants. Variations on the radiant cut are included in the "square" and "rectangular" categories that together represent 52% of all the diamonds studied (figure 6).

Color Appearance. Figure 7 illustrates the range of tones and saturations in which these yellow diamonds occur. As these charts illustrate, the colors of yellow diamonds transition smoothly throughout the ranges of hue, tone, and saturation (i.e., the changes in appearance are gradual without abrupt differences between them). The lighter, most-saturated colors are located toward the upper right corner of the charts (Fancy Intense, Fancy Vivid), while the darker, less-saturated colors lie toward the opposite corner (Fancy Dark). It is important to note that this distribution of color appearances differs from those of pink and blue diamonds (see King et al., 1998, 2002), where the stronger colors are darker in tone (i.e., toward the lower right corner of the chart). Five percent of the samples exhibited a brownish yellow, brownish greenish yellow, or brown–greenish yellow color appearance.

GIA Fancy Color Grades. The study samples covered all the GIA "fancy" grades associated with yellow diamonds (i.e., Fancy Light, Fancy, Fancy Intense, Fancy Dark, Fancy Deep, and Fancy Vivid). Unlike other colored diamonds (except brown), yellow diamonds with grades of Faint, Very Light, and Light are not considered to be fancy-colored diamonds, but are part of GIA's D-to-Z color grading scale.

The pie charts in figure 8 show how the yellow diamonds in our study fell into the fancy grade categories for 1998 and 2003. Colored diamond grading activity at GIA more than doubled from 1998 to 2003, but, as seen in figure 8, the general color-grade distribution remained consistent during these two years.

DISTRIBUTION BY WEIGHT
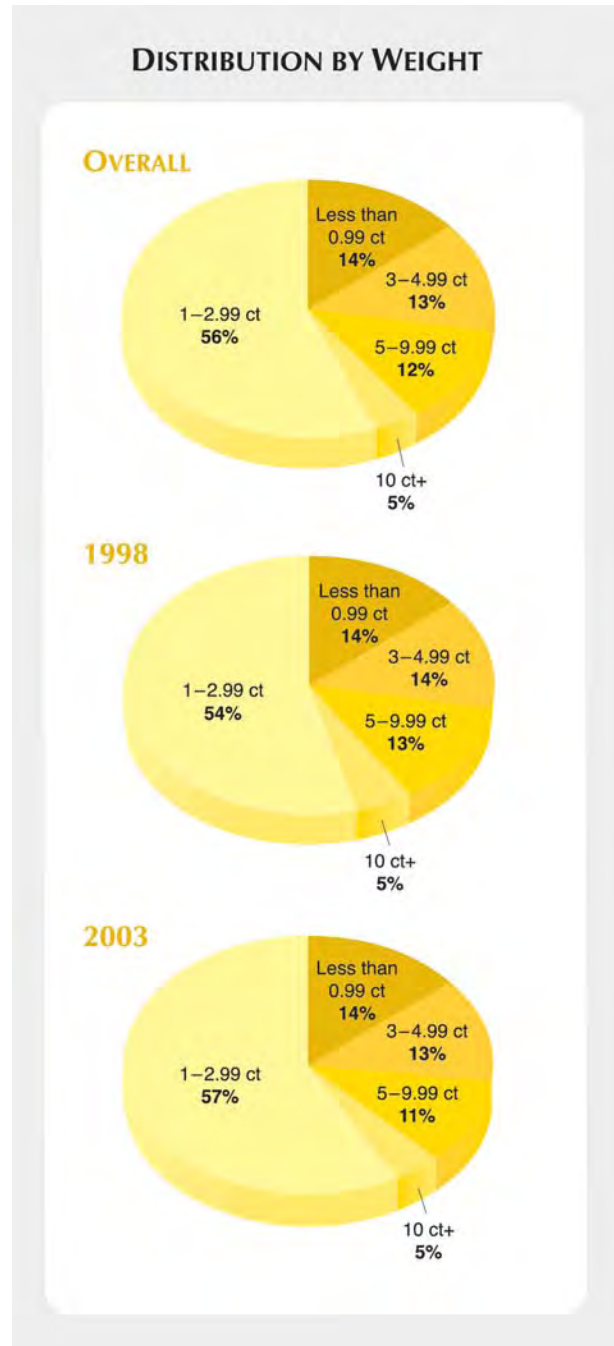
Figure 5. These three pie charts illustrate the distribution of the 24,668 diamonds in the study in several weight categories. The bottom two charts show that there was very little difference seen in the weight categories between 1998 and 2003.

Hue. As noted above, the diamonds in this study transition smoothly throughout the yellow hue range. This is consistent with GIA's observations of yellow diamonds over the past 50 years. At the extremes, two subtly different color appearances are

observed ("cooler" toward the greenish yellow boundary and "warmer" toward orangy yellow) that are still described as *yellow* with no modifying terms (figure 9). In the more saturated grades of Fancy Intense and Fancy Vivid, the diamond community sometimes refers to these two appearances as "lemony" and "golden," respectively (N. Livnat, pers. comm., 2004).

Tone and Saturation. Yellow diamonds occur in broad ranges of tone and saturation. They reach their strongest saturation at relatively light tones (again, see figure 7), with saturation strengths as high as we have encountered for any other diamond color.

Microscopic Examination. *Clarity Grades.* Of the 17,152 diamonds examined for clarity, 30% were VVS or Flawless/Internally Flawless (FL/IF), 50% were Very Slightly Included (VS), and 20% were Slightly Included (SI) or Included (I). Some variations were noted between samples graded in 1998 versus

Figure 6. This pie chart illustrates the percentage breakdown for the various shapes in which the yellow diamonds in our study were fashioned. Each shape category may include different cutting styles (such as step, modified brilliant, and brilliant cuts). Included in the miscellaneous category are shapes such as marquise, triangle, shield, kite, and briolette. The "cut-cornered or round-cornered rectangular/square" sections include variations on the radiant cut, which helped revolutionize the availability of fancy-color yellow diamonds in the marketplace.
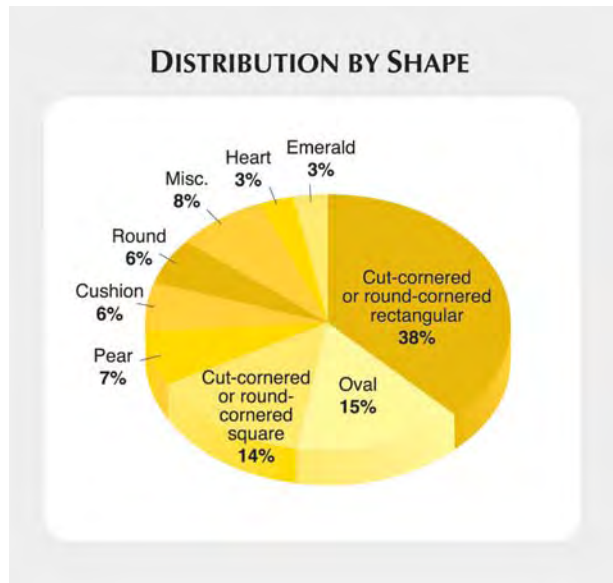

DISTRIBUTION BY SHAPE

2003 (figure 10). For example, there was a decrease in the percentage of FL/IF (from 9% to 5%) and an increase in those graded SI (from 14% to 19%).

We were interested to see if there might be a correlation between depth of color and the clarity of the yellow diamonds in our study, so we reviewed the overall distribution of clarity grades for those diamonds graded Fancy Vivid versus those graded Fancy Light (as these two grades would represent the extremes in strength of color). In general, the distribution was similar (figure 11), although a higher percentage of Fancy Vivid diamonds received grades of Flawless or Internally Flawless (12% versus 4% for the Fancy Light group); conversely, a higher percentage of Fancy Light diamonds received VS grades (55% versus 45% for the Fancy Vivid group).

Inclusions. It is common to encounter small clouds or strings of pinpoint-like solid inclusions in yellow diamonds (figure 12; see also Crowningshield, 1994). Occasionally dark crystals are seen as well (figure 13). We also noted the presence of small pinpoint or cloud-like inclusions toward the center of a number of the large (over 30 ct) diamonds in our study.

Graphite was the most common mineral inclusion observed, typically occurring in fractures of various sizes, displaying a flat shape. We occasionally observed euhedral crystals of both peridotitic and eclogitic minerals. Olivine (colorless), pyrope garnet (purple), and diopside (green) were observed as inclusions from the peridotitic group, which in general is more abundant in natural diamonds than the eclogitic group. From the eclogitic group, we usually found almandine-rich garnet (orange; figure 14), omphacite (grayish blue), and rutile (dark reddish orange). These inclusions were generally smaller than 100 μm, but they ranged up to several hundreds of micrometers in longest dimension. In rare cases, these inclusions displayed octahedral morphology. Over 80% of all natural diamonds are peridotitic (Meyer, 1987). However, in the majority of the yellow diamonds, it seems that macro inclusions of eclogitic group minerals were as common as those of peridotitic groups. Euhedral macro inclusions rarely occur in diamonds dominated by isolated nitrogen, and this was also the case for most of the type Ib diamonds examined in this study. What we did observe in a few of these type Ib samples, however, were small, needle-like fractures surrounding solid pinpoint inclusions.

GIA Yellow Diamond Color Chart

"Warmer" Yellow

Fancy Light		Fancy Intense	Fancy Vivid
	Fancy		
		Fancy Deep	
Fancy Dark			

Figure 7. These two tone/saturation charts illustrate the color appearances at two locations in the yellow hue range: "warmer" yellow diamonds that lie toward the orangy yellow/yellow hue boundary, and "cooler" ones that lie toward the greenish yellow/yellow boundary. In each case, the lighter, more saturated colors are seen in the upper right of the diagram, whereas the darker, weaker colors are located toward the lower left. On each diagram, the inset chart shows the generalized boundaries of the GIA Gem Laboratory fancy grades. The shaded areas on the two charts indicate the areas in

"Cooler" Yellow

Fancy Light | Fancy Intense | Fancy Vivid
Fancy
Fancy Deep
Fancy Dark
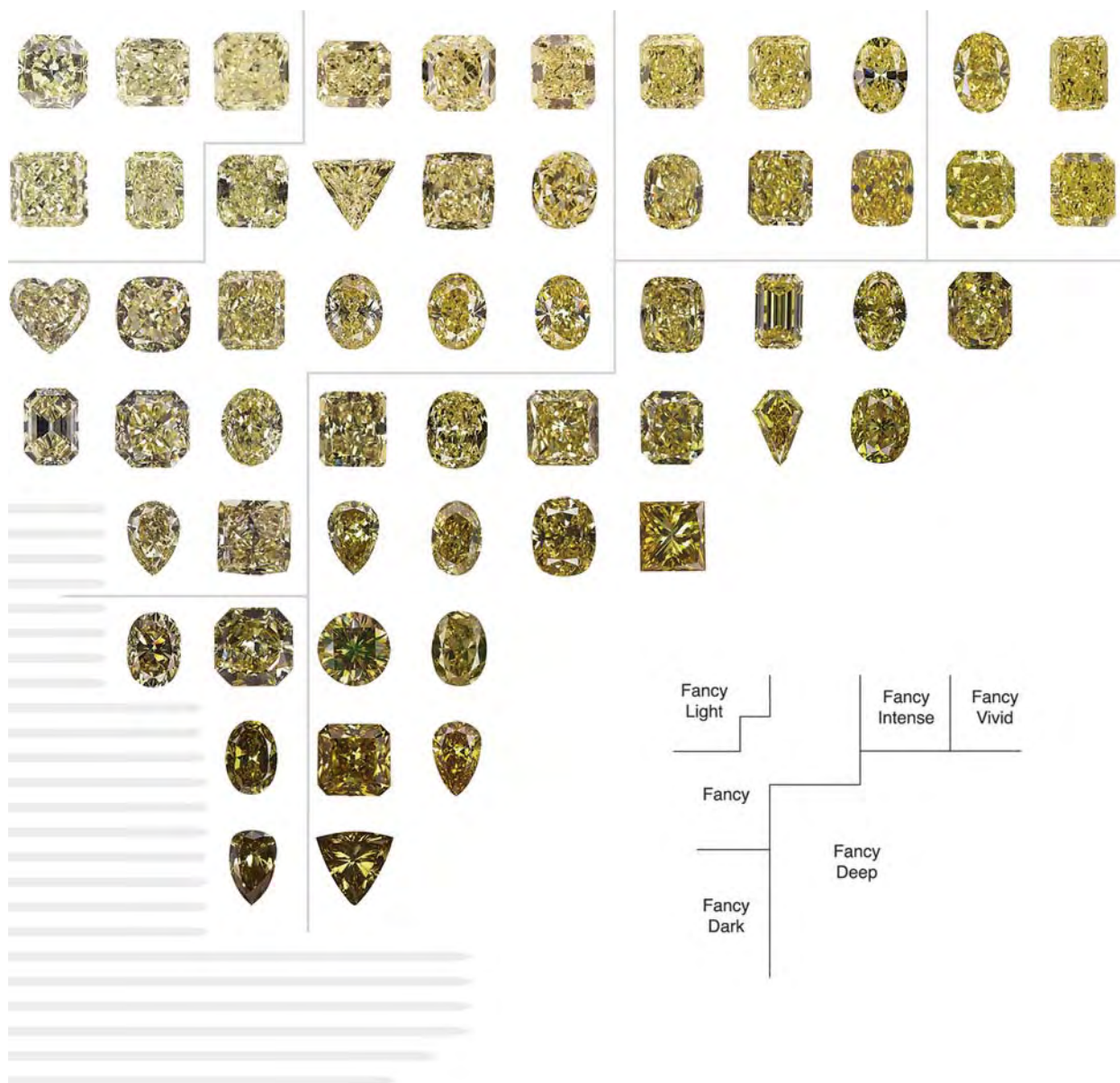
the yellow hue range in which diamonds described as predominantly brown (not part of this study) occur. Note that these two diagrams are for illustrative purposes only; by themselves, they are not adequate for use in color grading. Because of the inherent difficulties of controlling color in printing (as well as the instability of inks over time), the colors of the images shown here may differ from the actual colors of the diamonds. Photos by Elizabeth Schrader and C.D. Mengason.

DISTRIBUTION BY FANCY GRADE

1998

- Fancy Intense 26%
- Fancy Vivid 4%
- Fancy Deep 3%
- Fancy Dark less than 1%
- Fancy Light 17%
- Fancy 49%

2003

- Fancy Intense 24%
- Fancy Vivid 6%
- Fancy Deep 2%
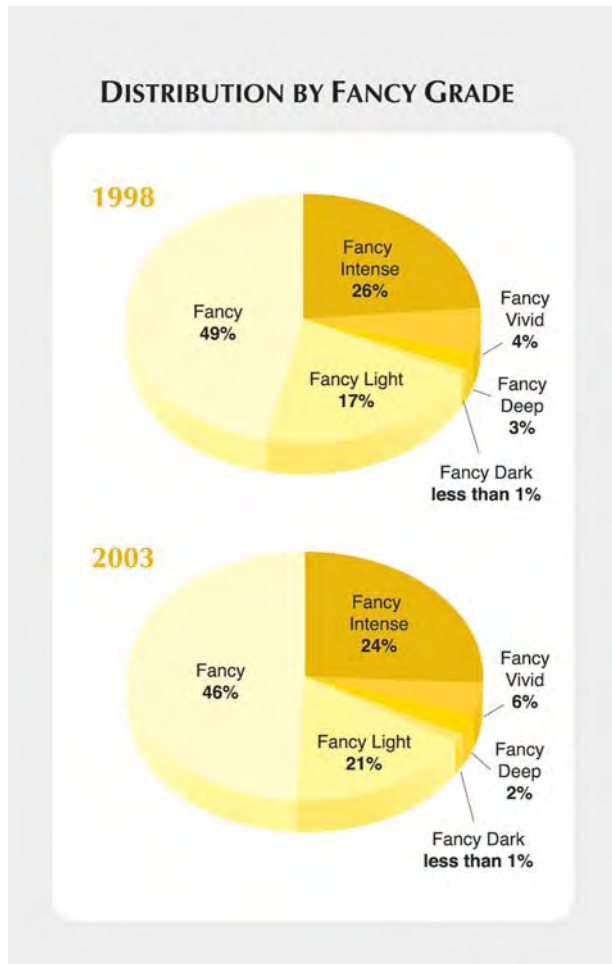- Fancy Dark less than 1%
- Fancy Light 21%
- Fancy 46%

Figure 8. These pie charts show the percentages of the diamonds in the study in each of the GIA Gem Laboratory fancy-color grade categories for the years 1998 and 2003. Note the relatively consistent distribution between 1998 and 2003, even though requests for laboratory services more than doubled over this time period.

Figure 9. These Fancy Intense yellow diamonds illustrate four different positions within this color group. Members of the diamond trade sometimes describe those colors that lie near the yellow/greenish yellow boundary (like the diamond on the far right) as "lemony," and those near the orangy yellow/yellow boundary (as seen in the diamond on the far left) as "golden." Photos by Elizabeth Schrader.

DISTRIBUTION BY CLARITY

OVERALL

- Flawless or Internally Flawless 6%
- VVS 24%
- SI 18%
- I 2%
- VS 50%

1998

- Flawless or Internally Flawless 9%
- VVS 26%
- SI 14%
- I 2%
- VS 49%

2003

- Flawless or Internally Flawless 5%
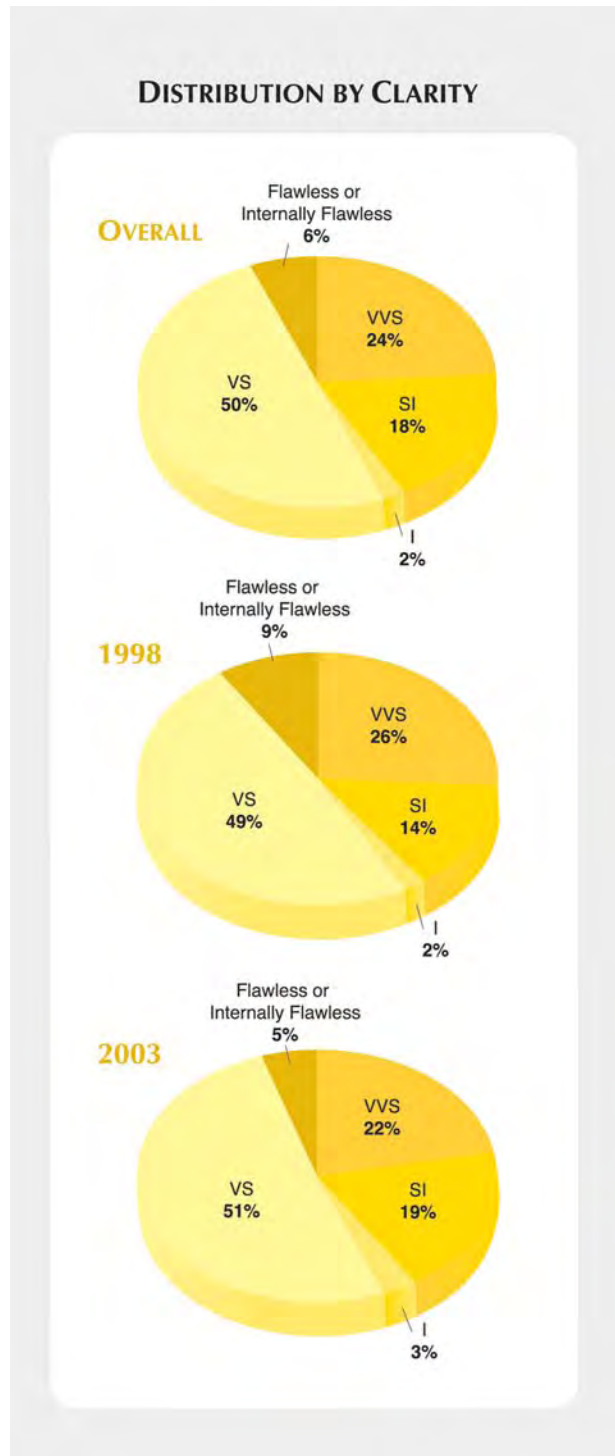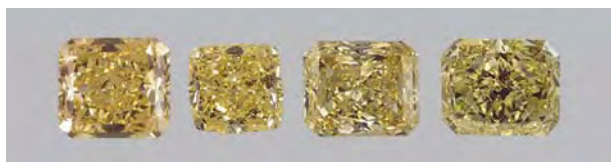- VVS 22%
- SI 19%
- I 3%
- VS 51%

Figure 10. The diamonds studied were relatively high in clarity, with approximately 80% of the studied samples receiving grades of VS or higher. These percentage distributions were relatively consistent between the sample groups examined in 1998 and 2003.

DEPTH OF COLOR VERSUS CLARITY

FANCY VIVID

- VVS 23%
- Flawless or Internally Flawless 12%
- SI 18%
- I 2%
- VS 45%

FANCY LIGHT

- VVS 21%
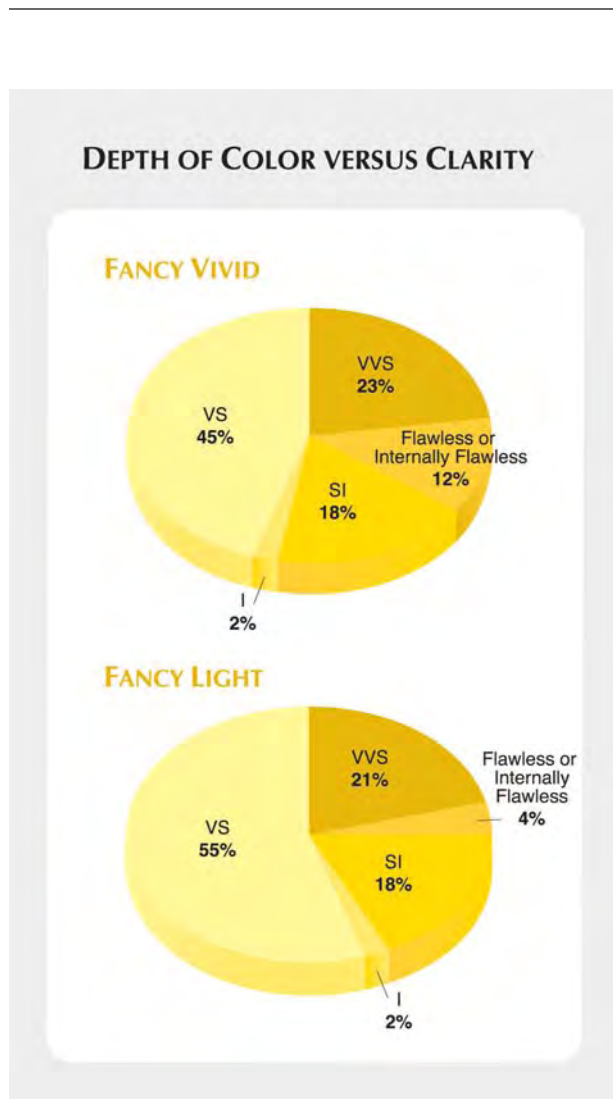- Flawless or Internally Flawless 4%
- SI 18%
- I 2%
- VS 55%

Figure 11. These two pie charts show the clarity grade distributions among those yellow diamonds in our total sample population with Fancy Vivid and Fancy Light color grades (which represent the extremes in yellow color saturation).

Graining. When observed under standard diamond grading conditions, the vast majority of the yellow diamonds did not exhibit typical forms of internal graining such as reflective planes or colored banding (i.e., whitish or brown). However, we found that one form of internal graining not commonly encountered in other fancy colors occurs more frequently in yellow diamonds. In this type of graining, the internal reflective graining plane exhibits a dispersion of color (figure 15) and maintains this appearance through a range of viewing angles. Because of the dispersive color appearance, this graining is described as "rainbow" graining; in some cases, it may affect the clarity grade.
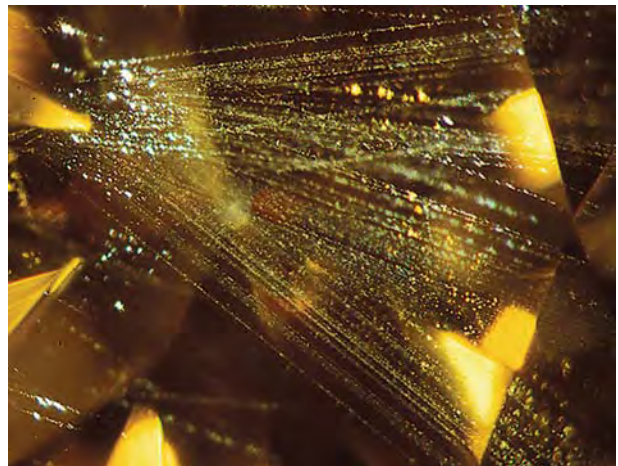

Figure 12. Stringers of numerous tiny inclusions, some in reflective orientation, create an interesting cloud formation in this brownish yellow diamond. The presence of this cloud further supports the diamond's natural-color determination. Photomicrograph by John I. Koivula; magnified 30x.

Color Zoning. Only 8% of the diamonds in our study exhibited noticeable color zoning. When present, the zoning often took the form of diffused or concentrated patches of color (an appearance occasionally referred to as "scotch and water").

Ultraviolet Fluorescence. We found that 71% of our samples showed either no or a very faint reaction

Figure 13. Clusters of small black and metallic-looking needles and platelets, such as this triangular grouping, were seen in some of the yellow diamonds. These inclusions are probably composed of sulfides and graphite. The triangular form of this cluster suggests that it might also be a phantom plane. Photomicrograph by John I. Koivula; magnified 25x.
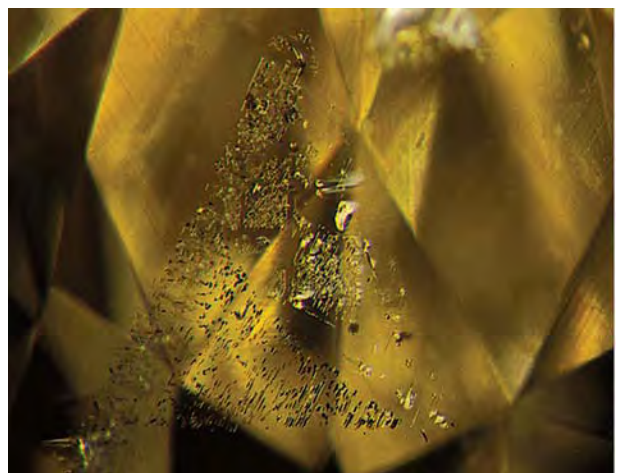
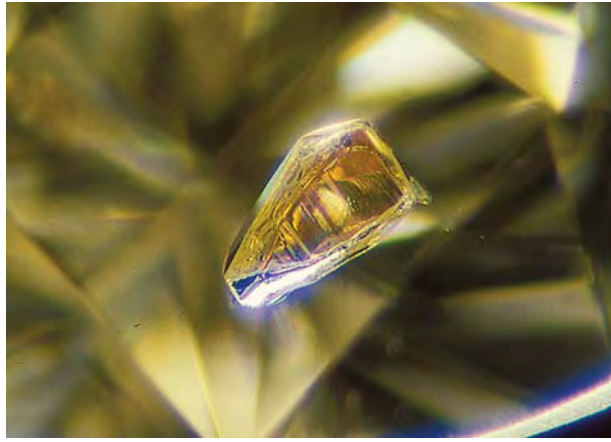Figure 14. The most recognizable color for an eclogitic garnet inclusion in a diamond is orange. Such garnets are mixtures of almandine and pyrope. Their presence also provides proof of the diamond's natural origin. Photomicrograph by John I. Koivula; magnified 20x.

(both of which are referred to as "none" on grading reports) when exposed to long-wave UV radiation, while 25% displayed a faint to medium reaction. A

Figure 15. This 5.04 ct yellow diamond exhibits "rainbow" graining, a type of graining seen more commonly in yellow diamonds than in other colors. When this dispersion of colors remains visible through a range of motion, it can affect the clarity grade. Photo by Vincent Cracco; magnified 12x.

strong or very strong reaction was observed in less than 4% of the total group (figure 16). Of these latter samples, 92% exhibited blue fluorescence, while the remainder displayed other colors (including green, yellow, orange, and white).

Eighty-eight percent of the samples displayed no reaction or a very faint to faint reaction to short-wave UV radiation. The remainder had medium (11%) or strong reactions (1%). In terms of their fluorescence colors, 91% were yellow. The remainder fluoresced various other colors, but predominantly blue or green.

Spectrometry and Diamond Type Groups. Based on our subset of 10,399 diamonds, we found that type I yellow diamonds may be broadly categorized into five groups based on their UV-visible and infrared spectroscopy. Representative samples for each group are illustrated in figure 17.

Group 1. This first group represents the vast majority of yellow diamonds in the subset (92.8%). Based on the intensity of features in their spectra, they demonstrated a high concentration of nitrogen and highly aggregated nitrogen impurities, consistent with type Ia diamond. Spectral features arising from isolated nitrogen were rarely seen in the samples in this group. The UV-visible and infrared spectra for a representative 1.31 ct Fancy Vivid yellow diamond are displayed in figure 17A. The UV-visible spectrum is dominated by absorptions due to the N3 center, with zero-phonon-line absorption at 415 nm and its related sidebands with peaks at 376, 384, 394, and 403 nm. Other absorption features present—at 425, 438, 452, 465, and 478 nm—are all related to the N2 center (Collins, 1982). The absorption features seen between 1400 and 1000 cm^{-1} of the infrared spectrum suggest high concentrations of aggregated nitrogen. Due to the completely radiation-absorbing nature of the type Ia nitrogen, spectral fitting could not be performed to calculate exact concentrations of nitrogen; however, these features suggest that this diamond has nitrogen concentrations of at least 200 ppm. Other spectral features characteristic of this group include a strong peak at about 1370 cm^{-1} associated with platelets—an extended defect composed of interstitial carbon and, possibly, nitrogen atoms (Collins, 2001)—and weak absorption peaks at 1547, 1520, and 1495 cm^{-1}. At higher wavenumbers, weak peaks at 3236 and 3106 cm^{-1} are present, which are indicative of the presence of a trace hydrogen impurity (Field, 1992).

Group 2. These diamonds comprise approximately 4% of the sample set, and they share many of the same nitrogen-related infrared and UV-visible spectral features as the diamonds detailed in Group 1. However, they differ significantly from the Group 1 samples due to strong absorption features related to hydrogen. This group is represented by a 1.26 ct Fancy brownish yellow diamond. The infrared spectrum (figure 17B) displays high concentrations of type Ia nitrogen (similar to Group 1 diamonds) but clearly differs from them by features at 4495, 4168, 3236, 3106, 2813, 2785, and 1405 cm^{-1}—all related to hydrogen defects (Fritsch and Scarratt, 1992). The UV-visible spectrum also displays the N3 and N2 features associated with Group 1 diamonds, but it contains hydrogen-related absorptions at 474 and 563 nm—and two weak but broad bands at 545 and 555 nm—as well. Furthermore, a weak rise from a broad band resulting from a broad band center around 700 nm to longer wavelengths, possibly hydrogen related, is present (Fritsch and Scarratt, 1992).

Group 3. We found that 1.7% of the sample set fell into this group. These diamonds differed from all the other yellow diamonds because of their green luminescence to visible light. The 0.40 ct Fancy Intense yellow diamond seen in figure 17C is an example of this group. The UV-visible spectrum displays absorption due to the N3 center and weak N2-related absorption features situated on a gradual rise at the blue end of the spectrum (which are collectively responsible for the predominantly yellow color). The weak green luminescence observed in these diamonds is a result of the H3 center (a defect consisting of two nitrogen atoms and a vacancy) at 503.2 nm. The infrared spectrum suggests that almost all of the infrared active nitrogen is type IaB, with a calculated total B-aggregate nitrogen concentration of more than 350 ppm.

Group 4. This group encompassed 0.8% of the sample set and is represented by a 2.03 ct Fancy Vivid yellow diamond. Unlike the other groups, the infrared spectrum (figure 17D) displays a relatively low concentration of nitrogen (calculated to be 16 ppm by means of spectral fitting). The nitrogen is mostly unaggregated (~11 ppm), and these predominantly type Ib diamond spectra exhibit a sharp absorption line at 1344 cm^{-1}, and a broader peak at ~1130 cm^{-1}. A small amount (~5 ppm) of aggregated type IaA nitrogen, represented by an absorption at 1282 cm^{-1}, is also present. Notably, the 1600–1450
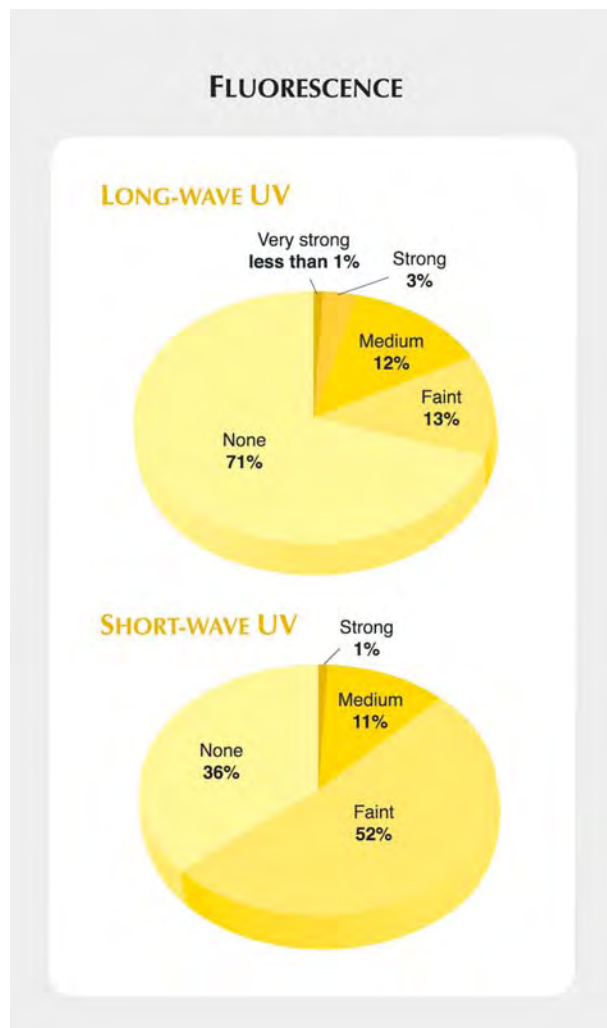
FLUORESCENCE

Figure 16. These two pie charts illustrate the strength of fluorescence of the studied diamonds to long- and short-wave UV radiation. In general, more than 80% of the samples displayed no fluorescence or faint fluorescence to both wavelengths. The most common colors observed were blue (92%) for long-wave and yellow (91%) for short-wave UV.

cm^{-1} region lacks any distinctive features. The visible spectrum is virtually featureless aside from a rise in absorption from 500 nm to shorter wavelengths. However, some diamonds in this group showed nitrogen-vacancy (NV) related absorption features at 575 and 637 nm.

Group 5. The fifth group of yellow diamonds made up 0.7% of the sample set. It is represented by a 1.56 ct Fancy Intense yellow diamond. Absorption features related to N2 are generally much weaker than those in Group 1 for comparable color saturations. Similar to the samples in Group 4, the UV-
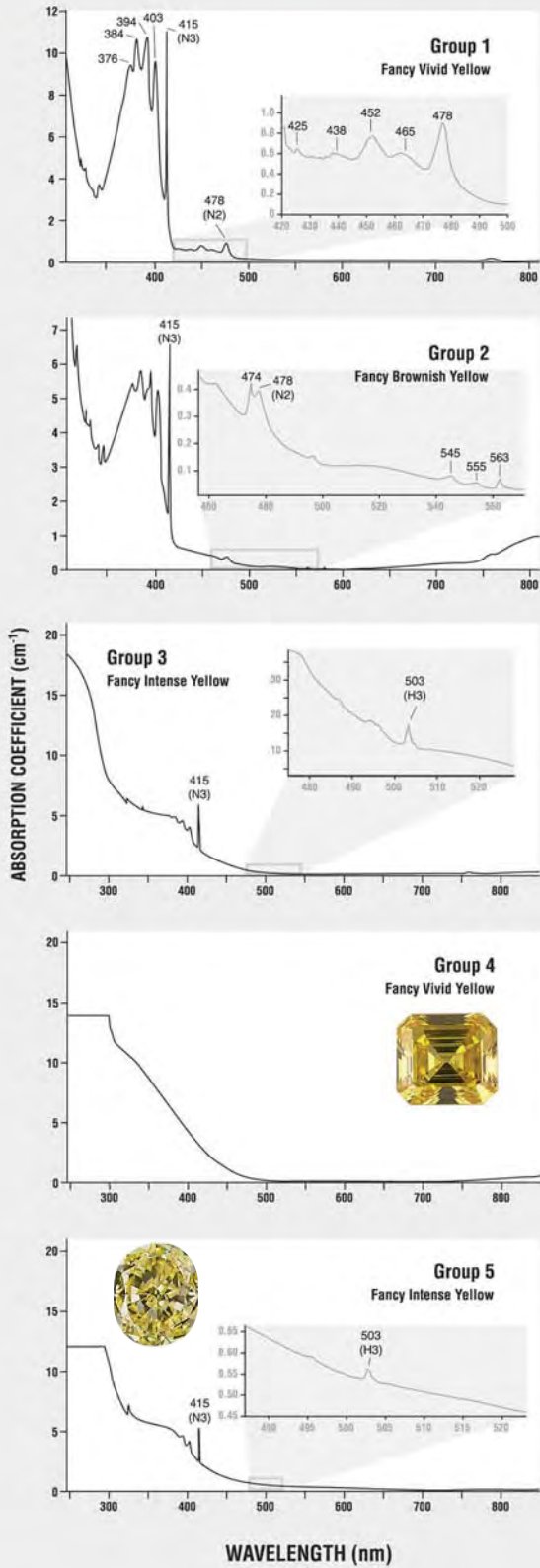
Figure 17A–E. Yellow diamonds may be broadly divided into five different groups based on their UV-visible and infrared spectra. One set of spectra for each of the five diamonds illustrated was chosen to represent the individual groups.

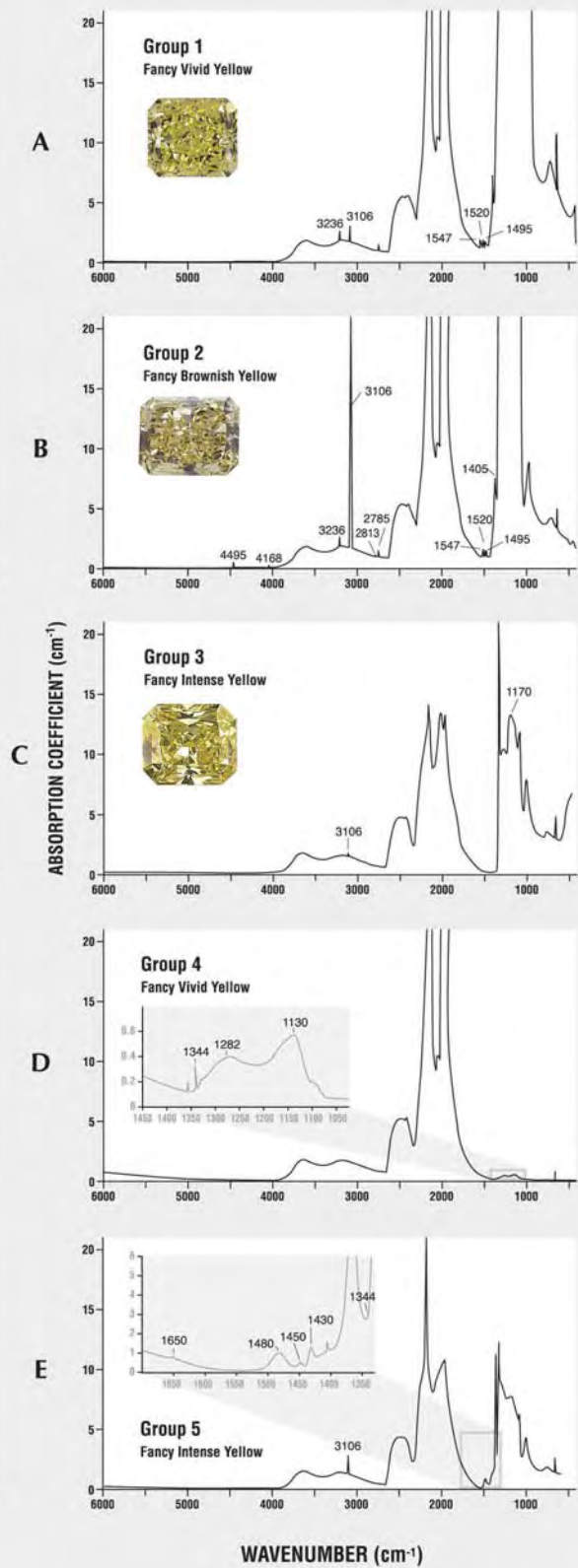visible spectrum displays a gentle rise in absorption from 500 nm to shorter wavelengths, but with an obvious N3 zero-phonon line and its related sidebands. A weak H3 absorption was also observed. The infrared spectrum, like the spectra for diamonds in Groups 1 and 2, typically consists of totally absorbing type Ia nitrogen and the platelet peak. However diamonds of this group commonly had a broad absorption at 1650 cm^{-1}; three absorptions at ~1480, 1450, and 1430 cm^{-1} of varying sharpness; and, in many cases, a very weak absorption at 1344 cm^{-1} due to isolated (type Ib) nitrogen (figure 17E).

DISCUSSION

Weight. With nearly one-third of our samples for both years of our study weighing more than 3 ct, it appears that the likelihood of encountering comparatively large yellow diamonds is significantly higher than for other colored diamonds, which typically occur in small sizes (see, e.g., Hofer, 1998; King et al., 1998, 2002). To confirm this, we looked at the average weight for colored diamonds submitted to the laboratory in the various hues in 2003. The average weight for yellows (3.23 ct) exceeded that for all other hues and was more than one-third larger than the average for blues. King et al. (1998) indicated that 14% of the blue diamonds studied were over 5 ct, compared to 17% for this study. While these percentage differences do not initially appear great, the largest diamond in the blue study weighed 45 ct, whereas the present study included 23 diamonds over 50 ct and three larger than 100 ct. Indeed, from our experience, no other colored diamond color occurs so consistently in such large sizes.

Cut. As discussed in previous studies (King et al., 1998, 2002), the primary goal of the cutter of colored diamonds is to enhance the final face-up color appearance. As shown by our data, yellow diamonds are typically cut as fancy shapes to help attain the most intense face-up color appearance. For a detailed discussion on manufacturing aspects of yellow diamonds, see box A.

Clarity. As with other natural-color diamonds, color is the primary factor in the valuation of yellow diamonds. Still, their relative abundance causes the diamond trade to seek additional means to differentiate among them, so the value placed on clarity is higher than for more rarely encountered colors (N. Livnat, pers. comm., 2005). This situation is evident in the shift in requests for specific GIA colored diamond reports between the two years of our study. Of the two colored diamond grading services offered by the laboratory, the Colored Diamond Grading Report includes clarity grading, while the Identification and Origin of Color Report (which focuses on the diamond's color information) does not. Requests for reports that included a clarity grade for the yellow diamonds described here increased from 57% in 1998 to 75% in 2003. The increased desire for more grading information (as represented by clarity grades) appears to parallel the increasing interest in yellow diamonds over this time frame.

Because a higher clarity grade can be a positive marketing factor, it is not unusual for a manufacturer to try to attain a minimum "VS" grade when possible (M. Witriol, pers. comm., 2005). Such an approach is consistent with the finding that 80% of the diamonds in our study were graded VS or higher. Manufacturers indicate that it is easier to attain a higher clarity grade with yellow diamonds than with diamonds in other colors because of the relative purity of some of the larger yellow rough (M. Witriol, pers. comm., 2005).

Interestingly, our data showed a percentage *decrease* for the clarity grade categories of FL/IF and VVS (from 9% to 5% and 26% to 22%, respectively) between the two years of our study, but an *increase* from 14% to 19% for SI. We do not know if these changes in clarity grade distribution are a result of more requests for reports with clarity grades (from 57% to 75%, as noted above), greater effort to quickly fill market need (i.e., manufacturers are working toward quicker turn-around rather than higher clarity), a change in the quality of rough being used, or a combination of these factors.

The analysis of clarity grade versus strength of color supported our assumption that there was little or no relationship between these two characteristics. As noted in our results, the distribution of clarity grades for Fancy Light and Fancy Vivid was similar, with the exception of FL/IF, where there were three times more diamonds in this category for Fancy Vivid than Fancy Light. The rarer a diamond's inherent color, the more likely it is that a manufacturer

BOX A: THE IMPORTANCE OF CUT IN YELLOW DIAMONDS

Manufacturing. Today, yellow diamonds (and colored diamonds in general) are typically cut as fancy shapes to enhance their color appearance (see figure A-1). It is not unusual for yellow rough to occur as octahedra (I. Wolf, pers. comm., 2005). The best yield and potential color retention for such crystals is found in square or near-square shapes such as radiants, emeralds, or cushions (which comprised as many as 61% of the samples in this study; see again figure 6).

Given the relative lack of inclusions and color zoning in large yellow rough, manufacturers can focus more on weight retention and color appearance (M. Witriol, pers. comm., 2004).

Cutting Innovations. Much of the framework on which today's cutting decisions are based originated with innovations begun in the 1970s. Previously, diamonds with light yellow bodycolor were manufactured in the shapes, cutting styles, and proportions of diamonds on the D-to-Z scale. Recent personal accounts to one of the authors (JMK) described how some of these changes came about (M. Blickman and J. Doppelt, pers. comms., 2005). By the mid-1970s, New York manufacturers such as Stanley Doppelt and Henry Grossbard had begun experimenting with variations on Basil Watermeyer's 1971 Barion cut, a square mixed cut whose step crown and modified-brilliant pavilion improved brilliancy and increased yield from the traditional step cut (see Kerr, 1982), in an attempt to hide imperfections in "cheap, square-cut diamonds." The assumption was that the increased scintillation from the mixed cut would better disguise inclusions, thus giving a more pleasing appearance to the eye. From an early point in this experimentation, Mr. Doppelt (and later Mr. Grossbard) realized these variations also enhanced the color of the yellow diamonds they were recutting, especially light yellow hues. Throughout the mid- to late 1970s, other experienced cutters experimented with the angles on these diamonds (from "off-color" to noticeably yellow) to produce the best face-up color appearance.

In the late 1970s and early 1980s, the trade became aware of these potential cutting benefits. Mr. Doppelt, in conjunction with Louis Glick, introduced the "Star-Burst" cut, which helped gain popularity for yellow diamonds. Mr. Grossbard, for his part, patented the radiant cut (Overton, 2002). Mr. Grossbard's 1976 purchase at Sotheby's Zurich of an off-color 109 ct diamond then named the Cross of Asia would eventually add to trade interest as well. He decided to recut that diamond to his new cut. Industry observers felt that the resultant 79 ct Flawless, Fancy yellow renamed the Radiant Cut diamond was significantly more valuable than the original Cross of Asia (M. Blickman, pers. comm., 2005; this stone was graded prior to the 1995 modifications to the

Figure A-1. This 10.12 ct Fancy Vivid yellow pear shape illustrates the effect a fancy shape can have on intensifying the color in a yellow diamond. Courtesy of the Scarselli family; photo by Elizabeth Schrader.

GIA colored diamond color grading system).

As others in the trade became aware of this recut diamond and the effectiveness of these new cuts in the market, more manufacturers began recutting light yellow diamonds into these styles in an effort to achieve grades of Fancy Light or Fancy (M. Kirschenbaum, pers. comm., 2004). Key features of these cuts were half-moon facets on the pavilion, French culets, and a greater number of facets in general. The most dramatic differences in face-up color appearance were often seen when the starting material was a round brilliant (figure

Figure A-2. Some of the most striking differences are seen when a light yellow round brilliant is recut into a shape and cutting style, such as the radiant, that can accentuate the color appearance. For example, the 6+ ct round brilliant diamond on the left was graded in the W-X range of the D-to-Z scale. When recut as a 4.61 ct radiant (right), it was graded Fancy yellow. Courtesy of the Scarselli family; composite photo by Elizabeth Schrader.

Figure A-3. Use of a diamond cut that highlights brightness can cause a light-toned yellow diamond to appear even lighter. The diamond on the left has numerous small, bright spots as a result of the manufacturer's cutting decisions. The one on the right is the same diamond with the spots digitally removed and replaced with the average face-up color. When the small bright spots are removed, the color appearance is subtly deeper (i.e., it appears slightly darker and stronger). If such a diamond were near a grade boundary, this subtle difference in appearance could move the diamond into a higher grade. Composite photo by Elizabeth Schrader.

A-2). Over time, the new shapes and cutting styles were used on diamond rough—a practice that resulted not only in better color grades but also in better weight retention, so manufacturing light yellow rough became more profitable (I. Wolf, pers. comm., 2004). Even more than the opening of new mines or a mine's increased production, these cutting activities were responsible for the greater number of more intensely colored yellow diamonds that appeared in the marketplace.

Effects of Cut on Yellow Diamond Color Appearance. As noted above, the appearance of light-toned colors is easily influenced by the effects of cut. Cutting can create brightness (white or near-white light return), fire (the dispersion of various colors), windows ("see-through"), and dark areas (extinction). Because colored diamonds are graded in the face-up position, the overall blend of sensations—small areas of brightness, windowing, and/or extinction—may intermingle with the yellow face-up color and affect the overall color appearance. For example, brightness can visually blend with color to cre-

ate a softer, lighter appearance. If the color is near a grade boundary, such an appearance often results in the diamond being placed in a lower grade (i.e., with a weaker color; figure A-3). Similarly, small areas of windowing can mix with the color to create an overall washed out, weaker (i.e., less saturated) appearance. Overall darkness, or numerous dark areas due to extinction, can cause a "grayed-out," weaker look. Occasionally, these extinct areas can create a deeper appearance. Again, these effects can have an impact on color grade if the diamond is near a grade boundary.

Many diamond cutters are aware of the range of proportions that yield an attractive face-up cut appearance in colorless to near-colorless diamonds, but those who also cut colored diamonds often say "when it comes to color, you can throw away the book" (I. Wolf, pers. comm., 2005). An example of this is the rare Fancy Vivid yellow round brilliant in figure A-4. When observed by experienced staff and members of the trade, all agreed it was an exceptional color. But with a total depth of more than 65% and crown angles greater than 39°, it was unorthodox for a round brilliant and, if it had been near-colorless, would likely be considered less attractive than many other near-colorless diamonds. Clearly, the assessment of diamond cut for fancy-color diamonds is based on very different considerations than their D-to-Z counterparts.

Finally, cutting can also affect the perceived distribution of color when the diamond is viewed face-up. When the characteristic color does not predominate in the face-up position, it is reported as "uneven" for the "distribution" entry on grading reports (see King et al., 1994). Figure A-5 shows four examples of uneven color distribution in different shapes and cutting styles of yellow diamonds.

Figure A-4. With colored diamonds, cut is evaluated first in terms of its effect on the color. While this 1.51 ct Fancy Vivid yellow diamond has proportions that would be considered unorthodox for a colorless or near-colorless round brilliant, here they have produced a spectacular color appearance. Photo by Elizabeth Schrader.

Figure A-5. In some diamonds, the yellow color can appear limited to a minority of areas relative to the total area in the face-up position. Such yellow diamonds would be described as having an "uneven" color distribution on GIA grading reports. As illustrated here, the appearance produced by this uneven distribution can vary depending on the cut and proportions used. Composite photos by Elizabeth Schrader.

will consider working on other characteristics to further enhance its marketing potential (N. Smid, pers. comm., 2005). For the less-saturated colors, the manufacturer will factor in additional cutting (loss of weight), time costs, and current market salability into the decision to work toward the highest possible clarity. This approach is followed for colorless to near-colorless diamonds as well. It is much more likely for a manufacturer to try, when possible, to achieve a Flawless grade on a "D" color diamond than on a "K" color (N. Smid, pers. comm., 2005).

Inclusions. Given that the vast majority of the yellow diamonds in our sample group were type Ia, it is not surprising that their inclusions appeared to be the same as those encountered in diamonds on the D-to-Z scale (Koivula, 2000). Since the composition of these diamonds is essentially the same as those on the D-to-Z scale (differing only in concentration of defects), such a continuity of appearance would be expected.

Over the years, we have tracked the frequency with which pinpoint or small cloud-like inclusions occur toward the center of large (over 30 ct) diamonds submitted to the lab. A brief review of some of our historic records indicated that they were observed in more than half of 29 yellow diamonds weighing between 50 and 60 ct. The reason for this centrally located feature is not known, although these inclusions may represent growth conditions similar to those of symmetrical micro-inclusion "clouds" seen in other diamonds (see, e.g., Crowningshield, 1965). In our experience with yellow diamonds, the cloud-like inclusions may be distributed randomly throughout a stone, or they may follow specific growth sectors; in particular, cubic growth sectors {100} tend to contain more clouds than any other sector (see, e.g., Wang and Mayerson, 2002). Occasionally, the clouds are very obvious and can affect the color appearance as well as the clarity grade. Although little is known about the chemistry and phase relations of the tiny clouds, with few exceptions high levels of infrared-active hydrogen (see below) were commonly detected by infrared spectroscopy in the regions where these clouds were concentrated.

Color Zoning. To see if there was a relationship between our overall findings (8% of the samples exhibited color zoning) and the diamond type groups, we examined our subset of 10,399 diamonds for which type spectra were obtained. Most (92.3%) of our type Ia yellow study diamonds (Group 1) did not exhibit noticeable color zoning. However, diamonds with different kinds of nitrogen aggregations (as evidenced by features in their spectra) had much higher occurrences of uneven color zoning. Specifically, 62.3% of diamonds that showed hydrogen absorption lines in their visible spectra (Group 2) had uneven color zoning, usually in the form of brown growth sector–related zones. In addition, 65.1% of diamonds that had green visible luminescence (Group 3) showed uneven zoning, which usually appeared as straight yellow lines paralleling internal graining. The type Ib diamonds (Group 4) showed color zoning in 56.8% of its samples, most commonly in the form of diffused zones or concentrated patches of color, occasionally referred to as "scotch and water." Unlike in other colors, such as type I pinks and type IIb blues where the zoning tends to form in discrete bands, the "scotch and water" zoning has less effect on manufacturing decisions with regard to orientation of the zoning in relation to the face-up appearance (I. Wolf, pers. comm., 2005). Like Group 1, the diamonds in Group 5 did not show noticeable color zoning.

Ultraviolet Fluorescence. Of the 10,399 diamonds studied for diamond type, only 75 showed a short-wave UV reaction that was stronger than the long-wave reaction. Perhaps most interesting was that 58 (77.3%) of these diamonds were type Ib. While not a conclusive test, this observation may be helpful to the diamantaire who does not have access to sophisticated equipment but wishes to have an indication of diamond type.

Spectrometry and Diamond Type Groups. As noted earlier, the yellow color observed in natural diamond is mainly a result of nitrogen, the most common impurity found in this gem. Both aggregated and isolated forms of nitrogen within the diamond's lattice are responsible for the unique absorption features in the blue portion of the visible spectrum, which in turn give rise to the yellow coloration. Variations in nitrogen aggregation that begin during diamond formation (as well as the addition of other trace impurities and other defects) lead to the differences seen in nitrogen-related spectral features.

The complex stages of nitrogen aggregation in diamond take place over geologic time at high pressures and high temperatures within the earth. During the initial stages of growth, nitrogen atoms may substitute for single carbon atoms within the diamond lattice. Diamonds containing isolated

nitrogen are classified as type Ib (here, Group 4); they owe their unique "golden" yellow color to a rise in absorption from 500 nm to lower wavelengths (again, see figure 17D). In general, these yellow diamonds have low total nitrogen, even though their color is usually strongly saturated. As nitrogen-bearing diamonds continue to develop within the earth, the nitrogen atoms will migrate through the diamond lattice and over time may begin to form the commonly observed A, B, and N3 aggregates. Our spectroscopy results suggest that these optical centers are represented in the remaining four groups.

Group 1 diamonds contain a high concentration of N3 centers as well as N2 centers, which are attributed to a vibronic transition of the N3 center (Zaitsev, 2001). These are by far the most abundant yellow diamonds. Figure 18 shows overlain spectra of the Fancy Vivid yellow diamond in figure 17A and a Fancy Light yellow diamond also from Group 1. These spectra illustrate that the N2- and N3-related absorptions are stronger in the Fancy Vivid yellow diamond. Data from our entire subsample of diamonds on which spectra were taken suggest that the N2 centers in highly saturated yellow diamonds absorb more strongly than their less saturated counterparts; however, in many cases we observed that the N3 center in intensely colored yellow diamonds had the same absorbance as in their less intense counterparts. These data suggest that the N2 center plays a large role in determining the strength of yellow color saturation in Group 1 diamonds, as well as contributing to their "lemony" yellow color.

Group 2 diamonds are closely related to Group 1; however, our representative spectra for this group indicate high concentrations of hydrogen compared to Group 1 diamonds. Hydrogen-related absorptions in the UV-visible spectra may contribute to the modifying brownish and greenish appearances associated with these diamonds.

Similar to Groups 1 and 2, Group 3 diamonds contain aggregated N3 and N2 centers that contribute to the overall body color. In addition, however, Group 3 diamonds contain a green luminescence component that is attributed to small concentrations of another form of aggregated nitrogen, the H3 center, at 503.2 nm. Group 3 diamonds also tend to contain significant concentrations of highly aggregated type IaB nitrogen. In fact, our infrared data suggest that the vast majority of the type Ia nitrogen in most yellow diamonds with H3-
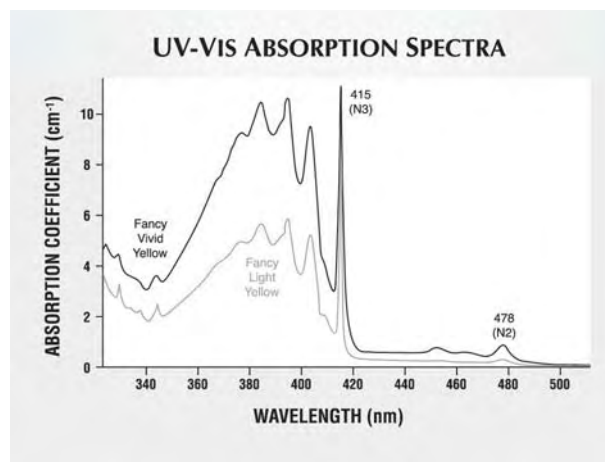

Figure 18. These two UV-visible spectra represent the Fancy Vivid yellow diamond from Group 1 (shown in figure 17A) and a Fancy Light yellow diamond from the same group. There are obvious differences in the strength of the N3 and N2 absorptions between these two diamonds of very different saturation.

attributed green transmission luminescence is in the form of B-aggregates.

As diamonds containing aggregated nitrogen mature in the mantle at elevated temperatures and pressures, it is possible that defects and nitrogen aggregates may begin to break up. Group 5 diamonds have spectral features similar to groups 1, 3, and 4, and some of these features may be linked to the destruction of defect centers and the disaggregation of nitrogen. The presence of the 1480 cm^{-1} peak in the IR spectrum has been linked to the degrading of the platelet peak at 1360 cm^{-1}; other features at 1650, 1450, and 1430 cm^{-1} may also be platelet related and increase in intensity as the platelets are destroyed by increased annealing (Kiflawi et al., 1998). In addition, Group 5 diamonds typically show trace amounts of isolated (type Ib) nitrogen, which suggests the breakdown of aggregated nitrogen after heating (Fisher and Spits, 2000).

Color Appearances as They Relate to the Diamond Type Groups. Despite the overlap, we did note different representative color appearances associated with the five groups. This can be seen in the photos accompanying the spectra of each group (again, see figure 17). The chart in figure 19 shows the general distribution of the diamonds in these groups in relation to the yellow fancy grades. The appearances associated with this larger distribution of tones and saturations can be seen when the areas noted in figure 19 are compared to the images in the corresponding locations in figure 7.

The diamonds associated with Group 1 (more than 90% of our samples) have the appearance most commonly associated with yellow diamonds. In the stronger grades of Fancy Intense or Fancy Vivid yellow, these diamonds are often described as "lemony." Group 5 diamonds were similar in appearance to those in Group 1.

The green luminescence characteristic of Group 3 diamonds can be strong enough to affect the apparent color. However, the luminescence in our study samples was not noticeable enough under standard grading conditions to place the diamonds outside of the yellow hue range, although they were located toward the "cooler" side of that range (i.e., toward the yellow/greenish yellow boundary).

Group 2 diamonds often appeared brownish or had brown and green components, which may be due to the hydrogen-related absorptions in the UV-visible spectra. It is also likely that the spectral features of Group 4 diamonds (all type Ib) are responsi-

ble for the strongly saturated, "warmer" yellow typical of these diamonds. Such "golden" color appearances are often associated with grades of Fancy Vivid and Fancy Deep yellow.

Color Appearance Transitions. As mentioned above, unlike other colors, the initial colored diamond grade associated with yellow is Fancy Light (again, see figure 7). The grade descriptions of Faint, Very Light, and Light are part of the D-to-Z scale, and they correspond to the K-M, N-R, and S-Z letter grade ranges, respectively (King et al., 1994). The transition in color appearance from these D-to-Z scale diamonds to fancy-color yellow diamonds is smooth, but the grading methodology and philosophy between the two scales changes abruptly.

A fundamental difference between these two grading scales is the value placed on "absence of color" in one (D-to-Z) versus "presence of color" in the other (colored diamond). The "absence of color" is primarily observed with the diamond in the table-down position, whereas the "presence of color" is *only* judged in the face-up position (King et al., 1994).

As the depth of color increases for diamonds on the D-to-Z scale, the role of face-up observation (in addition to table-down viewing) also increases in importance during grading. The transition boundary between the D-to-Z scale and a fancy-color grid is the "Z" grade. At this location, face-up appearance becomes *the* determining factor in assigning the color grade (i.e., a diamond must have a stronger face-up color appearance than the Z "master" to be considered a fancy color regardless of the bodycolor observed table down; figure 20).

Not only does methodology differ between these approaches, but the ranges of tone and saturation associated with a given grade are quite different as well. Grade ranges for fancy-color diamonds are significantly broader in both tone and saturation attributes than those on the D-to-Z scale.

In past observations, we have noted that some yellow color appearance transitions are more common than others, and this was supported by our data. The most common transition is throughout the saturation range rather than throughout tone or both tone and saturation. This is seen in the breakdown of our samples' fancy-color grades as well as their color descriptions. For example, about 97% of the diamonds in our study (representative of all diamonds in the yellow hue range submitted to the lab for 1998 and 2003) were Fancy Light, Fancy, Fancy

Figure 19. While there are overlapping color appearances among the five "spectral groups" of yellow diamonds identified in our study, some areas are more representative of each particular group than the others. This generalized tone/saturation chart (with the fancy grades for yellow diamonds overlaid) illustrates the most common areas in which the diamonds in the five groups occur.
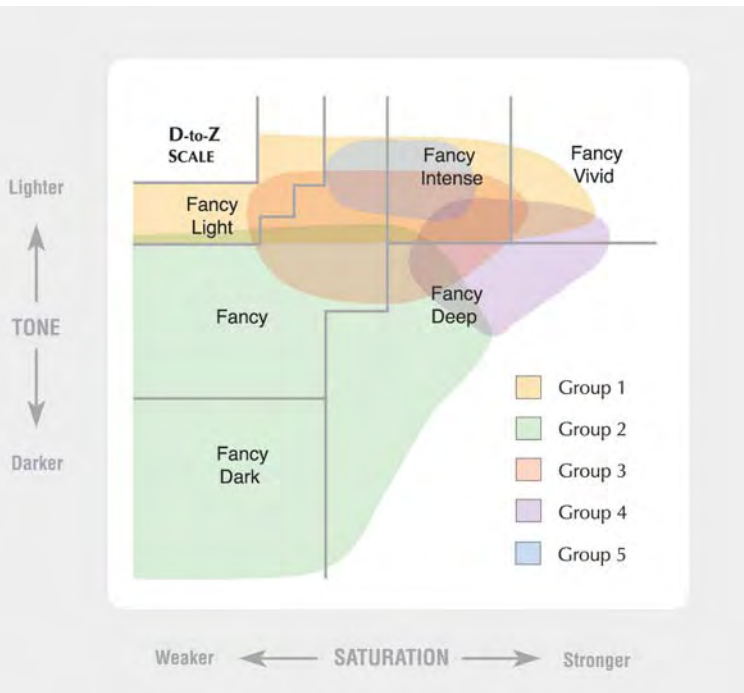
Intense, or Fancy Vivid. All of these grades occur in a restricted *tone* range of medium to light, but they span the entire *saturation* range for yellow diamonds. Just as fancy grades are defined by related areas of tone and saturation in color space, some of the word descriptions (i.e., *brownish* or *greenish*) associated with them are also determined by their area of tone and saturation within the grades. Many color order/description systems (e.g., Natural Bureau of Standards, 1976), including GIA's, arrange their terms in color space to accommodate increasing appearances of brown or gray that occur as colors darken in tone and weaken in saturation. Since most of the yellow diamonds in our study were lighter in tone and of relatively strong saturation, they did not have a brown or green component. Understanding this ordering convention, and the occurrence of our samples in color space, clarifies why so few of the yellow diamonds in our sample (5%) had descriptions of brownish yellow, brownish greenish yellow or brown–greenish yellow. It is understood, of course, that the GIA Gem Laboratory may not see the full range of yellow diamonds available. Nevertheless, given the large number of samples examined, this distribution may serve as a good indication of what goods are prominent in the marketplace.

Grade Distribution Over Time. It was interesting to note from our data that the distribution of fancy grades among our sample population was relatively consistent for the two separate years of our study. While far from being conclusive, these data give some indication as to the general distribution of yellow diamonds in that segment of the marketplace that uses GIA reports.

Figure 20. The transition from the D-to-Z scale to the fancy-color diamond scale for yellow diamonds is greatly affected by the cutter's ability to concentrate and intensify the face-up color, since it becomes the factor in determining the grade (not the "bodycolor" seen table down). In the diagram on the left, the X marks the location of a yellow diamond that lies near the end of the D-to-Z scale. The shaded area illustrates the range of potential tones and saturations and, in this case, grades the diamond could receive depending on how well the cutter was able to intensify the perceived face-up color. This is illustrated by the two yellow diamonds on the right. When observed table-down (top), both have a similar bodycolor. However, when the same diamonds are observed face-up (bottom), the differences in appearance are obvious. While the table-down bodycolor of these two diamonds placed them near the end of the D-to-Z scale, their face-up appearances resulted in the one on the left being placed on the D-to-Z scale and the other being graded as a fancy color. Photos by Elizabeth Schrader.
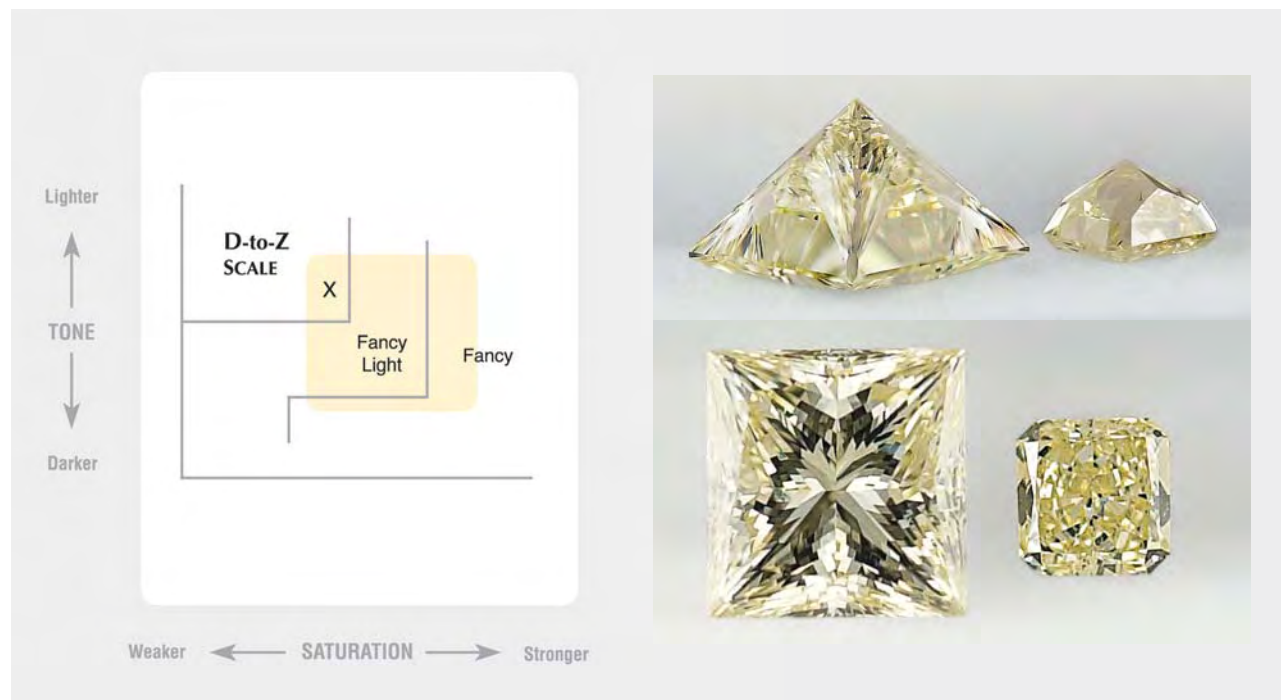
Figure 21. The evaluation of color in a colored diamond requires that the observer focus on overall blend (the characteristic color) rather than detail (individual components of the color). To see the overall blend, the observer uses a technique similar to that used when viewing a 19th century pointillist painting. The detail highlighted in this famous Georges Seurat work, A Sunday on La Grande Jatte, *shows a number of distinct, individual colors; when the observer steps back and looks at the painting as a whole, these colors blend into a single color sensation. When grading a colored diamond, one can also pick out colors from a mosaic of appearances in the diamond, but the grade assigned is based on the overall blend. 1884, oil on canvas, 81³¹⁄₄₄ × 121¹¹⁄₄₄ in.; image courtesy of The Art Institute of Chicago, Helen Birch Bartlett Collection.*

A REVIEW AND ELABORATION OF FACTORS INVOLVED IN COLOR GRADING

When GIA's colored diamond color grading system was first documented in this journal (King et al., 1994), we described our grading methods, environment, and terminology, to help those who use our reports understand the procedures and factors involved in assigning a color grade. Since that time, we have described the grading of blue diamonds and pink diamonds, specifically (King et al., 1998, 2002). Here, we would like to use yellow diamonds to review and elaborate on important aspects of color grading. From our discussions over the years, we have found that differences in grading interpretation can often be resolved by consistently answering two

important methodology questions: (1) Where and for what is the grader looking when grading color in a diamond (i.e., observation)? And (2) how does that diamond relate to other diamonds in terms of color appearance (i.e., bracketing)?

Observation. As mentioned before, when observing a colored diamond, the face-up position is the only view used. However, even when restricted to the face-up position, differences between observers in the "plane of focus" can yield different results. This plane can be thought of as an imaginary surface parallel to the table facet where the eyes of the observer are focused to evaluate the color. Depending on the location of this plane—near the table facet, at a depth near the girdle, or even deeper within the pavilion of the diamond—an observer can reach different conclusions about the color. At the GIA Gem Laboratory, this plane of focus is located close to the table facet, not deep inside the diamond, so the grader observes the overall blend that constitutes the predominant single color appearance (i.e., the characteristic color).

Figure 22. A thorough understanding of yellow diamond color evaluation requires an awareness of the full range in which the color occurs. For example, when the Fancy Deep yellow diamond on the left is shown next to a Fancy Intense yellow diamond (top right), the color of the former appears darker and slightly less saturated, which some might consider less attractive. However, when the same Fancy Deep yellow diamond is shown next to a Fancy Dark brown–greenish yellow diamond (bottom right), the attraction of its rich yellow hue is more evident. Photos by Elizabeth Schrader.
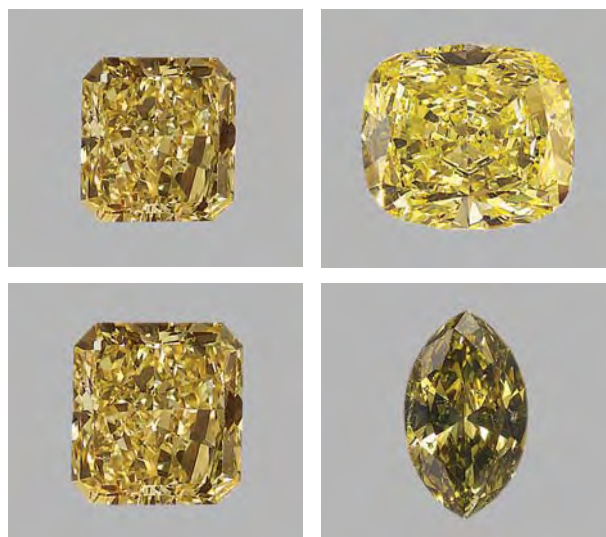
Figure 23. Yellow diamonds that lie near the yellow/greenish yellow boundary may appear less saturated if compared to a yellow diamond of similar strength that lies near the yellow/orangy yellow boundary. The two Fancy Intense yellow diamonds seen here are of similar saturation in GIA's grading system. To the inexperienced observer, however, the cooler yellow diamond on the right might appear weaker than the warmer one on the left. Photos by Elizabeth Schrader and C.D. Mengason.

Even with consistent lighting, environment, and viewing geometry, if one grader focuses deep into the diamond (or changes his/her focus to "pick out" highlights at different depths), it is possible to arrive at a conclusion different from that of another grader who is focusing on the table plane and observing the overall blend of face-up appearance.

The blended appearance that results from using a plane of focus near the table of a colored diamond can be likened to the merging effect that viewing distance has on color appearance in a 19th century pointillist painting such as Georges Seurat's *A Sunday on La Grande Jatte* (figure 21), a commercially printed page (produced with very small dots of cyan, yellow, magenta, and black ink), or a checkerboard pattern. In each instance, more than one color is visible on close inspection, but they blend to a single overall color appearance when viewed at a distance.

Bracketing. Thorough bracketing of the characteristic color with color references of known location is crucial to understanding the grading of a colored diamond. This process allows the observer to understand the color's location in color space and the description related to that location. Without that understanding, proper evaluations may be lacking. For example, a diamond that appears darker and weaker when compared to lighter, stronger reference diamonds (figure 22, top) will appear rich in color when compared to its darker and weaker counterparts (figure 22, bottom).

Bracketing is also important to accurately grade yellow diamonds of similar tone and saturation but at opposite ends of the hue range. The appearance of

those toward the "cooler" end of the range is different from those at the "warm" end, and this difference may be confused with strength of color if the diamond is not compared and bracketed consistently (figure 23).

Because yellow diamonds commonly transition in color appearance through a relatively narrow range of lighter tones, it is easy to misinterpret those falling outside that norm. To prevent this, observers need to be aware of the appearance relationships seen throughout the complete tonal range. Unless compared to known samples, the saturation of less commonly encountered colors of darker tone may be considered stronger than they are (figure 24). For example, the difference in appearance between a typical Fancy Light yellow diamond and one that is

Figure 24. If a diamond is near a grade boundary, darker tone can be confused with increasing saturation if known references are not used. Here, two examples illustrate this situation. On the far left are three diamonds near the Y-Z/Fancy Light yellow saturation boundary; the diamonds are of similar saturation and differ only in tone. Comparison to the Fancy Light yellow reference diamond to their right establishes their grade on the D-to-Z scale. On the right, a similar situation is seen with three diamonds near the Fancy Intense/Fancy Vivid boundary; their Fancy Intense grade is clear when they are compared to the Fancy Vivid yellow reference diamond to their right. These tonal differences can be misinterpreted by an inexperienced observer. Photos by Elizabeth Schrader.
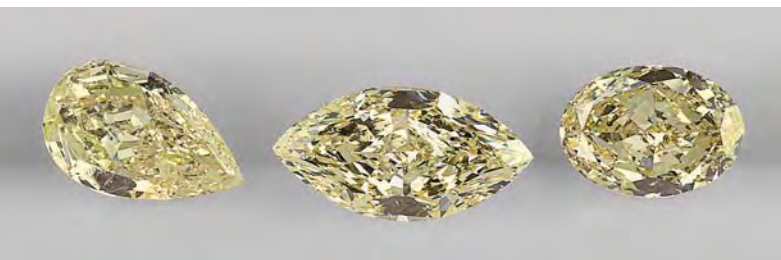
Figure 25. The light-toned yellow diamond shown in the center appears to "stand out" relative to the other two diamonds. Nonetheless, all three diamonds have the same Fancy yellow color grade. Photo by Elizabeth Schrader.

darker toned might lead to the incorrect assumption that there is a difference in saturation, and hence to the diamond being graded Fancy yellow. Similarly, fancy-color yellow diamonds that are light in tone often appear to "stand out"' from darker diamonds of similar hue, resulting in the misinterpretation of a "higher" grade. Lightness does not necessarily mean they are stronger or weaker in saturation and therefore fall into a different grade (figure 25).

Even though saturation-based grade transitions are relatively common among yellow diamonds, the observer may not know the full range of appearances within a grade, especially since grade ranges are quite different from those on GIA's D-to-Z scale. One can incorrectly assume that two yellow diamonds near the upper and lower boundaries of a grade's saturation range are in different grades if the entire range is not understood.

A number of the examples above illustrate the fact that there is a different appearance associated with each transition step in each one of a color's three attributes. The change in appearance between a tonal step (lightness to darkness) is different from that seen in a saturation (strength of color) step. Similarly, a transition in hue appears different from one in tone or saturation. Without understanding the difference between these appearance transitions, it is difficult to locate one color in relation to others. The process is further complicated by the complex face-up appearance of diamonds. In our experience, by working consistently with known references (and, preferably, the same references), a grader can develop an understanding of the appearance relationships between them and consistently interpret the transition. Changing references may result in less consistency because the observer risks misinterpreting an attribute in the changed reference that is not the determining factor for a grade.

An interesting aspect of grading observation that occurs at the laboratory but is more common in the

marketplace is the occasional need to make a general assessment of a diamond's color while it is in a jewelry mounting. The appearance of yellow diamonds may be influenced by jewelry mountings to various degrees, as the color of the metal (especially yellow gold) can affect the apparent color of the diamond. It is important to keep this in mind when making color comparisons. At the laboratory, we follow our standard grading methodology when grading colored diamonds mounted in jewelry, but we assign a more generalized, multiple grade range for the diamond. Figure 26 shows a loose diamond that was near the Y-Z, Light yellow/Fancy Light yellow grade boundary before it was mounted (top) in an 18K gold ring (bottom). The color appearance of the diamond when mounted was well within the Fancy yellow range; depending on the cut, this effect can be more or less pronounced.

Figure 26. The color of most yellow diamonds may appear noticeably darker and stronger when set in a mounting. The diamond on the left in the top image is near the Y-Z, Light yellow/Fancy Light yellow boundary and is shown next to a Fancy yellow reference diamond. In the bottom image, the larger diamond is mounted in a ring and placed next to the same reference diamond. While the jewelry designer can use these effects to enhance the appearance of a yellow diamond, it is important that the observer be aware of this difference when evaluating the color of mounted diamonds. Courtesy of the Scarselli family; photos by Elizabeth Schrader.

SUMMARY AND CONCLUSIONS

Yellow diamonds occur in a wide range of tones and saturations, but the majority encountered in the industry fall into the saturation range represented by the grades Fancy Light, Fancy, Fancy Intense, and Fancy Vivid. Yellow diamonds occur in some of the highest levels of saturation we have seen in colored diamonds to date. The fact that they also occur in larger sizes than other colored diamonds offers greater versatility for the jewelry designer (figure 27). With clarity grades that are commonly "VS" or higher, the manufacturer is often able to cut to proportions that offer maximum weight yield and the most intensified face-up color appearance without requiring as many modifications for clarity characteristics as with other colors. An important manufacturing consideration with yellow diamonds is that the lighter tones are more readily affected by cutting decisions than darker, deeper colors. Brightness, windows, and extinction can affect the grade if the color is already near a grade boundary. Understanding the effect of jewelry mountings on the color is also important for the designer or laboratory/jewelry professional who needs to evaluate yellow diamonds when mounted.

Many of the routine manufacturing decisions used for colored diamonds today had their roots in the cutting innovations first seen with yellow diamonds in the 1970s (again, see box A). Early experiments with cut variations employed to hide inclusions were found to also intensify the face-up appearance of light yellow diamonds. Soon these techniques were applied to a broader tone and saturation range of yellow diamonds and, eventually, other colors.

While it is difficult to define groupings within type

Figure 27. Increasing numbers of yellow diamonds are appearing in haute couture jewelry, as seen in these Gypsy earrings and the Bull's Eye necklace. Composite photo courtesy of Graff Diamonds.

I yellow diamonds due to the many overlapping spectral features, we were able to establish five groups with distinct spectral characteristics. We have shown the spectral relationships between these representative groups within yellow type I diamonds and noted a general relationship of these groups to color appearance.

An important goal of this study was to provide a better understanding of the range of color appearances associated with yellow diamonds. Understanding this range will help the growing number of traders in yellow diamonds evaluate these diamonds properly.

REFERENCES

Anderson B.W. (1943a) Absorption and luminescence in diamond, Part I. *The Gemmologist*, Vol. 12, No. 138, pp. 21–22.

Anderson B.W. (1943b) Absorption and luminescence in diamond, Part II. *The Gemmologist*, Vol. 12, No. 139, pp. 25–27.

Anderson B.W. (1962) Lines and line systems in the fluorescence spectra of diamonds. *Journal of Gemmology*, Vol. 8, No. 5, pp. 193–202.

Anderson B.W. (1963) The classification of diamonds on the basis of their absorption and emission of light. *Journal of Gemmology*, Vol. 9, No. 2, pp. 44–54.

Anderson B.W., Payne C.J. (1956) The spectroscope and its applications to gemmology. *The Gemmologist*, Vol. 25, No. 300, pp. 115–119.

Balfour I. (1997) *Famous Diamonds*. Christie, Manson and Woods Ltd., London.

Balfour I. (2000) *Famous Diamonds*, 4th ed. Christie, Manson and Woods Ltd., London.

Bauer M. (1904) *Precious Stones*, translated by L.J. Spenser. Charles Griffin & Company Ltd., London.

Briddon P.R., Jones R. (1993) Theory of impurities in diamond. *Physica B*, Vol. 185, pp. 179–189.

Bursill L.A., Glaisher R.W. (1985) Aggregation and dissolution of small and extended defect structures in Type Ia diamond. *American Mineralogist*, Vol. 70, pp. 608–618.

Cassedanne J.P. (1989) Diamonds in Brazil. *Mineralogical Record*, Vol. 20, No. 5, pp. 325–336.

Clark C.D., Ditchburn R.W., Dyer H.B. (1956a) The absorption spectra of natural and irradiated diamonds. *Proceedings of the Royal Society*, Vol. A234, pp. 363–381.

Clark C.D., Ditchburn R.W., Dyer H.B. (1956b) The absorption spectra of irradiated diamonds after heat treatment. *Proceedings of the Royal Society*, Vol. A237, pp. 75–89.

Collins A.T. (1978) Investigating artificially colored diamonds. *Nature*, Vol. 273, No. 5664, pp. 654–655.

Collins A.T. (1980) Vacancy enhanced aggregation of nitrogen in diamond. *Journal of Physics C: Solid State Physics*, Vol. 13, pp. 2641–2650.

Collins A.T. (1982a) Colour centres in diamond. *Journal of Gemmology*, Vol. 18, No. 1, pp. 37–75.

Collins A.T. (1982b) A spectroscopic survey of naturally-occurring vacancy-related colour centres in diamond. *Journal of Physics D: Applied Physics*, Vol. 15, pp. 1431–1438.

Collins A.T. (1984) Pitfalls in color grading diamonds by machine. *Gems & Gemology*, Vol. 20, No. 1, pp. 14–21.

Collins A.T. (2001) The colour of diamond and how it may be changed. *Journal of Gemmology*, Vol. 27, No. 6, pp. 341–359.

Collins A.T., Davies G., Woods G.S. (1986) Spectroscopic studies of the H1b and H1c absorption lines in irradiated, annealed type-Ia diamonds. *Journal of Physics C: Solid State Physics*, Vol. 19, pp. 3933–3944.

Copeland L.L., Martin J.G.M. (1974) *Diamonds: Famous, Notable and Unique*, revised by R.A.P. Gaal and J. Taylor. Gemological Institute of America, Santa Monica, CA.

Crowningshield G.R. (1957–8) Spectroscopic recognition of yellow bombarded diamonds and bibliography of diamond treatment. *Gems & Gemology*, Vol. 9, No. 4, pp. 99–104, 117.

Crowningshield G.R. (1959) Highlights at the Gem Trade Lab in New York. *Gems & Gemology*, Vol. 9, No. 9, p. 269.

Crowningshield G.R. (1965) Developments and highlights at the Gem Trade Lab in New York: Clouds in natural-color brown diamonds. *Gems & Gemology*, Vol. 11, No. 9, pp. 269–270.

Crowningshield G.R. (1994) Gem Trade Lab Notes: Characteristic inclusions in fancy-color diamonds. *Gems & Gemology*, Vol. 30, No. 1, pp. 41–42.

Davies G. (1972) The effect of nitrogen impurity on the annealing of radiation damage in diamond. *Journal of Physics C: Solid State Physics*, Vol. 5, pp. 2534–2542.

Davies G. (1981) The origin of the "N2" absorption band in natural yellow diamonds. *Portugaliae Physica*, Vol. 13, No. 1–2, pp. 241–261.

Davies G. (1994) *Properties and Growth of Diamond*. Institution of Electrical Engineers, London.

Davies G., Summersgill I. (1973) Nitrogen dependent optical properties of diamond. *Diamond Research 1973*, pp. 6–15.

Davies G., Welbourn C.M., Loubser J.H.N. (1978) Optical and electron paramagnetic effects in yellow Type Ia diamonds. *Diamond Research 1978*, pp. 23–30.

De Weerdt F., Van Royen J. (2001) Defects in coloured natural diamonds. *Diamond and Related Materials*, Vol. 10, pp. 474–479.

Dyer H.B., Matthews I.G. (1957) The fluorescence of diamond. *Proceedings of the Royal Society*, Vol. A243, pp. 320–335.

Dyer H.B., Raal F.A., Du Preez L., Loubser J.H.N. (1965) Optical absorption features associated with paramagnetic nitrogen in diamond. *Philosophical Magazine*, Vol. 11, No. 112, pp. 763–773.

Field J.E. (1992) *The Properties of Natural and Synthetic Diamonds*. Academic Press, London.

Fisher D., Spits R.A. (2000) Spectroscopic evidence of GE POL HPHT-treated natural type IIa diamonds. *Gems & Gemology*, Vol. 36, No. 1, pp. 42–49.

Fritsch E. (1998) The nature of color in diamonds. In G. Harlow, Ed., *The Nature of Diamonds*, Cambridge University Press, Cambridge, UK.

Fritsch E., Scarratt K. (1992) Natural-color nonconductive gray-to-blue diamonds. *Gems & Gemology*, Vol. 28, No. 1, pp. 35–42.

GIA Diamond Dictionary (1993) Gemological Institute of America, Santa Monica, CA.

Gleason B. (1985) *Notable Diamonds of the World*. Diamond Promotion Service, New York.

Harris J.W., Hawthorne J.B., Oosterveld M.M. (1979) Regional and local variations in the characteristics of diamonds from southern Africa kimberlites. In F.R. Boyd and H.O.A. Meyer, Eds., *Kimberlite, Diatremes and Diamonds: Their Geology, Petrology, and Geochemistry*, Vol. 1, Proceedings of the Second International Kimberlite Conference, American Geophysical Union, Washington. D.C., pp. 27–41.

Haske M.D. (2000) Yellow diamonds. *The Guide*, Vol. 19, Issue 5, Part 1, pp. 8–10.

Hofer S.C. (1998) *Collecting and Classifying Coloured Diamonds—An Illustrated History of the Aurora Collection*. Ashland Press, New York.

Janse A.J.A. (1995) A history of diamond sources in Africa: Part 1. *Gems & Gemology*, Vol. 31, No. 4, pp. 228–255.

Kaminsky F.V., Khachatryan G.K. (2001) Characteristics of nitrogen and other impurities in diamond, as revealed by infrared absorption data. *The Canadian Mineralogist*, Vol. 39, pp. 1733–1745.

Kerr W.C. (1982) A report on the new Watermeyer split-facet diamond cuts. *Gems & Gemology*, Vol. 18, No. 3, pp. 154–159.

Kiflawi I., Bruley J., Luyten W., VanTendeloo G. (1998) "Natural" and "man-made" platelets in type Ia diamonds. *Philosophical Magazine B*, Vol. 78, No. 3, pp. 299–314.

King J.M., Moses T.M., Shigley J.E., Liu Y. (1994) Color grading of colored diamonds at the GIA Gem Trade Laboratory. *Gems & Gemology*, Vol. 30, No. 4, pp. 220–242.

King J.M., Moses T.M., Shigley J.E., Welbourn C.M., Lawson S.C., Cooper M. (1998) Characterizing natural-color type IIb blue diamonds. *Gems & Gemology*, Vol. 34, No. 4, pp. 246–268.

King J.M., Shigley J.E., Guhin S.S., Gelb T.H., Hall M. (2002) Characterization and grading of natural-color pink diamonds. *Gems & Gemology*, Vol. 38, No. 2, pp. 128–147.

King J.M., Shigley J.E. (2003) An important exhibit of seven rare gem diamonds. *Gems & Gemology*, Vol. 39, No. 2, pp. 136–143.

Koivula J.I. (2000) *MicroWorld of Diamonds: A Visual Reference*. Gemworld International, Northbrook, Illinois, 157 pp.

Liddicoat R.T. (1976) Developments and Highlights at GIA's Lab in Santa Monica: A true canary. *Gems & Gemology*, Vol. 15, No. 8, p. 235.

Mani A. (1944) The fluorescence and absorption spectrum of diamond in the visible region. *Proceedings of the Indian Academy of Sciences*, Vol. A19, pp. 231–252, plates 8–13.

Mawe J. (1813) *A Treatise on Diamonds and Precious Stones*. Longman, Hurst, Rees, Orme and Brown, London.

Meyer H.O.A. (1987) Inclusions in diamond. In P.H. Nixon, Ed., *Mantle Xenoliths*, New York, John Wiley and Sons, pp. 501–523.

Mita Y. (1996) Change of absorption spectra in type Ib diamond with heavy neutron irradiation. *Physical Review B*, Vol. 53, No. 17, pp. 11360–11364.

National Bureau of Standards (1976) *Color: Universal Language and Dictionary of Names*. NBS Special Publication 440, S.D. Catalog No. C13.10:440, U.S. Government Printing Office, Washington D.C.

Nayar P.G.N. (1941) The luminescence, absorption and scattering of light in diamonds: Part III. Absorption. *Proceedings of the Indian Academy of Sciences*, Vol. A14, pp. 1–17, plates 1–3.

Overton T.W. (2002) Legal protection for proprietary diamond cuts. *Gems & Gemology*, Vol. 38, No. 4, pp. 310–325.

Robertson R., Fox J.J., Martin A.E. (1934) Two types of diamond. *Philosophical Transactions of the Royal Society of London*, Vol. A232, pp. 463–535.

Sato K., Sunagawa I. (1982) Quantitative evaluation of colour of diamonds by spectrophotometric method. *Journal of the Gemmological Society of Japan*, Vol. 9, No. 4, pp. 3–17 [in English; pp. 87–101 in Japanese].

Scarratt K. (1979) Investigating the visible spectra of coloured diamonds. *Journal of Gemmology*, Vol. 16, No. 7, pp. 433–447.

Scarratt K. (1982) The identification of artificial coloration in diamond. *Gems & Gemology*, Vol. 18, No. 2, pp. 72–78.

Tavernier J-B. (1676) *Travels in India*. Translated by V. Ball, W. Crooke, Ed., republished in 1977 by Oriental Books Reprint Corp., New Delhi, India.

Vendrell-Saz M., Nogués-Carulla J.M., Mones-Roberdeau L., Bosch-Figueroa J.M. (1980) Transmission et absorption des diamantes taillés de la série "cape." *Revue de Gemmologie a.f.g.*, Vol. 64, pp. 20–24.

Wade F.B. (1920) A few words on fancy colored diamonds. *The Jeweler's Circular*, Vol. 80, No. 1, pp. 187–189.

Wang W., Mayerson W. (2002) Symmetrical clouds in diamond: The hydrogen connection. *Journal of Gemmology*, Vol. 28, No. 3, pp. 143–152.

Wilks J., Wilks E. (1994) *Properties and Applications of Diamond*. Butterworth Heinemann Ltd., Oxford, UK.
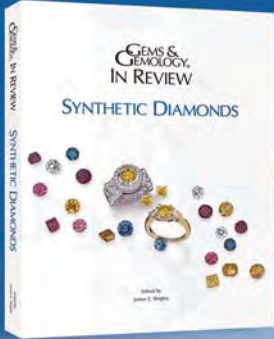
Woods G.S. (1984) Infrared absorption studies of the annealing of irradiated diamonds. *Philosophical Magazine B*, Vol. 50, pp. 673–688.

Woods G.S., Collins A.T. (1982) The 1450 cm^{-1} infrared absorption in annealed, electron-irradiated type Ia diamonds. *Journal of Physics C: Solid State Physics*, Vol. 15, pp. L949–L952.

Woods G.S., Collins A.T. (1986) New developments in spectroscopic methods for detecting artificially coloured diamonds. *Journal of Gemmology*, Vol. 20, No. 2, pp. 75–82.

Zaitsev A.M. (2001) *Optical Properties of Diamond: A Data Handbook*. Springer Verlag, Berlin.

Emeralds from the Kafubu Area, Zambia

J. C. (Hanco) Zwaan, Antonín V. Seifert, Stanislav Vrána, Brendan M. Laurs, Björn Anckar, William B. (Skip) Simmons, Alexander U. Falster, Wim J. Lustenhouwer, Sam Muhlmeister, John I. Koivula, and Héja Garcia-Guillerminet

Zambia is considered the world's second most important source of emeralds by value (after Colombia). The deposits are located near the Kafubu River in the Ndola Rural Restricted Area. Emeralds have been known from this region since 1928, but significant commercial production began only in the 1970s. As of mid-2004, most of the emeralds were being mined 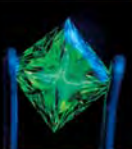from large open-pit operations at the Kagem, Grizzly, and Chantete concessions. Economic emerald mineralization is confined almost entirely to phlogopite reaction zones adjacent to Be-bearing quartz-tourmaline veins that metasomatically altered Cr-bearing metabasite host rocks. Nearly all of the rough is cut in India and Israel. Zambian emeralds have relatively high R.I. and S.G. values, with inclusions typically consisting of partially healed fissures, as well as actinolite, phlogopite, dravite, fluorapatite, magnetite, and hematite. They contain moderate amounts of Cr, Mg, and Na, moderate-to-high Fe contents, and relatively high Cs and Li. Although many features of Zambian emeralds are comparable to those from other commercially important localities, in many cases they may be separated by a combination of their physical properties, microscopic characteristics, and chemical composition.

Zambia is one of the world's most significant sources of fine-quality emerald and has been called the second most important producer by value after Colombia (see, e.g., Suwa, 1994; Giuliani et al., 1998). For years, the mines in the Kafubu area (near the Kafubu River in the Ndola Rural Restricted Area) have produced emeralds of uniform color and size, which supported the cutting of vast quantities of calibrated goods. In addition, relatively large, fine stones are occasionally found (see, e.g., figure 1).

Several articles have been published on Zambian emeralds, especially the geology of the Kafubu area, physical properties, and inclusions (see, e.g., Koivula, 1982; Graziani et al., 1983; Milisenda et al., 1999; Seifert et al., 2004c). The present article provides an overview on various aspects of these emeralds, and includes updated information on the geology of the area, mining and production, and gemological properties. Much of the historic and geologic information was obtained during several months of fieldwork in 2001 by two of the authors (AVS and SV), who studied all the major Zambian emerald deposits and several minor ones (Seifert et al., 2004b,c). In July-August 2004, these authors also examined a new emerald area in the Musakashi area of north-central Zambia (see box A). Other authors (JCZ in 1995 and BA since 2002) have visited the deposits, and in September 2004 BA collaborated with authors JCZ, BML, and WBS on visits to four mines (Chantete, Grizzly, Pirala, and Twampane). Subsequently, JCZ visited Ramat Gan, Israel, to learn more about the production and distribution of Zambian emeralds.

Figure 1. Zambia has been an important source of emeralds since the 1980s. Much of the production is polished into beads, such as those in these strands (maximum bead diameter is 16.2 mm). Relatively large, fine-quality Zambian emeralds also are faceted, such as the center stone (10.42 ct) in this ring. Courtesy of Pioneer Gems, New York; photo © Harold & Erica Van Pelt.

HISTORY

According to Sliwa and Nguluwe (1984), beryl mineralization was first discovered in the Kafubu area (at a locality that later became known as the Miku mine) in 1928 by geologists working for the Rhodesia Congo Border Concession Co. Although initial investigations did not reveal good-quality gems, Rhokana Co. and Rio Tinto Mineral Search of Africa continued small-scale exploration work into the 1940s and '50s. In 1966, the claim was passed to Miku Enterprises Ltd., and in 1971 the rights to the Miku area were taken over by Mindeco Ltd., a government-owned company. The region was subsequently mapped and the Miku deposit verified by Zambia's Geological Survey Department (Hickman 1972, 1973).

During the 1970s, when local miners discovered several more deposits, the Kafubu area became a major producer of good-quality emeralds. Due to the significant economic potential and extensive illegal mining, the government established a restricted zone and forcibly removed the population of this sparsely inhabited area.

In 1980, a new government-controlled agency, the Reserved Minerals Corp., took over the major deposits and prospecting rights to the surrounding region (Sliwa and Nguluwe, 1984). Kagem Mining Ltd. (owned 55% by Reserved Minerals and 45% by Hagura, an Indian-Israeli corporation) was authorized to conduct exploration and mining in the Kafubu area. A privatization agreement was signed between Hagura and the Government of Zambia in May 2001,

and the transfer of shares recently was completed by the government (Govind Gupta, pers. comm., 2005).

Outside the Kagem properties, which lie on the north side of the Kafubu River, the emerald area has been subdivided into nearly 500 prospecting plots. However, many of these claims were established without the benefit of a thorough geologic evaluation. Small-scale mining currently takes place on dozens of claims, whereas mechanized activity is mostly concentrated on the Kagem, Grizzly, Chantete, and Kamakanga properties.

LOCATION AND ACCESS

The emerald mines are located in the Kafubu area (also known as the Ndola Rural Restricted Area) of central Zambia, about 45 km southwest of the town of Kitwe (figure 2). This region lies in the southern part of an important copper mining area known as the Copperbelt (Coats et al., 2001). The emerald deposits are distributed over ~200 km^2 within 13°02′–13°11′S latitude and 28°03′–28°11′E longitude, on both sides of the Kafubu River.

From Kitwe, the Kafubu area is accessed by a 15 km paved road to Kalulushi, and then by 30 km of poorly maintained gravel road. The principal mining localities are reached by several dirt tracks, most of which remain passable throughout the year.

The Kafubu River, a western tributary of the Kafue River, drains the area together with small perennial streams. Except for the quartzite ridges in the southeast, there are no prominent topographic

Figure 2. The Kafubu emerald mines are located in north-central Zambia, 45 km southwest of Kitwe, the nearest town. A relatively new emerald occurrence was discovered in the Musakashi area to the northwest of Kafubu in 2002.

features and the entire area is typically flat. The average altitude is around 1,200 m above sea level. Over much of the area, the residual clay-rich soils are yellow-brown or reddish brown with extensive crusts of laterite, and support relatively thick vegetation. Access to the area is restricted, although the workers' settlements are located near the producing mines.

GEOLOGY

Regional Geology. The region encompassing the Zambian Copperbelt and the Kafubu area comprises a complex assemblage of geologic units (figure 3) that evolved during three successive orogenies of mostly Proterozoic age (i.e., mountain-building events ranging from about 2 billion to 500 million years ago [My]). The emerald deposits are hosted by metamorphic rocks of the Muva Supergroup (Daly and Unrug, 1983) that overlay the basement granite gneisses along a structural unconformity. The Muva rocks consist of quartzites, mica schists, and metabasites. Emerald mineralization is hosted by the metabasites, which consist of talc-chlorite-actinolite ± magnetite schists (Hickman 1973; Sliwa and Nguluwe, 1984). These schists are thought to represent metamorphosed volcanic rocks that were dominated by komatiites (i.e., highly magnesian ultramafic rocks; Seifert et al., 2004c). Their high chromium content provides a necessary component for emerald mineralization.

In the Kafubu area, thick layers (up to 200 m) of the metabasite are intercalated in the mica schist–quartzite sequence. Deposition of the Muva Supergroup is dated to ~1,700 My. Subsequent folding and metamorphism, which also involved the basement granite gneisses, took place during the Irumide orogeny (~1,010 My; De Waele et al., 2002). Importantly, with the exception of the Kafubu area, the metabasites are unknown in other portions of the 1,000-km-long Irumide belt of northeastern Zambia (see, e.g., Daly and Unrug, 1983; De Waele and Mapani, 2002).

The basement granite gneisses and the Muva Supergroup were later buried under sediments of the Katanga Supergroup during the Neoproterozoic era (i.e., 570–900 My). The entire crustal domain then underwent folding, thrusting, and metamorphism during the Pan-African orogeny, culminating at ~530 My (John et al., 2004). This tectonic event produced the most observable deformation and metamorphic features in the Muva rocks of the Kafubu area (Hickman, 1973).

1 Mitondo	8 Akala	15 Kagem Dabwisa
2 Gerntina	9 Ebenezer	16 Kagem Fibolele
3 Kamakanga	10 Mbuwa	17 Chantete
4 Miku	11 Kagem D8	18 Pioneer
5 Twampane	12 Kagem Fwaya-Fwaya	19 Solid Rock
6 Pirala	13 Kagem Fwaya-Fwaya Ext. F10	
7 Grizzly	14 Kagem Libwente	

Muva Supergroup (Mesoproterozoic)
- Metabasite
- Quartzite
- Quartz-mica schist

- Katanga Supergroup (Neoproterozoic)
- Basement granite gneiss (Paleoproterozoic)
- Kafubu pegmatite field
- Fault
- Mine

Figure 3. This simplified geologic sketch map of the Kafubu emerald area, modified after Hickman (1973) and Sliwa and Nguluwe (1984), shows the distribution of major rock types and the main emerald deposits in the area. The extent of the Kafubu pegmatite field is based on field observations of mining pits visited by two of the authors (AVS and SV).

During late stages of the Pan-African orogeny, rare-element pegmatites and some beryllium-rich granites intruded various crustal units in central, eastern, and possibly also northwestern parts of Zambia (see, e.g., Cosi et al., 1992; Parkin, 2000). In the Kafubu area, field studies at numerous mines and exploration pits indicate the existence of a major field of beryllium-bearing pegmatites and

Box A: Emerald from the Musakashi area, North-Western Province, Zambia

By Antonín V. Seifert, Stanislav Vrána, Björn Anckar, and Jaroslav Hyrsl

Figure A-1. The abandoned open-pit Hope mine in the Musakashi area reportedly was a source of emeralds. Photo by A. V. Seifert.

Figure A-2. This emerald fragment (8 × 6 mm) from the Musakashi area shows good color and transparent areas between fractures. Photo by V. Žáček.

A minor emerald "rush" occurred in 2002 at Chief Mujimanzovu's village in the Musakashi area, Solwezi district, central Zambia. In August 2002, one of the authors (BA) saw some high-quality emeralds with some Senegalese dealers in Kitwe. The color of these emeralds was significantly different from those of the Kafubu area, showing an intense bluish green reminiscent of emeralds from Muzo, Colombia. A field visit to their reported source was arranged with a Senegalese dealer, but the miners refused to grant access due to fierce disputes over the property. Visits to nearby outcrops and artisanal workings (mined for rock crystal quartz) showed the presence of abundant hydrothermal veins in the area. The European Union's Mining Sector Diversification Programme subsequently sponsored the Geological Survey Department of Zambia to map and explore the area, with field work undertaken in June 2004. By this time, it was reported that there was very little activity and the locals thought the deposit was mined out (Ng'uni and Mwamba, 2004). No in-situ emeralds were found, but small emerald fragments were recovered from eluvial lateritic soil adjacent to quartz veins at two mines (Hope and Musakashi) in the Chief Mujimanzovu village area.

When two of the authors (AVS and SV) visited the Musakashi area in July-August 2004, the pits were inactive (see, e.g., figure A-1), and data on the production and quality of the emeralds proved elusive to obtain. Nevertheless, a few emerald fragments were obtained for gemological examination and chemical analyses (see, e.g., figure A-2).

The gemological properties of three irregular polished emerald fragments (up to 6 mm in maximum dimension) were obtained by one of us (JH) using standard instruments and techniques. Refractive indices measured on two of the samples were 1.580–1.587, yielding a birefringence of 0.007. The specific gravity could not be measured accurately, due to abundant fissures in available stones. The dichroism was blue-green and yellow-green. The samples were inert to UV radiation. They had a typical chromium-type absorption spectrum and appeared red with the Chelsea filter. The most interesting characteristic was the presence in all the stones of three-phase inclusions, consisting of a bubble and a cube-shaped crystal in a liquid (figure A-3), almost identical to those commonly seen in Colombian emeralds. Note that these inclusions were very tiny—up to 0.1 mm but usually much smaller.

Mineral inclusions in these samples were examined by AVS and SV, and identified by electron microprobe. They consisted of minute crystals of sphene (titanite),
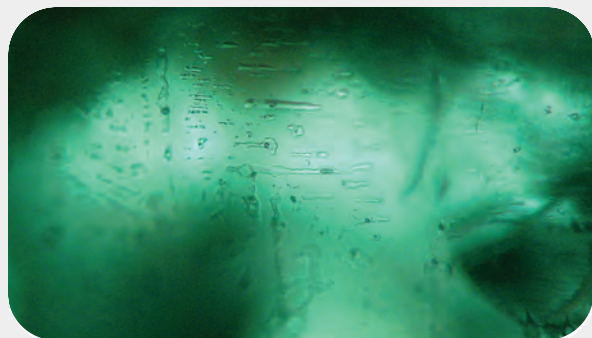
Figure A-3. All three samples of emerald from the Musakashi area contained minute three-phase inclusions that consisted of a bubble and a cube-shaped crystal that were suspended within liquid. Photomicrograph by J. Hyrsl; width of view is 0.5 mm.

Fe-oxides, Na-K feldspar, and quartz, with zeolite aggregates occurring along fissures. In comparison, the Kafubu emeralds typically contain phlogopite, actinolite, and apatite. The difference in mineral inclusions is consistent with field relations that suggest the two emerald areas are geologically unrelated.

The chemical composition of the three Musakashi samples is compared to Kafubu emeralds in table A-1. The Musakashi analyses show significantly higher Cr and V than those from Kafubu. By comparison, they also contain higher Cr and lower Mg than representative analyses of dark green emeralds from Colombia.

Although none of the authors are aware of any faceted emeralds from the Musakashi area, there appears to be potential for the production of facetable material.

TABLE A-1. Representative electron-microprobe analyses of Zambian emeralds from the Musakashi and Kafubu areas, with comparison to Colombian emeralds.

	Kafubu	Musakashi			Colombia[a]	
Oxides (wt.%)						
SiO_2	61.9–65.4	66.58	66.24	66.58	64.93	64.89
TiO_2	bdl	bdl	0.01	0.01	<0.02	0.03
Al_2O_3	12.5–17.9	15.90	15.70	15.64	15.60	18.10
Cr_2O_3	bdl–0.84	1.31	1.45	1.36	0.68	0.28
V_2O_3	bdl–0.08	0.48	0.47	0.55	1.87	0.12
FeO^{tot}	0.06–1.75	0.23	0.27	0.31	0.05	0.39
MnO	bdl–0.01	bdl	0.03	0.01	<0.02	0.05
MgO	0.27–2.90	0.73	0.72	0.72	1.27	1.24
CaO	bdl–0.12	0.02	bdl	0.01	<0.01	0.01
Na_2O	0.16–1.99	0.65	0.62	0.66	0.68	1.12
K_2O	bdl–0.27	0.03	0.02	bdl	<0.10	0.07

[a] *Representative dark green emeralds from La Pita (left column; Fritsch et al., 2002) and Somondoco (right column; Kozlowski et al., 1988). Abbreviation: bdl = below detection limit.*

hydrothermal veins that is nearly 20 km long. This field overlaps major horizons of metabasites that are enriched in chromium, resulting in emerald mineralization over a large area (again, see figure 3). Potassium-argon dating of muscovite from a pegmatite and an associated quartz-tourmaline vein gave cooling ages of 447–452 My (Seifert et al., 2004c). This corresponds to the approximate time of emerald mineralization, when the rocks cooled below 350 ± 50°C (which is the approximate temperature at which muscovite becomes "closed" to argon loss; see Viana et al., 2003).

Local Geology. Emerald miners in the Kafubu area use a local geologic vernacular that is summarized in the *G&G* Data Depository (www.gia.edu/gemsandgemology). Knowledge of this terminology is critical to understanding their observations of the geology and emerald mineralization. The emerald mineralization is directly related to the metasomatic alteration of the Cr-bearing metabasites by Be-bearing fluids derived from hydrothermal veins (see, e.g., Coats et al., 2001; Seifert et al., 2004c). For the most part, economic quantities of emerald are restricted to the phlogopite reaction zones (typically 0.5–3 m wide) between quartz-tourmaline veins and metabasite. These reaction zones locally contain aggregates of emerald (figure 4), of which a minor proportion is gem quality. Only rarely are good stones found in the quartz-tourmaline veins, or very exceptionally in less altered, partially phlogopitized host rocks (e.g., at the Grizzly mine).

Localized phlogopite reaction zones in the metabasites also were caused by emplacement of simple quartz-feldspar pegmatites, which are typically 2–10 m thick and steeply dipping. Field observations by two of the authors (AVS and SV) indicate that these pegmatites were emplaced shortly after the quartz-tourmaline veins. Since fluids from the pegmatite system contained some Be, minor emerald mineralization occurs locally in the phlogopite alteration zones associated with these pegmatites, too. The best emerald mineralization is found in phlogopite schist near intersections between the quartz-tourmaline veins and the pegmatites—particularly at the intersection between steeply dipping pegmatites and flat-lying veins.

The abundance of quartz-tourmaline veins with associated phlogopite reaction zones in the

Figure 4. Emerald aggregates are locally found in phlogopite schist, as shown in this specimen from Kagem's Fibolele mine. Only a small portion of the emeralds found in these aggregates are gem quality. Photo by V. Žáček.

Kafubu area suggests a "regional" influx of hydrothermal fluids containing Si, B, K, F, and other elements (Seifert et al., 2004c). The Be-bearing fluids that altered the metabasites, causing emerald mineralization, are most likely related to a hidden granitic source. Information from a fluid inclusion study (Seifert et al., 2004c) is consistent with the results of the regional geology described above, which indicates emerald mineralization occurred at temperatures of 360–390°C and pressures of 400–450 MPa.

EXPLORATION

About 2% of the Kafubu area is currently being mined (i.e., 5 km^2), and exploration activities are limited mostly to the immediate surroundings of known deposits. The nearly omnipresent cover of residual soil (2–10 m thick) is a serious obstacle to prospecting.

Exploration methods range from witchcraft and gut feel to the use of advanced geophysical methods, core drilling, and geologic mapping. Kagem has several highly qualified geologists who methodically monitor exploration and mining activities. Smaller companies rely on local consultants who provide geologic interpretation and basic geophysical surveying (described below). Local miners, many of whom have decades of experience working the area, also are an important resource. These miners (locally called "sniffers") are experts at locating emeralds through careful field observations (e.g., quartz-rich soil uplifted in tree roots).

The target ore geology at Kafubu is favorable for magnetic surveying. This rather simple geophysical technique has been used in the area for years, and remains the main tool for emerald prospecting. A magnetic survey measures variations in the earth's magnetic field intensity over an area of interest (see, e.g., Cook, 1997). Ferromagnetic minerals and their contrasting proportions in the earth's crust produce magnetic anomalies that can help define the underlying geology of the target area. However, the expression of magnetic anomalies is highly dependent on the surrounding geology. For example, low-magnetic sedimentary rocks together with high-magnetic igneous or metamorphic rocks will typically result in distinct anomaly patterns. In the Kafubu area, the host metabasites are usually the only rocks with high contents of magnetite, which is the primary mineral causing magnetic-high readings. The metabasites are contained within generally low-magnetic quartz-muscovite schists, so the surveys usually produce easily interpreted anomaly patterns.

In addition to magnetic surveying, radiometry (see Cook, 1997) is often used at Kafubu. With this method, a gamma ray spectrometer measures U, Th, and K anomalies to distinguish different rocks on the basis of their mineralogy; it may also reveal geologic contacts and major fault structures. However, the penetration depth of this technique is very shallow, so only surface or very near-surface anomalies can be detected. Nevertheless, this technique has successfully revealed underlying pegmatites and hydrothermal veins in the Kafubu area. Combinations of magnetic highs and radiometric highs indicate a very favorable geologic setting, and such geophysical anomalies are tested by digging pits to verify the presumed occurrence of metabasites and hydrothermal veins. When favorable conditions are encountered, local geologic indicators may point toward areas with high potential for emerald mineralization.

Geochemical soil and rock sampling has been attempted in the area but has not been done systematically. The samples have been analyzed for Ni, Cr, Co, and similar elements to look for metabasites, as well as for Be, Rb, Cs, and Li as pathfinders for pegmatites and hydrothermal veins.

Although expensive and time consuming, oriented drilling exploration programs may reveal important new emerald accumulations. For example, an extensive drilling survey at a grid spacing of 25 m—carried out in the southern continuation of Kagem pit D8 in 2003—intersected a new and very promising emerald-

Figure 5. The Grizzly mine employs large earth-moving equipment in a highly mechanized operation. The excavators used in the Kafubu emerald mines typically weigh 25–30 tons and have a bucket capacity of approximately 1.6 m³. Photo by B. M. Laurs.

bearing zone at a depth of 75 m. A similar survey in 2002 revealed additional emerald mineralization in the southeastern continuation of the Fwaya-Fwaya Ext. F10 mine (J. G. Dey, pers. comm., 2003).

So far, emerald mineralization has been mined to a maximum depth of 50–60 m (e.g., at the deepest Grizzly, Kamakanga, and Kagem mines). However, structural and lithologic criteria suggest that mineralization continues to deeper levels. Field surveys and laboratory analyses (Seifert et al., 2004c), as well as a study of the structural geology (Tembo et al., 2000), have demonstrated that the potential for substantial reserves and new emerald occurrences in the Kafubu area remains very high.

MINING

The Kafubu mining area (or Ndola Rural Restricted Area) has been subdivided into several hundred small concessions at around 100 hectares each. Most of these concessions are located in areas with unpromising geology. However, many others are in favorable areas, and a few of these have been amalgamated into larger entities such as the one operated by Kagem. The current license system has many disadvantages ("Zambia cranks up…," 2004), as these 100-hectare concessions are too small to support the investment needed to start financially viable operations, but there is no system in place to have such licenses relinquished and offered to capable mining companies. Furthermore, the area is rife with disputes and lengthy court cases that delay promising operations.

As of August 2004, the main emerald mining activities took place at the Kagem, Grizzly, and Chantete concessions. At Kagem, which at 46 km² is by far the largest license area, producing mines include Fwaya-Fwaya Ext. F10, Fwaya-Fwaya, Fibolele, D8, and Dabwisa. The Grizzly mine recently expanded its operations by acquiring licenses to additional concessions and investing in new machinery. The Chantete mine is also an active producer with modern equipment. Other producers include the Kamakanga, Twampane, and Akala mines, with sporadic production from the Pirala, Miku, Ebenezer, and Mitondo mines.

In June 2004, United Kingdom–based Gemfields Resources Plc started systematic exploration at its Plots 11A-1 and 11A-2 adjacent to the Pirala mine. The company is now undertaking a full feasibility study after having carried out drilling, ore body modeling, and bulk sampling. The initial results are promising, and the company expects to be in full operation by late 2005.

All the Kafubu emerald deposits are worked by open-pit mining. Because of abundant water during the rainy season (November to March), underground work is not considered an option; the groundwater level is too high for sinking shafts, as it would be too expensive to pump water continuously. Only one operator, at the Mitondo mine, has tried underground mining, but they recently ceased these activities.

Mining is done by removing the overburden rock with bulldozers, excavators, and large dump trucks (see, e.g., figure 5). At all the big pits, the miners drill

Figure 6. At the Grizzly mine, workers drill holes that will be filled with explosives to open up the area adjacent to an emerald-bearing zone. Photo by B. M. Laurs.

a series of holes (figure 6), so that explosives can be used to open the areas adjacent to the veins. Once emerald-bearing schist is exposed, mining is done manually with hammer and chisel, by so-called "chiselers." The recovered emeralds are put into cloth sacks or deposited into padlocked metal boxes. Security is a major problem during the manual extraction phase. The emerald-bearing zones must be heavily guarded at night to prevent access by the numerous illegal miners who become active after sunset. It is also not uncommon for a chiseler to cover a newly discovered emerald concentration for later nighttime excavation.

Standard washing/screening plants are used to process the ore at some of the mines. A new processing plant at the Grizzly mine was recently put into operation, with a capacity of 20 tons per hour. After crushing, the ore is washed and sized, with larger and smaller pieces separated in a rotating trommel. Additional vibrating screens further separate the material into specific size ranges for hand sorting on slow-moving conveyor belts. At Kagem, the operators rent the equipment used at the washing and sorting plant to keep costs down.

The smaller operations do not use washing plants due to a lack of funding and/or security. For instance, at the Chantete mine, 24-hour-a-day shifts keep the emerald-bearing rock moving, and all the emeralds are sorted by hand. This is done throughout the year, except during the rainy season when the pit fills with water.

Although it is expected that the Kafubu area will be able to supply a large quantity of emeralds over the next 20 years (A. Eshed, pers. comm., 2005), there is growing concern about the expenses involved in extracting them. For instance, at present the cost of running the Kagem mines is estimated to be around US$10,000 per day. The output is always uncertain; due to the irregular distribution of the emerald mineralization, it is extremely difficult to estimate reserves realistically, which makes emerald mining a high-risk business.

ENVIRONMENTAL IMPACT

A detailed study of the environmental impact of the emerald mines was performed by Seifert et al. (2004b). The mining activities affect the landscape and natural media—water, soil, rocks, and air—as well as human health. Fortunately, there are no enriched heavy metals or toxic elements in the Kafubu area.

Various environmental interactions and impacts are associated with each phase of a mine's lifespan

Figure 7. This 40 g emerald crystal fragment from the Chantete mine is illuminated from behind to show its transparency and attractive color. Photo by H. Zwaan.

Figure 8. This prismatic single crystal of emerald (slightly more than 8 cm long) was recovered from the Chantete mine. Photo by Dirk van der Marel, © Naturalis, the Netherlands.

sist throughout the year.

PRODUCTION AND DISTRIBUTION

Description of the Rough. The information in this section was derived from communications with the mine owners and from the personal experience of the authors. Much of the emerald rough is recovered as fragments that show only a few crystal faces (e.g., figure 7), but well-formed hexagonal crystals are sometimes produced (figure 8). Typically, though, these are broken segments that rarely have natural flat (pinacoidal) terminations. Also seen are emerald clusters or aggregates (figure 9), which may show well-formed crystals with perfectly developed terminations, as well as hexagonal prisms with irregular terminations. The aggregates may contain several to dozens of individuals within the host schist. Step-growth crystal surfaces are frequently present, caused by abrupt changes in diameter. The surface quality of the crystal faces is often rough, but it may be glassy smooth.

The color of the emerald crystals ranges from light bluish green to dark green. Very pale green or blue (rarely colorless) beryl also is found. As with emeralds from other localities, color zoning is common. Larger crystals typically have a core that is light yellowish green to greenish blue surrounded

Figure 9. This cluster of well-formed emerald crystals was found at the contact of a quartz vein with phlogopite schist at the Chantete mine. The width of this specimen is 9 cm. Photo by Dirk van der Marel, © Naturalis, the Netherlands.

(i.e., prospecting, exploration, mine development, mining, and closure). The most serious impacts include deforestation and vegetation removal, land degradation, increased soil erosion and siltation of watercourses, habitat loss (resulting in a reduction of biodiversity), and dangerous sites (e.g., pit walls). The amount of mined material from the entire Kafubu area that must be disposed of or stockpiled is roughly estimated at approximately 25,000 tonnes per day at current levels of activity, with a total of 70 million tonnes displaced since the 1970s.

The dozens of abandoned mines in the area do not always have negative consequences. They are filled by seasonal rainwater, and previously dry bush can benefit from the presence of a reservoir by creating new wetland ecological systems that per-

by a deep green rim; other crystals may show both a core and rim that are deep green, with internal zones of light and/or medium green.

The crystals typically range from less than 1 mm to several centimeters long, with pieces exceeding 10 cm encountered occasionally. The largest crystal observed by the authors was about 14 cm long and weighed over 3 kg (see, e.g., figure 25 inset in Laurs, 2004). According to a local mine manager, exceptionally large emerald crystals up to 60 cm long were found in the phlogopite schist at the Kamakanga Old Pit during the 1980s.

Production of the Rough. Emerald mineralization is very irregular, with the crystals often aggregated together (figure 4). These local concentrations may have grades of several kilograms of emerald per ton of ore rock. More typical is a dispersed mineralization of a few grams per ton of ore.

Run-of-mine (ROM) emerald typically yields only a small percentage of material that can be faceted. Most of it is of bead to cabochon quality. According to information supplied by T. Schultz (pers. comm., 2005) and Milisenda et al. (1999), a typical 10 kg of ROM emerald from a favorable deposit would yield about 5 g of extra-fine material, about 100 g of fine material, about 300 g of good material (in terms of both color and clarity), about 600–800 g of material with good color but included, about 3,000 g of low-quality material, and the remaining 6–7 kg of very low commercial value.

At Kagem, an average production of 300 kg (including low-grade emerald and beryl) every 2–3 months contains 10% facetable and cab-quality emeralds, with the remainder usable for beads and carvings. Typically, the emeralds occur as crystals up to 60 g each, but occasionally crystals as large as 1 to 3 kg are found. However, these large specimens usually contain only 1–2% cuttable material (A. Eshed, pers. comm., 2005). In terms of quality, F10 is currently the best-producing Kagem mine, with better (higher clarity) crystals than the former top producer, Fwaya-Fwaya (I. Eliezri, pers. comm., 2005). The Fibolele and D8 mines generally produce "medium-quality" stones—that is, good colors, but included, both facetable and cab quality. The Dabwisa mine mainly produces cabochon material, some of which is referred to as "metallic green" (caused by "rusty" looking inclusions; A. Eshed, pers. comm., 2005).

The Grizzly mine produces a quantity similar to that from the Kagem mines but generally bigger

pieces (often 50 g to 1 kg), although most are of "medium quality." Large crystals also are found. Production at the Chantete mine is typically 150–300 kg per month, and large crystals are produced occasionally there as well. Only about 10% is suitable for cutting, and just 1% is facet grade (see, e.g., figure 7). Stones from this mine tend to be somewhat lighter in color than those from elsewhere in the Kafubu area.

Production of rough reportedly exceeded US$100 million in the late 1980s (Milisenda et al., 1999). More recently, the value of emerald production from the Kafubu area was reported to be about US$20 million annually—according to 2002 statistics from the Export Board of Zambia for the officially declared export value of rough emerald. A conservative estimate is that at least another US$5 million worth of rough is smuggled out of Zambia (Douglas Ng'andu, DN Consulting Associates Ltd., Kitwe, pers. comm., 2005), although some sources (mainly the Zambian media) place the number much higher. However, it is difficult to imagine where such large quantities of emerald would originate, given that there are only two large operators and the presence of secret "bonanza" mines is not realistic.

Distribution of the Rough. Most of Zambia's emeralds are exported to India, mainly for use in that country's domestic market, and to Israel for international distribution. According to D. Tank (pers. comm., 2005), India receives 80% of Zambia's emerald production by weight, and 70–75% by value, with the cutting done in Jaipur. Israeli buyers usually purchase the higher-quality material.

The larger mining operators have well-established trading arrangements. For example, Kagem offers their production four times a year at a closed-tender auction in Lusaka. The dates are flexible, depending on when sufficient material is available. The very small operators and illegal miners rely on local traders, who are mainly of West African origin (e.g., Senegal and Mali) and often supply them with food and other necessities in exchange for emeralds.

The Informal Local Market. Rough emeralds are frequently traded on the streets of Lusaka and Kitwe, usually as run-of-mine material sold by illegal miners. Occasionally, large top-quality emeralds also turn up on the informal street market.

Buyers who visit Zambia should be aware of various scams. Green glass (stolen from local traffic lights) is molded to simulate hexagonal emerald

crystals, and quartz crystals are colored by green marker pens. While these imitations are easy to identify, there also are more clever imitations such as pieces of Russian hydrothermal synthetic emerald that are carefully coated in clay and mica.

Production and Sorting of Cut Emeralds. Gemstar Ltd., based in Ramat Gan, is the largest manufacturer of Zambian emeralds for the international market; it consumes most of the higher-quality rough material. Gemstar produces 2,000–3,000 carats per month of cut emeralds, from approximately 15,000 carats of rough. As an example of how the company approaches the rough from a commercial viewpoint, the following case was demonstrated to the senior author: While evaluating a 312 ct piece of rough that was of very good quality, the manufacturer decided that, instead of cutting this piece into a few stones weighing 5–10 ct, he would aim for smaller stones of high clarity, because there is strong demand for such emeralds. In the preform phase, 105 carats were recovered from the piece of rough, from which 60 carats of faceted gems (0.50–5 ct) were produced—for a yield of only 20% of the original high-quality crystal. An example was also provided for medium-quality (i.e., more included) rough: Four pieces weighing a total 84 carats had a yield of 20% after preforming and only 10% after faceting (including very small stones with little commercial value). For cabochon-grade material, the recovery is sometimes not more than 7%.

As explained by Daniel Madmon, manager of Gemstar's cutting factory, the typical cutting procedure is outlined below:

Figure 11. The sawn pieces of emerald are evaluated by the Robogem machine to predict the maximum yield and preshape the rough. Photo courtesy of E. Eliezri.

1. Using a strong lamp, the cutter assesses how and where to trim the rough, and the sawing is done carefully by hand (figure 10).

2. The sawn pieces go to the office for evaluation, and the cutting style is chosen according to demand.

3. Next, the sawn pieces are sent to a computerized robot, called "Robogem" (figure 11). Manufactured by Sarin Technologies Ltd., this equipment uses the Sarin DiaExpert system (as described by Caspi, 1997) to measure each sawn piece and predict the best possible yield. The robot is then used to make the girdle of each stone.

4. Once returned to the factory, the emerald preforms are placed on a dop and faceted by hand (figure 12), rather than by machine, because a "soft touch" is needed for emeralds. First, the

Figure 10. At Gemstar, after a piece of rough has been assessed, it is typically sawn into several transparent pieces for faceting. Photo by H. Zwaan.
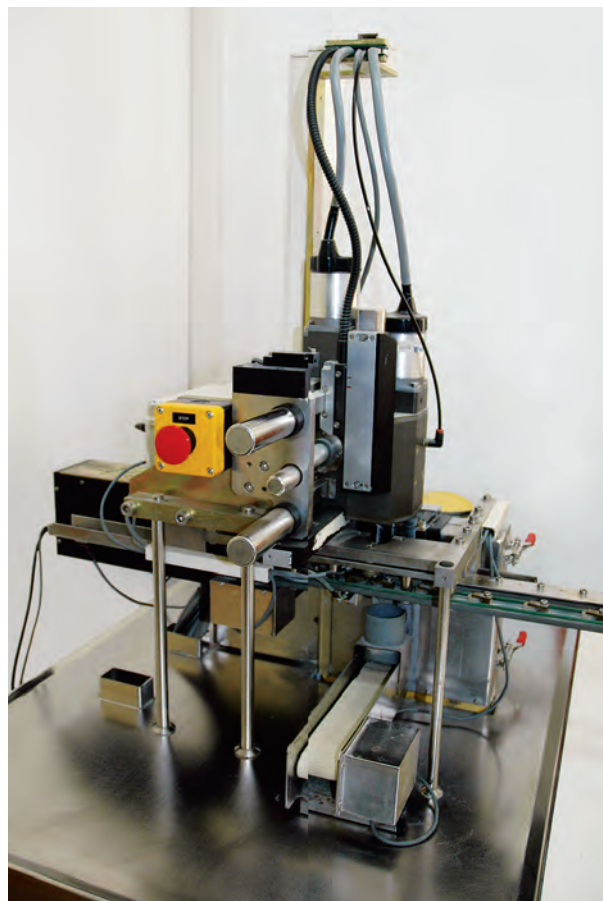
Figure 12. After they have been preshaped by Robogem, the emeralds are cut and polished by hand, using precise cutting and polishing wheels and equipment. Photo by H. Zwaan.

table and crown facets are cut and (with the girdle) polished.

5. The cutter then turns the stone on the dop and cuts/polishes the pavilion side. Taking an emerald cut as an example, the cutter places a maximum of three steps on the pavilion to get the best color, with more steps (up to four or five) used if greater sparkle is the goal.

Figure 13. At Gemstar, emeralds cut in calibrated sizes are sorted by color and clarity into numerous categories. Photo by H. Zwaan.
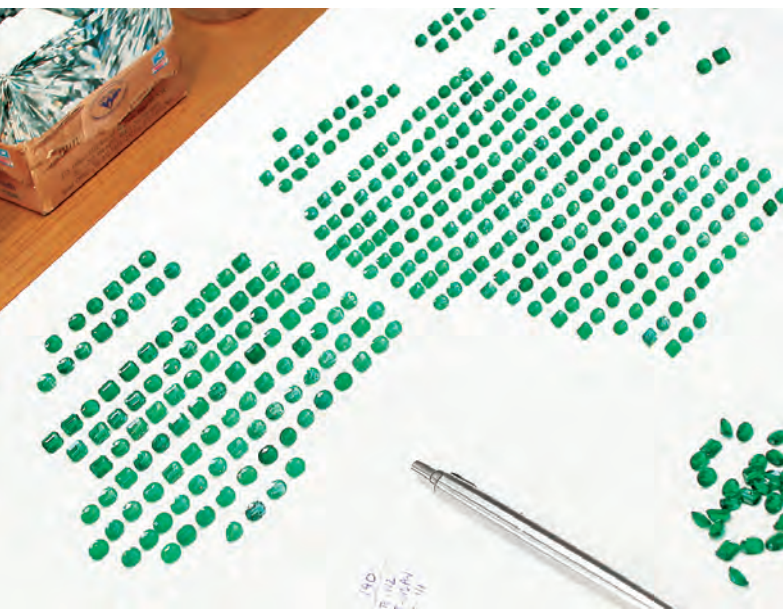
6. Once cutting and polishing is complete, the dop is gently iced so that the emerald can be easily removed. Subsequently, the finished gem is cleaned in an alcohol solution.

Each step of the cutting process is monitored by the master cutter, so that minor adjustments can be made when necessary. After polishing, stones with fissures are clarity enhanced by Gemstar using paraffin oil (i.e., mineral oil), a near-colorless transparent oil that the company has used for nearly 30 years. Gemstar declares at the time of sale that its emeralds are enhanced in this way. Resins like Opticon are never used.

Commercial production is done in calibrated sizes, such as 5 × 3, 6 × 4, 7 × 5, 8 × 6, and 10 × 8 mm. Typically, these are divided equally between emerald and oval cuts, although other shapes, such as hearts and pears, also are produced.

Next, the stones are sorted according to color and clarity into numerous categories (figure 13), based on master sets. Gemstar keeps an inventory of about 35,000 carats, so they can repeatedly produce the same colors, makes, and sizes. The steady availability of calibrated sizes of consistent quality is extremely important to customers, and the Zambian emerald is prized for such consistency (A. Eshed, pers. comm., 2005).

Commercial goods typically weigh up to 5 ct. Zambian emeralds over 10 ct are rare (again, see figure 1). During a visit to Ramat Gan, the senior author encountered a rare 14.29 ct medium-dark green stone (figure 14) that was only slightly included.

Consuming Countries. As mentioned before, most Zambian emeralds end up in India, where they are cut and distributed, mainly to the domestic market. In Israel, Gemstar Ltd. sells 70% of its stones to the U.S., 15% to the Far East, and roughly 15% to Europe. It is expected that in the future the growing markets will be in China, Russia, and eastern Europe.

MATERIALS AND METHODS

For this study, we examined a total of 127 emeralds (0.07–5.69 ct), of which 69 were faceted and 2 were cabochon cut. Almost all the 56 rough samples were transparent and suitable for faceting. At least two windows were polished on each rough sample; the resulting pieces ranged from 0.46 to 6.98 ct. The samples were obtained from several mines: 34 from

Figure 14. This exceptional Zambian emerald weighs 14.29 ct. It shows a deep "Zambian" bluish green color and is only slightly included. Courtesy of Gemstar Ltd.; photo by H. Zwaan.

Figure 15. The emeralds studied for this report represented a range of color, as evident in these samples from the Kagem mines (0.55–5.69 ct). Photo by Jeroen Goud, © Naturalis, the Netherlands.

the Chantete mine, 51 from the Kagem mines (specific pits not known), and one from the Kamakanga mine. In addition, a thin section was cut from a light bluish green emerald from the Mbuwa mine; this emerald, which was not of gem quality, was hosted by a quartz-tourmaline vein in phlogopitized metabasite. The other 40 samples were from unspecified mines in the Kafubu area.

All of the rough samples and 59 of the cut stones (see, e.g., figure 15) were examined at the Netherlands Gemmological Laboratory (NGL). Twelve faceted emeralds (0.22–4.28 ct) were examined at GIA in Carlsbad; these were cut from rough produced at the Chantete mine during the 2004 mining season (see, e.g., figure 16).

Standard gemological properties were obtained on all the emeralds. We used a GIA GEM Instruments Duplex II refractometer (at GIA) and a Rayner refractometer with an yttrium aluminum garnet prism (at NGL), both with near-sodium equivalent light sources, to measure the refractive indices and birefringence. Specific gravity was determined by the hydrostatic method. We tested the samples for fluorescence in a darkened room with four-watt long- and short-wave UV lamps. Absorption spectra of the stones examined at NGL were observed using a System Eickhorst Modul 5 spectroscope with a built-in light source. Internal features were observed with a standard gemological microscope; in some cases, a polarizing (Leica DMRP Research) microscope was used as well. In 29 samples, we analyzed inclusions with Raman spectroscopy using 514 nm laser excitation and two instruments: a Renishaw 2000 Ramascope (3 sam-

ples at GIA) and a Renishaw Invia (26 samples at the CCIP French Gemmological Laboratory in Paris). Polarized absorption spectra of 15 representative samples examined at NGL were taken with a Unicam UV540 spectrometer, in the range of 280–850 nm. Spectroscopy of the 12 samples studied at GIA was performed with a Hitachi U-4001 spectrophotometer (oriented UV-Vis spectra, range 280–850 nm) and a Nicolet Magna-IR 760 spectrometer (mid-IR spectra, 400–6000 cm^{-1}). Additional mid-IR spectra were taken of 12 representative samples at NGL using a Thermo Nicolet Nexus FT-IR-NIR spectrometer.

EDXRF spectroscopy was performed on the 12

Figure 16. Many Zambian emeralds are an attractive saturated medium bluish green, as evident in this selection from the Chantete mine (0.66–1.35 ct). Courtesy of Chantete Emerald Ltd.; photo © GIA and Jeff Scovil.

GIA samples with a Kevex Omicron instrument. The instrument was operated at a voltage of 15 kV without a filter for low-Z elements, with an aluminum filter at 20 kV for transition metals, and with an iron filter at 25 kV for heavier elements. An Eagle μProbe EDXRF spectrometer was used at NGL to analyze the composition of surface-reaching inclusions on the pavilions of 16 faceted samples. This instrument has a focus spot of 200 × 200 μm and a beam diameter of 300 μm. A voltage of 25 kV and a count time of 100 seconds were used for each measurement.

Quantitative chemical analyses were carried out on 27 selected emeralds from the Kagem and Chantete mines at two electron microprobe facilities—the Institute of Earth Sciences, Free University of Amsterdam, the Netherlands (JEOL model JXA-8800M) and the University of New Orleans, Louisiana (ARL SEMQ instrument). In Amsterdam, 78 spot analyses were performed on the table surfaces of 12 light to dark bluish green faceted emeralds from the Kagem mines and 3 polished fragments from the Chantete mine. Twenty analyses were done on surface-reaching inclusions. Analyses were performed at 15 kV, with a beam current of 25 nA and a spot size of 3 μm. The count time for the major elements was 25 seconds, and for the trace elements, 36 seconds (except 50 seconds were counted for V, Cr, F, and Rb). From two to 16 spots per sample were analyzed. In New Orleans, the tables of 12 faceted Chantete emeralds were analyzed at 15 kV, with a beam current of 15 nA and a spot size of 2 μm, and a count time of 45 seconds for each element. Three spots per

---

TABLE 1. Physical properties of emeralds from the Kafubu area, Zambia.[a]

Color	Colors range from light to dark green to slightly bluish to bluish green; typically a saturated bluish green with a medium to medium-dark tone
Clarity	Very slightly to heavily included
Refractive indices	n_o = 1.585–1.599; n_e = 1.578–1.591 n_o = 1.589–1.597; n_e = 1.581–1.589[b] n_o = 1.602; n_e = 1.592[c]
Birefringence	0.006–0.009 (0.008[b], 0.010[c])
Optic character	Uniaxial negative
Specific gravity	2.71–2.78 (except one 0.22 ct sample, which gave a value of 2.81) 2.69–2.77[b]
Pleochroism	Strong yellowish green (o-ray) and bluish green (e-ray); some stones showed strong greenish yellow (o-ray) and greenish blue (e-ray)
Fluorescence	Usually inert to long- and short-wave UV radiation; sometimes faint green to long-wave
Chelsea filter reaction	No reaction or light pink to red (deep green samples)
Absorption spectrum	Some absorption between 580 and 630 nm; distinct lines at approximately 636, 662, and 683 nm
Internal features	• "Feathers" in flat, curved, (rarely) conchoidal forms or undulatory/scalloped shapes • Partially healed fissures with various shapes of two- and three-phase fluid inclusions, but typically equant or rectangular • Isolated negative crystals containing CO_2 and CH_4 • Parallel oriented decrepitated inclusions appearing as silvery disks or brownish spots, depending on the lighting • Mineral inclusions (this study): randomly oriented actinolite needles, platelets of phlogopite or rare chlorite, equant to columnar dravite, fluorapatite, magnetite, hematite, chlorite, quartz, fluorite; carbonates (magnesite/siderite, ferroan dolomite, ankerite and calcite); niobian rutile, pyrite, talc, zircon, barite, albite, calcite, sphene (titanite), and beryl • Characteristic inclusions described by other authors: phlogopite/biotite, actinolite-tremolite, and square- and rectangular-shaped fluid inclusions (Milisenda et al., 1999); phlogopite, glauconite, talc, apatite, quartz, and Fe-Mn and Fe-Cr oxides (Moroz and Eliezri, 1999); apatite, quartz, chrysoberyl, margarite, muscovite, and rutile or brookite (Graziani et al., 1983); tourmaline, limonite, magnetite, mica, rutile, hematite, and apatite (Koivula, 1982; 1984), and also chrysotile (Gübelin and Koivula, 1986) • Cavities, representing dissolved columnar mineral inclusions • Either homogeneous color distribution or medium to strong color zoning may occur (as planar zones oriented parallel to the prism faces)

[a] All data are from the present study unless otherwise noted.
[b] Data from Milisenda et al. (1999), obtained from an unspecified number of samples that they described as representative. Other data on refractive indices, birefringence, and specific gravity, such as reported by Graziani et al. (1983) on a single sample, and the average values given by Campbell (1973) for Zambian emeralds, fall within the ranges that are indicated.
[c] Data from Schmetzer and Bank (1981) on one dark bluish green sample.

sample were analyzed.

In addition, three emerald fragments from the Musakashi area (box A) were analyzed using a Cameca SX 100 electron microprobe (15 kV, 40 nA) at Masaryk University, Brno, Czech Republic.

GEMOLOGICAL PROPERTIES

The gemological properties are summarized in table 1, with details described below.

Visual Appearance. The emeralds showed a wide variety of colors, ranging from green to slightly bluish green to bluish green with a light to dark tone (figure 15). Many were an attractive saturated bluish green with a medium to medium-dark tone (figure 16). Typically, the color was evenly distributed, although we saw strong color zoning in some crystals and polished material. Color zoning in the faceted stones was best seen from the side, when looking parallel to the table through the pavilion.

Physical Properties. Roughly 70% of the stones tested showed refractive indices of n_o = 1.591–1.595 and n_e = 1.583–1.587. Some light green stones showed values lower than 1.583, and some dark green stones had R.I.'s above 1.595. The birefringence of most of the emeralds ranged between 0.007 and 0.008. Only one stone had a birefringence of 0.006, and only two stones showed 0.009.

Specific gravity values ranged from 2.71 to 2.78. The majority of the stones (78%) had an S.G. between 2.72 and 2.76.

The emeralds were typically inert to long- and short-wave UV radiation, except for a few samples that fluoresced faint green to long-wave UV. All of the emeralds with more saturated colors appeared pink to red under the Chelsea filter; the other samples showed no reaction. Dichroism was strong, in yellowish green and bluish green; or even stronger, in greenish yellow and greenish blue. Most of the emeralds, even the light-colored stones, showed well-defined absorption spectra when viewed with the handheld spectroscope. The spectra showed some absorption between 580 and 630 nm, and distinct lines at approximately 636, 662, and 683 nm. The violet range (beyond 430 nm) was completely absorbed. A few light-colored emeralds showed a weaker spectrum with only a clear line at 683 nm.

Microscopic Characteristics. The stones were very slightly to heavily included. The most obvious clarity characteristics were fractures, partially healed fissures, fluid inclusions, needles, and occasional brown flakes.

Fractures and Fluid Inclusions. The most conspicuous inclusions consisted of "feathers" and partially healed fractures, which both exhibited wide variations in appearance. Feathers had flat, curved, or rarely conchoidal forms with mirror-like reflections, or undulatory/scalloped shapes with a white appearance caused by rough surfaces. Less commonly, the feathers were present in parallel formations or in tight clusters with no preferred orientation. One sample from Chantete contained larger fractures that locally showed blue "flash-effect" colors due to filling with a foreign organic substance.

Partially healed fractures were marked by planar groups of equant, elongated, wispy, or irregularly shaped fluid inclusions that often showed low relief and contained relatively small bubbles (figure 17), indicating that they are probably H_2O rich (e.g., Samson et al., 2003). Partially healed fractures also were represented by arrays of pinpoints that formed parallel lines (see, e.g., figure 18) or "fingerprints."
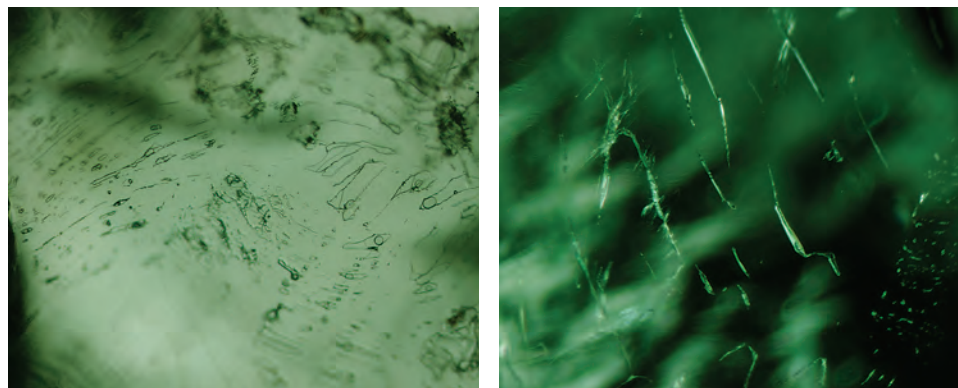

Figure 17. Irregularly shaped (left) and wispy (right) fluid inclusions, such as those present in these two emeralds from the Chantete mine, were widespread in the Zambian emerald samples. Photomicrographs by H. Zwaan; magnified 50× and 55×, respectively.
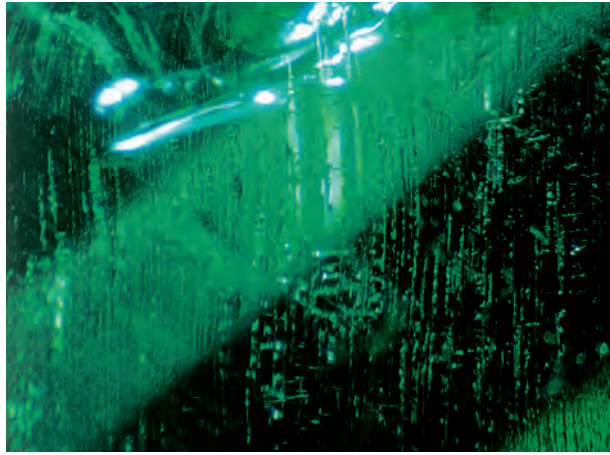
Figure 18. Parallel arrays of secondary fluid inclusions were relatively common in the Chantete emeralds, as were fractures of various sizes. Photomicrograph by J. I. Koivula; magnified 10×.
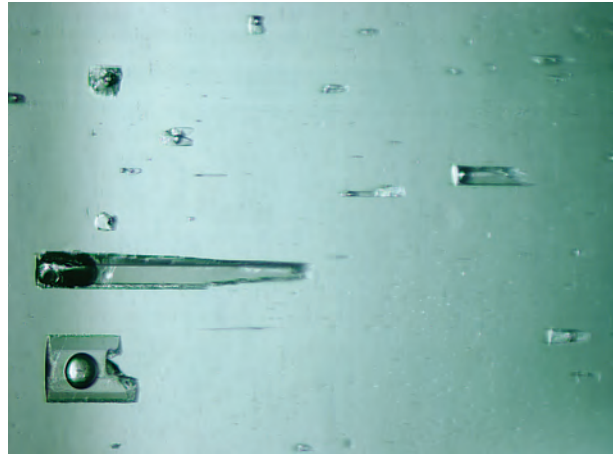

Figure 19. Rectangular pseudosecondary two-phase inclusions, typically present in healed fissures in many Zambian emeralds, mainly contain H_2O (liquid) and CO_2 (gas). Photomicrograph by H. Zwaan; magnified 100×.

Many of the Zambian emeralds had healed fissures consisting of pseudosecondary rectangular to square fluid inclusions (a hundred or more microns) that each contained a bubble (figure 19). These inclusions generally contained either two phases (liquid and gas, mainly H_2O [by inference] and CO_2 [identified by Raman analysis]) or three phases (liquid, gas, solid), which often looked like two-phase inclusions because the solids were only clearly visible with crossed polarizing filters (figure 20). The solids were tentatively identified by optical means as carbonates. In heavily included emeralds, the healed fissures were often accompanied by minute fluid inclusions, causing a milky translucency. Fluid-filled tubes oriented parallel to the c-axis were commonly seen in light-colored emeralds (figure 21), but they were rare in the saturated medium to dark green stones.

Compared to the abundant pseudosecondary fluid inclusions in healed fissures, primary inclusions were less common, and were not present in every stone. They formed isolated negative crystals with a roughly hexagonal outline and high relief in

transmitted light (figure 22). They appeared to be CO_2-rich, each with a large bubble occupying most of the available space. Raman analysis confirmed that these inclusions contained CO_2 as well as CH_4 (an example spectrum is in the *G&G* Data Depository). Other isolated, irregular-shaped primary three-phase fluid inclusions, containing an obvious solid phase, were very rare (figure 23).

Parallel planes of decrepitated inclusions, containing remnants of fluid, were observed in a number of stones. When viewed with oblique illumination, these features only showed up clearly in a specific orientation when the light was properly reflected; in transmitted light, they appeared as parallel faint brownish spots with a vague hexagonal outline (figure 24).

Mineral Inclusions. Mineral inclusions were common in the lower-clarity Zambian emeralds. Colorless needles with diamond-shaped cross sections were visible in many of the stones (figure 25) and were identified as actinolite in five of the sam-

Figure 20. Many rectangular three-phase inclusions look like two-phase inclusions (left), because the solid phase (carbonate) only became apparent when viewed with crossed polarizers (right). Photomicrographs by H. Zwaan; magnified 100×.
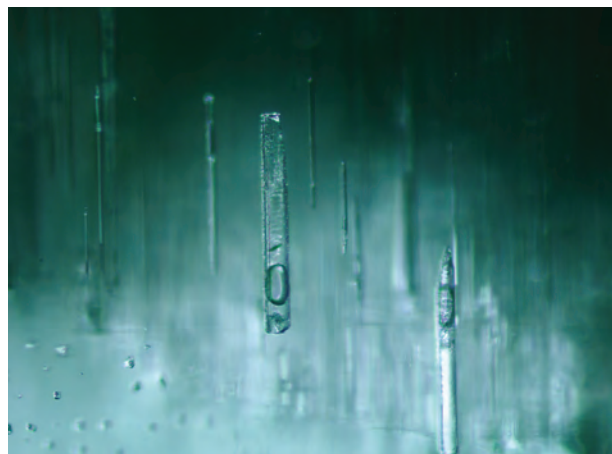
Figure 21. Parallel-oriented tubes commonly were present in the light-colored emeralds. In this particular sample, the tubes are seen only in the light green portion. Photomicrograph by H. Zwaan; magnified 100×.
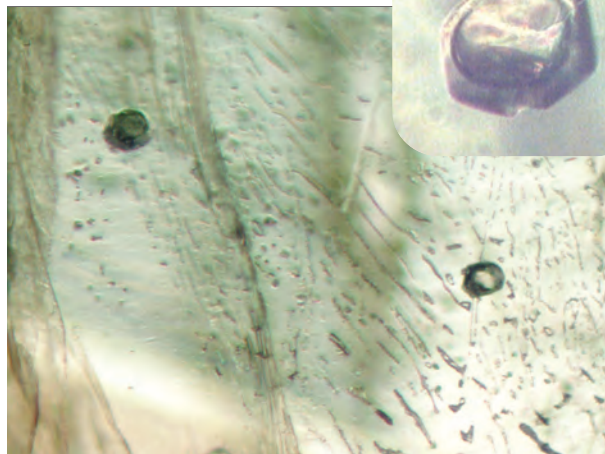

Figure 22. Primary inclusions appear as small isolated negative crystals in the Zambian emeralds, with high relief evident in transmitted light at 50× magnification. The "curtain" behind the two negative crystals is a partially healed fissure. Only under strong magnification could a large bubble be observed inside each cavity (see inset, magnified 250×). Photomicrographs by H. Zwaan.

ples by Raman analysis. Two microprobe analyses of a surface-reaching inclusion gave $Mg/(Mg + Fe^{2+})$ ratios of 0.77 and 0.78, indicating a Mg-rich actinolite (per the classification of Leake et al., 1997). This was similar to the composition of actinolite in the host metabasites (ratio of 0.78–0.86; Seifert et al., 2004c). Some of the actinolite needles were surrounded by material with a fuzzy appearance (probably microfractures; figure 26). The needles were typically straight, although a needle in one emerald from the Chantete mine was obviously curved.

Also common were pale to moderate brown platelets (figure 27) that provided Raman spectra consistent with biotite/phlogopite. Microprobe analyses of eight grains in four different emerald samples gave phlogopite compositions, which is in agreement with the compositions of micas in the altered metabasite host rock as documented by Seifert et al. (2004c) and with the composition of an inclusion in a "bluish green Zambian emerald" given by Moroz and Eliezri (1999). In a few stones that contained a fair amount of phlogopite, dark green mica also was found. One such inclusion (figure 28) was identified

as chlorite by Raman analysis.

Less abundant than actinolite or phlogopite were high-relief, dark brown to black, equant to columnar crystals (figures 25 and 29). These inclusions had a rounded triangular cross section that is typical of tourmaline. Raman spectra of two such inclusions were consistent with schorl-dravite tourmaline. A semiquantitative EDXRF analysis of the crystal in figure 29 revealed nearly twice as much MgO as FeO, and little Ca, identifying it as dravite. This is consistent with earlier studies of tourmaline from the Kafubu area by Koivula (1984) and Seifert et al. (2004c), who found Fe-rich or Ca-Fe rich dravites, with individual crystals showing significant compositional variations.

Apatite was identified by Raman analysis in four emeralds from the Kagem mining area. It usually formed colorless euhedral crystals (figure 30) or small colorless grains with irregular surfaces. One

Figure 23. This primary three-phase fluid inclusion was observed in a Chantete emerald. Rotating the microscope's polarizer showed the yellowish green (left) and greenish blue (right) dichroic colors of the emerald. Photomicrographs by J. I. Koivula; magnified 15×.
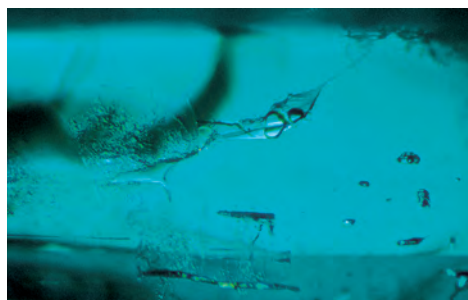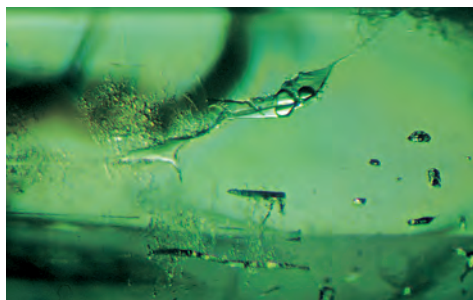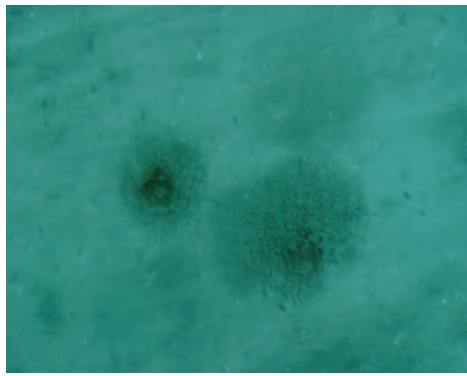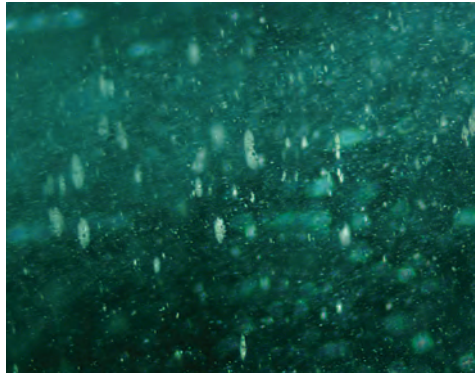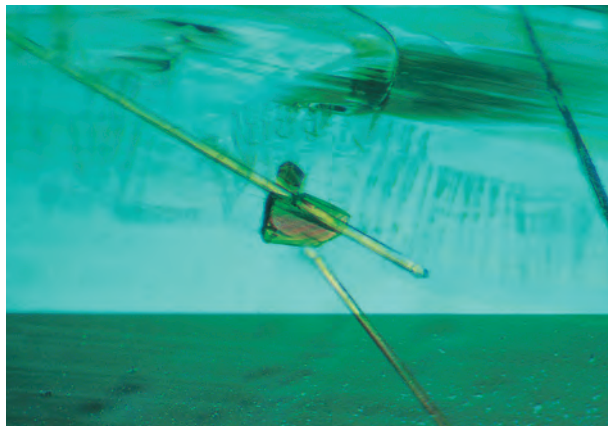
heavily included dark bluish green emerald contained numerous hexagonal prisms of apatite, with two crystals at the surface identified by microprobe analysis as fluorapatite. Interestingly, this tiny inclusion itself contained even smaller inclusions of actinolite and magnetite (figure 31). Minute opaque black "crumbs" and larger euhedral-to-anhedral opaque grains, which formed skeletal features in parallel planes (figure 32) and had a submetallic luster, were identified as magnetite by both Raman and microprobe analyses. In a few emeralds, brown-red inclusions with similar skeletal shapes were identified by Raman analysis as hematite (again, see figure 32). This suggests the presence of martite, a variety of hematite that is a pseudomorph after magnetite.

Cavities that appeared to represent casts of dissolved mineral inclusions with a euhedral columnar habit were seen in a few samples (figure 33).

Small, slightly rounded, euhedral transparent crystals were encountered in some emeralds. In most cases, they were too deep within the stone to be identified by Raman analysis. One sample showed many of these crystals, both isolated and in clusters. Some crystals had very low relief and were doubly refractive, whereas others had higher relief and were isotropic. At the surface, a few crystals of both types were identified by microprobe as quartz and fluorite, respectively (figure 34). In one sample, between a quartz and a fluorite crystal, three carbonates also were identified: a magnesite/siderite mixture, ferroan dolomite, and ankerite. Interestingly, these carbonates contained a fair amount of Cr (e.g., up to 1.34 wt.% Cr_2O_3 in the ankerite). A small beryl inclusion seen in association with these carbonates contained less Mg and Fe than the emerald host. Raman analysis confirmed the presence of additional carbonate inclusions in a few other stones.

Other rare inclusions identified in the Zambian

Figure 25. Colorless needles of actinolite in a Chantete emerald appear brownish yellow in this image taken between crossed polarizers. The dark grain between the two actinolite needles in the center of the image is probably tourmaline. A network of fractures also is present in this view. Photomicrograph by J. I. Koivula; magnified 13×.

Figure 26. A fuzzy-looking white "coating" of micro cracks and/or fluid inclusions hides the identity of the rod-shaped solid inclusion inside this Chantete emerald. Similar coatings were seen associated with the needles that were identified as actinolite in other samples. Photomicrograph by J. I. Koivula; magnified 15×.
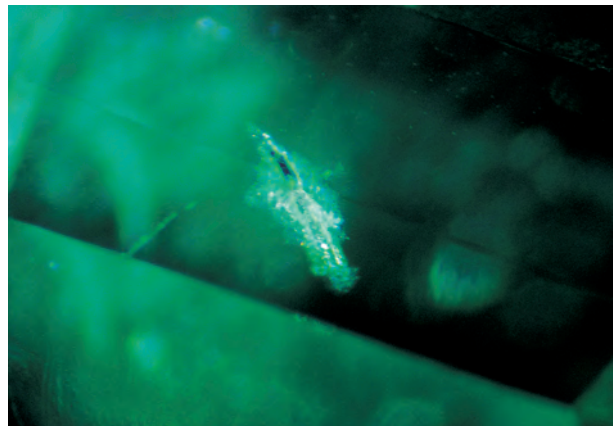
Figure 27. Platelets of phlogopite, as seen here in one of the Chantete emeralds, are quite common inclusions in Zambian emeralds. Photomicrograph by H. Zwaan; magnified 80×.
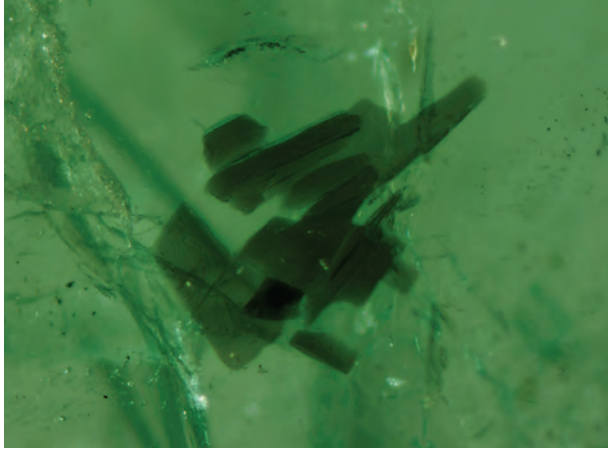

Figure 28. A few stones contained chlorite—like the crystal in the center here—as well as phlogopite. Photomicrograph by H. Zwaan; magnified 80×.

emeralds were pyrite and talc, present as fairly large crystals in one heavily included sample; very small grains of zircon, which were also observed in some phlogopite inclusions, where they had caused dark brown radiation halos; and minute grains of barite, albite, and calcite. In one cut emerald from the Kagem mining area, calcite was present in surface-reaching fractures. A small euhedral crystal of sphene (titanite) was found in one faceted emerald; its identity was confirmed by Raman analysis. All of

the other inclusions in this paragraph were identified by a combination of visual appearance and EDXRF spectroscopy, microprobe, or Raman analysis.

In the thin section of the Mbuwa mine emerald, some reddish orange inclusions were identified as niobian rutile (figure 35). Rutile inclusions in Zambian emerald have previously been described by various authors (e.g., Graziani et al., 1984; Gübelin and Koivula, 1986; Seifert et al., 2004c), but the reddish orange color in the thin section suggested the presence of Fe^{3+}, Nb, and/or Ta. Raman analysis showed a rutile spectrum with fundamental

Figure 29. Equant black-appearing crystals of dravite (Mg-bearing tourmaline) also were observed, as seen here in an emerald from the Kagem mining area; the crystal with the rounded triangular cross section shows the typical crystal habit of tourmaline. Most of the tourmaline crystals observed appeared to have grown where actinolite needles intersect. Photomicrograph by H. Zwaan; magnified 80×.

Figure 30. Large and small euhedral apatite crystals are seen in this emerald from the Kagem mining area. The apatite inclusions are transparent and show virtually no color. The size (1.0 mm long) of the large crystal is quite unusual; typically apatite seen in Zambian emerald is smaller, like the crystal near the bottom of this image, which is about 0.15 mm. Photomicrograph by H. Zwaan; magnified 80×.

vibrations at 442 and 616 cm^{-1}, and a qualitative EDXRF micro-analysis confirmed the abundance of Ti, with lesser amounts of Nb and Fe, and some Ta.

Growth Features. Widespread in the Chantete emeralds were parallel growth lines with a fine lamellar appearance (again, see figure 32). When observed between crossed polarizers, two samples showed strain that was oriented parallel to the growth lines; none of the other samples showed evidence of strain. In many of the samples, the color was evenly distributed. Others exhibited moderate to strong narrow zoning of straight, alternating light green to medium-dark green bands (figure 36), which was oriented parallel to the prism faces of the crystals (figure 37). When this color zoning was present in faceted stones, it was often well disguised by cutting the table of the emerald parallel to one of the prismatic faces, so that the color zoning could be observed only when looking at the stone from the side, through the pavilion. In some cuttable rough samples, hexagonal color zoning was prominent, often showing a darker green rim and a lighter or darker green core, with alternating lighter and darker green zones in between.

Figure 32. Magnetite in Kafubu emeralds occurs as tiny opaque inclusions, sometimes in parallel planes and showing skeletal shapes. The red-brown inclusions are hematite. Note also the fine-scale parallel growth lines traversing the image. Photomicrograph by H. Zwaan; magnified 65×.

CHEMICAL COMPOSITION

Representative electron-microprobe analyses of emeralds from the Chantete mine and Kagem mining area are shown in table 2 (see *G&G* Data Depository for all analyses). In total, we obtained 78 microprobe analyses of 15 Chantete samples, and 36 analyses of 12 Kagem emeralds. Data from both mining areas were quite similar, although slightly higher

Figure 31. This backscattered electron image shows a minute euhedral inclusion that was identified as fluorapatite by electron-microprobe analysis at the surface of a heavily included emerald. The fluorapatite itself contains small laths of actinolite (darker gray) and magnetite (white). Micrograph by W. J. Lustenhouwer.

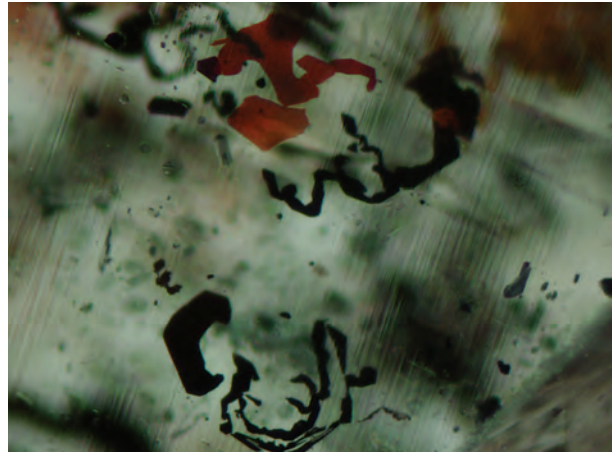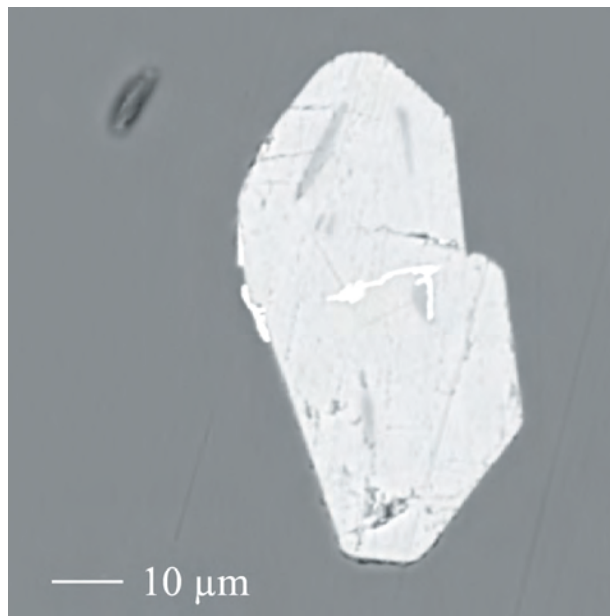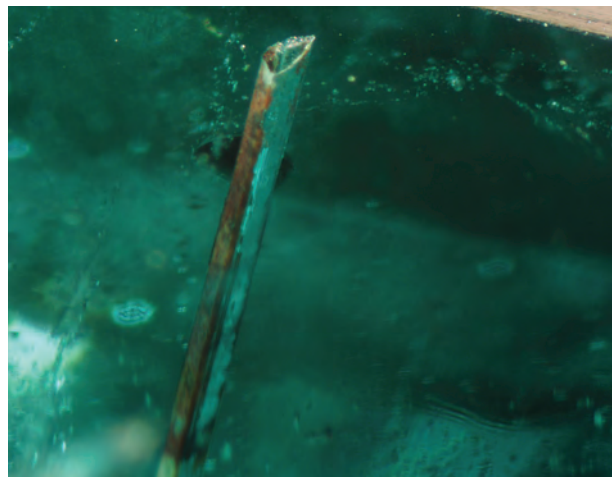*Figure 33. A few of the faceted Zambian emeralds contained large, open-ended, sharp-edged columnar cavities that have the appearance of dissolved actinolite inclusions. These cavities were partially filled with epigenetic debris. Photomicrograph by H. Zwaan; magnified 65×.*
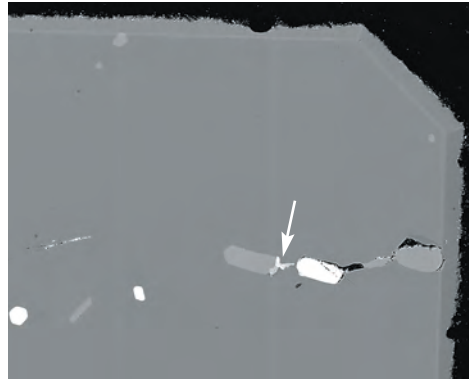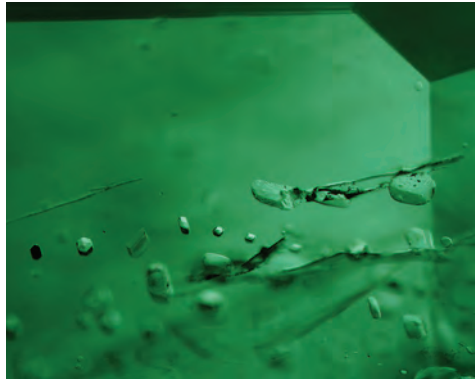
Figure 34. Inclusions showing low and higher relief (left) were identified as quartz and fluorite, respectively. (Photomicrograph by H. Zwaan; magnified 100×.) In the backscattered electron image on the right, the fluorite crystals appear white, while the quartz grains look gray. Carbonates (light gray, see arrow) also were present. Micrograph by W. J. Lustenhouwer; width of view 1.0 mm.

Cr and Fe concentrations were measured in the Kagem stones overall. In addition, the Kagem emeralds showed larger overall variations in the concentration of these elements, as well as in Mg and Na.

The Kagem emeralds were carefully selected to include the lightest to darkest colors seen in commercially available cut stones (see, e.g., figure 15). The color range of the faceted Chantete emeralds tested was more restricted to a typically desirable medium bluish green (see, e.g., figure 16), although considerable color variations were present in one of the rough gem-quality samples of Chantete emerald (again, see figure 37). The most important chromophore in Zambian emeralds is Cr, which averaged 0.26 wt.%—and ranged up to 0.84 wt.%—Cr_2O_3. Overall, the darkest green stones had significantly higher Cr contents than the lighter and medium green stones, which often showed no straightforward correlation between color intensity and average Cr content. In contrast, V concentrations

were consistently low, averaging just 0.02 wt.% V_2O_3 and attaining a maximum of 0.09 wt.% V_2O_3. The only other significant chromophoric element was Fe, which averaged 0.76 wt.% oxide (as FeO) and showed a maximum of 1.75 wt.% FeO.

The emeralds contained relatively high concentrations of Mg (average of 1.90 wt.% MgO) and somewhat less Na (average of 1.10 wt.% Na_2O). We detected trace amounts of Ca and K in many of the samples. In the 12 Chantete emeralds analyzed at the University of New Orleans, Ti and Mn were near or below the detection limits in all stones. In the 15 emeralds analyzed at the Free University of Amsterdam, traces of Cs were detected in most samples, Sc was documented in some of them, and Rb was below the detection limit in all the analyses.

Distinct compositional variations were recorded in analyses of fine-scale color zones in a rough emerald from the Chantete mine (again, see figures 37

Figure 35. Reddish orange inclusions of niobian rutile were identified in a thin section of an emerald from the Mbuwa mine. Photomicrograph by H. Zwaan; width of view 1.8 mm.
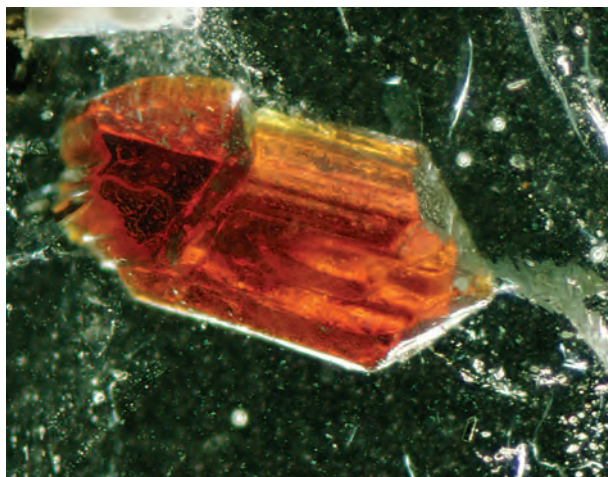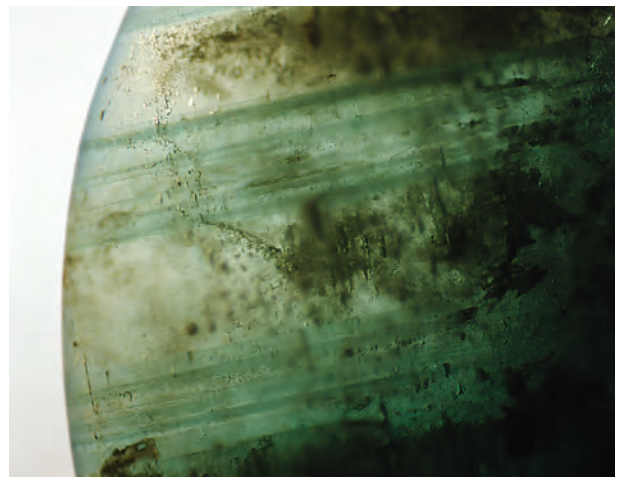

Figure 36. Although an even color appearance is very common in Zambian emeralds, straight narrow color zoning, as in this heavily included 5.69 ct cabochon, was also seen in certain orientations. Photomicrograph by H. Zwaan.
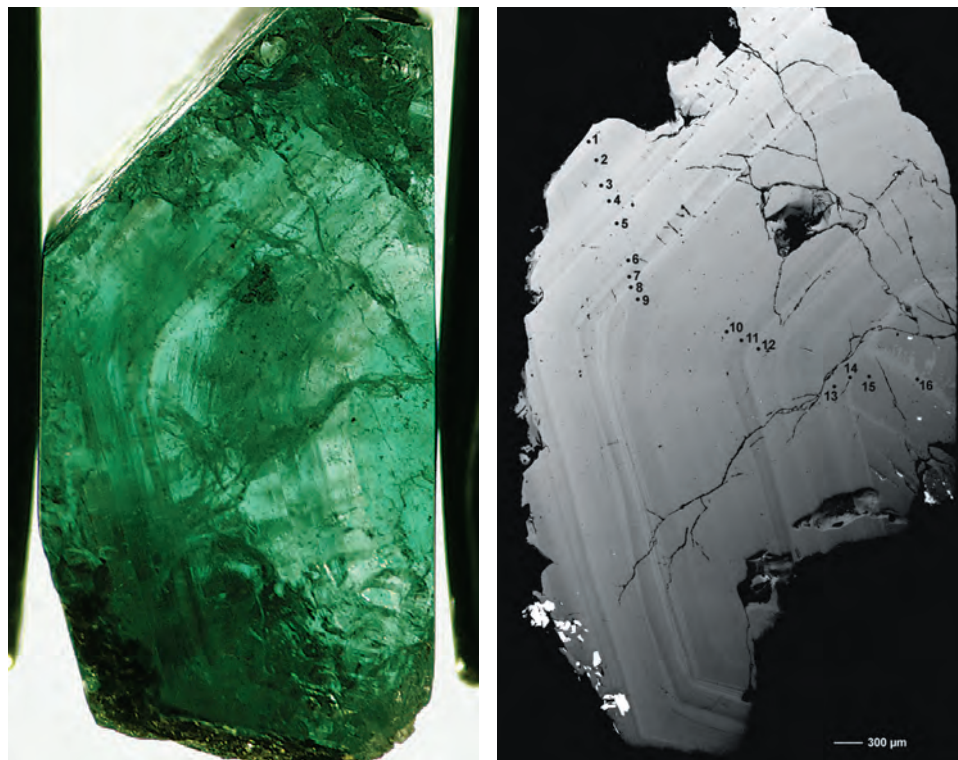
Figure 37. On the left, hexagonal color zoning was observed parallel to the prismatic crystal faces in this 4.93 ct cuttable emerald crystal from the Chantete mine (no. r29, table 2). (Photomicrograph by H. Zwaan; magnified 10×). The backscattered electron image of this same crystal, on the right, also reveals fine-scale growth zoning as well as the position of the spots that were analyzed by electron microprobe. The white-appearing grains are phlogopite. Composite micrograph by W. J. Lustenhouwer.

and 38). The Cr_2O_3 for this emerald ranged from not detectable in a narrow colorless zone to 0.46 wt.% in the darkest green zone, with an average of 0.22 wt.%. As shown in figure 38, there was a good correlation between color and Cr content. Compared to Cr, similar trends were shown by Fe, Mg, and Na, and an inverse pattern was found for Al. The Cs content, which ranged from 0.05 to 0.23 wt.% Cs_2O, was highest in the outer portion of the crystal.

In addition to the elements detected by electron microprobe, EDXRF analysis of the faceted Chantete emeralds found traces of Ga and Zn in separate emeralds, with Ga possibly present in an additional sample. This technique, which is more sensitive than the electron microprobe, detected Mg, K, Ca, Cr, Fe, Rb, and Cs in all 12 of the samples analyzed. V also was detected in five samples, and possibly in two others.

SPECTROSCOPY

Typical UV-Vis-NIR absorption spectra for Zambian emeralds are illustrated in figure 39. The ordinary ray ($E\perp c$) showed bands at 372, 440, 478, 610, 637, and 830, as well as a doublet at 680 and 683 nm. The bands at 440, 610, and 830 nm are broad and the positions were estimated. The extraordinary ray ($E\|c$) displayed bands at 425 and 650 nm, as well as absorptions at 632, 662, 684, and 830 nm.

Though the intensities varied, all the samples showed the same bands for both the ordinary and extraordinary rays. The bands at 440 and 610, and at 425 and 650 nm, and the peak at 684 nm, indicate the presence of Cr^{3+}, which causes the green color (Wood and Nassau, 1968; Schmetzer et al., 1974). Additional weaker peaks at 478, 662, 684, and the doublet at 680 and 683 nm also are caused by the presence of Cr^{3+}. The shift in absorption from 440 to 425 nm and from 610 to 650 nm causes an absorption minimum at about 512 nm for the ordinary ray, producing a yellowish green color, and a shift toward a minimum at about 500 nm for the extraordinary ray, producing a bluish green color. The band at 830 nm indicates the presence of Fe^{2+} (Platonov et al., 1978), whereas the peak at 372 nm denotes the presence of Fe^{3+} (Schmetzer et al., 1974). The exact Fe^{2+}/Fe^{3+} ratio cannot be determined by this method.

The FTIR spectra of the emeralds contained the typical features caused by vibration of H_2O molecules (see, e.g., figure 40). The most obvious peaks, at 7096 and 5265 cm^{-1}, are caused by type II H_2O molecules, which are present in the channels of the crystal structure of beryl. These water molecules are located adjacent to alkali-metal ions in the channels (Wood and Nassau, 1968), which in the Zambian emeralds are mainly Na^+, Cs^+, and Li^+. The H-H direction of the type II H_2O molecules is

TABLE 2. Representative chemical compositions of Zambian emeralds by electron microprobe.[a]												
	Chantete mine						Kagem mining area						
Sample	0.95-2	0.66-2	3.47-2	r29-7	r29-12	r29-5	z01r-1	z08b	z08d	z04c	z03c	z09c	z43a
Weight (ct)	0.95	0.66	3.47	4.93	4.93	4.93	0.55	0.91	0.91	0.66	1.04	0.89	0.98
Color[b]	Med. bG	Med. bG	Med. bG	Color- less	Med. bG	Int. med. bG	Lt. bG	Med. sl. bG	Med. sl. bG	Med. bG	Med. bG	Int. med. sl. bG	Dark bG
Laboratory	UNO[c]	UNO	UNO	FUA[d]	FUA	FUA	FUA	FUA	FUA	FUA	FUA	FUA	FUA
Oxides (wt.%)													
SiO_2	65.39	65.24	64.86	63.52	63.21	62.29	63.40	62.44	62.14	63.17	63.08	62.71	63.35
TiO_2	bdl	bdl	bdl	na	na	na	na	na	na	na	na	na	na
Al_2O_3	15.42	15.33	14.81	15.81	14.97	13.58	15.96	13.65	13.62	14.09	14.39	13.63	14.62
Cr_2O_3	0.08	0.20	0.63	bdl	0.25	0.46	0.25	0.04	0.29	0.15	0.31	0.33	0.70
V_2O_3	0.01	0.04	0.02	0.04	0.02	0.04	0.06	0.02	0.02	0.02	0.02	0.03	0.03
Sc_2O_3	na	na	na	bdl	0.01	0.03	0.03	bdl	bdl	bdl	bdl	bdl	bdl
BeO (calc.)	13.61	13.57	13.52	13.20	13.10	12.89	13.21	12.93	12.88	13.12	13.08	12.99	13.19
FeO^{tot}	0.37	0.34	0.90	0.58	0.72	1.31	0.36	1.11	1.05	1.10	0.96	0.93	1.01
MnO	bdl	bdl	0.01	na	na	na	na	na	na	na	na	na	na
MgO	2.39	2.22	2.47	1.48	1.84	2.36	1.26	2.77	2.68	2.45	2.11	2.90	1.81
CaO	bdl	bdl	bdl	0.02	0.02	0.02	0.03	0.03	0.06	0.06	0.05	0.07	0.04
Na_2O	1.46	1.71	1.36	0.76	0.74	0.98	1.04	0.99	0.94	1.49	1.15	0.86	1.45
K_2O	bdl	bdl	bdl	0.02	0.03	0.04	0.02	0.26	0.25	0.05	0.04	0.21	0.03
Rb_2O	na	na	na	bdl	bdl	bdl	bdl	bdl	bdl	bdl	bdl	bdl	bdl
Cs_2O	na	na	na	0.23	0.06	0.20	0.04	bdl	0.05	0.08	0.11	0.04	0.15
Total[e]	98.72	98.65	98.59	95.65	94.98	94.20	95.64	94.24	93.97	95.78	95.30	94.71	96.39
Ions based on 18 oxygens													
Si	6.001	6.000	5.990	6.010	6.026	6.035	5.996	6.031	6.024	6.013	6.021	6.027	5.997
Ti	bdl	bdl	bdl	na	na	na	na	na	na	na	na	na	na
Al	1.668	1.662	1.612	1.763	1.682	1.551	1.779	1.554	1.556	1.581	1.619	1.544	1.631
Cr	0.006	0.014	0.046	bdl	0.019	0.035	0.019	0.003	0.023	0.011	0.023	0.025	0.053
V	0.001	0.003	0.001	0.003	0.002	0.003	0.004	0.001	0.001	0.002	0.002	0.002	0.003
Sc	na	na	na	bdl	0.001	0.003	0.002	bdl	bdl	bdl	bdl	bdl	bdl
Be	3.001	2.999	3.000	3.000	3.000	3.000	3.000	3.000	3.000	3.000	3.000	3.000	3.000
Fe	0.028	0.026	0.070	0.046	0.057	0.106	0.028	0.090	0.085	0.087	0.076	0.075	0.080
Mn	bdl	bdl	0.001	na	na	na	na	na	na	na	na	na	na
Mg	0.327	0.304	0.340	0.208	0.262	0.340	0.178	0.398	0.387	0.347	0.300	0.415	0.256
Ca	bdl	bdl	bdl	0.002	0.002	0.002	0.003	0.003	0.006	0.006	0.005	0.007	0.004
Na	0.260	0.305	0.244	0.139	0.137	0.185	0.190	0.186	0.176	0.276	0.212	0.160	0.265
K	bdl	bdl	bdl	0.002	0.004	0.005	0.002	0.032	0.031	0.006	0.005	0.026	0.003
Rb	na	na	na	bdl	bdl	bdl	bdl	bdl	bdl	bdl	bdl	bdl	bdl
Cs	na	na	na	0.009	0.002	0.008	0.002	bdl	0.002	0.003	0.005	0.001	0.006

[a] BeO was calculated based on an assumed stoichiometry of 3 Be atoms per formula unit. Abbreviations: bdl = below detection limit, bG = bluish green, Int. = intense, Lt. = light, med. = medium, na = not analyzed, and sl = slightly.

[b] Refers to overall color appearance, except for sample r29, in which specific color zones that correspond to each analysis are listed for this gem-quality crystal (which had an overall color appearance of medium slightly bluish green). The relatively low values for Cr measured in some stones does not appear to correlate with their bluish green color. Since the electron microprobe is a microbeam technique, the particular points analyzed on each of those stones may not be representative of the bulk composition of those samples, particularly if color zoning is present.

[c] Analyses performed at the University of New Orleans, Louisiana. Background counts were determined by a mean atomic number (MAN) method (Donovan and Tingle, 1996). Analytical standards included both natural and synthetic materials: albite (Na), adularia (K), quartz and clinopyroxene (Mg, Ca, Fe, and Ti), chromite (Cr), rhodonite (Mn), V_2O_5 (V), PbO (Pb), ZnO (Zn), Bi-germanate (Bi), and sillimanite (Si and Al). MAN standards in addition to the above as appropriate: MgO, hematite, rutile, strontium sulfate, and ZrO_2. Detection limits (in wt.%): TiO_2 = 0.009, CaO = 0.008, MnO = 0.005, and K_2O = 0.012. Cl was analyzed but not detected.

[d] Analyses performed at the Free University of Amsterdam, the Netherlands. Analytical standards included both natural and synthetic materials: diopside (Si, Mg, and Ca), corundum (Al), fayalite (Fe), Sc_2O_3 (Sc), jadeite (Na), orthoclase (K), V_2O_5 (V), Cr_2O_3 (Cr), RbBr (Rb), Cs_2ReCl_6 (Cs), fluorite (F), and marialite (Cl). Detection limits (in wt.%): Cr_2O_3 = 0.018, Sc_2O_3 = 0.012, Cs_2O = 0.028, and Rb_2O = 0.029. Cl was analyzed but not detected. Low overall totals appear mainly due to low analytical SiO_2 data.

[e] Analyses do not include H_2O. Data on Kafubu emeralds from Hickman (1972) and Banerjee (1995) showed 2.5 wt.% H_2O, and 2.61 and 2.69 wt.% H_2O, respectively.

Figure 38. Electron-microprobe analyses of the Chantete emerald in figure 37 revealed systematic variations in the composition of the various growth zones. There was a good correlation between color and Cr content, with similar trends shown by Fe, Mg, and Na; the trends for all these elements were opposite that of Al. A significant increase in Cs was evident in the outer portion of the crystal.

perpendicular to the c-axis; the intensity of these peaks was very strong in all the spectra we obtained. Wood and Nassau (1967) demonstrated that their intensity increases as the amount of alkalis increases. The broad band between roughly 3900 and 3400 cm⁻¹ is caused by type I and type II H_2O molecules. Type I H_2O molecules are freely present in the channels, without being linked to other ions, and their H-H direction is parallel to the c-axis of the beryl crystal. The peak at 2357 cm⁻¹ is caused by CO_2. This peak was present in all the samples

for which spectra were taken, but the intensity varied between samples. Similar UV-Vis-NIR and FTIR spectra were described by Milisenda et al. (1999), and UV-Vis spectra of a light green emerald from the Miku mine were illustrated by Schmetzer and Bank (1981).

FTIR spectroscopy also is helpful to identify possible fillers used for clarity enhancement (see e.g., Johnson et al., 1999; Kiefert et al., 1999). None of the spectra we obtained indicated the presence of an artificial resin in any of the stones examined. Also, we did not observe any yellow or blue flash effects (a possible indication that an artificial resin might be present) in the fissures, except for an apparent local blue flash effect observed in one stone from the Chantete

Figure 39. These polarized absorption spectra of an emerald from the Chantete mine show bands that are representative of all the Kafubu samples, and indicate the presence of not only Cr^{3+} and Fe^{2+}, but also Fe^{3+}. The intensities of the bands varied somewhat between samples, but no straightforward relationship could be established between band intensities and Cr and Fe concentrations (or FeO/Cr_2O_3 ratios) measured by electron microprobe. The spectra shown here were collected on a 4.27 ct emerald cut that contained an average of 0.17 wt.% Cr_2O_3 and 0.36 wt.% FeO^{tot}.
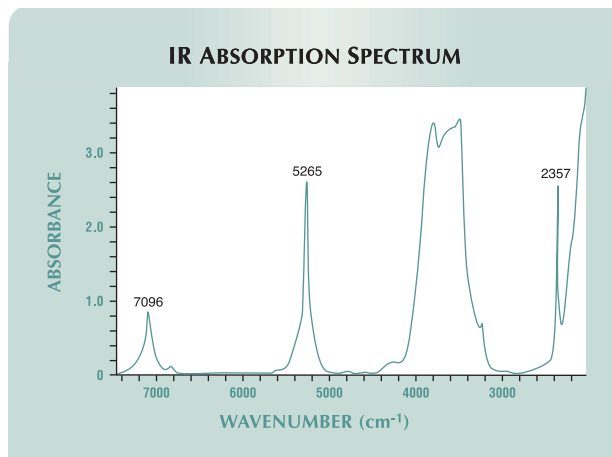
IR Absorption Spectrum
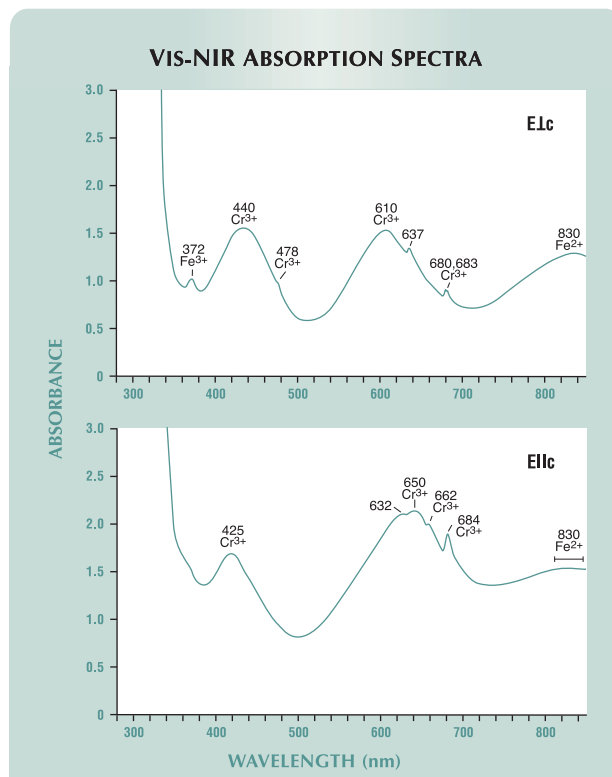
Figure 40. This representative FTIR spectrum of a Kafubu emerald shows peaks at 7096 and 5265 cm⁻¹ that are caused by the vibrations of water molecules adjacent to alkali-metal ions in the channels of the beryl structure. The broad band between 3900 and 3400 cm⁻¹ also is caused by water molecules in this position, and by free water molecules. The peak at 2357 cm⁻¹ is due to CO_2. The intensity of this peak varied substantially between samples.

Figure 41. Peaks in the 3100–2800 cm⁻¹ range were seen in the FTIR spectra of both faceted and cuttable rough specimens of Kafubu emerald, indicating the presence of oil. No artificial resin was found in the stones that were tested. Spectra have been offset vertically for clarity.

IR Absorption Spectra
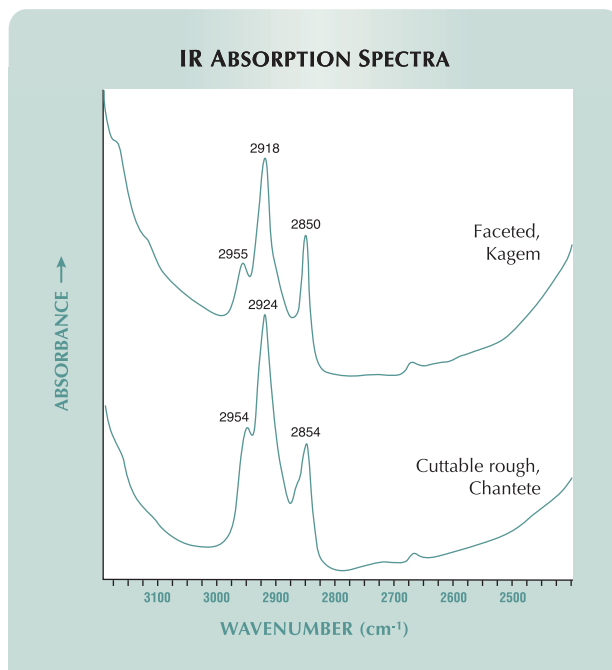
mine, as described in the Microscopic Characteristics section. Stones with sufficient fractures containing a near-colorless filler showed FTIR spectra that are typical for an oil (figure 41). Although the type of oil cannot be established with this method, at the Chantete mine we were told that Johnson's baby oil (mineral oil) is used on the rough. Likewise, mineral oil is reportedly used by emerald cutters in Israel. No green fillers were seen in any of the samples.

DISCUSSION

Physical Properties. The measured refractive indices and specific gravity values (table 1) are fairly consistent with those presented by Milisenda et al. (1999). An unusual dark bluish green emerald described by Schmetzer and Bank (1981) showed extreme values for refractive indices, n_o = 1.602 and n_e = 1.592, with a birefringence of 0.010.

Inclusions in Zambian emeralds have been described by Campbell (1973), Koivula (1982, 1984), Graziani et al. (1984), Gübelin and Koivula (1986), Milisenda et al. (1999), and Moroz and Eliezri (1999). These studies largely agree with and support our findings (table 1). However, in the present study, we did not encounter glauconite, chrysoberyl, margarite, muscovite, or chrysotile, which suggests these mineral inclusions are rare. It should also be noted that the chrysoberyl, margarite, and muscovite were identified in a heavily included crystal fragment (Graziani et al., 1983), which may not be representative of gem-quality material. The presence of isolated CO_2-CH_4–bearing negative crystals has not been reported previously in Zambian emerald.

Chemical Properties. Our chemical analyses showed a wider range of trace-element concentrations than was indicated by the seven analyses presented by Milisenda et al. (1999). Our Cr content was fairly consistent with their results but was slightly higher in some stones; V, Fe, Mg, Ca, Na, and K also showed a much wider range. In addition, our study indicated the presence of Cs and occasionally Sc. The values we measured for the main trace elements all fell within the ranges that were presented earlier by Graziani et al. (1984) on one emerald, Hänni (1982) on two emeralds, Schwarz and Henn (1992) on 11 emeralds from the Kamakanga mine (mean concentrations only), and Moroz et al. (1998) and Moroz and Eliezri (1998) on three samples. Our data also were consistent with the

analyses of noncuttable rough Zambian emeralds reported by Seifert et al. (2004c), except those rough samples had slightly higher Na. Moreover, we found a wider range of Mg and Fe concentrations, with lower values in light green cut emeralds.

Using Schwarz's empirical subdivision of low, medium, and high concentrations of elements in emerald (see, e.g., Schwarz, 1990a,b; Schwarz and Henn, 1992), the Zambian stones generally show a low V content, a moderate amount of Cr, Mg, and Na, and a moderate-to-high Fe content. Notable is the relatively high Cs content in many of our samples. As observed by Bakakin and Belov (1962), Cs is typically present in Li-rich beryl. Li could not be analyzed by electron microprobe, but PIXE/PIGE analyses of 11 Zambian crystal fragments by Calligaro et al. (2000) indicated an average Li content of 580 ppm, along with a high average Cs content of 1,150 ppm.

Examination of the growth zoning in the Chantete emerald crystal (figure 38) showed that as Cr, Fe, and Mg increase, Al decreases. This is expected from the known substitutions in emerald (Aurisicchio et al., 1988), namely of Al^{3+} in the octahedral site by Fe^{2+} and Mg^{2+}, plus Fe^{3+}, Cr^{3+}, and V^{3+}. The presence of Cs^+, which is located in the channel of the beryl structure, is coupled with the substitution of Li^+ for Be^{2+} in the tetrahedral site and clearly follows a different trend. Na appears to reflect mainly the trend of Cr, Fe, and Mg, but also seems to follow the general trend of Cs. This could be explained by the fact that Na^+ can be involved in coupled substitutions for Al^{3+} in the octahedral site, but also for Be^{2+} in the tetrahedral site (compare, e.g., to Aurisicchio et al., 1988; Barton and Young, 2002). From the trend shown in figure 38, it is clear that the main substitution in the Chantete emerald crystal took place in the Al^{3+} octahedral site.

The analyses of the faceted emeralds did not show a consistent correlation between color and Cr content (see table 2 and the *G&G* Data Depository). However, analysis of the various color zones in the Chantete emerald described above provided a good opportunity to explore the relationship between color and trace-element content within a single crystal. When the data from this crystal are graphed according to the atomic ratios that were plotted by Barton and Young (2002), a clear trend is revealed that confirms Cr as the main chromophore (figure 42). Also plotted in figure 42 are two of the darkest green emeralds analyzed for this study (from Kagem), which extend the trend shown by the zoned Chantete sample. This trend resembles the one diagramed by
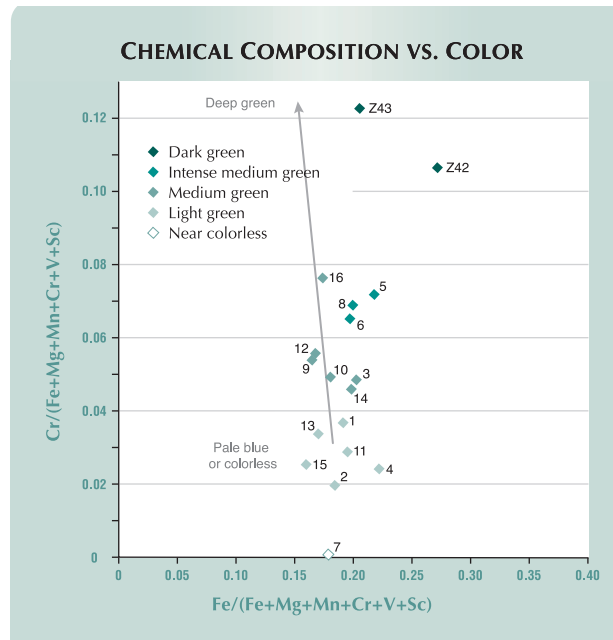

Figure 42. Data from the color-zoned Chantete emerald crystal in figures 37 and 38, together with two of the darkest green emeralds analyzed for this study, are plotted on this beryl composition diagram from Barton and Young (2002) to reveal the relationship between composition and color. The data points are labeled according to the growth zones shown in figure 37, and plotted by color. A clear correlation is revealed between the depth of emerald coloration and Cr content. The arrow (from Barton and Young, 2002) indicates the general trend of beryls from Somondoco (Colombia) and Khaltaro (Pakistan) that range from colorless or pale blue to deep green.

Barton and Young (2002) for pale blue to dark green beryls from Somondoco, Colombia and Khaltaro, Pakistan. The non-emerald analyses from those localities contained very little or no Cr and plotted along the X-axis, like the colorless zone (analysis no. 7) of the Chantete emerald in this study.

Identification. *Separation from Synthetics.* The higher R.I. values of Zambian emeralds (table 1) make them easy to distinguish from their synthetic counterparts. Synthetic emeralds typically have lower refractive indices—roughly between 1.56 and 1.58—and lower specific gravities of 2.65–2.70 (see, e.g., Schrader, 1983; Liddicoat, 1989; Webster, 1994; Schmetzer et al., 1997), although some Russian hydrothermal synthetic emeralds have shown R.I.'s up to 1.584 and S.G.'s up to 2.73 (Webster, 1994;

Koivula et al., 1996). Russian hydrothermal synthetic emeralds can be readily separated from natural emeralds by their distinctive chevron growth zoning or, if present, by unusual internal characteristics such as tiny red-brown particles. Only in the absence of these features would infrared or EDXRF spectroscopy be needed to identify this synthetic (Koivula et al., 1996).

Separation from Emeralds of Different Geographic Origin. The commercially important Colombian emeralds typically show lower refractive indices of 1.569–1.580 (e.g., Ringsrud, 1986; Gübelin, 1989; Boehm, 2002), although Bosshart (1991) gave a wider R.I. range of 1.565–1.588. Colombian emeralds can be further distinguished by their distinctive inclusion scenery, including abundant three-phase inclusions containing halite cubes.

A comparison of other commercially available emeralds with R.I., birefringence, and S.G. values similar to those from Kafubu is shown in table 3 and discussed below. As previously mentioned, roughly 70% of the Zambian stones tested showed n_o = 1.591–1.595 and n_e = 1.583–1.587. Only some light green stones had R.I. values below 1.583, and dark green stones may show R.I.'s above 1.595. According to these data, accurate measurement of the R.I. can distinguish most of the commercial medium and dark green Zambian emeralds from the emeralds of Itabira, Brazil. In addition, the R.I.'s of most Zambian emeralds appear to show only a slight overlap with those of emeralds from the Ural Mountains.

The internal features seen in emeralds from the various localities in table 3 show many similarities, so their use for determining geographic origin is rather limited (for further discussion, see Schwarz, 1998). This overlap is due to the similar geologic environment in which these emeralds form (various types of metamorphic schist). Nevertheless, some distinguishing internal features are listed in table 3. When present, these characteristics can be used to clearly separate Kafubu emeralds from those of Santa Terezinha de Goiás (Brazil), Sandawana (Zimbabwe), and the Swat Valley (Pakistan).

The UV-Vis spectra can only help distinguish between the various emerald occurrences to a limited extent, by indicating differences in the valence state of iron. Only the UV-Vis spectra of Sandawana and, possibly, Ural emeralds show distinctive features. Interestingly, this method can also be used effectively to distinguish between emeralds from Nigeria (containing Fe^{2+} and Fe^{3+}) and Colombia (virtually no iron and no Fe^{3+}; Henn and Bank, 1991;

Moroz et al., 1999), which may contain very similar three-phase inclusions. Note that Nigerian emeralds also fall outside the scope of our discussion due to their lower optical properties.

The chemical composition of the various emeralds in table 3 shows considerable overlap. However, trace elements may help eliminate some localities for a specific stone. For instance, relatively high K contents have been documented in emeralds from Kafubu and Mananjary.

PIXE/PIGE analysis, which is a highly sensitive technique that is capable of measuring light elements such as Li, has revealed interesting trends for Cs, Li, and Rb (Calligaro et al., 2000; table 3). Compared to Kafubu, emeralds from Mananjary showed lower Li content, and those from Habachtal had smaller amounts of Rb. Enriched Cs is indicative of emeralds from Kafubu, Mananjary, and Sandawana. The validity of these trends should be tested further with additional analyses of representative samples from the various deposits.

Measuring stable oxygen isotope ratios is another (not entirely nondestructive) technique that can provide additional information. This technique was first applied to Zambian emeralds by Eliezri and Kolodny (1997), and has seen wider application to emeralds from various deposits by Giuliani et al. (1998, 2000). The oxygen isotope data are expressed as $\delta^{18}O$, which is the relative difference between the $^{18}O/^{16}O$ ratio of the sample and that of SMOW (standard mean ocean water), expressed in per mil (‰). The $\delta^{18}O$ values of emeralds from some of the localities in table 3 show considerable overlap (figure 43). Data for Kafubu emeralds exhibit a range similar to that reported for emeralds from the Ural Mountains.

This brief overview shows that even when optical properties, internal characteristics, and chemical data are carefully combined and evaluated, it may not always be possible to differentiate Kafubu emeralds from those of other localities. It appears, however, that in many cases the use of chemical analysis is helpful. Even so, more analyses of representative emeralds from various deposits are needed to better characterize their variations in chemical composition.

SUMMARY AND CONCLUSION
The Kafubu area became a significant producer of good-quality emeralds in the 1970s. As of August 2004, the main production took place at the Kagem, Grizzly, and Chantete concessions, which are all

TABLE 3. Properties of emeralds with R.I. and S.G. values similar to those from Kafubu, Zambia.

Properties	Kafubu area, Zambia	Santa Terezinha de Goiás, Brazil	Itabira district, Brazil	Ural Mountains, Russia	Mananjary region, Madagascar
Physical and optical properties					
References	This study, Milisenda et al. (1999)	Lind et al. (1986), Schwarz (1990a; 2001)	Hänni et al. (1987), Schwarz et al. (1988), Epstein (1989), Henn and Bank (1991); Gübelin (1989), Schwarz (1998), Zwaan (2001)	Gübelin (1974), Sinkankas (1981), Bank (1982), Mumme (1982), Schmetzer et al. (1991), Gübelin and Koivula (1986), Laskovenkov and Zhernakov (1995)	Hänni and Klein (1982), Schwarz and Henn (1992), Schwarz (1994)
R.I.					
n_o	1.585–1.599	1.592–1.600	1.580–1.590	1.581–1.591	1.588–1.591
n_e	1.578–1.591	1.584–1.593	1.574–1.583	1.575–1.584	1.580–1.585
Birefringence	0.006–0.009	0.006–0.010	0.004–0.009	0.007	0.006–0.009
S.G.	2.69–2.78	2.75–2.77	2.72–2.74	2.72–2.75	2.68–2.73
Distinguishing internal features	Skeletal magnetite and hematite (if present)	Abundant opaque inclusions, such as black spinel octahedrons; pale brown to colorless carbonate rhombohedra; fluid inclusions are very small and rare	Numerous parallel growth tubes (with remarkable variation of fluid inclusions)	Irregular color distribution (if present)	Elongate quartz crystals, parallel to the c-axis, often associated with growth tubes; fibrous aggregates of talc (if present); rhombohedral carbonate crystals (rare)
Iron peaks in UV-VIS spectra	Fe^{2+} and Fe^{3+} features	Fe^{2+} and Fe^{3+} features	Fe^{2+} and Fe^{3+} features	Fe^{2+} features only, or Fe^{2+} and Fe^{3+} features	Fe^{2+} and Fe^{3+} features
Electron-microprobe data[a]					
References	This study[b]	Schwarz (1990a)	Schwarz (1990b), Zwaan (2001)	Schmetzer et al. (1991), Schwarz (1991)	Hänni and Klein (1982), Schwarz and Henn (1992)
No. analyses	114	15	71	27	7
Oxide (wt.%)					
SiO_2	61.9–65.4	63.8–66.5	63.3–67.0	64.6–66.9	63.3–65.0
TiO_2	bdl	–	≤ 0.04	≤ 0.05	bdl
Al_2O_3	12.5–17.9	12.2–14.3	13.9–16.9	14.2–18.3	12.8–14.6
Cr_2O_3	bdl–0.84	0.06–1.54	0.06–1.42	0.01–0.50	0.08–0.34
V_2O_3	bdl–0.08	≤ 0.08	≤ 0.07	≤ 0.04	≤ 0.03
FeO^{tot}	0.06–1.75	0.77–1.82	0.41–1.30	0.10–1.16	0.91–1.46
MnO	bdl–0.01	≤ 0.02	≤ 0.08	≤ 0.03	–
MgO	0.27–2.90	2.48–3.09	1.39–2.64	0.29–2.23	1.71–3.00
CaO	bdl–0.12	–	≤ 0.10	≤ 0.03	–
Na_2O	0.16–1.99	1.46–1.73	0.79–1.93	0.61–1.72	1.28–2.16
K_2O	bdl–0.27	≤ 0.03	≤ 0.08	≤ 0.07	0.05–0.21
Cs_2O	bdl	–	bdl	–	–
Rb_2O	bdl–0.23	–	bdl	–	–
Sc_2O_3	bdl–0.07	–	–	–	–
Mo_2O_3	–	–	≤ 0.06	–	–
PIXE/PIGE data[c]					
No. samples	11	8	–	20	12
Trace elements (ppm)					
Li	580 (230)	170 (90)	–	720 (260)	130 (70)
Cs	1150 (540)	350 (300)	–	360 (230)	610 (580)
Rb	140 (60)	15 (2)	–	40 (60)	190 (70)

[a] Abbreviations: bdl = below detection limit; – = no data.

[b] The range of composition reported in the literature for Zambian emeralds falls within the analyses obtained for this study.

[c] Data from Calligaro et al. (2000), average elemental content from three point analyses per sample in ppm by weight. Standard deviations are given in parentheses. Detection limits (in ppm) for Rb=2, Li=50, and Cs=100.

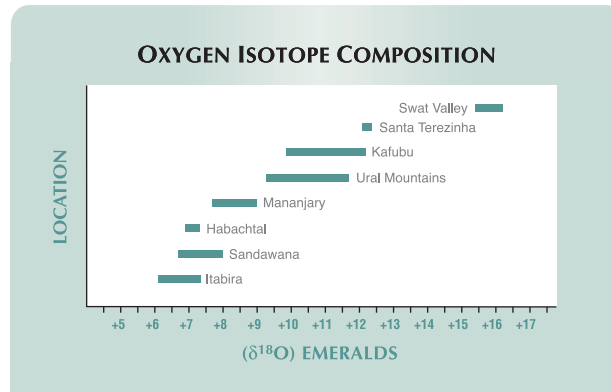| Sandawana, Zimbabwe	Swat Valley, Pakistan	Habachtal, Austria
Gübelin (1958), Zwaan et al. (1997)	Henn (1988), Gübelin (1989)	Gübelin (1956), Morteani and Grundmann (1977), Nwe and Grundmann (1990), Schwarz (1991), Gübelin and Koivula (1986), Grundmann (2001)
1.590–1.594	1.584–1.600	1.582–1.597
1.584–1.587	1.578–1.591	1.574–1.590
0.006–0.007	0.006–0.009	0.005–0.007
2.74–2.77	2.70–2.78	2.70–2.77
Abundant thin needles and curved fibers of amphibole; extremely small fluid inclusions (if present); black grains of chromian ilmenorutile (very rare); phlogopite virtually absent	Many two-and three-phase inclusions (similar to Colombia), but with no rectangular to square shapes; common black chromite and rhombohedral dolomite	Commonly show patchy color distribution; most stones are heavily included and fractured (rarely cuttable and only in small sizes)
Fe^{2+} features only	Fe^{2+} and Fe^{3+} features	Fe^{2+} and Fe^{3+} features
Zwaan et al. (1997)	Henn (1988), Hammarstrom (1989)	Schwarz (1991)
41	176	47
62.6–63.2	62.2–65.8	64.6–66.1
≤ 0.05	≤ 0.02	≤ 0.03
13.0–13.7	13.1–15.0	13.3–14.5
0.61–1.33	0.15–2.05	0.01–0.44
0.04–0.07	0.01–0.06	≤ 0.04
0.45–0.82	0.20–2.51	0.61–1.87
bdl	bdl	≤ 0.05
2.52–2.75	2.21–3.10	2.33–2.92
–	bdl	0.02–0.04
2.07–2.41	1.08–2.11	1.54–2.24
0.03–0.06	≤ 0.02	0.01–0.10
0.06–0.10	–	–
–	–	–
bdl	≤0.19	–
bdl	–	≤ 0.04
22	4	13
800 (310)	350 (130)	190 (210)
710 (320)	120 (80)	370 (390)
350 (200)	6 (3)	18 (13)

OXYGEN ISOTOPE COMPOSITION

Figure 43. Significant overlap is evident in the oxygen isotopic values of emeralds reported from some of the localities in table 3. The range of $\delta^{18}O$ values for Kafubu emeralds is similar to that for emeralds from the Ural Mountains. Data from Eliezri and Kolodny (1997), Giuliani et al. (1998), Cheilletz et al. (2001), Gavrilenko (2001), and Zwaan et al. (2004).

open-pit mines. Research and exploration activities (e.g., Tembo et al., 2000; Seifert et al., 2004c) demonstrate that the potential for new emerald occurrences in the Kafubu area remains very high.

During a late stage of the Pan-African orogeny, probably around 450 million years ago, emerald mineralization at Kafubu was caused by metasomatic alteration of Cr-bearing metabasites, which were invaded by Be-bearing fluids derived from hydrothermal veins. Economic emerald concentrations are almost entirely confined to phlogopite reaction zones between quartz-tourmaline veins and the metabasites.

Kafubu emeralds show large variations in physical properties, with refractive indices and specific gravities higher than those of emeralds from Colombia, but comparable to emeralds from many other commercially important localities. Kafubu emeralds are characterized by partially healed fractures with various shapes of fluid inclusions. Characteristic mineral inclusions are randomly oriented actinolite needles and phlogopite platelets, and dravite, fluorapatite, magnetite, and hematite. Skeletal magnetite and hematite have not been described as inclusions in emeralds from other occurrences. Inclusions such as dravite, fluorapatite, and fluorite, as well as niobian rutile identified in one stone, confirm a metasomatic origin related to the intrusion of a rare-element pegmatite-hydrothermal vein system.

The chemical composition of the Kafubu emeralds is characterized by a wide range of trace-ele-

Figure 44. Zambia is a recognized source of attractive emeralds that are readily available in calibrated sizes, but occasionally exceptional stones are produced, as shown by the 15.32 ct emerald in this platinum pendant that is set with diamonds. The emerald is unusually large and clean for a Zambian stone, and a laboratory report has verified that it has not been treated in any way. Courtesy of Kothari and Company Inc., Los Angeles, CA; photo © Harold and Erica Van Pelt.

ment contents, with generally moderate amounts of Cr, Mg, and Na, and a moderate-to-high iron content as both Fe^{2+} and Fe^{3+}. Notable is a relatively high content of Cs and Li in many samples. The V content is low, and Sc may be detected.

Most of Zambia's emeralds are exported to India, mainly for use in the domestic market, and to Israel for international distribution. Commercial production of emeralds for the international market is done in calibrated sizes; commercial faceted goods typically weigh up to 5 ct, are slightly bluish green to bluish green with medium to dark tones,

REFERENCES

Aurisicchio C., Fioravanti G., Grubessi O., Zanazzi P.F. (1988) Reappraisal of the crystal chemistry of beryl. *American Mineralogist*, Vol. 73, No. 7–8, pp. 826–837.

Bakakin V.V., Belov N.V. (1962) Crystal chemistry of beryl. *Geokhimiya*, Vol. 5, pp. 420–433.

Banerjee A. (1995) Investigation of fluid inclusion in emeralds of different geological origins by microchemical analysis and IR-reflexion-spectroscopy. *Boletín de la Sociedad Española de Mineralogía*, Vol. 18-1, pp. 18–19.

Bank H. (1982) Geschliffene zonar gebaute Smaragde aus dem Gebiet der Tokowaya, Ural, UdSSR. *Zeitschrift der Deutschen Gemmologischen Gesellschaft*, Vol. 31, No. 3, pp. 193–194.

Barton M.D., Young S. (2002) Non-pegmatitic deposits of beryllium: Mineralogy, geology, phase equilibria and origin. In E.S. Grew, Ed., *Beryllium: Mineralogy, Petrology and Geochemistry*, Reviews in Mineralogy and Geochemistry, Vol. 50, Chapter 14, pp. 591–691.

Boehm E. (2002) Gem News International: New emerald find from the Chivor region, Colombia. *Gems & Gemology*, Vol. 38, No. 4, pp. 350–351.

Bosshart G. (1991) Emeralds from Colombia, part 2. *Journal of Gemmology*, Vol. 22, No. 7, pp. 409–425.

Calligaro T., Dran J.C., Poirot J.P., Querré G., Salomon J., Zwaan J.C. (2000) PIXE/PIGE characterisation of emeralds using an external micro-beam. *Nuclear Instruments and Methods in Physics Research B*, Vol. 161–163, pp. 769–774.

Campbell I.C.C. (1973) Emeralds reputed to be of Zambian origin. *Journal of Gemmology*, Vol. 13, No. 5, pp. 169–179.

Caspi A. (1997) Modern diamond cutting and polishing. *Gems & Gemology*, Vol. 33, No. 2, pp. 102–121.

Cheilletz A., Sabot B., Marchand P., de Donato P., Taylor B., Archibald D., Barrès O., Andrianjaffy J. (2001) Emerald deposits in Madagascar: Two different types for one mineralising event. *EUG XI*, Strasbourg, France, April 8–12, p. 547.

Coats J.S., Mosley P.N., Mankelow J.M., Mwale M., Chikambwe E.M., Muibeya B., Ndhlovu K.C., Nzabara F. (2001) *The Geology and Mineral Resources of Zambia*. Geological Survey Department Memoir 6, Ministry of Mines and Minerals Development, Lusaka, Zambia.

Cook F.A. (1997) Applications of geophysics in gemstone exploration. *Gems & Gemology*, Vol. 33, No. 1, pp. 4–23.

Cosi M., de Bonis A., Gosso G., Hunziker J., Martinotti G., Moratto S., Robert J.P., Ruhlman F. (1992) Late Proterozoic thrust tectonics, high-pressure metamorphism and uranium mineralization in the Domes area, Lufilian Arc, northwestern Zambia. *Precambrian Research*, Vol. 58, No. 1–4, pp. 215–240.

Daly M.C., Unrug R. (1983) The Muva Supergroup of northern Zambia; A craton to mobile belt sedimentary sequence. *Transactions of the Geological Society of South Africa*, Vol. 85, No. 3, pp. 155–165.

de Waele B., Mapani B. (2002) Geology and correlation of the central Irumide belt. *Journal of African Earth Sciences*, Vol. 35, No. 3, pp. 385–397.

de Waele B., Wingate M.T.D., Fitzsimons I.C.W., Mapani B. (2002) Untying the Kibaran knot: A re-assessment of Mesoproterozoic correlations in southern Africa based on SHRIMP U-Pb data from the Irumide belt. *Geology*, Vol. 31, No. 6, pp. 509–512.

Donovan J.J., Tingle T.N. (1996) An improved mean atomic number correction for quantitative microanalysis. *Journal of Microscopy*, Vol. 2, No. 1, pp. 1–7.

Eliezri I.Z., Kolodny Y. (1997) The isotopic composition of oxygen in emeralds as an indicator of origin. *26th International Gemmological Conference*, Idar-Oberstein, Germany, p. 14.

Epstein D.S. (1989) The Capoeirana emerald deposit near Nova Era, Minas Gerais, Brazil. *Gems & Gemology*, Vol. 25, No. 3, pp. 150–158.

Fritsch E., Rondeau B., Notari F., Michelou J.-C., Devouard B., Peucat J.-J., Chalain J.-P., Lulzac Y., de Narvaez D., Arboleda C. (2002) Les nouvelles mines d'émeraude de La Pita (Colombie) 2ᵉ partie. *Revue de Gemmologie*, No. 144, 2002, pp. 13–21.

Gavrilenko E. (2001) Emeralds of the Ural mountains (Russia): Geology, fluid inclusions and oxygen isotopes. *28th International Gemmological Conference*, Madrid, Spain, pp. 36–40.

Giuliani G., France-Lanord C., Coget P., Schwarz D., Cheilletz A., Branquet Y., Girard D., Martin-Izard A., Alexandrov P., Piat D.H. (1998) Oxygen isotope systematics of emerald: Relevance for its origin and geological significance. *Mineralium Deposita*, Vol. 33, No. 5, pp. 513–519.

Giuliani G., Chaussidon M., Schubnel H.J., Piat D.H., Rollion-Bard C., France-Lanord C., Giard D., Narvaez D.D., Rondeau B. (2000) Oxygen isotopes and emerald trade routes since antiquity. *Science*, Vol. 287, No. 5453, pp. 631–633.

Graziani G., Gübelin E., Lucchesi S. (1983) The genesis of an emerald from the Kitwe District, Zambia. *Neues Jahrbuch für Mineralogie, Monatshefte*, Vol. 4, pp. 75–186.

Graziani G., Gübelin E., Lucchesi S. (1984) Report on the investigation of an emerald from the Kitwe District, Zambia. *Australian Gemmologist*, Vol. 15, No. 7, pp. 227–234.

Grundmann G. (2001) Die Smaragde der Welt. In D. Schwarz and R. Hochleitner, Eds., *Smaragd—der kostbarste Beryll, der teuerste Edelstein*, extraLapis No. 21, pp. 26–37.

Gübelin E.J. (1958) Emeralds from Sandawana. *Journal of Gemmology*, Vol. 6, No. 8, pp. 340–354.

Gübelin E.J. (1956) The emerald from Habachtal. *Gems & Gemology*, Vol. 8, No. 10, pp. 295–309.

Gübelin E.J. (1974) *Die Innenwelt der Edelsteine*. Hanns Reich Verlag, Düsseldorf, Germany.

Gübelin E.J. (1989) Gemological characteristics of Pakistani emeralds. In A.H. Kazmi and L.W. Snee, Eds., *Emeralds of Pakistan: Geology, Gemology and Genesis*, Van Nostrand Reinhold, New York, pp. 75–92.

Gübelin E., Koivula J.I. (1986) *Photoatlas of Inclusions in Gemstones*. ABC Edition, Zürich, Switzerland.

Hammarstrom J.M. (1989) Mineral chemistry of emeralds and some associated minerals from Pakistan and Afghanistan: An electron microprobe study. In A.H. Kazmi and L.W. Snee, Eds., *Emeralds of Pakistan: Geology, Gemology and Genesis*, Van Nostrand Reinhold, New York, pp. 125–150.

Hänni H. (1982) A contribution to the separability of natural and synthetic emeralds. *Journal of Gemmology*, Vol. 18, No. 2, pp. 138–144.

Hänni H.A., Klein H.H. (1982) Ein Smaragdvorkommen in Madagaskar. *Zeitschrift der Deutschen Gemmologischen Gesellschaft*, Vol. 31, No. 1/2, pp. 71–77.

Hänni H.A., Schwarz D., Fischer M. (1987) The emeralds of the Belmont mine, Minas Gerais, Brazil. *Journal of Gemmology*, Vol. 20, No. 7/8, pp. 446–456.

Henn U. (1988) Untersuchungen an Smaragden aus dem Swat-Tal, Pakistan. *Zeitschrift der Deutschen Gemmologischen Gesellschaft*, Vol. 37, No. 3/4, pp. 121–127.

Henn U., Bank H. (1991) Außergewöhnliche Smaragde aus Nigeria. *Zeitschrift der Deutschen Gemmologischen Gesellschaft*, Vol. 40, No. 4, pp. 181–187.

Hickman A.C.J. (1972) *The Miku Emerald Deposit*. Geological Survey Department Economic Report No. 27, Ministry of Mines and Mining Development, Republic of Zambia, 35 pp.

Hickman A.C.J. (1973) *The Geology of the Luanshya Area*. Report of the Geological Survey No. 46, Ministry of Mines, Republic of Zambia, 32 pp.

John T., Schenk V., Mezger K., Tembo F. (2004) Timing and PT evolution of whiteschist metamorphism in the Lufilian Arc–Zambezi Belt Orogen (Zambia): Implications for the assembly of Gondwana. *Journal of Geology*, Vol. 112, No. 1, pp. 71–90.

Johnson M.L., Elen S., Muhlmeister S. (1999) On the identification of various emerald filling substances. *Gems & Gemology*, Vol. 35, No. 2, pp. 82–107.

Kiefert L., Hänni H.A., Chalain J.-P., Weber W. (1999) Identification of filler substances in emeralds by infrared and Raman spectroscopy. *Journal of Gemmology*, Vol. 26, No. 8, pp. 487–500.

Koivula J.I. (1982) Tourmaline as an inclusion in Zambian emeralds. *Gems & Gemology*, Vol. 18, No. 4, pp. 225–227.

Koivula J.I. (1984) Mineral inclusions in Zambian emeralds. *Australian Gemmologist*, Vol. 15, No. 7, pp. 235–239.

Koivula J.I., Kammerling R.C., DeGhionno D., Reinitz I., Fritsch E., Johnson M.L. (1996) Gemological investigation of a new type of Russian hydrothermal synthetic emerald. *Gems & Gemology*, Vol. 32, No. 1, pp. 32–39.

Kozlowski A., Metz P., Estrada Jaramillo H.A. (1988) Emeralds from Somondoco, Colombia: Chemical composition, fluid inclusions and origin. *Neues Jahrbuch für Mineralogie, Abhandlungen*, Vol. 159, No. 1, pp. 23–49.

Laskovenkov A.F., Zhernakov V.I. (1995) An update on the Ural emerald mines. *Gems & Gemology*, Vol. 31, No. 2, pp. 106–113.

Laurs B. (2004) Gem News International: Update on several gem localities in Zambia and Malawi. *Gems & Gemology*, Vol. 40, No. 4, pp. 347–350.

Leake B.E., Woolley A.R., Arps C.E.S., Birch W.D., Gilbert M.C., Grice J.D., Hawthorne F.C., Kato A., Kisch H.J., Krivovichev V.G., Linthout K., Laird J., Mandarino J., Maresch W.V., Nickel E.H., Rock N.M.S., Schumacher J.C., Smith D.C., Stephenson N.C.N., Ungaretti L., Whittaker E.J.W., Youzhi G. (1997) Nomenclature of amphiboles: Report of the subcommittee on amphiboles of the International Mineralogical Association Commission on New Minerals and Mineral Names. *Mineralogical Magazine*, Vol. 61, No. 2, pp. 295–321.

Liddicoat R.T. (1989) *Handbook of Gem Identification*, 12th ed., 2nd rev. printing. Gemological Institute of America, Santa Monica, CA.

Lind T., Henn U., Bank H. (1986) Smaragde von Sta. Terezinha de Goias, Brasilien, mit relativ hoher Lichtbrechung. *Zeitschrift der Deutschen Gemmologischen Gesellschaft*, Vol. 35, No. 4, pp. 186–187.

Milisenda C.C., Malango V., Taupitz K.C. (1999) Edelsteine aus Sambia—Teil 1: Smaragd. *Zeitschrift der Deutschen Gemmologischen Gesellschaft*, Vol. 48, No. 1, pp. 9–28.

Moroz I., Eliezri I.Z. (1998) Emerald chemistry from different deposits. *Australian Gemmologist*, Vol. 20, No. 2, pp. 64–69.

Moroz I., Eliezri I.Z. (1999) Mineral inclusions in emeralds from different sources. *Journal of Gemmology*, Vol. 26, No. 6, pp. 357–363.

Moroz I., Panczer G., Roth M. (1998) Laser-induced luminescence of emeralds from different sources. *Journal of Gemmology*, Vol. 26, No. 5, pp. 316–320.

Moroz I., Roth M.L., Deich V.B. (1999) The visible absorption spectroscopy of emeralds from different deposits. *Australian Gemmologist*, Vol. 20, No. 8, pp. 315–320.

Morteani G., Grundmann G. (1977) The emerald porphyroblasts in the penninic rocks of the central Tauern Window. *Neues Jahrbuch für Mineralogie, Mitteilungen*, Vol. 11, pp. 509–516.

Mumme I. (1982) *The Emerald*. Mumme Publications, Port Hacking, New South Wales, Australia.

Ng'uni B., Mwamba K. (2004) *Evaluation of the Potential and Authentication of Emerald Mineralization in North-Western Province, Musakashi Area, Chief Mujimanzovu–Solwezi District*. Draft Economic Report, Geological Survey Department, Lusaka, Zambia.

Nwe Y.Y., Grundmann G. (1990) Evolution of metamorphic fluids in shear zones: The record from the emeralds of Habachtal, Tauern Window, Austria. *Lithos*, Vol. 25, No. 4, pp. 281–304.

Parkin J. (2000) *Geology of the St. Francis Mission and Musakashi River Areas. Explanation of Degree Sheet 1226 NE and SE Quarters and Part of 1126 SE Quarter*. Report No. 80, Geological Survey Department, Lusaka, Zambia, 49 pp.

Platonov A.N., Taran M.N., Minko O.E., Polshyn E.V. (1978) Optical absorption spectra and nature of color of iron-containing beryls. *Physics and Chemistry of Minerals*, Vol. 3, No. 1, pp. 87–88.

Ringsrud R. (1986) The Coscuez mine: A major source of Colombian emeralds. *Gems & Gemology*, Vol. 22, No. 2, pp. 67–79.

Samson I., Anderson A., Marshall D. (2003) *Fluid Inclusions, Analysis and Interpretation*. Mineralogical Association of Canada Short Course Series, Vol. 32, 374 pp.

Schmetzer K., Bank H. (1981) An unusual pleochroism in Zambian emeralds. *Journal of Gemmology*, Vol. 17, No. 7, pp. 443–445.

Schmetzer K., Berdesinski W., Bank H. (1974) Über die Mineralart Beryll, ihre Farben und Absorptionsspektren. *Zeitschrift der Deutschen Gemmologischen Gesellschaft*, Vol. 23, No. 1, pp. 5–39.

Schmetzer K., Bernhardt H., Biehler R. (1991) Emeralds from the Ural Mountains, USSR. *Gems & Gemology*, Vol. 27, No. 2, pp. 86–99.

Schmetzer K., Kiefert L., Bernhardt H.-J., Zhang B. (1997) Characterization of Chinese hydrothermal synthetic emerald. *Gems & Gemology*, Vol. 33, No. 4, pp. 276–291.

Schrader H.W. (1983) Contributions to the study of the distinction of natural and synthetic emeralds. *Journal of Gemmology*, Vol. 18, No. 6, pp. 530–543.

Schwarz D. (1990a) Die brasilianischen Smaragde und ihre Vorkommen: Santa Terezinha de Goiás/Go. *Zeitschrift der Deutschen Gemmologischen Gesellschaft*, Vol. 39, No. 1, pp. 13–44.

Schwarz D. (1990b) Die chemische Eigenschaften der Smaragde I. Brasilien. *Zeitschrift der Deutschen Gemmologischen Gesellschaft*, Vol. 39, No. 4, pp. 233–272.

Schwarz D. (1991) Die chemische Eigenschaften der Smaragde III. Habachtal/Österreich und Uralgebirge/UdSSR. *Zeitschrift der Deutschen Gemmologischen Gesellschaft*, Vol. 40, No. 2/3, pp. 103–143.

Schwarz D. (1994) Emeralds from the Mananjary region, Madagascar: Internal features. *Gems & Gemology*, Vol. 30, No. 2, pp. 88–101.

Schwarz D. (1998) The importance of solid and fluid inclusions for the characterization of natural and synthetic emeralds. In D. Giard, Ed., *L'émeraude*, Association Française de Gemmologie, Paris, pp. 71–80.

Schwarz D. (2001) Gemmologie des Smaragds—Ist die Herkunftsbestimmung von Smaragden möglich? In D. Schwarz and R. Hochleitner, Eds., *Smaragd, der kostbarste Beryll, der teuerste Edelstein*, extraLapis No. 21, pp. 68–73.

Schwarz D., Henn U. (1992) Emeralds from Madagascar. *Journal of Gemmology*, Vol. 23, No. 3, pp. 140–149.

Schwarz D., Bank H., Henn U. (1988) Neues Smaragdvorkommen in Brasilien entdeckt: Capoeirana bei Nova Era, Minas Gerais. *Zeitschrift der Deutschen Gemmologischen Gesellschaft*, Vol. 37, No. 3/4, pp. 146–147.

Seifert A.V., Vrána S., Lombe D.K. (2004a) *Evaluation of Mineralization in the Solwezi area, Northwestern Province, Zambia. Final Report for the Year 2004*. Czech Geological Survey, Record Office – File Report No. 2/2004, Prague, Czech Republic, 20 pp.

Seifert A., Vrána S., Lombe D.K., Mwale M. (2004b) *Impact Assessment of Mining of Beryl Mineralization on the Environment in the Kafubu Area; Problems and Solutions*. Final Report for the Year 2003. Czech Geological Survey, Record Office – File Report No. 1/2004, Prague, Czech Republic, 63 pp.

Seifert A.V., Žáček V., Vrána S., Pecina V., Zachariáš J., Zwaan J.C. (2004c) Emerald mineralization in the Kafubu area, Zambia. *Bulletin of Geosciences*, Vol. 79, No. 1, pp. 1–40.

Sinkankas J. (1981) *Emerald and Other Beryls*. Chilton Book Co., Radnor, PA.

Sliwa A.S., Nguluwe C.A. (1984) Geological setting of Zambian emerald deposits. *Precambrian Research*, Vol. 25, pp. 213–228.

Suwa Y. (1994) *Gemstones: Quality and Value*, 8th ed. Gemological Institute of America and Suwa & Son Inc., Santa Monica, CA.

Tembo F., Kambani S., Katongo C., Simasiku S. (2000) *Draft Report on the Geological and Structural Control of Emerald Mineralization in the Ndola Rural Area, Zambia*. University of Zambia, School of Mines, Lusaka, 72 pp.

Viana R.R., Mänttäri I., Kunst H., Jordt-Evangelista H. (2003) Age of pegmatites from eastern Brazil and implications of mica intergrowths on cooling rates and age calculations. *Journal of South American Earth Sciences*, Vol. 16, pp. 493–501.

Webster R. (1994) *Gems: Their Sources, Descriptions and Identification*, 5th ed. Revised by P.G. Read, Butterworth-Heinemann, Oxford, England.

Wood D.L., Nassau K. (1967) Infrared spectra of foreign molecules in beryl. *Journal of Chemical Physics*, Vol. 47, No. 7, pp. 2220–2228.

Wood D.L., Nassau K. (1968) The characterization of beryl and emerald by visible and infrared absorption spectroscopy. *American Mineralogist*, Vol. 53, No. 5–6, pp. 777–799.

Zambia cranks up the emerald sector (2004) *ICA Gazette*, June, pp. 1, 10–11.

Zwaan J.C. (2001) Preliminary study of emeralds from the Piteiras emerald mine, Minas Gerais, Brazil. *28th International Gemmological Conference*, Madrid, Sprain, pp. 106–109.

Zwaan J.C., Kanis J., Petsch E.J. (1997) Update on emeralds from the Sandawana mines, Zimbabwe. *Gems & Gemology*, Vol. 33, No. 2, pp. 80–100.

Zwaan J.C., Cheilletz A., Taylor B.E. (2004) Tracing the emerald origin by oxygen isotope data: The case of Sandawana, Zimbabwe. *Comptes Rendus Geoscience*, Vol. 336, pp. 41–48.

MT. MICA:
A RENAISSANCE IN MAINE'S GEM TOURMALINE PRODUCTION

William B. (Skip) Simmons, Brendan M. Laurs, Alexander U. Falster, John I. Koivula, and Karen L. Webber

The Mt. Mica area in southwestern Maine has been mined for tourmaline and other pegmatite gems since the 1820s. Most tourmaline production occurred during the late 1800s to the 1910s, with occasional finds made from the 1960s to 1990s. Since May 2004, a new mining venture has produced gem- and specimen-quality tourmaline in a variety of colors. The faceted stones typically are yellowish green to greenish blue, although pink and bicolored or tricolored stones have been cut. Their gemological properties are typical for gem tourmaline. Chemical analysis shows that the tourmaline mined from pockets at Mt. Mica is mostly elbaite, with lesser amounts of schorl, rossmanite, and foitite.

The Mt. Mica deposit has been famous for 185 years as a producer (and the original source) of gem tourmaline in Maine. Tourmaline crystals and cut gems from this historic locality are found in museums and private collections worldwide, and they have been documented in classic works of literature (Hamlin 1873, 1895). After years of no or little activity, recent mining by Coromoto Minerals (Gary and Mary Freeman) has yielded large tourmaline crystals and a modest amount of gem rough. Several stones have been cut, in a wide range of colors (see, e.g., figure 1). Prior to this venture, from 1998 to 2003, Coromoto Minerals successfully mined the Orchard pegmatite in Maine for aquamarine and heliodor.

With the cooperation of Coromoto Minerals, two of the authors (WBS and KLW) recently documented some of the gem pockets as they were excavated, and chemically characterized the tourmalines that were produced. This article first reviews the history of Mt. Mica and then examines the gemological and chemical properties of tourmaline from this historic locality.

HISTORY

Mt. Mica is the site of the first reported occurrence of gem tourmaline in the U.S. (Hamlin, 1895). Since tourmaline was discovered there in 1820 by Elijah L. Hamlin and Ezekiel Holmes (Hamlin, 1873), the pegmatite deposit has been worked by numerous ventures. Some of these activities, as they relate to tourmaline production, are summarized in table 1.

An important development occurred in 1886, when a large pocket found by Augustus C. Hamlin and mine superintendent Samuel Carter yielded a great number of specimens, including a 24 x 5 cm green tourmaline crystal that was broken into four pieces. Faceting of this tourmaline produced the 34.25 ct center stone for the famous Hamlin necklace (Perham, 1987). This necklace, commissioned by A. C. Hamlin, featured 70 cut stones from Mt. Mica with a total weight of 228.12 carats, which included pink,

Figure 1. Recent mining at the historic Mt. Mica pegmatite has produced gem tourmaline in a variety of colors. Shown here are some of the samples that were characterized for this report (0.78–11.72 ct). The stones were faceted by Dennis Creaser (Creaser Jewelers, South Paris, Maine) and are courtesy of Coromoto Minerals Inc.; photo © Jeff Scovil.

blue-green, blue, and green tourmaline, as well as colorless tourmaline and beryl (figure 2). It was donated to the Harvard Mineralogical Museum in 1934 and is considered one of the most significant pieces of North American jewelry ever produced (Fales, 1995).

Using simple drilling and blasting techniques, the early miners at Mt. Mica uncovered numerous pockets from shallow workings (figure 3). As these excavations progressed to deeper levels of the pegmatite, the miners began employing more innovative techniques. During the period from 1890 to 1913, when Loren B. Merrill and L. Kimball Stone had the miner-

al exploration rights at Mt. Mica, they used a large derrick to remove boulders from a deep trench (figure 4). The location of the stacked boulders that formed one side of the trench is shown in figure 5, along with the sites of other workings and discoveries.

Mining activity at Mt. Mica was eventually affected by the fabulous new tourmaline finds in southern California that began in the early 1900s. The abundance of tourmaline from California contributed to the decline in mining at Mt. Mica, where activity was sporadic at best from the 1920s until recently.

TABLE 1. Chronology of gem tourmaline production at Mt. Mica, prior to mining by Coromoto Minerals.

Year	Event	Reference
1822	Cyrus and Hannibal Hamlin produce red and green tourmaline.	Hamlin (1873)
~1866	Ordesser Marion Bowker[a], owner of the farm that encompasses Mt. Mica, opens a large pocket of tourmaline. This creates a renewed interest in the mine by Augustus and Elijah Hamlin.	Hamlin (1895)
1868–1890	Augustus and Elijah Hamlin produce numerous fine tourmaline specimens and gem material from several pockets; much of the top-quality material is acquired by Harvard University and Tiffany & Co. in New York.	Hamlin (1895); Perham (1987)
1891	Loren B. Merrill and L. Kimball Stone recover exceptional blue tourmalines.	Hamlin (1895)
1899	Merrill and Stone find a 411 ct blue-green tourmaline gem nodule that was part of a crystal over 20 cm long. A second 584 ct gem nodule found in a later pocket is now in the Harvard Mineralogical Museum collection.	Perham (1987)
1904	Merrill and Stone open a large pocket that produces over 75 pounds (34 kg) of tourmaline crystals, including near-colorless nodules and a single multicolored tourmaline crystal over 30 pounds (13.6 kg).	Perham (1987)
1926	Howard Irish purchases Mt. Mica, but the deposit lays idle until the 1940s. In 1949 he leases the deposit to the United Feldspar Corp.	King (2000)
1964–65	Frank Perham produces green and bicolored tourmaline.	King (2000)
1979	Plumbago Mining Corp. excavates the large "Dagenais" pocket.	Francis (1985)
1990s	Specimen- and gem-quality tourmalines are occasionally produced by Plumbago Mining Corp.	R. Naftule, pers. comm. (2005)

[a] *Although the spelling is commonly indicated as "Odessa" Bowker in the literature, independent research by R. Sprague (e.g., 1870 U.S. Federal Census, State of Maine) indicated that the farm owner and miner of the tourmaline pocket was a man named Ordesser.*

Figure 2. The Hamlin necklace is considered one of the most significant pieces of North American jewelry. It was commissioned by Augustus C. Hamlin after he and Samuel Carter found a large pocket of tourmaline at Mt. Mica in 1886. The necklace contains 228.12 carats of colored tourmaline, as well as colorless tourmaline and beryl. Courtesy of Harvard Mineralogical Museum; photo © Tino Hammid.

Figure 3. The yellow flags mark the location of gem pockets in the early days of mining at Mt. Mica, circa 1890. Shown are L. Kimball Stone (left) and Loren B. Merrill (right); modified from Bastin (1911, plate 12, p. 84).

In 1964–65, Frank Perham mined the old Merrill and Stone diggings and produced some notable tourmalines, from which an eye-clean 25 ct green stone and a flawless 59.59 ct blue-green stone were cut (King, 2000). The latter stone and the original crystal were documented by Crowningshield (1966a,b). Perham continued to work the property after it was purchased by Plumbago Mining Corp. in 1973. In 1979, the large "Dagenais" pocket (4 x 5.5 x 16 m) was found and required two months to excavate (Francis, 1985). Later, after a brief period of inactivity, Plumbago and private investors re-opened Mt. Mica in 1989. Although tourmaline was recovered sporadically, the results were not considered economically viable, and mining ceased in the late 1990s.

Coromoto Minerals acquired the Mt. Mica property in 2003 and soon started to systematically remove portions of the entire pegmatite. This approach has proven highly successful, with 43 pockets found in the first two years of mining. Two of the pockets have produced large gemmy crystals of tourmaline, which rival the best material that has come from Mt. Mica in its 185-year history (see Mining and Production section).

LOCATION AND ACCESS

The Mt. Mica mine, which is closed to the public, is located about 6 km northeast of the small town of South Paris in Oxford County, southwestern Maine (figure 6). The mine is situated on a small hill, at an elevation of 295 m (970 feet), in forested terrain. Due to typically severe winter conditions, most of the pegmatite mines in this area are operated from March through October. The Mt. Mica mine is operated year round, weather permitting.

GEOLOGY

The Mt. Mica tourmaline deposit is a large, pocket-bearing granitic pegmatite that belongs to the Oxford pegmatite field of southwestern Maine (Wise and Francis, 1992). The Oxford field is spatially related to the Sebago batholith. Pegmatites are concentrated within and around the northeastern margin of this batholith, and they are therefore inferred to be genetically related. Uranium-lead isotopic data indicate that the age of the Sebago Batholith is 296 ± 3 million years (Foord et al., 1995).

According to recent observations by the authors, the Mt. Mica pegmatite strikes northeast and dips moderately southeast (typically about 30°) within

Figure 4. The images on these post cards show mining activities at Mt. Mica around the turn of the 20th century. A large derrick (left; printed by The Hugh C. Leighton Co., Portland, Maine) was used to remove boulders from a deep trench (right; printed by The Metropolitan News Co., Boston, Massachusetts). Remnants of the stacked boulders shown in the right image still can be seen today. From the private collection of Jane C. Perham.

the metasedimentary host rock. It is exposed for about 135 m along strike and ranges in thickness from about 1.5 m at the western exposure near the surface to over 8 m thick in places further down dip. The pegmatite is poorly zoned, with a thin (2–5 cm) wall zone and a 1.5-m-thick intermediate zone in the thicker portion of the dike. The intermediate zone consists principally of quartz and K-feldspar, with lesser amounts of schorl and muscovite. The core consists mainly of quartz, microcline, and schorl, with local pods of cleavelandite and rare areas of lepidolite with spodumene, pollucite, cassiterite, columbite, and very rare beryl. Pockets are relatively abundant in the central area of the dike

(again, see figure 5), where Coromoto Minerals has averaged about one cavity every 3 m. In this area, the miners have learned to recognize several indications of pocket mineralization, including wisps of lepidolite, large muscovite "books" (particularly near pods of massive quartz), masses of friable cleavelandite, rust-colored fractures crosscutting the inner zones, and large schorl crystals that point downward toward the cavities.

MINING AND PRODUCTION

Coromoto Minerals began mining at Mt. Mica in July 2003; they have posted detailed reports about
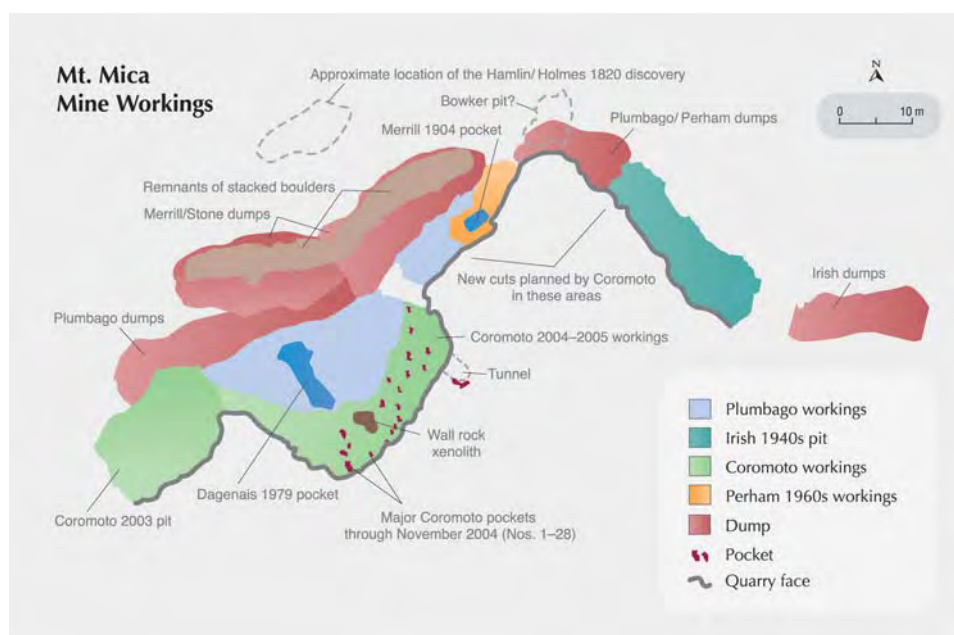
Figure 5. The locations of both historic and modern mining activities at Mt. Mica are shown on this diagram. From a drawing by Gary Freeman.

Figure 6. Mt. Mica is located in southwestern Maine near the small town of South Paris.

Figure 7. An excavator and dump truck are used to remove mined material from the open cut at Mt. Mica, as shown in this October 2004 photo by Gary Freeman.

Figure 8. The entrance to a large pocket (no. 7) containing mostly green tourmaline is marked by the small tunnel just in front of the men in the pit. Note the location of this pocket within a pronounced bulge in the thickness of the predominantly light-colored pegmatite. Photo by Alexander Falster.

significant finds on the Internet at www.coromotominerals.com. In addition, a separate article (Simmons et al., 2005) will review the history and recent specimen mining in more detail.

The miners (Gary and Mary Freeman, together with Richard Edwards) initially used an excavator to expose the pegmatite from beneath the old dump material. Subsequently, they used drilling and blasting to mine the pegmatite in an open cut, and they removed material from the pit using an excavator and dump truck (figure 7).

Several small pockets containing smoky quartz and blue apatite were encountered in 2003, but the first significant tourmaline discovery did not occur until May 2004, when pocket no. 7 was entered. This cavity was found in an area where the pegmatite showed a local bulge in thickness (figure 8). Hundreds of gemmy crystals of predominantly green tourmaline were produced. Most ranged up to 3 cm long and 0.5 cm in diameter, with pink cores that were commonly altered to a pink clay. The zoned crystals with unaltered pink cores resembled the classic "watermelon" pieces pictured in Hamlin (1895). A modest number of small gem-quality pink crystals also were recovered from this pocket. In all, about 1 kg of gem rough was produced, and most of the faceted stones examined for this article came from this pocket.

Figure 10. Two of the most significant tourmaline crystals recently recovered by Coromoto Minerals are shown here. On the left is a 19-cm-tall tricolored elbaite crystal (reassembled from three pieces) on a matrix of cleavelandite and lepidolite that was recovered from pocket no. 10. On the right is a multicolored crystal from pocket no. 28 that measures 22 cm tall, and forms the top portion of a crystal that was originally 54 cm long. Chemical analyses showed the colored portion to be elbaite, while the thin black flat termination is foitite. Composite photo by Gary Freeman.

Figure 9. In June 2004, fine tourmaline crystals were recovered from pocket no. 10. The crystal on the left (approximately 10 cm long) forms the top portion of the reassembled specimen shown in figure 10. The crystal on the lower right is part of a separate specimen. A chisel is shown for scale. The dark material consists of fragments of the overlying metasedimentary host rock. Photo by Gary Freeman.

In June 2004, the miners opened a series of pockets that appeared to line up with pocket no. 7 and the 1979 Dagenais pocket (again, see figure 5). It is possible that this zone of pockets extends even further down dip. Most notable was pocket no. 10, which contained more well-formed green and multicolored tourmalines (figure 9), including a broken 19-cm-long color-zoned crystal that is probably the finest tourmaline specimen found at Mt. Mica and one of the best ever mined in New England (see the left crystal in figure 10).

From June through December 2004, an additional 18 pockets were encountered. The company's most important discovery was made in late December 2004, with the opening of pocket no. 28 (figure 11). This cavity, which exceeded 7 m long, consisted of three connected chambers. Several cathedral-type smoky quartz crystals weighing ~20 kg were found at the edges of the pocket. The miners eventually recovered several hundred bicolored green/pink and green/colorless tourmaline crystals ranging up to 5–8 cm long and <1 cm in diameter

Figure 11. The largest and most important cavity found by Coromoto Minerals at Mt. Mica was 2004 pocket no. 28. Here, Richard Edwards (left) and Frank Perham are shown at the beginning of the excavation in late December. Photo by Gary Freeman.

by screening the pocket mud. They also recovered some much larger tourmalines, including a 22-cm-tall elbaite crystal that grades from reddish pink to orange with a thin black flat termination (see figure 10, right). When four additional pieces of this crystal were subsequently recovered, it was determined that the entire crystal was originally 54 cm long—the largest elbaite tourmaline known from Maine and perhaps the largest from North America.

The 2005 mining season began in March, with the miners clearing debris from the pit and driving a

Figure 12. A small loader is used to remove pegmatite material from the underground workings at Mt. Mica. June 2005 photo by Brendan Laurs.

decline (tunnel) into the pegmatite from the northeastern portion of the 2004 open cut, near pocket no. 28. A new loader for working underground was purchased (figure 12), and Jim Clanin—an experienced gem pegmatite miner from southern California—joined the mining crew. As of mid-June 2005, the decline reached approximately 20 m deep and they had encountered nine small pockets—some with fine green and greenish blue gem tourmaline.

The crystal specimens produced by Coromoto Minerals are being marketed to mineral collectors through Graeber & Himes, Fallbrook, California. As a byproduct of the crystal mining, the mine owners have accumulated a few kilograms of gem rough. Most of this material shows various shades of green (from pocket nos. 7 and 11). So far, a few dozen gemstones (described below) have been faceted from broken crystals. As mining progresses in 2005, such rough material will continue to be stockpiled for future cutting and marketing.

MATERIALS AND METHODS

Standard gemological properties were obtained on 45 faceted Mt. Mica tourmalines that were cut from material produced from May 2004 to early 2005. The samples weighed 0.78–16.48 ct and were faceted in a variety of shapes, including rectangular (some with a checkerboard style), round, oval, pear, square, and freeform. The samples reportedly were not treated in any way.

We used a GIA Instruments Duplex II refractometer with a near-sodium equivalent light source for refractive index readings, and determined specific gravity by the hydrostatic method. The samples were tested for fluorescence in a darkened room with four-watt long- and short-wave UV lamps. Internal features were observed with a standard gemological microscope, and a polariscope was used to view optic figures and check for strain. Inclusions in four samples were investigated by Raman spectroscopy at GIA in Carlsbad, using a Renishaw 2000 Ramascope.

Quantitative chemical analyses were obtained by electron microprobe at the University of New Orleans, Louisiana, on 363 fragments of tourmaline from pocket nos. 7 and 28. Some of these samples were taken from the same pieces of rough used to facet the stones described above. The fragments were mounted on 1 inch (2.5 cm) glass disks with epoxy, and were ground and polished with 0.05 μm alumina powder. The mounted samples were then

ultrasonically cleaned and carbon coated. When possible, the samples were mounted so that analytical traverses could be performed from core to rim. Also analyzed were two Mt. Mica tourmaline crystals that were collected in 1890 by A. C. Hamlin (from the collection of Peter Lyckberg) and 10 additional tourmaline crystals mined in 1964 by Frank Perham (from the collections of Ray Sprague and Jane Perham). These crystals were partially mounted in epoxy so that the smoothest, glass-like prism surfaces could be used for analysis.

Analyses were conducted with an ARL SEMQ electron microprobe operated at an acceleration potential of 15 kV, a beam current of 15 mA, and a spot size of 2 μm. An acquisition time of 45 seconds per spot was used. The number of cations in the formula of each analysis was calculated so that the data could be plotted and the tourmaline species identified. Since some elements in tourmaline (i.e., boron, lithium, and hydrogen) cannot be measured by electron microprobe, we calculated the cations (and wt.% oxides) according to standard assumptions and conventions (see Deer et al., 1992).

RESULTS AND DISCUSSION

The gemological properties are summarized in table 2, with details described below.

Visual Appearance. Overall, the faceted samples could be separated by color into groups of yellowish green, pink (including orangy pink and brownish purplish red), greenish blue, and bicolored or tricolored with green, pink, and/or near-colorless zones. Most of the stones showed weak-to-moderate saturation and light-to-medium tone—with dark tones seen in some of the green stones that were cut with their tables oriented perpendicular to the c-axis.

All of the samples were transparent. In general, the pink, yellowish green, and greenish blue stones were lightly included (commonly with no inclusions visible to the naked eye), whereas the multicolored samples contained obvious partially healed fractures and feathers.

Physical Properties. There were only slight variations in the refractive indices, which could not be correlated to color. The most typical values were $n_o = 1.639$ and $n_e = 1.620$ (yielding a birefringence of 0.019). Although S.G. values ranged from 3.04 to 3.08, the lower values (3.04–3.05) were obtained for the multicolored stones, probably due to the presence of abundant fluid inclusions. Most of the samples that were only lightly included had S.G. values ranging from 3.05 to 3.07.

In the polariscope, typical uniaxial optic figures could be resolved in all of the stones in which the faceting did not obscure view of the optic axis. Subtle patchy or sector-like patterns were seen along the optic axis direction in a few samples; no evidence of significant strain was noted in any of the tourmalines.

The gemological properties of the Mt. Mica samples are consistent with those reported in the litera-

---

TABLE 2. Properties of the 45 faceted samples of tourmaline from Mt. Mica, Maine.

| Property	Description
Color	Most were yellowish green or multicolored in yellowish green, pink, and/or near colorless. Other stones were pink, orangy pink, brownish purplish red, and greenish blue.
Pleochroism	*Yellowish green:* Weak to strong (depending on color saturation), in yellowish green and slightly bluish green *Pink:* Weak, in purplish pink and orangy pink *Greenish blue:* Weak or very weak, distinguishable by a slight brown tint
Clarity	Transparent; lightly to heavily included
Optic character	Uniaxial negative
Refractive indices	
$\quad n_o$	1.638–1.640
$\quad n_e$	1.619–1.622
Birefringence	0.018–0.020
Specific gravity	3.04–3.08
UV fluorescence	
$\quad$ Short-wave	Inert
$\quad$ Long-wave	Inert
Internal features	Most common were partially healed fractures, "feathers," and growth zoning. Other features included color zoning, fine needle-like tubes, linear or planar trails of pinpoints, planar two-phase (liquid-gas) inclusions, mineral inclusions (feldspar and low-relief grains that could not be identified), and cavities.
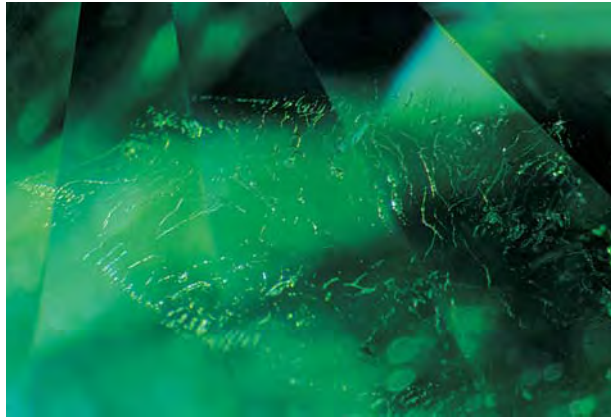
Figure 13. Network stringers of filamentary fluid inclusions known as "trichites" are characteristic of tourmalines from many localities, including Mt. Mica. Photomicrograph by John I. Koivula; magnified 10x.
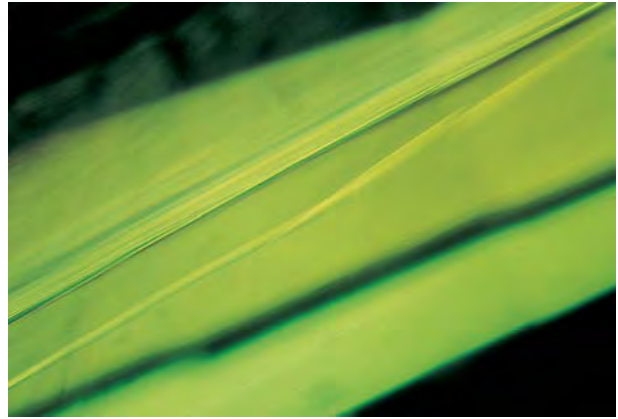

Figure 14. Sharp-edged, elongated straight-to-angular growth zoning, as revealed by shadowed illumination in this Mt. Mica tourmaline, is often encountered in tourmalines in general. Photomicrograph by John I. Koivula; magnified 15x.

ture for gem tourmaline (see, e.g., Webster, 1994). Although the lowest R.I. values we obtained were slightly below the range reported by Webster (1994), they fell within the values given by Dunn (1975) for tourmaline from Newry, Oxford Co., Maine (1.612–1.644). The lack of any correlation between R.I. and color in our Mt. Mica samples also was documented for Newry tourmaline by Dunn (1975). However, the weak violet fluorescence to short-wave UV observed by Dunn (1975) in pink and red Newry tourmaline was not found in the similar-colored samples from Mt. Mica that we studied.

Microscopic Features. The most conspicuous inclusions consisted of partially healed fractures and "feathers". A wide diversity of characteristics related to healed fractures were recorded: flat planar-to-curved aggregates of minute fluid inclusions, spindle- and irregular-shaped "trichites" (figure 13), linear or planar trains of pinpoints, and flat two-phase inclusions with conspicuous gas bubbles suspended within fluid. Growth zoning was also quite common, but relatively inconspicuous, forming linear, planar, or angular patterns (figure 14). The growth zoning was most prevalent in the greenish blue samples and the multicolored stones; in the latter, the growth lines were oriented parallel to the color zoning.

Other microscopic features included fine needle-like tubes (often in parallel arrays) and small

Figure 15. This inclusion in a Mt. Mica tourmaline was identified as feldspar by Raman analysis. Fluid inclusions also are visible in the immediate vicinity. Photomicrograph by John I. Koivula; magnified 20x.

Figure 16. Cross-polarized light has produced interference colors in this inclusion, which is probably a crystal of tourmaline within tourmaline from Mt. Mica. Photomicrograph by John I. Koivula; magnified 15x.
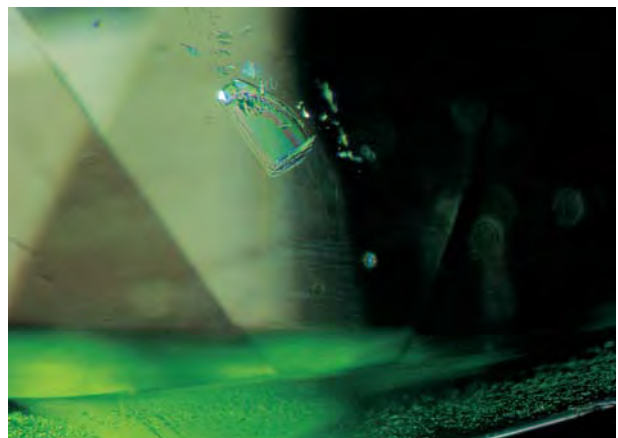
cavities. Mineral inclusions were seen in six of the 45 samples, typically as isolated, high-relief, rather equant colorless grains. In three of the samples, these inclusions were identified as feldspar by Raman analysis (see, e.g., figure 15), probably sodic plagioclase (i.e., "cleavelandite"), since this variety of albite is commonly associated with the tourmaline in the Mt. Mica gem pockets. Two additional samples contained low-relief colorless grains exhibiting strong birefringence (figure 16), but these could not be identified by Raman analysis due to their small size and/or position within the stones. Their appearance suggested that they were inclusions of tourmaline within their tourmaline hosts.

Chemical Composition. The tourmalines analyzed for this study were found to consist of four species: elbaite, schorl, foitite, and rossmanite (table 3). Notably, all four species were present in one pocket (no. 28). Representative electron-microprobe data for tourmalines from pocket nos. 7 and 28 are shown in table 4. As shown in figure 17, the analyses mostly fell in the elbaite field, although a few corresponded to rossmanite. The elbaite colors ranged from dark green/black to lighter green to pink. Most of the pink and red elbaites were distinctly enriched in Ca (liddicoatite component) relative to other colors. The green tourmalines were mostly lower in Ca and richer in Na (elbaite component). Near-colorless samples tended to have low Ca and greater X-site vacancies (rossmanite component).

TABLE 3. General chemical formulas of tourmaline species found at Mt. Mica.	
Species	Formula[a]
Elbaite	$Na(Li_{1.5},Al_{1.5})Al_6(BO_3)_3Si_6O_{18}(OH)_4$
Schorl	$NaFe_3^{2+}Al_6(BO_3)_3Si_6O_{18}(OH)_4$
Rossmanite	$\square(LiAl_2)Al_6(BO_3)_3Si_6O_{18}(OH)_4$
Foitite	$\square(Fe_2^{2+}Al)Al_6(BO_3)_3Si_6O_{18}(OH)_4$

[a] $\square$ = vacancy

Figure 17. This diagram shows the X-site composition of all the tourmaline samples analyzed from Mt. Mica pocket nos. 7 and 28. The analyses predominantly fell within the elbaite field, although a few points fell on the border or slightly into the rossmanite field. Black tourmaline samples from these pockets consisted of schorl or foitite, but these compositions are not shown on this diagram.
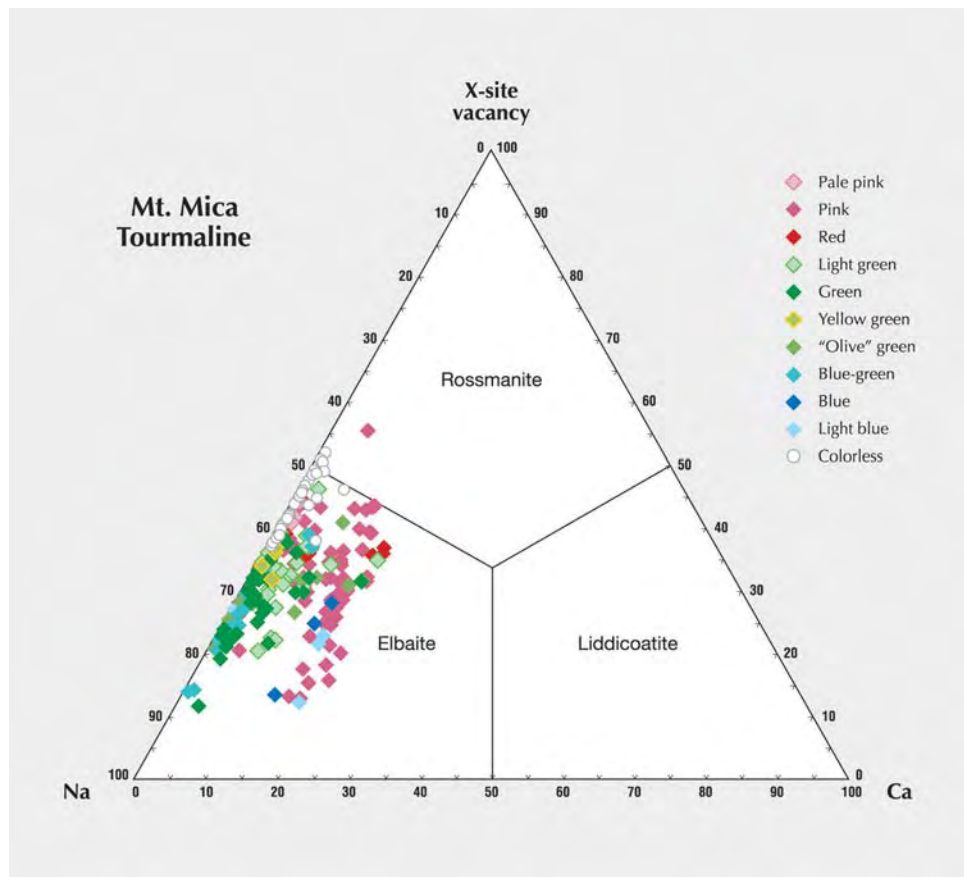
TABLE 4. Representative compositions by electron microprobe of various colors and species of Mt. Mica tourmaline.[a]

Chemical composition	Pale pink Elbaite	Pink Elbaite	Red Elbaite	Light green Elbaite	Green Elbaite	Yellow-green Elbaite	"Olive" green Elbaite	Blue-green Elbaite	Blue Elbaite
Oxides (wt.%)									
SiO_2	36.80	36.78	36.84	36.79	36.59	36.63	36.76	36.55	36.78
TiO_2	bdl	bdl	bdl	bdl	0.08	bdl	0.18	bdl	bdl
B_2O_3 (calc.)	11.02	11.10	11.07	10.99	10.80	10.97	11.00	10.79	10.83
Al_2O_3	42.89	42.46	42.70	41.78	38.67	41.93	41.57	39.55	38.49
FeO^{tot}	0.07	0.11	bdl	1.33	4.46	0.96	1.79	4.35	5.22
MnO	0.12	0.55	0.29	0.44	1.70	0.41	0.82	0.43	1.20
MgO	bdl	bdl	bdl	0.03	0.03	bdl	0.02	bdl	bdl
CaO	0.07	1.11	1.01	0.32	0.15	0.22	0.14	0.06	0.75
Li_2O (calc.)	1.90	2.11	2.02	1.82	1.43	1.87	1.71	1.48	1.49
Na_2O	2.00	2.01	1.55	2.07	2.38	2.22	2.12	2.10	2.00
K_2O	bdl	0.04	0.01	0.02	bdl	0.02	0.02	0.02	0.03
H_2O (calc.)	3.33	3.36	3.40	3.33	3.18	3.27	3.35	3.31	3.12
F	0.99	1.01	0.88	0.97	1.14	1.09	0.95	0.88	1.31
Subtotal	99.18	100.62	99.78	99.91	100.60	99.61	100.42	99.52	101.22
−O=F	0.42	0.42	0.37	0.41	0.48	0.46	0.40	0.37	0.55
Total	98.76	100.20	99.41	99.50	100.12	99.15	100.02	99.15	100.67
Ions on the basis of 31 (O,OH,F)									
Si	5.802	5.755	5.783	5.815	5.889	5.801	5.805	5.886	5.900
Al	0.198	0.245	0.217	0.185	0.111	0.199	0.195	0.114	0.100
Tet. sum	6.000	6.000	6.000	6.000	6.000	6.000	6.000	6.000	6.000
B	3.000	3.000	3.000	3.000	3.000	3.000	3.000	3.000	3.000
Al (Z)	6.000	6.000	6.000	6.000	6.000	6.000	6.000	6.000	6.000
Al	1.771	1.585	1.683	1.599	1.226	1.628	1.541	1.394	1.177
Ti	bdl	bdl	bdl	bdl	0.009	bdl	0.021	bdl	bdl
Fe^{2+}	0.009	0.015	bdl	0.176	0.600	0.126	0.236	0.586	0.700
Mn	0.015	0.073	0.039	0.059	0.231	0.055	0.109	0.059	0.163
Mg	bdl	bdl	bdl	0.006	0.007	bdl	0.005	bdl	bdl
Li	1.204	1.326	1.277	1.160	0.927	1.190	1.087	0.961	0.960
Y sum	3.000	3.000	3.000	3.000	3.000	3.000	3.000	3.000	3.000
Ca	0.011	0.186	0.170	0.054	0.026	0.038	0.024	0.011	0.129
Na	0.610	0.609	0.471	0.634	0.743	0.683	0.648	0.654	0.620
K	bdl	0.007	0.002	0.004	bdl	0.004	0.005	0.005	0.005
Vacancy	0.378	0.198	0.357	0.308	0.231	0.275	0.324	0.330	0.245
X sum	1.000	1.000	1.000	1.000	1.000	1.000	1.000	1.000	1.000
F	0.496	0.498	0.435	0.486	0.582	0.548	0.472	0.446	0.664
OH	3.503	3.502	3.564	3.514	3.417	3.451	3.528	3.553	3.335

[a] Selected from analyses of 363 samples from pocket nos. 7 and 28, as well as the two 1890 Hamlin and the ten 1964 Perham crystals. Backgrounds were determined by the mean atomic number (MAN) method (Donovan and Tingle, 1996). Standards used include both natural and synthetic materials: albite (Na), adularia (K), quartz and clinopyroxene (Mg, Ca, Fe, Ti), chromite (Cr), rhodonite (Mn), V_2O_5 (V), PbO (Pb), ZnO (Zn), Bi-germanate (Bi), silli-manite (Si and Al), and fluortopaz (F). MAN standards used in addition to those above were corundum, fayalite, hematite, rutile, MgO, $SrSO_4$, and ZrO_2. Detection limits (in wt.% oxide): Ti = 0.008, Fe = 0.005, Mn = 0.006, Mg = 0.012, Ca = 0.007, and K = 0.014. Detection limits of elements analyzed but not detected (in wt.% oxide): V = 0.007, Cr = 0.013, Zn = 0.022, Pb = 0.009, and Bi = 0.016. Li_2O, B_2O_3, and H_2O were calculated based on an assumed elbaite tourmaline stoichiometry. Abbreviation: bdl = below detection limit.

Foitite is a rare tourmaline species that is iron rich in the Y-site and has an X-site that is more than 50% vacant (MacDonald et al., 1993); it formed the thin black flat terminations on some of the pink elbaite crystals (e.g., figure 10, right). The schorl analyses corresponded to the black basal portions of some of the elbaite crystals. The analyzed crystals that were mined in 1890 and 1964 were all elbaite, with compositions that overlapped the more recent-ly mined tourmaline.

As expected, the chromophoric elements Fe, Ti, and Mn showed strong correlation with color (see table 4 and figure 18). Fe was highest in the black tourmaline, and virtually absent in the near-color-less and pink tourmaline. The next-highest Fe val-ues were found in the "olive" green, green, and blue tourmaline. Ti correlated with elevated Fe in the black and green to "olive" green samples. All other colors had very low Ti contents. On average, Mn was highest in the blue and green tourmaline, and was lowest in all light-colored tourmaline.

Fluorine contents were relatively constant, aver-aging 1.08 wt.% and ranging from 0.8 to 1.31 wt.% in all analyses. Mg was present mainly in the black tourmaline, where it averaged 0.54 wt.% MgO and ranged from below the detection limit to 1.38 wt.%

Light blue Elbaite	Colorless Elbaite	Colorless Rossmanite	Black Schorl	Black Foitite
36.60	36.83	37.26	36.51	36.36
bdl	bdl	bdl	0.54	0.07
10.87	11.02	11.10	10.48	10.45
39.50	42.90	43.43	32.65	34.77
3.45	bdl	0.05	13.20	12.54
1.11	bdl	0.20	0.26	0.63
bdl	bdl	bdl	1.30	bdl
0.88	bdl	bdl	0.09	bdl
1.69	1.91	1.79	0.54	0.52
2.04	2.03	1.48	1.82	0.92
0.02	bdl	bdl	0.03	bdl
3.20	3.27	3.38	3.08	3.19
1.17	1.11	0.94	0.88	0.88
100.53	99.09	99.63	101.38	100.32
0.49	0.47	0.40	0.47	0.37
100.03	98.62	99.24	100.91	99.95
5.853	5.809	5.832	6.055	6.046
0.147	0.191	0.168	0.000	0.000
6.000	6.000	6.000	6.055	6.046
3.000	3.000	3.000	3.000	3.000
6.000	6.000	6.000	6.000	6.000
1.299	1.785	1.843	0.381	0.814
bdl	bdl	bdl	0.068	0.008
0.461	bdl	0.007	1.831	1.743
0.151	bdl	0.026	0.036	0.088
bdl	bdl	bdl	0.322	bdl
1.089	1.214	1.124	0.361	0.346
3.000	3.000	3.000	2.999	3.000
0.151	bdl	bdl	0.015	bdl
0.633	0.622	0.449	0.586	0.298
0.004	bdl	bdl	0.007	bdl
0.212	0.378	0.551	0.393	0.702
1.000	1.000	1.000	1.000	1.000
0.590	0.555	0.467	0.589	0.463
3.409	3.444	3.533	3.411	3.537

MgO. In all other colors, Mg was very low to below the limit of detection.

Schorl is found as black tourmaline along the pocket margins, and therefore formed early in crystallization of the miarolitic cavities. As the crystals grew into the pocket, they were progressively enriched in Al relative to Fe. As Fe diminished, elbaite became the dominant tourmaline. Foitite, and possibly rossmanite, represent the final stages of tourmaline compositional evolution in the pockets. Interestingly, the black foitite "caps" noted on some Mt. Mica tourmalines are similar to the "Mohrenköpfe" found on elbaite crystals from

Elba, Italy (Pezzotta, 2001). Elba is the only locality besides Mt. Mica where four tourmaline species have been documented from a single gem pocket (Pezzotta et al., 1998). Although it is not uncommon for multiple tourmaline species to be present in a particular pegmatite deposit or district (see, e.g., Selway, 1999), the occurrence of such a diverse composition of tourmaline in a single pocket appears to be quite unusual.

CONCLUSIONS AND FUTURE POTENTIAL

Gem- and specimen-quality tourmalines were produced in a wide variety of colors at Mt. Mica, mainly in the late 19th century and sporadically from the 1960s to 1990s. In 2004–2005, renewed mining by

Figure 18. These graphs show the average compositions of chromophoric elements Fe, Ti, and Mn (as wt.% oxides) in various colors of tourmaline from Mt. Mica. Fe and Ti are found mainly in the black and green samples, whereas Mn is present in tourmaline of all colors to varying degrees.
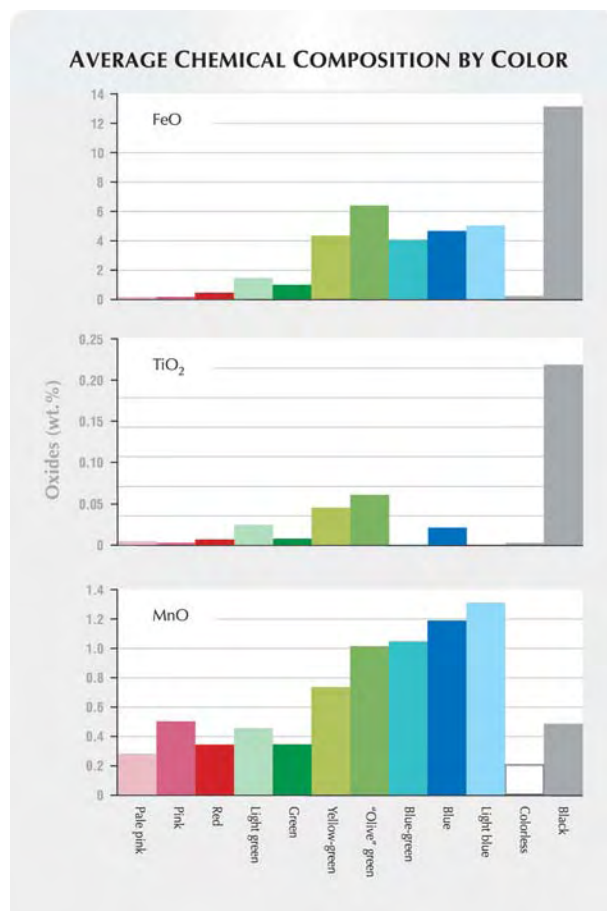

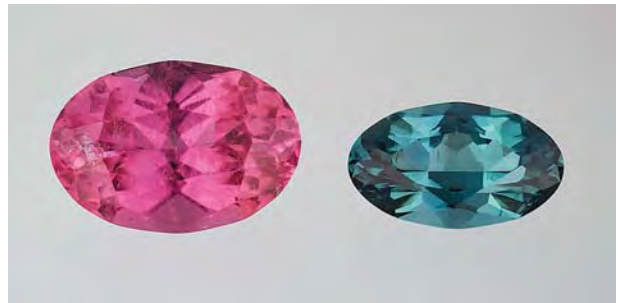AVERAGE CHEMICAL COMPOSITION BY COLOR

Figure 19. Well-formed gem-quality crystals of green tourmaline such as this one (5.4 cm long) from Mt. Mica pocket no. 11 are prized by collectors and connoisseurs. Courtesy of Graeber & Himes, Fallbrook, California; photo © Jeff Scovil.

Coromoto Minerals again produced attractive crystals and cut stones (figures 19 and 20), including some of the finest tourmaline ever recovered from the deposit.

Based on the deposit geology and on the projected mineralization of the pegmatite down dip, Mt. Mica shows considerable potential for additional tourmaline production. Future mining will focus on the deeper extension of the 2004–2005 mineralized zone, as well as on areas of the pegmatite to the northeast that are closer to the surface. As the pegmatite is explored by both open-cut and underground methods, the miners anticipate that more tourmaline will be found at this historic deposit.

Figure 20. Continued mining of the Mt. Mica deposit is expected to yield additional gem tourmaline, such as the bright pink and bluish green stones shown here (9.86 and 4.77 ct). These tourmalines were faceted in early 2005 by Dennis Creaser and studied for this report. Courtesy of Coromoto Minerals Inc.; photo by C. D. Mengason.

REFERENCES

Bastin E.S. (1911) *Geology of the pegmatites and associated rocks of Maine*. U.S. Geological Survey Bulletin 445, 152 pp.

Crowningshield R. (1966a) Developments and highlights at the Gem Trade Lab in New York: Maine tourmaline. *Gems & Gemology*, Vol. 12, No. 2, pp. 43–44.

Crowningshield R. (1966b) Developments and highlights at the Gem Trade Lab in New York: Maine tourmaline. *Gems & Gemology*, Vol. 12, No. 3, pp. 70–71.

Deer W.A., Howie R.A., Zussman J. (1992) *An Introduction to the Rock-forming Minerals*, 2nd ed. Longman Scientific & Technical, Essex, England.

Donovan J.J., Tingle T.N. (1996) An improved mean atomic number correction for quantitative microanalysis. *Journal of Microscopy*, Vol. 2, No. 1, pp. 1–7.

Dunn P.J. (1975) On gem elbaite from Newry, Maine, U.S.A. *Journal of Gemmology*, Vol. 14, No. 8, pp. 357–368.

Fales M.G. (1995) *Jewelry in America*. Martha Gandy Fales and Antique Collector's Club Ltd., Suffolk, England.

Foord E.E., Snee L.W., Aleinikoff J.N., King V.T. (1995) Thermal histories of granitic pegmatites, western Maine, USA. *Abstracts with Programs*, Geological Society of America Annual Meeting, New Orleans, LA, Vol. 27, No. 6, p. A468.

Francis C.A. (1985) Maine tourmaline. *Mineralogical Record*, Vol. 16, pp. 365–388.

Hamlin A.C. (1873) *The Tourmaline*. James R. Osgood & Co., Boston, MA, 107 pp.; republished in 2004 by Rubellite Press, New Orleans, LA.

Hamlin A.C. (1895) *The History of Mount Mica of Maine, U.S.A. and Its Wonderful Deposits of Matchless Tourmalines*. Publ.

by A.C. Hamlin, 72 pp. plus color plates; republished in 2004 by Rubellite Press, New Orleans, LA.

King V.T., Ed. (2000) *Mineralogy of Maine, Vol. 2: Mining History, Gems, and Geology*. Maine Geological Survey, Augusta, ME, 524 pp.

MacDonald D.J., Hawthorne F.C., Grice J.D. (1993) Foitite, $[Fe_2^{2+}(Al,Fe^{3+})]Al_6Si_6O_{18}(BO_3)_3(OH)_4$, a new alkali-deficient tourmaline: Description and crystal structure. *American Mineralogist*, Vol. 78, pp. 1299–1303.

Perham J.C. (1987) *Maine's Treasure Chest—Gems and Minerals of Oxford Co.*, 2nd ed. Quicksilver Publications, West Paris, ME, 267 pp.

Pezzotta F. (2001) Heiss Begehrt: die Mohrenköpfe. *Elba*, extraLapis No. 20, pp. 48–49.

Pezzotta F., Guastoni A., Aurisicchio C. (1998) La rossmanite di Roznà e dell' Elba. *Revista Mineralogica Italiana*, Vol. 22, No. 1, pp. 46–50.

Selway J.B. (1999) Compositional Evolution of Tourmaline in Granitic Pegmatites. Ph.D. dissertation, University of Manitoba, Canada, 363 pp.

Simmons W.B., Freeman G., Falster A., Laurs B., Webber K. (2005) New tourmaline production from Mount Mica: America's first gem pegmatite. *Rocks & Minerals*, Vol. 80, No. 6 (accepted for publication in November-December issue).

Webster R. (1994) *Gems: Their Sources, Descriptions and Identification*, 5th ed. Revised by P.G. Read, Butterworth-Heinemann, London.

Wise M.A., Francis C.A. (1992) Distribution, classification and geological setting of granitic pegmatites in Maine. *Northeastern Geology*, Vol. 14, No. 2–3, pp. 82–93.

LAB NOTES

DIAMOND

Fracture Filled, with Varying Results

Fracture filling is usually effective at making a diamond's fractures less obvious both to the unaided eye and when viewed with magnification, although a trained gemologist often can identify the treatment relatively easily. When the filling is not complete or is poorly executed, however, identification can be much more challenging. Two diamonds recently submitted to the East Coast laboratory highlighted these challenges.

The 9.01 ct rectangular modified brilliant in figure 1 was quickly identified as an artificially irradiated diamond, but as noted in the last issue of this journal (Spring 2005 Lab Notes, p. 46) identification of one treatment may not be the end of a gemologist's work. While the fractures in this diamond were generally quite visible, some contained an unusual texture and flow structure (figure 2) that led us to examine the stone more closely. A careful investigation at high magnification and with the light at varying angles revealed the telltale flash-effect colors associated with fracture filling.

We do not know exactly why the treatment was ineffective in this stone; however, a close look at figure 2 shows that the surface of the facet has a mottled, hazy appearance, which suggests that it may have been burned. Excessive heat can cause a high-lead glass filling to flow out of a fracture, and the dendritic patterns we observed (see also figure 3) support this possibility. One might further speculate that the excessive heat could have been generated during the color treatment process, since creating yellow color through artificial irradiation requires subsequent annealing. The heat necessary (~600°C) would certainly be sufficient to cause the filling material to break down. Thus, the fractures likely became much more visible than they were immediately after the fracture filling.

Another diamond, a 1.52 ct marquise, also had relatively obvious fractures that would not be expected in a clarity-enhanced stone. However, thorough examination with magnification revealed a very unusu-

Figure 1. This artificially irradiated 9.01 ct yellow diamond also showed unusual clarity enhancement features.

Figure 2. Heat treatment of the diamond in figure 1 may have created the unusual texture and flow structure visible within this fracture. Magnified 45x.

Figure 3. This dendritic pattern in another fracture in the 9.01 ct diamond indicates both the presence of a glass filler and exposure to high heat. Magnified 60x.
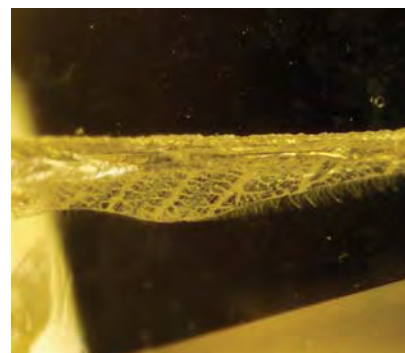
Figure 4. The unfamiliar pattern within this fracture led to closer examination of the 1.52 ct diamond for evidence of clarity enhancement. Magnified 75x.

Figure 5. These subtle flash-effect colors in the 1.52 ct marquise are further indications of clarity treatment. Magnified 50x.

al pattern within the fractures (figure 4), which led us to look closely for more classic indications of clarity treatment. Figure 5 shows the very weak flash-effect colors that we found at higher magnification with the aid of fiber-optic illumination. Again, we do not know the exact reason for this poor result. However, there may have been a problem with the contact between the host diamond and the filler. These situations usually arise when the glass does not fill the entire fracture or it has been altered in some way due to either mishandling or possibly a "flaw" in the treatment process.

Diamonds such as these can create great challenges for the practicing gemologist. Anything unusual bears careful scrutiny, but with diligence the proper identification can often be made using the standard instrumentation available to most gemologists and jewelers.

Thomas Gelb and Matthew Hall

Large Diamond with Micro-inclusions of Carbonates and Solid CO_2

Natural diamonds occasionally contain microscopic inclusions of carbonates, water, apatite, and silicates (see, e.g., O. Navon et al., "Mantle-derived fluids in diamond micro-inclusions," *Nature*, Vol. 335, 1988, pp. 784–789; Winter 2004 Lab Notes, pp. 325–326). These inclusions are encapsulated samples of mantle fluid, and thus are important for geochemical study of the mantle as well as for a better understanding of diamond formation. Although diamonds typically form at a depth of around 140–200 km, micro-inclusions of solid CO_2 were reported in a small rough type IaA diamond that is thought to have formed at a deeper origin, around 220–270 km (M. Schrauder and O. Navon, "Solid carbon dioxide in a natural diamond," *Nature*, Vol. 365, No. 6441, 1993, pp. 42–44). The discovery of solid CO_2 in diamond has very important implications in the study of the earth's mantle. However, that small crystal was the only specimen reported in which solid CO_2 micro-inclusions had been confirmed, except for a brief report of CO_2-bearing diamonds in a recent publication (T. Hainschwang et al., "HPHT treatment of different classes of type I brown diamonds," *Journal of Gemmology*, Vol. 29, 2005, pp. 261–273). Thus, the East Coast laboratory was very interested to examine a large faceted diamond that proved to contain micro-inclusions of solid CO_2 and carbonates, possibly from an even greater depth in the mantle.

The 5.04 ct pear-shaped diamond (14.94 x 9.26 x 6.27 mm; figure 6) of unknown geographic origin was graded D color. Although only a few very tiny pinpoint inclusions were visible with magnification, this stone displayed extremely strong colorless graining that created an undulating translucency throughout the entire diamond (figure 7). This severely affected its clarity, resulting in a grade of SI_2. Linear or planar graining occurred in a limited region close to the point of the pear shape. To the best of our recollection, the undulatory graining in this stone is the most prominent we have seen in the GIA Gem Laboratory.

The infrared spectrum (figure 8) showed no nitrogen- or boron-related absorption, which suggests that it is a type IIa diamond. This was supported by the ultraviolet (UV)-visible absorption spectrum, which did not show any absorption peaks. Unlike typical type IIa diamonds, this stone displayed a moderately strong yellow fluorescence

Figure 6. Spectroscopic analysis of this 5.04 ct D-color diamond revealed that it contains very unusual micro-inclusions of solid CO_2 as well as carbonates.
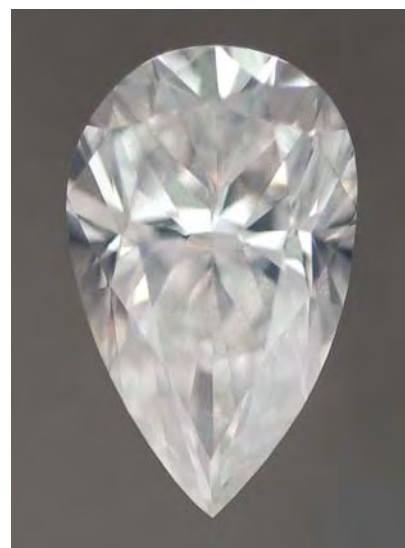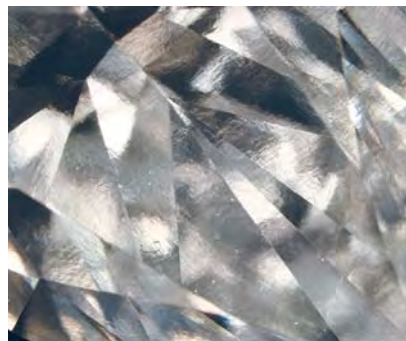
Figure 7. Hazy, undulatory graining is evident throughout the diamond in figure 6. This is the most intense graining seen so far in the laboratory, and it severely affected the diamond's clarity grade (SI_2). Image width is 8.0 mm.

Figure 8. In the IR spectrum of the diamond in figure 6, strong absorptions of solid CO_2 occur at approximately 2376 and 651 cm^{-1}. Weak combination modes at 5141.3, 5019.5, 3753.8, and 3625.3 cm^{-1} also were observed; the weak absorptions at 1474.1 and 886.2 cm^{-1} are most likely from micro-carbonate inclusions.

to short-wave UV radiation. In the Diamond Trading Company (DTC) DiamondView, a moderately strong blue-gray fluorescence and weak blue-gray phosphorescence were observed; the undulatory appearance was also apparent (figure 9). Natural type IIa diamonds rarely phosphoresce.

The IR spectrum exhibited strong absorptions of fundamental modes of solid CO_2 at ~2376 (v3) and ~651 (v2) cm^{-1}. These two absorptions were so strong that their positions could not be precisely determined. Weak combination modes at 5141.3, 5019.5, 3753.8, and 3625.3 cm^{-1} also were observed. Close examination of these absorption positions and comparison with high-pressure spectral data of solid CO_2 revealed that the positions of these combination modes closely fit those seen in solid CO_2 under a pressure of 6.3 ± 0.4 GPa at room temperature (see R. C. Hanson and L. H. Jones, "Infrared and Raman studies of pressure effects on the vibrational modes of solid CO_2," *Journal of Chemical Physics*, Vol. 75, 1981, pp. 1102–1112). This pressure is higher than the 5 ± 0.5 GPa in the stone reported by Schrauder and Navon (1993). Extrapolation to a mantle temperature of 1,200°C results in a pressure of 9.2–9.7 GPa, about 270–290 km in mantle depth. These very likely represent the conditions under which the

diamond originally crystallized. These pressure regimes are much higher than those in which most natural diamonds have grown (5–6 GPa), which further indicates that this diamond formed deeper in the mantle.

The weak absorptions observed at 1474.1 and 886.2 cm^{-1} (again, see figure 8) are most likely from micro-carbonate inclusions. These peak positions do not entirely fit with those of published calcite or magnesite positions at ambient conditions, and a pressure effect

Figure 9. The undulatory graining seen in figure 7 is also apparent in the DTC DiamondView fluorescence image.

like that of solid CO_2 is highly possible. The weak absorptions at 1274.3, 1113.5, 990.8, and 827.7 cm^{-1} may be from other components that also occur as micro-inclusions. However, their assignment is not clear at this moment. Raman spectroscopy showed no Raman peaks for solid CO_2 or carbonates, but it did reveal many unusual photoluminescence emissions at liquid-nitrogen temperature using 488 nm laser excitation (figure 10). Except for the 3H emission at 503.5 nm, little is known about the assignment of other observed lines, which rarely occur in "standard" natural diamonds.

We believe the micro-inclusions and associated graining are the main cause of the undulatory hazy appearance. The micro-inclusions of solid CO_2 and carbonates in this gem diamond indicate a localized pocket of carbonate-rich material within the deep mantle (>200 km). Furthermore, this environment must have been stable for an extended period, allowing for the growth of this fairly large gem-quality diamond. This diamond represents the largest of those so far reported from the deep mantle. It is an unusual

PHOTOLUMINESCENCE SPECTRUM
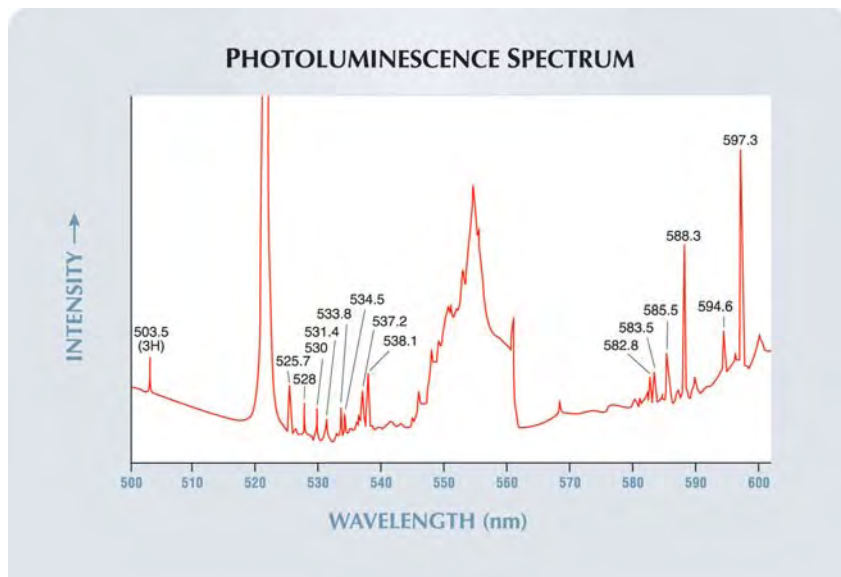
Figure 10. Except for the 3H emission at 503.5 nm, little is known about the assignment of the many photoluminescence emissions observed in the 5.04 ct diamond.

stone not only because of its special gemological properties but also for its importance in studying the earth's mantle and diamond formation.

Wuyi Wang, TM, Kyaw Soe Moe, and Andy Hsi-Tien Shen

Light Blue Diamond, with Type IIb and IIa Zones

Like some forms of nitrogen, boron occurs as individual atoms substituting for carbon in the diamond structure. However, boron and nitrogen typically do not coexist in natural diamonds. Unlike nitrogen-bearing diamonds and synthetic blue diamonds, which frequently exhibit distinctive growth zoning (best seen with the DTC DiamondView), most natural type IIb diamonds appear to have no—or only very subtle—zoning.

An interesting 0.67 ct light blue pear shape was recently submitted to the West Coast laboratory for grading (figure 11, left). Initial infrared absorption spectroscopy indicated that this diamond was type IIa, which suggested that the color was due to radiation-related defects. Low-temperature visible absorption spectroscopy, however, revealed the spectrum of a colorless IIa

diamond with no evidence of radiation damage. The discrepancy between the spectroscopy and the light blue body-color led us to undertake a careful gemological examination.

The diamond was inert to long-wave UV radiation and fluoresced a very weak yellow to short-wave UV, with brief, very weak blue phosphorescence. When tested with a gemological conductometer, the stone showed slight electrical conductivity in certain directions. No color zoning was apparent when the pear shape was viewed

with the microscope and diffused white light. Because in general these properties are consistent with type IIb diamonds, we decided to perform detailed UV imaging and collect spectroscopic data from different parts of the stone.

Phosphorescence in type IIb diamonds directly reflects the presence of boron, so we examined the diamond using the phosphorescence setup of the DiamondView to try to map the boron distribution. We were able to see small blue phosphorescent areas near the head and point of the pear shape that were not visible in the belly (figure 11, right). The degree to which the phosphorescent areas near the point represented boron enrichment is unclear, due to the tendency of pear-shaped brilliant cuts to collect color at the point. Our initial spectroscopic data had been collected by passing the beam through the girdle of the diamond at the belly; however, when the same measurements were taken near the head (where we saw the phosphorescent areas), the new absorption spectra revealed the presence of low concentrations of boron (figure 12). Although it is possible that hydrogen-boron complexes within the diamond may contribute to some of the observed features, the distinct differences in phosphorescence and the spectroscopic data collected from various parts of the stone strongly suggest that the diamond consisted of a mix-

Figure 11. This 0.67 ct Light blue pear-shaped diamond (left) was submitted for a colored diamond grading report. A DiamondView phosphorescence image (right) shows weak blue phosphorescence concentrated near the head and point of the pear shape.

MID-IR ABSORPTION SPECTRA

Type IIa zone **1**

Type IIb zone **2**

2803

4087

WAVENUMBER (cm⁻¹)

VISIBLE ABSORPTION SPECTRA

Type IIb zone **2**

Type IIa zone **1**

WAVELENGTH (nm)
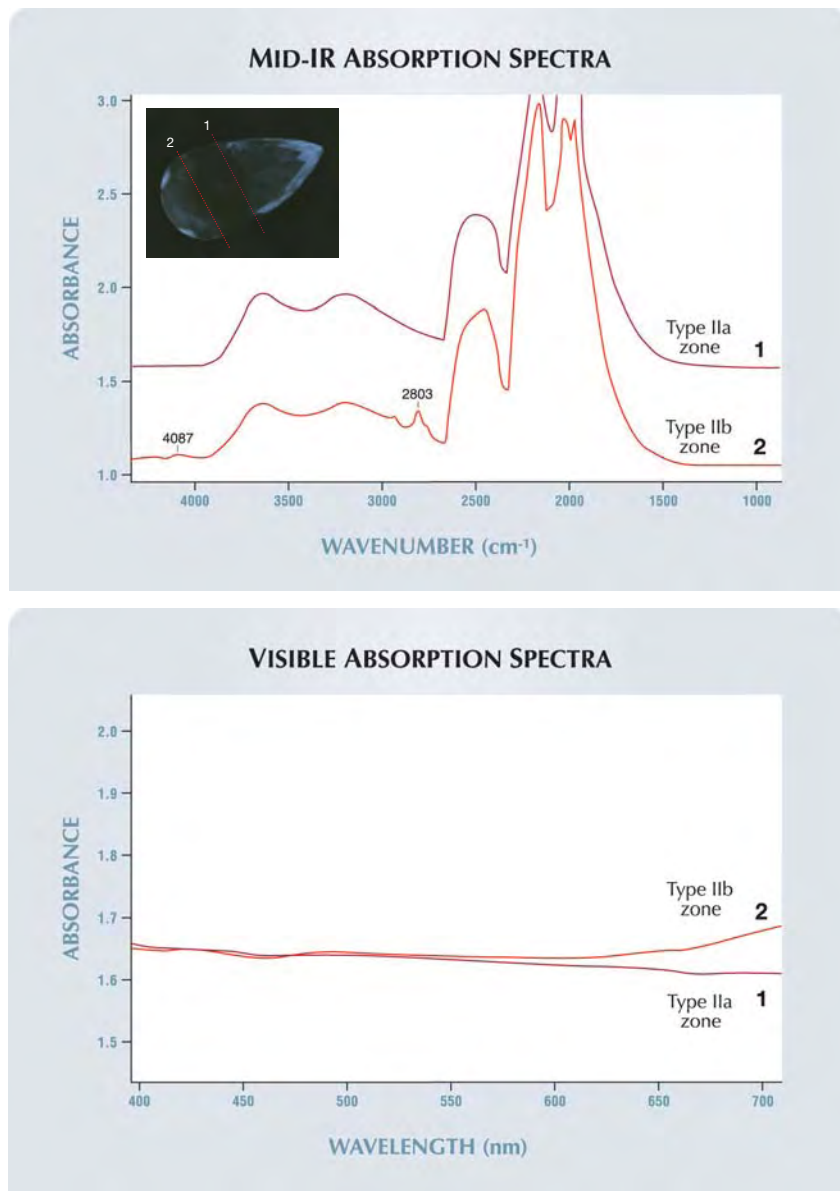
Figure 12. Mid-infrared (top) and visible (bottom) absorption spectra were collected from two different portions of the Light blue diamond, as indicated by the two lines in the phosphorescence image (top, inset). As would be expected from that image, the presence of boron is apparent only in the no. 2 spectra, as evident from the 2803 cm⁻¹ IR feature and the increase in absorption at the red end of the visible spectrum (~600–700 nm).

ture of type IIa and IIb zones.

The Lab Notes section has published reports on a few other mixed type IIa and IIb diamonds (see Fall 1963, p. 85; Winter 1966–1967, p. 116; Fall 1993, p. 199; Summer 2000, pp. 156–157). Although spectroscopic data were not available from these reports, the nature of the type IIa/IIb zoning appears very similar to that of the diamond described here. This type of zoning in blue diamonds may be more common than we have believed.

Christopher M. Breeding

Natural Type Ib Diamond with Unusually High Nitrogen Content

Nitrogen is by far the most common impurity in diamonds. If most of the nitrogen in a diamond is present as isolated nonaggregated atoms within the crystal lattice (i.e., single substitutional N, or C-centers), the diamond is considered to be type Ib. Even very small amounts of this type of nitrogen (<10 ppm) can produce vivid yellow or orange-yellow colors, sometimes resulting in the highly sought-after "canary" diamonds (see, e.g., the article by J. M. King et al. on pp. 88–115 of this issue). Most natural type Ib diamonds contain less than 100 ppm of single substitutional N, though synthetic diamonds commonly contain much more. The concentration of C-centers in synthetic yellow diamonds typically ranges up to ~200 ppm, but may be even higher in deeply saturated yellow-orange or brown colors.

The West Coast laboratory recently had the opportunity to examine a natural diamond with unusually high Ib nitrogen content. The 0.24 ct Fancy Dark pink-brown oval cut shown in figure 13 contained so much nitrogen that the signal intensity in the region of the mid-infrared absorption spectrum where nitrogen is measured (the one-phonon region, ~1400–800 cm⁻¹) exceeded the limits of our detector. Higher-resolution data revealed that the diamond was mostly type Ib with

Figure 13. This 0.24 ct Fancy Dark pink-brown oval-cut diamond proved to have an unusually high type Ib nitrogen content.

MID-IR ABSORPTION SPECTRUM
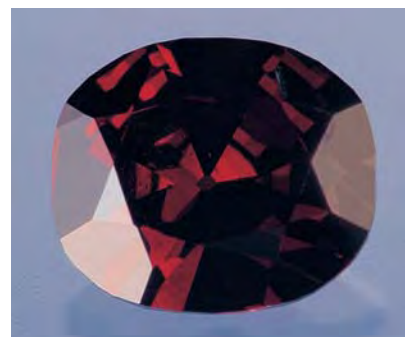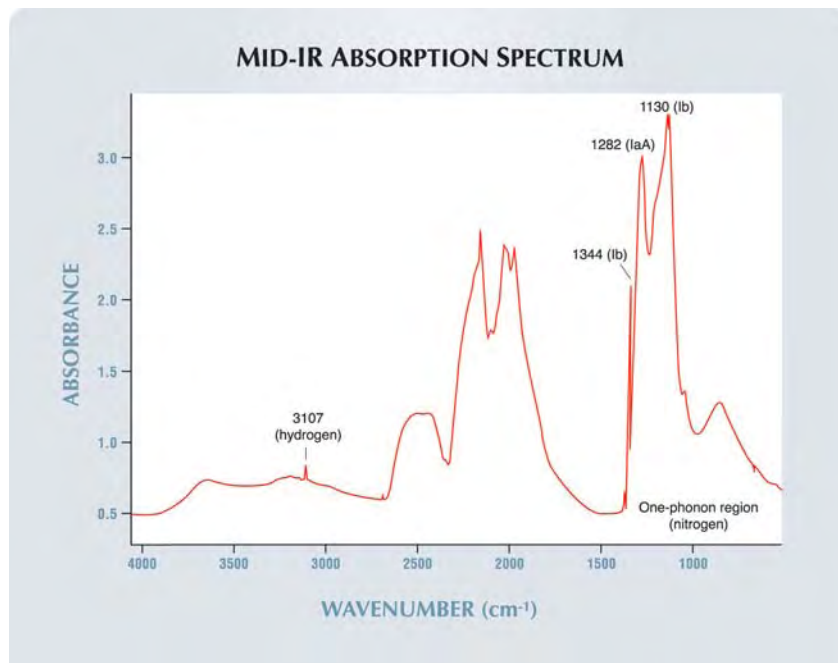
Figure 14. The mid-infrared absorption spectrum of the diamond in figure 13 displays peaks at 1344 and 1130 cm⁻¹, indicating a very high type Ib nitrogen content, as well as some type IaA nitrogen and small amounts of hydrogen.

Figure 15. The visible spectrum of the diamond in figure 13 shows complete absorption below ~515 nm and a broad band centered at ~610 nm; the latter probably contributes the pink component to the diamond's color.

VISIBLE ABSORPTION SPECTRUM
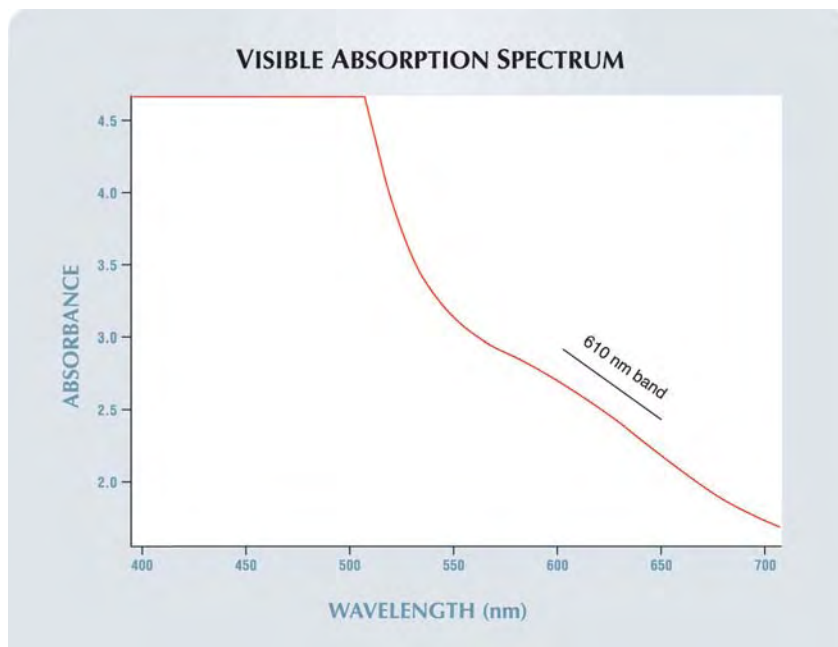
some type IaA (aggregated) N and also contained minor hydrogen (figure 14). Using FTIR software specially designed to measure nitrogen concentrations in diamond, we calculated levels of 364 ppm Ib nitrogen and 132 ppm IaA. This diamond contained more Ib nitrogen than any previous natural or synthetic diamond that we can recall examining in the laboratory. It is unusual that a diamond with such a high N content escaped aggregation and remained in its isolated form.

When examined with magnification, the diamond showed irregular color zoning and only a few small "feathers" and needle-like inclusions, similar to those we have previously seen in type Ib yellow diamonds (see, e.g., Spring 1994 Lab Notes, pp. 41–42; King et al., 2005). Strain was very weak and was localized around the inclusions. The diamond showed no reaction to either long- or short-wave UV radiation from a handheld lamp. In the desk-model spectroscope, general absorption was present below ~510 nm. More detailed data, collected at cryogenic temperatures using a high-resolution visible absorption spectrometer, revealed very strong absorption through most of the visible spectrum, with complete absorption below ~515 nm due to the abundance of Ib nitrogen (figure 15). The steady increase in absorption toward the blue end of the spectrum was accompanied by a broad band centered at ~610 nm that likely contributed the pink component of the face-up color. The origin of this band is unclear, but it may be an extension of the deformation-related 550 nm band that produces pink-red color in other natural diamonds.

The diamond was also examined with the DTC DiamondView. Several irregularly zoned areas of very weak green fluorescence were separated by more intense green boundaries. The zoning pattern of one region on the table was particularly interesting because it resembled the skeleton of a fish (figure 16). The reason for this unusual zoning pattern is not known at this time.

Figure 16. When exposed to strong short-wave UV radiation in the DTC DiamondView, the 0.24 ct pink-brown diamond shows zones that resemble the skeleton of a fish.

This stone is an excellent example of a rare and unique scientific treasure that belies its unremarkable appearance.

Christopher M. Breeding

Figure 17. This large cavity in an 8.38 ct diamond does not resemble any natural etch channels or laser drill holes seen previously in the laboratory. Magnified 35x.

With Unusual Laser Drill Holes

Over the past few years, the challenges posed by innovative diamond laser drilling techniques have increased markedly (see S. F. McClure et al., "A new lasering technique for diamond," Summer 2000 *Gems & Gemology*, pp. 138–146; Summer 2002 Lab Notes, pp. 164–165). Recently, a sharp-eyed diamond grader in the East Coast laboratory noticed something very strange in an 8.38 ct round brilliant and brought it to the attention of the Identification Department.

Our experience has been that laser drill holes are circular in appearance, while etch channels are angular, as they follow the diamond's crystal structure. The large cavities in this diamond (see, e.g., figure 17) were unlike any natural etching we have previously encountered. Yet, where they reached the surface, these "holes" were neither round nor angular; rather, their outlines consisted of numerous semicircles (figure 18). Long grooves, some of them with a black residue, ran down the length of the cavities (figure 19). These unusual striations mimicked what is characteristically seen in naturally occurring etch channels; if not scrutinized carefully, they could have been dismissed as natural inclusions.

Figure 18. Where the drill holes reach the surface of the diamond, they show an unusual outline, again unlike any previously encountered in the lab. Magnified 105x.

In this case, however, all of the questionable cavities tapered to solid inclusions (again, see figure 17). In addition, the grooves were rounded along their edges, and the dark color and sugary texture were reminiscent of laser drilling, which is known to leave a black residue. All of these clues led us to conclude that the cavities in this diamond were caused by laser drilling, perhaps the result of several holes drilled into the same area.

One could speculate that the drillers of this diamond were either trying to mimic natural etch channels or perhaps had outlined some near-surface crystals and drilled them completely out.

Joseph Astuto and Thomas Gelb

Yellowish Orange MAGNESIOAXINITE

The West Coast laboratory recently examined a 4.90 ct transparent brownish yellowish orange piece of rough (figure 20) that was submitted for identification by JOEB Enterprises of San Diego, California. This piece of rough, reportedly from Tanzania, was tabular in shape (17.75 x 8.86 x 3.64 mm) with parallel striations on some of its crystal faces.

Observation with a polariscope revealed a distinct biaxial optic figure.

Figure 19. Dark, rounded grooves along the length of this cavity in the 8.38 ct diamond are further indications of laser drilling. Magnified 45x.
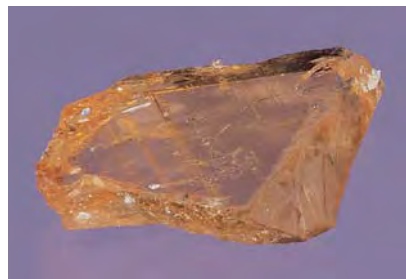
Figure 20. This 4.90 ct piece of rough, reportedly from Tanzania, is the first known sample of yellowish orange magnesioaxinite seen in the GIA Gem Laboratory.

The material also displayed moderate yellow and orange pleochroism. A small flat that had been polished on the surface allowed us to obtain refractive indices of $\alpha = 1.657$, $\beta = 1.660$, and $\gamma = 1.668$, resulting in a birefringence of 0.011 and indicating that the optic sign was positive. The specific gravity, measured hydrostatically, was 3.18. The sample fluoresced moderate orange to long-wave UV radiation and weak orange to short-wave UV. Using a desk-model spectroscope, we observed only a broad absorption band from 450 to 520 nm. Examination with a gemological microscope revealed "fingerprints," fractures, needles, negative crystals, and distinct orange-yellow and near-colorless zoning. The identification of this sample did not appear to be straightforward on the basis of physical and optical properties alone, so we proceeded with more advanced testing.

Both Raman and X-ray powder diffraction analysis identified the material as a member of the axinite group. Axinite, $Ca_2(Fe, Mn, Mg)Al_2B Si_4O_{15}(OH)$, is a borosilicate mineral group made up of a solid-solution series with three end members: ferroaxinite, manganaxinite, and magnesioaxinite. The species designation depends on the relative amounts of iron, manganese, and magnesium, respectively. The R.I. and S.G. of the sample in question were almost identical to those reported for blue magnesioaxinite from Tanzania (E. A.

Jobbins et al., "Magnesioaxinite, a new mineral found as a blue gemstone from Tanzania," *Journal of Gemmology*, Vol. 14, 1975, pp. 368–375). Puzzled by the fact that we were unable to locate any reference to magnesioaxinite with a yellowish orange color, we asked one of our research scientists to take the sample to Rutgers University in New Jersey for electron-microprobe analysis.

Analyses from three different spots indicated that the sample was chemically homogenous. Average results (reported in weight percent) were as follows: 46.74 SiO_2, below the detection limit for TiO_2, 18.39 Al_2O_3, 0.01 FeO, 0.80 MnO, 6.73 MgO, 21.53 CaO, 0.03 Na_2O, and 0.01 K_2O. This composition was consistent with that of the blue magnesioaxinite from Tanzania (see Jobbins et al., 1975; G. B. Andreozzi et al., "Crystal chemistry of the axinite-group minerals: A multi-analytical approach," *American Mineralogist*, Vol. 85, 2000, pp. 698–706). Vanadium was present as a minor constituent (0.13 wt.% V_2O_3) in the blue magnesioaxinite, and EDXRF analysis detected trace amounts of vanadium in the yellowish orange sample; unfortunately, quantitative microprobe data for vanadium were not collected.

In addition to the blue samples from Tanzania discussed above, brown-to-pink magnesioaxinite has been reported from Luning, Nevada. The material from Nevada has considerably less magnesium and more iron and manganese than the Tanzanian material (P. J. Dunn et al., "Magnesioaxinite from Luning, Nevada, and some nomenclature designations for the axinite group," *Mineralogical Record*, Vol. 11, 1980, pp. 13–15; Andreozzi et al., 2000). The Nevada samples contained just enough magnesium to fall within the broad magnesioaxinite range of the series, whereas the composition of the Tanzanian material was much closer to that of the pure magnesioaxinite end member. The difference in major-element chemistry between these two sources most likely explains their differences in color.

The brownish yellowish orange magnesioaxinite described here was similar in properties and chemistry to the blue Tanzanian material, which suggests that the yellowish orange color is probably not due simply to variations in iron, magnesium, and manganese. It is possible that variations in trace elements such as vanadium may contribute to the color, but as yet we do not know its true cause.

Elizabeth P. Quinn and
Christopher M. Breeding

CULTURED PEARL
With Cultured-Pearl Nucleus

It is always exciting to discover the unexpected on a pearl radiograph. When the pendant in figure 21 arrived at the West Coast laboratory for a routine identification, we anticipated nothing unusual. However, the X-radiographs used in pearl analysis sometimes reveal surprises, and this proved to be one such specimen.

The baroque pearl measured 16.00 x 13.50 mm in width and depth. (We could not measure the length because

Figure 21. This 16.00 x 13.50 mm baroque cultured pearl contained an unusual surprise.
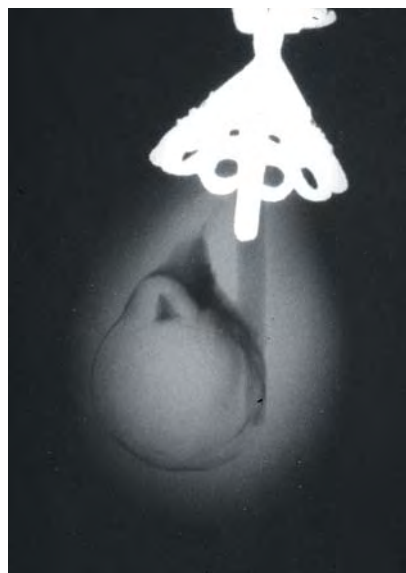
Figure 22. The X-radiograph of the cultured pearl in figure 21 revealed another cultured pearl as its nucleus, with bead and nacre clearly defined.

part of the pearl was covered by the mounting.) The X-ray luminescence was very weak, indicating that it might be a cultured pearl with thick nacre. However, X-radiography revealed that the nucleus did not merely consist of the expected mother-of-pearl bead, but it was in fact an *entire* cultured pearl with its own bead nucleus and nacre clearly defined on the radiograph (figure 22).

We have seen other cultured pearls with cultured-pearl nuclei; for example, we recently examined a semibaroque cultured pearl (approximately 18 ct) that appeared to contain a separate tissue-nucleated cultured pearl in its core (figure 23). The use of poor-quality cultured pearls as bead nuclei is a practice that has been known for a number of years, though it is unclear how common this practice is and we see very few such cultured-pearl nuclei in the laboratory. Nevertheless, gemologists relish having their routines broken by these small but delightful discoveries.

CYW
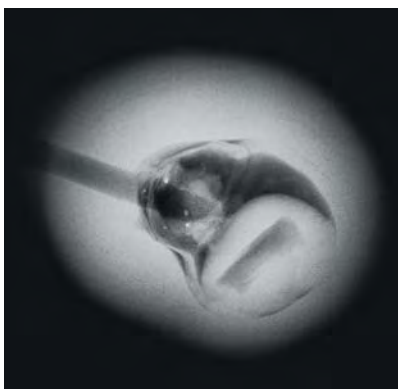
Figure 23. The ~18 ct cultured pearl in this X-radiograph appears to have a separate tissue-nucleated cultured pearl at its core.

Dyed "Golden" Freshwater Cultured Pearls

A graduated strand of what appeared to be "golden" South Sea cultured pearls arrived at the West Coast laboratory for identification (figure 24). We routinely examine these types of cultured pearls to determine whether or not they are dyed. This strand, however, provided another unexpected result.

Magnification revealed that the string knots between the cultured pearls were yellow, while the rest of

the string was white. There also were concentrations of darker yellow around some of the drill holes (figure 25). These preliminary observations suggested that the color was artificial in origin. The reaction to long-wave UV radiation also was characteristic of treated-color pearls: Some fluoresced medium orangy yellow (occasionally mottled with blue), while others were medium pink with uneven orange mottling (figure 26). Naturally and uniformly colored yellow pearls evenly fluoresce yellow to greenish yellow or greenish brown to brown to long-wave UV; pink and orange components, along with blue patches and other mottling, are inconsistent with an evenly distributed natural color.

UV-Vis reflectance spectra were collected by research gemologist Shane Elen. The spectra consistently revealed a strong absorption trough in the blue region at approximately 415–440 nm rather than a deeper trough in the UV region at approximately 330–385 nm. These results are consistent with dyed yellow saltwater cultured pearls (see S. Elen, "Spectral reflectance and fluorescence characteristics of natural-color and heat-treated 'golden' South Sea cultured pearls," Summer 2001 *Gems &*

Figure 24. This strand of 34 dyed freshwater cultured pearls (approximately 10.60–11.70 mm) at first appeared to be typical "golden" South Sea cultured pearls.

Figure 25. Color concentrations around the drill holes of these freshwater cultured pearls, along with the yellow coloring on the knots of the string, indicate the presence of dye.

Figure 26. The mottled pink and orange long-wave UV fluorescence of these cultured pearls is consistent with treated color.

Gemology, pp. 114–123).

Treated-color yellow South Sea cultured pearls have become commonplace. The surprise with this necklace came while examining the X-radiographs. Rather than the expected bead nuclei, the radiographs revealed the characteristic structure of tissue-nucleated cultured pearls, immediately raising suspicion of freshwater origin.

EDXRF analysis (also performed by Shane Elen) confirmed a level of manganese that was consistent with a Texas freshwater pearl in the reference file. Mn can be found as a trace element in some saltwater pearls, but the amount present in these cultured pearls excluded the possibility of saltwater origin, thus proving they were freshwater cultured pearls that had been dyed to resemble "golden" South Sea cultured pearls. It is interesting to note that while the varied

intensity (weak to strong) of the X-ray luminescence had supported the possibility of bead nucleation, it also was consistent with colored freshwater tissue-nucleated cultured pearls.

Although we do not have comparative UV-Vis spectra for dyed or natural-color yellow freshwater cultured pearls, the concentrations of color around the drill holes and unusual UV fluorescence behavior proved that these samples were dyed.

CYW

More on Copper-Bearing Color-Change TOURMALINE from Mozambique

The Fall 2004 Lab Notes section (pp. 250–251) reported on three unusual samples of copper-bearing tourmaline that displayed a strong and distinct "reverse" color change from grayish purple or purple in fluorescent light to gray–bluish green or

gray in incandescent light (figure 27). We have now obtained quantitative chemical data on all three of these samples; after the table of the pear-shaped preform was polished (with the client's permission), the stones were analyzed by electron microprobe by Dr. William B. (Skip) Simmons and Alexander U. Falster at the University of New Orleans in Louisiana.

The analyses (table 1) show that the tourmalines are elbaite, with slight variations in composition. Their major-element compositions are comparable to those reported for cuprian elbaite from the Paraíba and Rio Grande do Norte states in Brazil (see, e.g., J. E. Shigley et al., "An update on 'Paraíba' tourmaline from Brazil," Winter 2001 *Gems & Gemology*, pp. 260–276). However, their Cu contents were significantly lower than those reported for "Paraíba" tourmaline: They ranged from below the detection limit (< 0.008) to 0.09 wt.% CuO. These values also are significantly lower than those reported for most of the cuprian tourmalines from Nigeria that have been analyzed (see Gem News International, Fall 2001, pp. 239–240, and Spring 2002, pp. 99–100).

Only minute amounts of Fe and Ti were detected in some analyses of each stone. Although EDXRF analysis had detected Ga and Bi (again, see the Fall 2004 Lab Note), these elements were below the detection limits of the electron microprobe. The traces of Pb measured in some analyses are consistent with those found in cuprian elbaite from other localities, and the client confirmed that no

Figure 27. These three color-change tourmalines, reported to be from Mozambique (viewed in fluorescent light at left and incandescent light at right), contain Mn and Cu as their primary chromophores. They weigh 5.37, 5.47, and 5.68 ct.

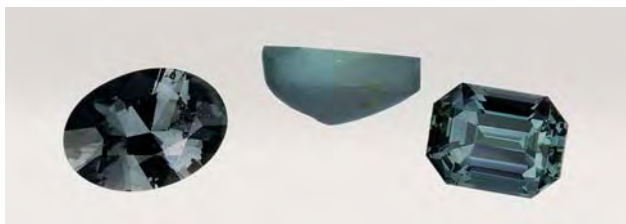| Chemical composition	5.37 ct grayish purple oval	5.68 ct purple emerald cut	5.47 ct purple pear preform
Oxides (wt.%)			
SiO_2	36.61–36.77	36.61–36.86	36.69–36.87
TiO_2	0.01–0.04	bdl–0.01	bdl–0.01
B_2O_3[b]	10.98–11.00	11.01–11.06	11.03–11.12
Al_2O_3	41.53–41.76	42.51–42.77	42.53–42.79
V_2O_3	bdl–0.02	0.08–0.15	0.08–0.11
FeO	0.02–0.05	bdl–0.01	bdl–0.01
MnO	1.94–2.14	0.07–0.11	0.11–0.15
CuO	bdl–0.09	bdl–0.03	bdl–0.03
SrO	0.02–0.08	0.02–0.04	0.02–0.03
CaO	0.45–0.51	0.72–0.89	0.60–0.68
PbO	bdl–0.02	bdl–0.04	bdl
ZnO	bdl	bdl–0.03	bdl–0.04
Li_2O[b]	1.77–1.84	1.94–2.06	1.95–2.16
Na_2O	1.95–2.14	1.48–1.78	1.67–1.80
K_2O	bdl	bdl–0.04	bdl
H_2O[b]	3.35–3.39	3.33–3.37	3.32–3.36
F	0.84–0.95	0.94–0.99	0.97–1.03
Sum	99.98–100.31	99.13–99.78	99.32–99.69
-O=F	0.35–0.40	0.40–0.42	0.41–0.43
Total	99.60–99.91	98.73–99.36	98.89–99.25
Ions on the basis of 31 (O,OH,F)			
Si	5.796–5.817	5.769–5.789	5.764–5.791
Al	0.183–0.204	0.211–0.231	0.209–0.236
T sum	6.000	6.000	6.000
B	3.000	3.000	3.000
Al (Z)	6.000	6.000	6.000
Al	1.545–1.575	1.661–1.741	1.601–1.729
V^{3+}	bdl–0.002	0.011–0.018	0.009–0.014
Ti	0.002–0.004	bdl–0.001	bdl–0.001
Fe^{2+}	0.003–0.006	bdl–0.001	bdl–0.001
Mn	0.259–0.287	0.009–0.014	0.014–0.019
Cu	bdl–0.011	bdl–0.004	bdl–0.003
Sr	0.001–0.007	0.002–0.003	0.001–0.003
Pb	bdl–0.001	bdl–0.002	bdl
Zn	bdl	bdl–0.004	bdl–0.004
Li	1.126–1.173	1.233–1.302	1.239–1.361
Y sum	3.000	3.000	3.000
Ca	0.076–0.086	0.121–0.150	0.101–0.115
Na	0.598–0.658	0.452–0.543	0.509–0.548
K	bdl	bdl–0.008	bdl
Vacancy	0.256–0.326	0.309–0.426	0.340–0.391
X sum	1.000	1.000	1.000
F	0.422–0.475	0.468–0.491	0.480–0.511
OH	3.525–3.578	3.509–3.532	3.489–3.520

[a] Analyzed with an ARL SEMQ electron microprobe, using an accelerating voltage of 15 kV, a beam current of 15 nA, a spot size of 2 μm, and 100-second count times for each spot. Ranges are shown for five points analyzed on each sample. Mg, Cr, Sc, Ga, Bi, and Cl were analyzed but were at or below the detection limit (except for 0.01 wt.% MgO in one analysis). Abbreviation: bdl = below detection limit.

[b] Values for B_2O_3, Li_2O, and H_2O were calculated based on an assumed elbaite tourmaline stoichiometry.

lead-containing compounds were used in the cutting and polishing process. Thus, the speculation in the previous entry about Pb contamination from the polishing compound residue was probably erroneous.

The transition metals Mn, Fe, Ti, and Cu are the primary color-causing agents in tourmaline, in addition to V and Cr (W. B. Simmons et al., "Gem tourmaline chemistry and paragenesis," *Australian Gemmologist*, Vol. 21, 2001, pp. 24–29). The oval stone contained much more Mn than the other two samples. Its Mn content was comparable to that found in "Paraíba" tourmaline and similar to or slightly higher than that reported in cuprian elbaite from Nigeria (again, see Gem News International, Fall 2001, pp. 239–240, and Spring 2002, pp. 99–100). The emerald cut and pear-shaped preform had appreciably less Mn than has been reported in "Paraíba" tourmaline and in three violet-blue cuprian elbaites from Nigeria, but it fell within the lower range reported for four greenish blue Nigerian cuprian elbaites.

By correlating the chemical composition with the UV-Vis-NIR spectra of all three stones (figure 28), the particular chromophores and the color-change phenomenon can be better understood. Each stone had a broad absorption peak centered around 515 nm (attributed to Mn^{3+}). In addition, Cu^{2+} peaks were centered at approximately 690 and 900 nm ($E\perp c$), or 720 and 910 nm ($E\|c$). The latest data confirm our preliminary conclusion that manganese—specifically, Mn^{3+} residing in the Y crystallographic site—is one of the primary coloring agents of this material. Although the Cu concentrations are significantly lower than those of cuprian elbaites from Brazil and Nigeria, the presence of copper is also contributing to the color; however, the absorption caused by Mn^{3+} in these specimens most likely explains their less saturated and more purplish color in fluorescent light, along with the presence of some pinkish zones, as compared to the more intensely colored copper-induced blue hues of "Paraíba" tourmaline.
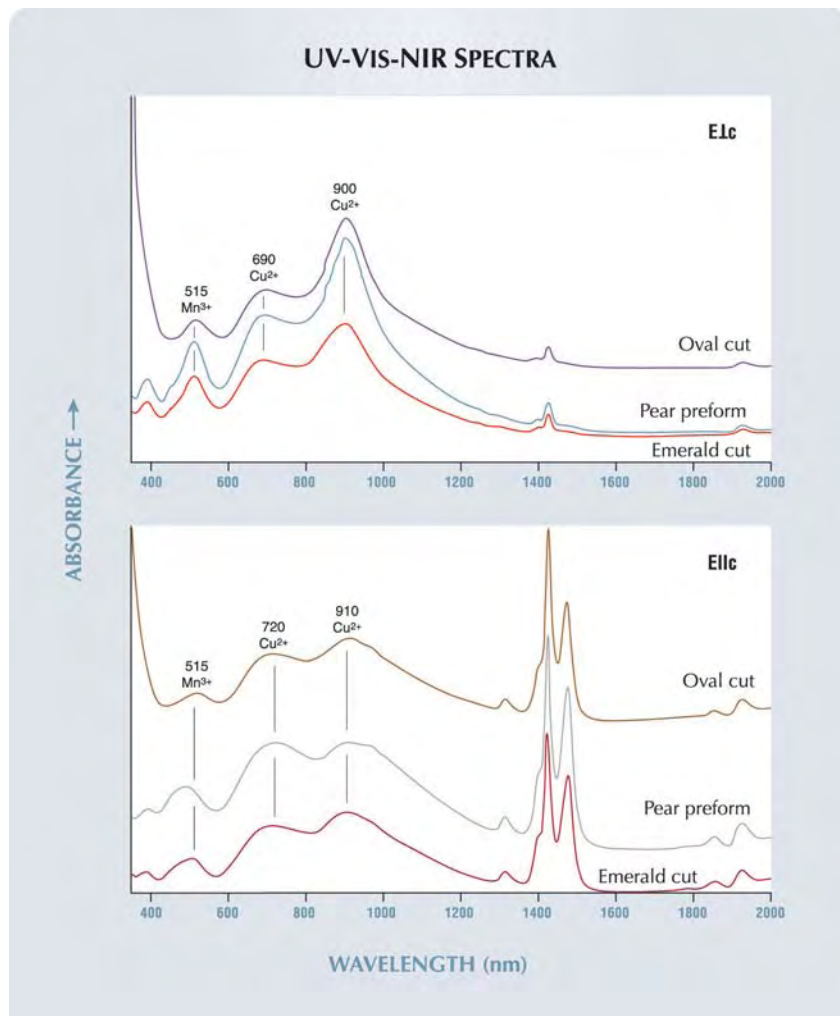
UV-VIS-NIR SPECTRA

Figure 28. These polarized UV-Vis-NIR spectra for the three Mozambique tourmalines (E⊥c, top; E∥c, bottom) show a broad absorption peak centered around 515 nm (attributed to Mn³⁺), with transmission "windows" on either side centered at approximately 420–450 nm and 570–580 nm. These separate transmission maxima could account for the color-change phenomenon observed in these stones. The peaks from approximately 1400 to 1500 nm are due to OH⁻ groups. The inferred optical path lengths are as follows: emerald cut ~7 mm, pear-shaped preform ~8 mm, and oval ~6–8 mm. Spectra have been shifted vertically for clarity.

The color-change phenomenon may be explained by the transmission "windows" on either side of the Mn^{3+} absorption peak. These separate transmission maxima are centered at approximately 420–450 nm (the violet to "purple" spectral region) and 570–580 nm (the greenish yellow to yellow-orange region; again, see figure 28). However, often it is not possible to explain the observed color of a sample on the basis of the absorption spectra alone. Although the colors of our samples correspond to the approximate regions of maximum transmission in the absorption spectra, they do not correlate exactly; additional factors such as variables in the composition of the stones, lighting and viewing conditions, the manner in which color perception varies between individuals, and other considerations combine to determine the actual hues observed by each viewer (Y. Liu et al., "A colorimetric study of the alexandrite effect in gemstones," *Journal of Gemmology*, 1999, Vol. 26, No. 6, pp. 371–385). Thus, the exact cause of the reverse nature of the color change (relative to the "alexandrite effect") remains unknown. We are confident, however, that the unusual phenomenon could be further explained with a detailed colorimetric study in conjunction with the absorption spectra.

Although these Mozambique tourmalines were found to have much lower copper contents than their Brazilian and Nigerian counterparts, they do expand the geographic locales where copper-bearing elbaite has been found.

CYW, Eric Fritz, and Sam Muhlmeister

Although the concentrations of V were nearly equal to those of Mn in both the emerald cut and pear-shaped preform, and they exceeded the contents of Cu in the same stones, the absorption spectra do not show any indication of the V^{3+} peaks (599–610 nm and 418–440 nm) that have been reported for tourmaline (K. Schmetzer, "Absorption spectroscopy and colour of V^{3+}-bearing natural oxides and silicates—A contribution to the crystal chemistry of vanadium," *Neues Jahrbuch für Mineralogie, Abhandlungen*, Vol. 144, No. 1, 1982, pp. 73–106 [in German]); therefore, there is no evidence that V^{3+} is contributing to the color of these stones.

COLORED STONES AND ORGANIC MATERIALS

Demantoid from northern Pakistan. At the February 2004 Tucson gem shows, one of us (BML) was shown some attractive demantoid that was reportedly from northern Pakistan. The dealer who had the material, Syed Iftikhar Hussain (Syed Trading Co., Peshawar, Pakistan), indicated that it came from the Kaghan Valley area (Hazara district), which is the same region that hosts Pakistan's famous peridot deposits. A visit to the mining area by Mr. Hussain revealed shallow open cuts within ultramafic rocks. The garnets occur as well-formed crystals in a soft white host rock that appears to consist mostly of talc. A small amount of rough was produced in 2003, yielding a few dozen carats of faceted stones up to 3 ct (most ranged from melee to 1 ct). Since that time, there has been little additional production.

One matrix specimen and three faceted demantoids (0.30–0.60 ct; figure 1) were donated to GIA by Mr. Hussain, and the cut stones were characterized by one of us (EPQ). Their color ranged from yellow-green to green, with two of the stones having fairly strong color zoning in green and lighter brownish greenish yellow. The face-up combination of these colors within the faceted stones created an almost pleochroic appearance. The three samples showed the following additional characteristics: diaphaneity—transparent; R.I.—over the limits of a standard refractometer; S.G.—3.85–3.95; anomalous birefringence—moderate to strong; fluorescence—inert to both long- and short-wave UV radiation; Chelsea filter reaction—weak pink; and a strong broad absorption band at 440 nm and lines in the red end of the spectrum were observed with the desk-model spectroscope. Microscopic examination revealed fine wavy and/or curved needles in all three stones, as well as a few fractures. In two samples, these needles occurred in clusters, creating partial "horsetail" inclusions. All three stones also contained

Figure 1. A small demantoid deposit, reportedly in northern Pakistan, is the source of these round brilliants (0.30–0.60 ct) and matrix specimen. Note the strong color zoning in the two larger cut stones. GIA Collection nos. 31930–31932; photo by Maha Calderon.
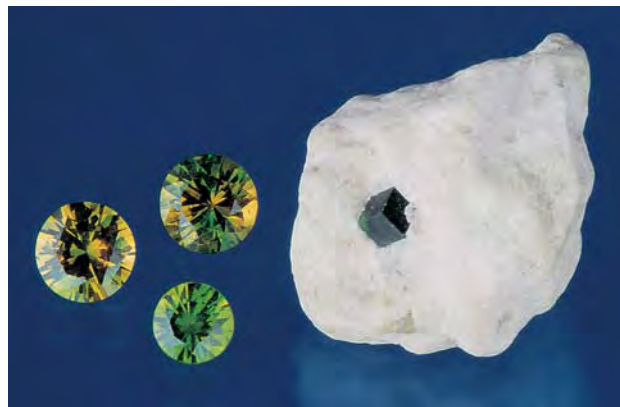
angular growth lines, and in two samples these lines formed an hourglass-like outline.

These properties are similar to those reported for demantoid from Iran (see Spring 2002 Gem News International, p. 96). However, while the Iranian material typically appears too dark in stones weighing more than 0.70 ct, this was not the case for the 1–3 ct samples from Pakistan that Mr. Hussain showed us.

Elizabeth P. Quinn (equinn@gia.edu)
GIA Gem Laboratory, Carlsbad

BML

Pyrope-almandine from Ethiopia. According to Scott Davies of American-Thai Trading, Bangkok, small quantities of purple to orange-red garnet from Ethiopia have been entering the gem trade in Thailand since June 2004. The slightly rounded rough pieces range up to 12 grams or larger. While most of the material is dark and contains abundant inclusions, a small percentage shows attractive color and good clarity. According to one supplier, Teferi Gobezie of Addis Ababa, Ethiopia, the garnet is mined at Baya Gundi, in the Hagare Mariam region of southern Ethiopia about 200 km from Kenya. Garnets are known from several localities in southern Ethiopia (see "Gem resources in Ethiopia," *Jewellery News Asia*, No. 209, 2002, p. 52)

Mr. Davies kindly loaned and donated several rough and cut samples of this garnet to GIA. Examination of three faceted stones (1.35, 1.31, and 0.89 ct; figure 2) by one of us (EPQ) showed the following properties (listed in respective order, as appropriate): color—red, dark orange-red, and purplish pink; R.I.—1.741, 1.744, and 1.757; S.G.—3.85, 3.84, and 4.00; and fluorescence—all three samples were inert to long- and short-wave UV radiation. With the desk-model spectroscope, all three samples showed weak absorption lines at 430, 460, and 620 nm, and stronger bands at 505, 520, and 570 nm. Microscopic examination revealed clusters of small, rounded, transparent, doubly refractive crystals in the red stone (which senior research associate Sam Muhlmeister identified as zircon by Raman analysis); small crystals, needles, and clouds of pinpoints in the dark orange-red sample; and pinpoint inclusions as well as large, transparent, flattened, doubly refractive crystals in the purplish pink stone (which could not be identified due to their position within the sample). The properties of these garnets are consistent with those reported for pyrope-almandine (see C. M. Stockton and D. V. Manson, "A proposed new classification for gem-quality garnets," Winter 1985 *Gems & Gemology*, pp. 205–218).

Elizabeth P. Quinn and BML

New ruby and pink sapphire deposit in the Lake Baringo area, Kenya. At the February 2005 Tucson gem shows, one of us (DB) was shown about 180 grams of rough ruby and pink sapphire that were reportedly mined from a new locality in Kenya. Subsequently more information has become available, along with both rough and cut samples of this new corundum that reportedly have not been treated in any way.

Figure 2. These samples (1.35, 1.31, and 0.89 ct) were selected to show the range of color of pyrope-almandine being produced from southern Ethiopia. GIA Collection nos. 31755–31757; photo by Maha Calderon.

The deposit is located in the Kenya Rift Valley in the west-central part of the country, approximately 70 km east of Eldoret near Lake Baringo. In October 2001, a local gem prospector was shown samples of pink and red corundum from this area by members of the Tugen tribe who lived in Barsemoi. The prospector later visited the locality and collected samples of gem-quality corundum from a dry river bed. He applied for a license with the Kenya Commissioner of Mines, and after a two-year process received a mining permit for a 5 km² area. In June 2004, he resumed collecting surface material from the site and has obtained more than 2 kg of corundum, ranging from red to pink to pinkish violet. So far, approximately 350 stones have been faceted at his office in Eldoret, and the largest weigh 2.80 and 3.71 ct (both oval cuts). Most of the stones range from 0.5 to 1.6 ct, and are bright purplish pink to purplish red (figure 3).

As of May 2005, approximately 400 local villagers were active in the region surrounding the original mining claim, expanding the corundum-bearing area to approximately 20 km². Preliminary indications suggest that this area has the potential to become a significant source of untreated ruby

Figure 3. A new corundum deposit in west-central Kenya is the source of these rubies and pink sapphires (0.34–1.64 ct). Courtesy of Dudley Blauwet Gems; photo by Maha Calderon.

Figure 4. Faceted sunstone from India was available in large quantities at this year's Tucson gem show. The loose stones shown here weigh 5.13–8.06 ct, and the pendant contains a 20 ct sunstone set in 18K white gold. Courtesy of Anil B. Dholakia Inc.; photo by Maha Calderon.

and pink sapphire. The gemological properties of this corundum are currently being studied at GIA, and will be reported in a future issue of *G&G*.

Dudley Blauwet (mtnmin@attglobal.net)
Dudley Blauwet Gems, Louisville, Colorado

BML

Faceted orange and brown sunstone from India. At the 2005 Tucson gem shows, Anil Dholakia of Anil B. Dholakia Inc., Franklin, North Carolina, had a large amount of faceted sunstone from Orissa, India. Although similar material has been produced from India in the past (see Summer 1995 Gem News, pp. 130–131), this sunstone
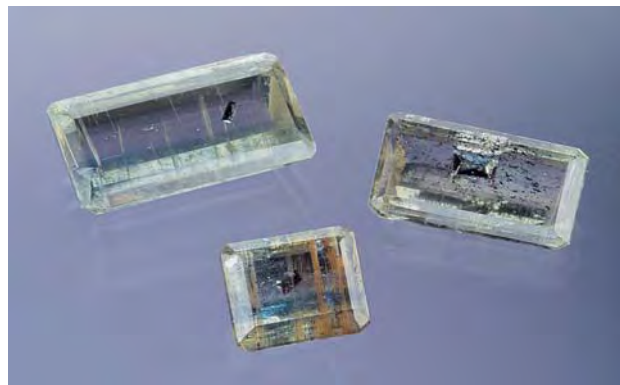
was notable for the huge quantity of faceted stones available. Mr. Dholakia had been accumulating the material for the past two years, and estimated that 75,000 carats were available, in calibrated rectangle and oval shapes from 6 x 4 to 12 x 10 mm. Some of the stones were set in bracelets and pendants (see, e.g., figure 4).

Mr. Dholakia loaned several samples to GIA for examination, and gemological properties were collected on three emerald cuts (5.13–8.06 ct; again see figure 4) by one of us (EPQ): color—brownish orange and brown (color created by inclusions); diaphaneity—semitransparent to translucent (due to numerous inclusions); R.I.—1.530 to 1.541; birefringence—0.009 or 0.010; S.G.—2.63–2.64; Chelsea filter reaction—weak orangy pink; and fluorescence—inert to longwave and weak red to short-wave UV radiation. Weak absorption in the blue and green areas of the spectrum was visible with the desk-model spectroscope. These properties are comparable to those reported for sunstone (aventurescent oligoclase feldspar) by R. Webster (*Gems*, 5th ed., revised by P. Read, Butterworth-Heinemann, Oxford, England, 1994, pp. 215–216). Microscopic examination of the three samples revealed numerous angular transparent-to-semitransparent thin platelets that were reddish orange in transmitted light and iridescent in reflected light. These inclusions had the distinctive appearance of hematite, and this was confirmed with Raman analysis by senior research associate Sam Muhlmeister.

Elizabeth P. Quinn and BML

INCLUSIONS IN GEMS

Staurolite in kyanite from Brazil. Faceted kyanite is generally considered to be a gem for collectors of the unusual. While the intense blue to greenish blue color that it sometimes displays can be quite attractive, its perfect cleavage and somewhat low directional hardness (5–7 on

Figure 5. Each of these three rectangular step-cut kyanites (2.31–7.39 ct) from Minas Gerais, Brazil, contains a well-formed inclusion of staurolite. Photo by Maha Calderon for microWorld of Gems.

Figure 6. This transparent dark yellowish brown crystal of staurolite formed a conspicuous inclusion in one of the Brazilian kyanites. Photomicrograph by John I. Koivula for microWorld of Gems; magnified 10x.
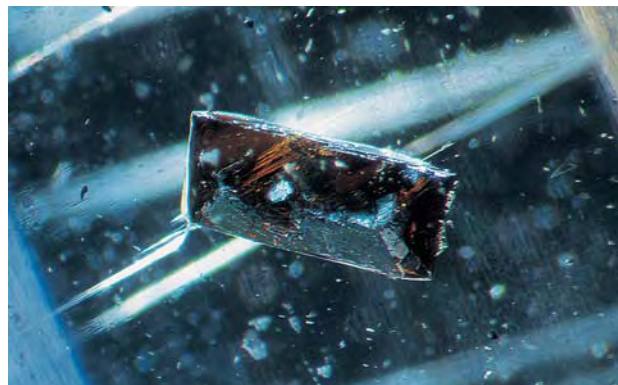
the Mohs scale) will always limit its use as a mainstream gemstone. One of the appealing features of kyanite for the gemologist, however, is the variety of interesting and colorful mineral inclusions it sometimes hosts. Among these are orange garnets, bright red rutile, and prisms of green tourmaline.

At the 2005 Tucson gem shows, a small selection of faceted light bluish green kyanites containing another interesting mineral inclusion were offered by Luciana Barbosa of the Gemological Center, Belo Horizonte, Minas Gerais, Brazil. They were cut from material recovered near Barra do Salinas in Minas Gerais.

Three rectangular step-cut kyanites (2.31, 3.44, and 7.39 ct; figure 5) were examined for this report. Two of the samples were obtained from Ms. Barbosa, and the third was provided by William Pinch of Pittsford, New York. Included in each stone was a single, transparent, dark yellowish brown crystal (figure 6), which was well-formed with chisel-point terminations and a diamond-shaped cross-section. Ms. Barbosa stated that these inclusions were pseudo-orthorhombic crystals of staurolite, a monoclinic iron-aluminum silicate. The smallest stone also contained a partial crystal of the same mineral that was exposed on the pavilion surface and polished flat during faceting. This made it ideal for Raman analysis, by which we verified the identification as staurolite.

Staurolite is virtually unknown as an inclusion. It has apparently only been reported as an unusual single inclusion in an eclogitic diamond (L. R. M. Daniels and J. J. Gurney, "A crustal mineral in a mantle diamond," *Nature*, Vol. 379, No. 6561, 1996, pp. 153–156) and may also be found in metamorphic corundum. The identification of staurolite inclusions in kyanite is not completely surprising, however, since both minerals are primarily products of medium-grade regional metamorphism and are known to form in association with each other.

John I. Koivula (johnkoivula@hotmail.com)
West Coast AGTA Gemological Testing Center
Carlsbad, California

Maha Calderon
Carlsbad, California

Obsidian with spessartine inclusions. Although generally uninspiring as gems from a superficial macroscopic standpoint, transparent-to-translucent natural volcanic glasses frequently contain interesting inclusions. For example, very rare euhedral indialite crystals and transparent rods of sillimanite have been found in obsidian (see J. Hyrsl and V. Zácek, "Obsidian from Chile with unusual inclusions," *Journal of Gemmology*, Vol. 26, No. 5, 1999, pp. 321–323).

At the 2005 Tucson gem shows, Dr. Jaroslav Hyrsl, from Kolin, Czech Republic, had a few semitransparent brown obsidians that were faceted from rough he had obtained in Bolivia. One of these gems, pictured in figure 7, had been cut into a 10.25 ct octagonal step cut. In strong incandescent light or bright direct sunlight, tiny sparkling
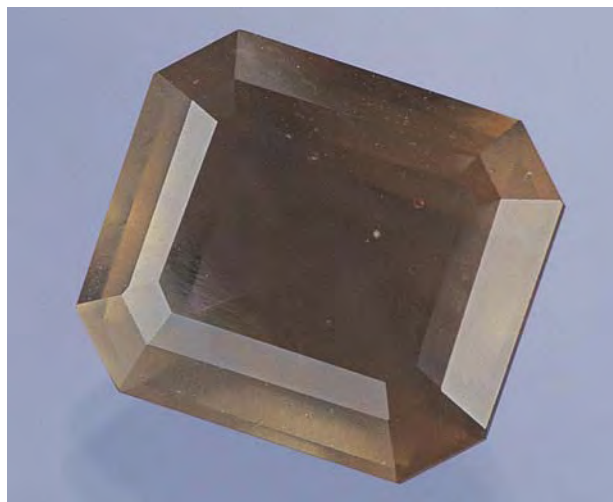
Figure 7. Even without magnification, small orange spessartine inclusions are clearly visible in this 10.25 ct Bolivian obsidian. Photo by Maha Calderon for microWorld of Gems.

orange inclusions could be seen even without magnification (again, see figure 7). Dr. Hyrsl stated that the inclusions had been identified as spessartine by X-ray diffraction and chemical analysis.

Gemological testing confirmed that the brown host gem was obsidian. With magnification, as seen in figure 8, the orange inclusions showed abundant crystal faces, and their isometric crystal form was consistent with the general appearance of garnet. Examination between crossed polarizers confirmed they were isotropic, while their high relief and Becke line reaction showed that they had a much higher refractive index than the surrounding obsidian. As a further gemological exercise, microspectroscopy of these inclusions (performed through the optical system of a Leica gemological microscope) showed weak but visible

Figure 8. Shown here are two of the more than a dozen well-formed spessartine inclusions observed in the Bolivian obsidian. Photomicrograph by John I. Koivula for microWorld of Gems; magnified 10×.

absorption features that would be expected from spessartine.

A literature search found only one other report of garnet inclusions in obsidian, from a volcano in northwestern Argentina (P. J. Gauthier et al., "Grenats des rhyolites de la caldéra de La Pava-Ramadas (NW Argentine) et de leurs xénolites granitiques," *Comptes Rendus de l'Académie des Sciences, Serie II. Sciences de la Terre et des Planetes*, Vol. 318, 1994, pp. 1629–1635). Obsidian blocks within rhyolite lava contained euhedral microcrystals of almandine-spessartine that ranged from 100 to 400 μm in diameter. By comparison, the garnet inclusions in the Bolivian obsidian reported in the present entry were much larger (i.e., up to about 1.5 mm in diameter).

John I. Koivula and Maha Calderon

Fluorite inclusions in quartz from Madagascar. One of the more interesting recent inclusion discoveries being offered to collectors at the 2005 Tucson gem shows were rough and cut samples of rock crystal quartz containing euhedral crystals of violet-to-blue fluorite. Most of this material was being sold at the Clarion Hotel by Frederic Gautier of Little Big Stone Co., Antananarivo, Madagascar. Although the locality was represented at the Tucson show as Miandrivazo, Mr. Gautier recently reported that the mine is actually situated about 17 km northeast of the village of Amborompotsy, Fianarantsoa Province, central Madagascar. The deposit can be reached from Amborompotsy only by motorcycle or on foot, due to the poor condition of the road. Large quantities of quartz crystals have been mined from this region for several years, but material containing fluorite inclusions was first recovered in late November 2004. The crystals were mined from a quartz vein approximately 80 cm wide that cross-cuts quartzite host rocks. The deposit was worked with hand tools by local miners until the end of February 2005, when a large cave-in buried the productive area.

Figure 10. Three large blue fluorite inclusions make this faceted 21.68 ct rock crystal gem from Madagascar much more interesting. Photo by Maha Calderon for microWorld of Gems.

Mr. Gautier estimated the total production of fluorite-included quartz at about 300 kg, with an approximately equal amount of quartz that did not contain any fluorite inclusions. Most of the fluorite-included material consists of single crystals, some doubly terminated, ranging up to 23 cm long. Only a few crystal clusters were produced. Mr. Gautier reported that Little Big Stone Co. acquired most of the production, which is being sold in three categories: (1) mineral specimens and rough for cutting, (2) polished points, and (3) polished material—consisting of emerald cuts (ranging from 2 to 30 ct), square slabs (from 1 cm to a few centimeters across), and cabochons. He believed the largest stone cut to date weighed approximately 100 ct.

One of us (JIK) has examined several hundred of these quartz crystals (see, e.g., figure 9). In all samples, the fluorite inclusions were confined to the near-surface outer

Figure 9. These intergrown crystals of quartz (up to 12.5 cm long) from central Madagascar contain directionally deposited inclusions of fluorite. Photo by Maha Calderon for microWorld of Gems.

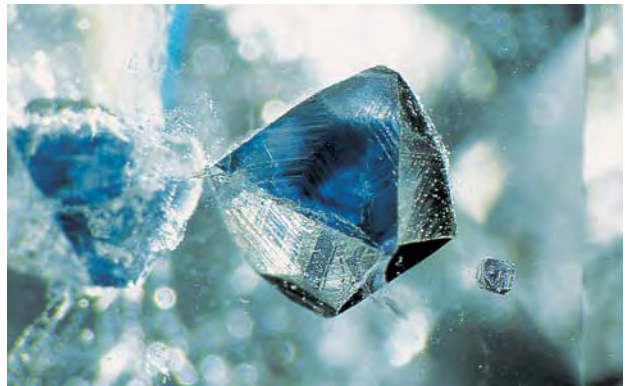Figure 11. Displaying sharp octahedral faces and an intense violet color, this 2.85 mm fluorite crystal was trapped during the final stage of growth near the surface of a quartz crystal from Madagascar. Photomicrograph by John I. Koivula for microWorld of Gems.

zones of their rock crystal hosts, which indicates late-stage crystallization of the fluorite in relation to the growth cycle of the quartz. The inclusions were situated only under certain crystal faces and on only one side of the quartz (again, see figure 9), suggesting a directional deposition of the fluorite.

The fluorite inclusions are particularly well displayed in faceted stones such as the 21.68 ct example in figure 10, which was cut by Leon M. Agee of Agee Lapidary, Deer Park, Washington. The fluorite inclusions ranged from blue to violet in light to dark tones, and many were strongly color zoned (figure 11). Some of the more prominent individual fluorite inclusions measured up to 7 mm in diameter, with clusters being somewhat larger. In a small percentage of the crystals, the fluorite formed together with clouds of green particles that had the appearance of chlorite. The fluorite inclusions were identified as such by means of Raman analysis. The refractive index (1.43) and isotropic nature of one partial fluorite inclusion extracted from the surface of a broken crystal was determined through Becke line testing using Cargille liquids.

A microscopic examination of several quartz crystals showed that some of the fluorite inclusions had been exposed to the surface through fine surface-reaching cracks. These inclusions were often either partially or completely dissolved away. The former case resulted in a loose crystallite of fluorite that was trapped, but free to move about in a fluorite-shaped cavity. In the latter case, the resulting cavity appeared to be colorless or, in some instances, was partially filled with light yellowish brown epigenetic debris.

The potential for large faceted stones, together with the relatively large size and the attractive violet-to-blue color of the fluorite inclusions, should make this new material from Madagascar quite popular among gemologists and others who appreciate inclusions in gemstones.

John I. Koivula, Maha Calderon, and BML

Bismuthinite inclusions in rose quartz from Madagascar. Eye-visible inclusions are common in almost all quartz varieties except rose quartz. Although massive rose quartz is colored by submicroscopic inclusions (see J. S. Goreva et al., "Fibrous nanoinclusions in massive rose quartz: The origin of rose coloration," *American Mineralogist*, Vol. 86, No. 4, 2001, pp. 466–472), only very rarely does this material contain macroscopic inclusions (see, e.g., Summer 2003 Gem News International, pp. 159–162). At the 2005 Tucson gem shows, one of these contributors (FD) had some unusual rose quartz from Madagascar that displayed abundant, conspicuous inclusions with a metallic luster (figure 12).

The material was recovered from the Itongafeno pegmatite (also known as Tsaramanga), located 23 km west of Antsirabe near the village of Mahaiza. This deposit is part of the Analalava pegmatite district and has been worked for asteriated rose quartz and dark blue aquamarine for

Figure 12. These faceted samples of rose quartz (5.74 and 12.55 ct) from the Itongafeno pegmatite in central Madagascar contain conspicuous inclusions of bismuthinite. Photo by J. Hyrsl.

almost 100 years. In addition to common pegmatite minerals, it has produced rare examples of emerald and native bismuth. Several vertically disposed zones of mineralization have been identified in the pegmatite, including rose quartz, smoky quartz adjacent to a thin Nb-Ta oxide and biotite layer, and rose quartz with metallic inclusions. About 60 kg of the included rose quartz was extracted between September 2003 and June 2004, although only a small percentage was suitable for cutting.

The inclusions in 10 faceted stones were examined, and with magnification they appeared metallic gray to black and had peculiar shapes (figure 13). They occurred in parallel rows of strongly elongated, sometimes striated crystals about 0.5 mm thick. Powder X-ray diffraction (XRD) analysis of an extracted crystal and chemical analyses of several surface-reaching inclusions in one sample with a Jeol 5800LV scanning electron microscope

Figure 13. The bismuthinite inclusions in the rose quartz from Madagascar appeared metallic gray to black, and showed a variety of irregular forms. A network of needle-like inclusions, possibly rutile, was responsible for the asterism in this rose quartz. Photomicrograph by J. Hyrsl; the field of view is approximately 3 mm.

equipped with a Princeton Gamma-Tech energy-dispersive IMIX detector identified the inclusions as bismuthinite (Bi_2S_3). These were sometimes accompanied by smaller, more equant, yellow-to-black chalcopyrite grains. XRD also suggested the possible presence of a Cu-Bi-sulfosalt close to gladite in composition, which probably was present as thin metallic needles seen in some samples.

In addition to the inclusions described above, the rose quartz also contained abundant tiny colorless needles (possibly rutile; again, see figure 13) oriented in three directions at angles of 120°. These needles are apparently the cause of asterism in samples that are cut as spheres or cabochons.

To our knowledge, this is the first confirmed report of bismuthinite in faceted quartz from a pegmatite. Previously, bismuthinite was identified in quartz from tin-tungsten deposits and from Alpine-type fissures (see J. Hyrsl and G. Niedermayr, *Magic World: Inclusions in Quartz*, Bode Verlag, Haltern, Germany, 2003, p. 48).

Jaroslav Hyrsl (hyrsl@kuryr.cz)
Kolin, Czech Republic

Fabrice Danet
Style Gems, Antsirabe, Madagascar

EF

SYNTHETICS AND SIMULANTS

Yellow hydrothermal synthetic sapphires seen in India. Since about mid-2004, the Gem Testing Laboratory in Jaipur, India, has encountered approximately 20 synthetic yellow sapphires (3.50–5.30 ct) grown by a hydrothermal technique (see, e.g., figure 14). Previously, the only yellow synthetic sapphires we had encountered were grown by a melt technique (e.g., flame-fusion). The physical properties of these hydrothermal samples were comparable to both natural and hydrothermal synthetic yellow sapphires (see, e.g., V. G. Thomas et al., "Tairus hydrothermal synthetic sapphires doped with nickel and chromium," Fall 1997 *Gems & Gemology*, pp. 188–202). Refractive indices were 1.760–1.770, with a birefringence of 0.007–0.008. Specific gravity varied between 3.98 and 4.01. All the specimens fluoresced weak orange to both long- and short-wave UV radiation, with a stronger reaction to short-wave.

With magnification, most of these synthetics exhibited some scattered flake-like inclusions (similar to "bread crumbs" seen in synthetic quartz). In approximately eight samples, these flake-like inclusions were concentrated in a single plane along one side of the seed plate (figure 15). Inclusions such as these have not been seen in natural sapphires (Thomas et al., 1997). A weak "chevron" growth pattern that is characteristic of synthetic hydrothermal growth (see, e.g., Thomas, et al., 1997; K. Schmetzer and A. Peretti, "Some diagnostic features of Russian hydrothermal synthetic rubies and sap-

Figure 14. The slightly brownish yellow body color of this 4.30 ct hydrothermal synthetic sapphire is characteristic of those encountered at the Gem Testing Laboratory in Jaipur, India. Photo by G. Choudhary.

phires," Spring 1999 *Gems & Gemology*, pp. 17–28) was visible in only about five of the specimens examined.

Infrared spectroscopy of all the synthetic sapphires showed absorption peaks in the region between 3600–3300 cm^{-1}, at 3563, 3483, 3383, and 3303 cm^{-1}. These peaks are related to OH- groups, and have been documented in both natural and synthetic corundum (Thomas et al., 1997). However, the samples were readily identified as synthetic by their characteristic "bread crumb" inclusions (present as scattered flakes and/or concentrated in a flat plane), as well as their occasional chevron growth patterns.

Gagan Choudhary (gtljpr_jp1@sancharnet.in)
Gem Testing Laboratory, Jaipur, India

Figure 15. Some of the yellow hydrothermal synthetic sapphires showed "bread crumb" inclusions that were concentrated in a plane along the seed plate. These flake-like inclusions have not been seen in natural sapphires. Photomicrograph by G. Choudhary; magnified 30×.

TREATMENTS

Interesting heated citrine. It is relatively well known that the vast majority of citrine quartz is the product of heat treating amethyst. Material from Brazil and Uruguay has often been used for this purpose. Both large and small amethyst-lined geodes are converted to citrine using simple low-temperature heat treatment in air. Because so much of this heat-treated material is available, and it is cost prohibitive to attempt to determine the cause of color (natural or heated) for most of these stones, the trade typically assumes that all citrine is heated and this yellow quartz is priced accordingly.

At the 2005 Tucson gem shows, well-known quartz specialists Si and Ann Frazier (El Cerrito, California) noticed clusters of brownish orange heat-treated citrine crystals from Uruguay that showed an unusual near-surface phenomenon. Many of the faces on these crystals had a pearly, reflective, almost mirror-like luster that was reminiscent of the silvery white adularescence characteristic of Sri Lankan moonstones. According to the dealer, Marcelo Valadares of General Brazilian Gems, Governador Valadares, Brazil, only a small proportion of the citrines showed this unusual surface feature after they were heated to approximately 400°C.

The Fraziers provided one of these contributors (JIK) with a specimen of the heated citrine that measured 23.9 x 21.4 x 11.1 mm (figure 16). With magnification, the reflective surfaces appeared to show true adularescence (figure 17), though the effect was apparent only on the minor rhombohedral crystal faces.

Figure 16. The interesting adularescent areas shown by the minor rhombohedral faces on this 23.9-mm-wide citrine crystal group formed during the heat treatment of an amethyst cluster from Uruguay. Photo by Maha Calderon for microWorld of Gems.

Figure 17. The adularescence shown by certain crystal faces of the heated citrine specimen provides an example of an interesting treatment-induced optical phenomenon. Photomicrograph by John I. Koivula for microWorld of Gems; magnified 10x.

The cause of this heat-induced adularescence is unknown. A curious rumor concerning this phenomenon was that the pearly-looking surfaces were actually individually cut and glued onto the surfaces of the crystals, but we found no evidence of this procedure (which, from an economic standpoint alone, seems quite unviable). The adularescence could be related to the delamination of twin planes or of ultra-fine growth structures during heating. Prior to this delamination, these submicroscopic planar features were perhaps similar to those that produce an unusual play-of-color in the minor rhombohedral faces of some amethyst and rock crystal specimens (referred to as the "Lowell Effect"; see Winter 1987 Gem News, p. 240). Other theories are possible, and we welcome any observations from *Gems & Gemology* readers.

John I. Koivula and Maha Calderon

"Chocolate" Tahitian cultured pearls. At the 2005 Tucson gem shows, Emiko Pearls International Inc. (Bellevue, Washington) had some Tahitian cultured pearls, marketed as "chocolate pearls," that were processed to lighten their color (figure 18). Although this attractive product has been available for 4–5 years, many in the trade are still unaware of it (see "Trade raises questions about 'chocolate pearls,'" *Jewellery News Asia*, No. 241, September 2004, pp. 160, 162). The colors range from a pleasing dark brown to light yellow-brown, and have been described in the trade as "copper," "bronze," or "honey" colored; these hues are not typical of natural-color Tahitian cultured pearls. The luster of the "chocolate" cultured pearls varies from satin-like to metallic. The available sizes range from 9 to 15 mm, although larger ones have been produced. Production is limited to a few hundred per month because only certain Tahitian cultured pearls can be successfully treated.

The coloration of these cultured pearls results from a proprietary two-stage process. Ron Greenidge of Emiko

Figure 18. The coloration of the "chocolate" Tahitian cultured pearls in this strand (13.6–16.7 mm in diameter) is the result of a proprietary two-stage process. Courtesy of Emiko Pearls International Inc.; photo by Maha Calderon.

Pearls International kindly provided the following general information from the company that performs the procedure. The first step is to remove color from the selected Tahitian cultured pearls, which could be compared to the bleaching process used on Akoya cultured pearls. In the second step, the bleached color is stabilized. The company reported that the process does not involve the use of dye or heat, and the brown color is stable under conditions associated with routine wear. Since Emiko Pearls International began selling the "chocolate" cultured pearls when they

were first introduced to the market, they have not encountered any problems with color stability.

The exact nature of the process remains undisclosed, and future studies are needed to establish identification criteria. Preliminary research suggests that careful observation of the long-wave UV fluorescence will likely be helpful in identifying these cultured pearls, when compared to known natural colors as a reference (see "US gem labs seek to uncover process behind brown pearls," *Jewellery News Asia*, No. 241, September 2004, p. 162).

Marisa Zachovay (marisa.zachovay@gia.edu)
GIA Education, Carlsbad

Lead glass–filled rubies appear in the Middle East. The Middle East—especially the countries along the Arabian Gulf—has long been an important gold market, but recently the region has gained importance in trading gems and jewelry. This can clearly be observed in Dubai, where the Dubai Metal and Commodities Centre has been established, incorporating the Dubai Diamond Exchange and a future GIA campus. Moreover, since the Gem & Pearl Testing Laboratory of Bahrain issued its first report in 1991, the region has also seen an increase in the number of gemological laboratories.

When a new treatment such as the lead-glass filling of rubies appears, it usually takes some time to be recognized in the smaller markets around the world. Most new treatments are initially reported in the U.S., the Far East, and Europe. In recent months, these major gem markets have encountered lead glass–filled rubies (see Fall 2004 Lab Notes, pp. 247–249, and references therein). Now such rubies are being seen in the Middle East as well.

Figure 19. This 10.35 ct faceted ruby with lead glass–filled fractures was submitted to the Gem & Pearl Testing Laboratory of Bahrain. Photo by N. Sturman.

Figure 20. With magnification, the presence of a lead-glass filler was evident from the vivid flash-effect colors and gas bubbles seen in some of the fractures. Photomicrograph by N. Sturman; magnified 20x.
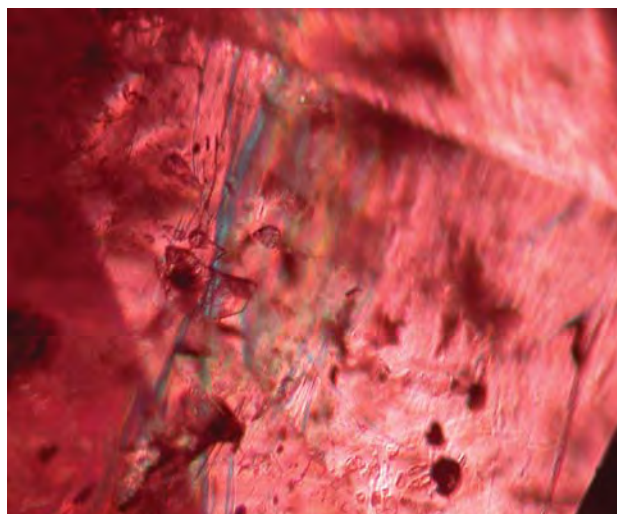
In February 2005, the 10.35 ct orangy red natural ruby shown in figure 19 was submitted via a Saudi Arabia–based client to the Gem & Pearl Testing Laboratory of Bahrain, and two more lead glass–filled rubies have subsequently appeared from a separate source. The 10.35 ct stone exhibited all the characteristic features associated with this treatment: loupe-visible flash effects and flattened gas bubbles within surface-reaching fractures (figure 20); differences in surface luster between the corundum and the glass filling in reflected light; and a filling material that was opaque to X-rays (again, see the Lab Note referenced above).

The appearance of these lead glass–filled rubies in the Middle East confirms that this treatment is reaching gem markets worldwide.

Nick Sturman (metalgem@commerce.gov.bh)
Gem & Pearl Testing Laboratory
Manama, Bahrain

CONFERENCE REPORTS

GemmoBasel 2005. This "International Colloquium of Gemmology" was held April 29–May 2 in honor of the 60th birthday of renowned Swiss gemologist (and GNI contributing editor) Dr. Henry A. Hänni. Approximately 170 participants from 29 countries gathered at the University of Basel to hear two days of presentations. **Dr. W. Stern** of the University of Basel opened the session with an entertaining biography of Dr. Hänni, noting that this celebration coincided with the anniversary in August of Dr. Hänni's 25 years with the SSEF Swiss Gemmological Institute.

The first technical session, on diamonds, began with a presentation by **Dr. Paul Spear** of the Diamond Trading Company (DTC) Research Centre in Maidenhead, U.K. Dr. Spear noted that the DTC Research Centre has developed methodology to rapidly screen for and identify both HPHT- and CVD-grown synthetic diamonds, down to 0.03 ct, as well as synthetic moissanite, using the Diamond-Sure and DiamondView verification instruments. **Dr. Emmanuel Fritsch** of the University of Nantes, France, and collaborators reported on advances in identifying and classifying the origin of color in brown and black diamonds. Significantly, most type Ia (nitrogen containing) diamonds with brown graining have a series of absorptions in the near-infrared region called "amber centers," the most common of which (AC1) shows a main absorption around 4168 cm^{-1}. The more intense the brown color is, the more intense this AC1 absorption is, and the more A aggregates are detected (figure 21). This and other results indicate that AC1 may be the cause of the visible-range absorption inducing the brown color. **Jean-Pierre Chalain** of SSEF stressed the importance of a database of natural-color diamonds for treatment research. Microscopic observation and extensive spectroscopic analyses of an historic (1907) 1.18 ct greenish yellow diamond crystal showed
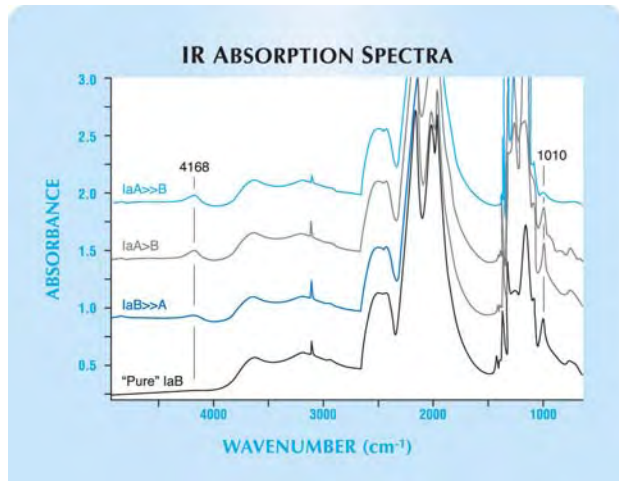
Figure 21. The intensity of the infrared absorption of the most common amber center in diamond (AC1) at about 4168 cm^{-1} correlates to that of the A aggregates, as well as with brown color. This indicates that the brown color of certain gem diamonds may be caused by this amber center. The spectra are offset vertically for clarity, and have all been normalized to the intrinsic absorption of diamond at about 2450 cm^{-1}. From top to bottom, the samples consist of a very dark brown (nearly black) 1.22 ct briolette, a dark reddish brown 0.75 ct round brilliant, a dark reddish brown 0.45 ct round brilliant, and a pinkish brown 0.31 ct single-cut diamond. All spectra were taken with the beam in the girdle plane, except for the briolette, in which the shortest dimension was chosen; the inferred optical path lengths are 5.2, 5.2, 4.9, and 4.1 mm, respectively.

strong overlap with the properties of HPHT-treated diamonds of similar color, indicating the need for further testing of such material.

Leading the Gemstone session was **John I. Koivula** of the West Coast AGTA Gemological Testing Center (AGTA GTC) in Carlsbad, California. Reiterating his conviction that the microscope is the gemologist's most important tool, he showed photomicrographs of distinctive inclusions, such as pink covellite in quartz, reportedly from Bahia, Brazil; intense blue fluorite in quartz from Madagascar; and turquoise in selenite from New Mexico. **Tay Thye Sun** of the Far East Gemmological Institute, Singapore, stressed the importance of classifying jade correctly, not only jade vs. nephrite and their simulants, but also the many treated jades. Today, most of the jadeite in the market is B-jade, which is bleached and polymer impregnated; it can be identified by distinctive features in the infrared spectrum. **Edward Boehm** of Joeb Enterprises, Solana Beach, California, presented an update on mining at Mogok, Myanmar, for **Richard Hughes**, also of the West Coast AGTA GTC. He reported that the mining methods used at Mogok have been virtually unchanged for decades, with the area pockmarked by tunnels and as many as 250,000 people working the area at the height of its activity.

Figure 22. Increasingly sophisticated gem treatments and synthetics have made laboratory reports indispensable to auction houses. This 8.01 ct untreated Burmese ruby recently sold for $2.2 million—a record auction price of $275,000 per carat—at Christie's New York. Courtesy of Christie's Images.

Dr. Karl Schmetzer of Petershausen, Germany, reported on taaffeite and musgravite, and compared the optical and chemical properties of "typical" samples of both gem minerals with iron-rich (taaffeite and musgravite) and zinc-rich (taaffeite) samples, all from Sri Lanka, to expand the compositional range of this material. During the question-and-answer session, gem dealer Werner Spaltenstein of Chanthaburi, Thailand, noted that gem-quality taaffeites have been found in Tunduru (Tanzania) as well. **Dr. Ulrich Henn** of the German Gemmological Laboratory, Idar-Oberstein, reported on feldspars, the most common minerals in the earth's crust, which provide an interesting link between mineralogy and gemology. The main gem feldspars are orthoclase, amazonite (microcline), moonstone (perthite or antiperthite), albite, sunstone (oligoclase or labradorite), and andesine.

Dr. Hänni began the Instrumentation session with a review of instruments used in gem identification at SSEF over the past 25 years. In addition to the adoption of analytical techniques such as EDXRF, FTIR, Raman spectroscopy, and—most recently—laser-induced breakdown spectroscopy (LIBS), the gem laboratory has seen significant advances in lighting, especially fiber-optic illumination. He recommended that if a laboratory could not afford to purchase needed instrumentation, they should make arrangements to access equipment at a local university. **This contributor** gave participants a glimpse "behind the pages" of *Gems & Gemology*, emphasizing the importance of a strict peer review, editing, and production process. She also offered several tips for publishing in *G&G*: Choose a topic with a strong application to gemology; organize the paper logically, including separate sections on the materials and methods, results, and discus-

sion; describe every test and say how many (and which) samples were used for each; and do a thorough literature review. **Manfred Eickhorst** of Eickhorst & Co., Hamburg, Germany, discussed various lighting needs for aging eyes: less glare, brighter light, and stability (i.e., nonflickering light). A high-frequency (40,000 Hz) lamp can eliminate flicker, whereas the use of two dimmable bulbs (with a color temperature of 5,500 K and 6,500 K) can help refresh the eyes as well as provide more efficient color evaluation. **Dr. Gaston Giuliani** of IRD and CRPG/CNRS, Vandoeuvre-lès-Nancy, France, reported on the use of oxygen isotopes to study emeralds from nearly 70 deposits. Although there is overlap among deposits, he found that emeralds could be classed into three groups based on their $\delta^{18}O$ values. He also found that oxygen isotopic analysis could be used to separate Mogok from Mong Hsu rubies.

In the Trade Issues session, **Helen Molesworth** of Christie's London reported that auction houses today require gem lab reports on virtually all stones (especially the most important ones, as shown in figure 22). However, gemology is advancing rapidly, and clients are reminded that reports are only an opinion based on current knowledge and technology. **Werner Spaltenstein** reported on his mining and buying activities in Tunduru and Madagascar, two areas that have great future promise because there was so little systematic gem exploration in the past. Also, tastes and interests change; for example, spinel was actually discovered at Mahenge (Tanzania) 20 years ago, but not until recently was there a market for it.

Eric Emms of the Precious Stone Laboratory, London, led the Treatments and Synthetics session by describing the three-fold impact on gemologists of the proliferation of treatments: (1) They must have sufficient funds to acquire the needed equipment and technical support staff, (2) they must have knowledge beyond the basic FGA or GG diploma, and (3) they must disclose to buyers/clients if treatment is detected or may be present. **Dr. Roy Walters** of Ocean Optics, Dunedin, Florida, and **Dr. Michael Krzemnicki** of SSEF recently determined that surrounding a sample with argon during LIBS analysis greatly improves the resolution of the main Be feature at 313 nm, so Be can be detected down to 2 ppm.

Dr. V. S. Balitsky of the Institute of Experimental Mineralogy, Moscow, reported that inclusions, growth zoning, and IR spectra may be useful to separate some synthetic from natural quartz, but not all types can be identified. **Dr. Lore Kiefert** of the East Coast AGTA GTC in New York explained the various factors involved in determining the geographic origin of gemstones: the inclusion scene, trace-element chemistry, and spectroscopic characteristics. Because of overlap in some features in stones from various sources, it is critical that multiple lines of evidence are used in the determination.

The last session, on Pearls, was led by **Dora Fourcade** of Pacific Perles, Tahiti. She reported that only 5% of the cultured pearls produced in Tahiti are superior quality; by law, the 10% classified as "rejects" must be destroyed. Typically, only 20–25% of the harvest are rounds. Also in the pearl session, **Andy Müller** of Hinata Trading Co., Kyoto, Japan, reported that production of South Sea cultured pearls has increased 160% since 1999, with Indonesia leading by weight in 2005 and Australia the leader by value. He emphasized the need to balance supply and demand, and warned of the problem posed by global warming. Water temperatures exceeding 33°C are deadly to pearl oysters. **Elisabeth Strack** of the Hamburg Gemmological Institute, Germany, provided a comprehensive review of European freshwater mussel pearls. The European pearl mussel, *Margaritifera margaritifera*, can live 130 years, and is mature at 15. Ubiquitous at one time, the mussel population dropped by 80–90% in the 20th century, so only a few hundred thousand mussels remain today. **Nicholas Sturman** of the Gem & Pearl Testing Laboratory, Manama, Bahrain, described the natural pearls from the Arabian Gulf, once considered the best in the world, but now in short supply. Bahrain law forbids the sale of cultured pearls, so the local commerce depends on natural pearls.

Alice S. Keller (akeller@gia.edu)
GIA, Carlsbad

ANNOUNCEMENTS

Exhibits

Cameos at the Met. "Cameo Appearances," a display of more than 160 examples of the art of gem carving from Greco-Roman antiquity to the 19th century, will be on display until October 30, 2005, at the Metropolitan Museum of Art in New York City. Among the pieces featured will be works by the neoclassical Italian masters Benedetto Pistrucci, Giuseppe Girometti, and Luigi Saulini. A variety of educational programs will be offered in conjunction with the exhibition. Also on display at the Met (through January 2006) is the exhibit "The Bishop Jades," a selection of fine Chinese and Mughal Indian jades from the collection of Heber R. Bishop that was donated to the museum in 1902. Visit www.metmuseum.org/news/news_pr.asp or call (212) 535-7710.

Diamonds in London. "Diamonds," an exhibit of some of the world's largest and most valuable faceted diamonds, will be on display at the Natural History Museum in London through February 26, 2006. The exhibit includes the De Beers Millennium Star, the Steinmetz Pink, the Ocean Dream, and the Moussaieff Red (see J. M. King and J. E. Shigley, "An important exhibition of seven rare gem dia-

monds," Summer 2003 *Gems & Gemology*, pp. 136–143), in addition to a 616 ct rough diamond and a number of other notable gems. Visit www.nhm.ac.uk/diamonds.

Conferences

Raman spectroscopy. The 3rd International Conference on the Application of Raman Spectroscopy in Art and Archaeology will be held August 31–September 3, 2005, in Paris, France. The Raman analysis of gem materials will be among the topics covered. Visit www.ladir.cnrs.fr/ArtRaman2005/or e-mail artraman2005@glvt-cnrs.fr.

Agate symposium. On September 10–11, 2005, a symposium on agate and cryptocrystalline quartz will take place at the Colorado School of Mines in Golden, Colorado. Field trips to Colorado mineral localities are planned for September 12–13. These events will take place in conjunction with the 38th Annual Denver Gem and Mineral Show (September 16–18). Call 303-202-4766 or e-mail pmodreski@usgs.gov.

Diamond 2005. A review of the latest scientific and technological aspects of natural and synthetic diamond (as well as related materials) will take place at the 16th European Conference on Diamond, Diamond-like Materials, Carbon Nanotubes and Nitrides, September 11–16, 2005, in Toulouse, France. Visit www.diamond-conference.com.

Rapaport International Diamond Conference 2005. This conference will be held in New York on September 19, 2005, and feature an insider's look at the international diamond and jewelry industry. Visit www.diamonds.net/conference.

Hong Kong Jewellery & Watch Fair. Held at the Hong Kong Convention and Exhibition Centre on September 21–25, this show will also host GIA GemFest Asia 2005 on September 23. The free educational event, "Update on Diamond Cut," will take place from 9 am to 12 noon in Room 301B; RSVP to events@gia.edu, or call 760-603-4205 in the U.S. or +852-2303-0075 in Hong Kong. An educational seminar given by the Gemmological Association of Hong Kong will also take place on September 23. Visit www.jewellerynetasia.com/exhibitions.

ERRATUM

The Spring 2005 article "Coated pink diamond: A cautionary tale" contained an error in figure 2 on p. 37. The labels for the room temperature and cryogenic spectra in this figure were inadvertently transposed. We thank Nick Sturman of the Gem & Pearl Testing Laboratory of Bahrain for bringing this to our attention.

Book REVIEWS

2005

EDITORS

Susan B. Johnson
Jana E. Miyahira-Smith
Stuart Overlin

101 Bench Tips for Jewelers

By Alan Revere, 120 pp., illus., publ. by MJSA/AJM Press, Providence, RI, 2004. US$42.95 ($36.50 for MJSA members)*

Alan Revere's latest literary contribution to the goldsmith trade ranges from how to maximize the efficiency and functionality of a jeweler's bench to troubleshooting a wide array of situations that make up a typical day in the life of a bench jeweler.

There is one tip to each page, with the illustrations taking up a large portion of that page. As a seasoned educator, Mr. Revere has made the book easy to navigate via its index. The writing is concise, yet understandable and often quite witty in spite of the technical content that many might otherwise consider esoteric. Bear in mind that such a consistent and user-friendly format will occasionally sacrifice completeness. After all, how much detail can you give when discussing the intricacies of essential techniques such as soldering, riveting, engraving, and the like, in only a few hundred words?

Evidently, Mr. Revere has chosen hand-renderings by Sean Kane over photographs to avoid distracting glare, misleading reflections, and similar problems associated with shooting at the bench. Some illustrations have been cleverly augmented by the selective use of transparency, "exploded" views, cross-sections, and sequences.

In an era where conventional trade skills are no longer passed on from old masters to their apprentices through long and intensive relationships (that typically averaged more like *1001* bench tips per year), this book fills a need. Self-taught tradespeople, students, and graduates from trade schools and vocational schools alike, as well as bench jewelers learning on the job, will find *101 Bench Tips* a valuable reference, as will business owners and gemologists-cum-designers when planning out procedures for the shop floor.

Mr. Revere's *oeuvre* makes every attempt to transmit that professional trade mentality that we goldsmiths have cultivated for millennia: a tradition of ingenuity.

ROBERT ACKERMANN
Gemological Institute of America
Carlsbad, California

Identification of Gemstones

By Michael O'Donoghue and Louise Joyner, 313 pp., illus., publ. by Butterworth-Heinemann, Oxford, UK, 2003. US$59.95*

The authors have boldly taken on the subject of gemstone identification—properties, appearances, sources, imitations, synthetics, treatments, and separation procedures—and the result is a book of amazing scope.

To understand the depth of information covered, one only has to look at the first chapter—on diamonds—which begins with diamond properties, types, appearances, and typical inclusions. The more common diamond imitations are detailed, along with separation techniques such as the use of a 10∞ loupe, reflectivity meter, thermal conductivity probe, and immersion in various liquids. Gem-quality synthetic diamonds from General Electric, Sumitomo, De Beers, and Russia are covered next. Treatments such as the use of ink, radium salts, various irradiation procedures (sometimes combined with heat treatment), HPHT, fracture filling, and diamond thin films are covered. Their effect on a diamond's clarity and/or color and the various methods used to detect them are discussed. This chapter (like most of the other gem chapters) ends with a section titled "Reports of Interesting and Unusual Examples from the Literature."

The next two chapters cover corundum and beryl, giving varieties, properties, descriptions (including by source), treatments (heat and diffusion for corundum, fracture filling for emerald), synthetics by method and manufacturer, imitations, and composites (assembled stones). As in all gem chapters, the authors describe procedures and properties that can be used to separate the gem covered from other gem materials with which they are commonly confused.

The remaining gem chapters cover opal, quartz, the jade minerals, chrysoberyl (alexandrite, cat's-eye, and other varieties), topaz, tourmaline, the garnet group, spinel, peridot, zircon, moonstone and other feldspars, rhodochrosite, tanzanite (zoisite), rhodonite, turquoise, lapis lazuli, pearl, amber, ivory, jet, coral, shell, and natural and artificial glass.

Other chapters highlight information on basic gem testing equipment, metals, ceramics, plastics, assembled stones, less common gemstones, rarely fashioned species, gem materials in their rough state, how crystals are grown, synthetics for the collector, treatments, and locality

information. The book ends with a six-page glossary, recommended reference materials, and an index.

As stated earlier, the book covers an amazing scope and depth of information, but unfortunately the title is a bit misleading. Because of its organization mostly by gem species or group, one would have to be fairly far along in the identification of an "unknown" gemstone for this book to be of benefit. By not choosing to use a color or property (e.g., refractive index) format, identifying a gemstone with this book is a little like trying to look up a number in a telephone directory without knowing the person's name.

Although the book includes a collection of 60 full-color photomicrographs of various gemstone features, there is unfortunately no reference to any of the individual images in the text. As a result, the reader must try to understand difficult concepts through written descriptions alone. For example, the doubling of facet junctions seen in some directions of some diamond simulants is described as looking "like tramlines" (p. 15). This description could have been made much clearer by directing the reader to color plate 3, which shows the appearance of doubling as seen in synthetic moissanite.

One of the authors' stated goals is to keep updating gemstone information by use of a companion website. At the time of this writing, however, the only information that appeared on the website were biographies of the authors and some additional instrumentation procedures. For example, there was no mention of CVD synthetic diamonds or beryllium diffusion treatment of corundum.

Despite these drawbacks, the information in this book is considerable and valuable. The authors' personalities come through in the writing, which adds a human touch to the subject without compromising the science of gemology.

DOUGLAS KENNEDY
Gemological Institute of America
London, England

Minerals and Their Localities

By Jan H. Bernard and Jaroslav Hyrsl, edited by Vandall T. King, 807 pp., illus., publ. by Granit, Praha, Czech Republic, 2004. US$145.00

This superb mineralogical compendium provides basic descriptive information for more than 4,200 mineral species and lists more than 8,500 localities from which they come. Each mineral species entry (arranged alphabetically) begins with its name in boldface and its chemical formula, followed by a classification number (Strunz system), descriptive characteristics, physical properties, and crystallographic data, and concludes with a fairly comprehensive listing of its localities. There are also entries (in bold italics) for certain other materials that the authors deem worthy of inclusion (such as inadequately described minerals, intermediate compositional members, well-known mixtures, organic materials, etc.). A select number of varietal names (in italics) are cross-referenced in this alphabetical listing and are further described under the corresponding species entries. Several minerals that are pending formal approval as species are so marked, and species that may have utility as gemstones are also identified.

The 1,000 color photographs, though small, are well chosen to demonstrate a given species, highlight unusual occurrences, and add visual appeal to the overall presentation. The thick, glossy paper stock is durable and enhances the reproduction of the images. A colored border on the pages serves as an alphabetical index that is useful as well as attractive.

The book concludes with a table of "The Richest Type Localities of the World," a list of references, and an alphabetical list of mineral localities. This last section, which includes all 8,500 localities with associated species, is particularly valuable. While the locality list is extensive and well chosen to include virtually all important sources, it is by necessity not all-inclusive.

A unique feature of this compendium is the organization of locality information for each mineral according to geologic environment: magmatic, pegmatitic, contact metasomatic, hydrothermal, alpine fissure, sedimentary, regional metamorphic, and products of weathering. The authors call these environments "genetic classes." The discussion of this format in the introduction is required reading if one is to use the book to best advantage. This is particularly true when referring to entries for minerals that occur in several geologic environments. For example, all of the localities where quartz has formed by magmatic processes are listed first, followed by its pegmatitic occurrences, and so forth. While this organization is quite instructive, it can make scanning for specific information somewhat protracted, if not tedious, for extended entries. Both current and historical localities (including those no longer producing) are included.

The descriptive information is well written, even lively, and is effective in enabling readers to visualize the described species and varieties. Considering the enormous amount of information presented, there are relatively few spelling errors, although they may occasionally be disconcerting, such as when the same locality or mineral feature is spelled several different ways in the same entry.

Perhaps because of the length, the authors have employed many space-saving tricks, which create some minor readability problems. For example, there is no space between mineral entries, and while the boldface species names serve as clear demarcation, the non-boldface variety entries get lost. If space had not been an issue, it would have been useful to provide a glossary of geologic terms. As it is, the authors' occasional use of technical jargon makes it a good idea for the nontechnical user to have a geologic dictionary close at hand.

This book was a monumental undertaking, the product of a lifetime of work and a "hands-on" understanding of the sort of information that is helpful to anyone interested in miner-

als and their localities (and geologic environments). An international flavor comes through, assuring the reader that the book is truly global in perspective. The authors also have paid special attention to localities that produce gemstones. The descriptions associated with each "genetic class" and locality make this book unique. Each species entry can become a learning experience and enhance the reader's general knowledge of mineral occurrences.

Minerals and Their Localities is an excellent and extremely useful reference. For anyone interested in minerals and gems with particular reference to their localities, there is no better resource available.

DOROTHY ETTENSOHN
*Natural History Museum of
Los Angeles County
Los Angeles, California*

Masterpieces of the Mineral World: Treasures from The Houston Museum of Natural Science

By Wendell E. Wilson and Joel A. Bartsch with Mark Mauthner, 264 pp., illus., publ. by The Houston Museum of Natural Science and The Mineralogical Record *in association with Harry N. Abrams Inc., New York, 2004. US$75.00*

Mineral collecting has been around for centuries and continually becomes more sophisticated in its outlook. The finest mineral specimens are *objets d'art*, and there is a growing overlap between the mineral and gem markets. Therefore, this is an excellent time to expose gem dealers to a book explaining the finer points of mineral specimen appreciation. Unfortunately, the text of this handsome book is a little too biased to be entirely useful.

Masterpieces of the Mineral World uses a selection of gorgeous mineral specimens from the Houston Museum of Natural Science to explain connoisseurship in mineral collecting. There are three main parts: "The Discerning Eye," which explains the factors that make a mineral specimen desirable from an aesthetic point of view; a series of plates and a section called "The Paths of Discovery," which detail the individual histories of 80 mineral specimens; and "A Royal Passion," which reviews the history of mineral collecting by aristocrats in Europe.

In the first part, Wilson lists several factors that might qualify a mineral specimen for "masterpiece" status: crystal form, color, transparency, luster, size, perfection, crystal orientation/grouping and related aesthetic visual composition, and provenance (both natural origin and history in human hands). Other factors include associated species, durability, preparation, authenticity (persistence of the specimen's unmodified state), matrix, and rarity.

Yet some important considerations to a gemological audience are only touched on or are missing from this text. Every mineral specimen is a collaboration between nature and human beings, from the original collector to the final owner; at every stage, a human has had to recognize, preserve, and sometimes "improve" the specimen. Many aesthetic factors are subject to modification by human activity, and standards of preparation and restoration have changed over time. Current practices include trimming matrix with hand tools or saws; cleaning specimens with chemical solutions; improving color, transparency, and luster by oiling with mineral oil; and gluing broken crystals back together, or reattaching broken crystal groups to their matrix. All these practices can improve the aesthetic factors mentioned above, and some are specifically mentioned for individual specimens in the section that follows.

As with gems, though, the definition of what is considered an acceptable modification changes over time, and some previously accepted mineral enhancement practices may now be considered fakery. In addition, a mineral's locality is often an important factor in its value, yet often that information only loosely accompanies the piece. There is no overall disclosure practice in the mineral field; practices vary from dealer to dealer. Thus the transition from the gem market to the mineral market is as challenging as the opposite transition would be.

Photos of the 80 specimens by Jeff Scovil and Harold and Erica Van Pelt are excellent. The accompanying text, however, reads as though written from a seller's perspective, and sometimes verges on hyperbole. For instance, well-formed transparent grossular crystals are not "extremely" rare. Another entry claims "for size, luster, transparency, sharpness, and form, the Piuva [Russian] ferro-axinites have no rival"—except for, in this reviewer's opinion, the best from the New Melones Dam, California. Yet the mineral specimens are beautiful enough to speak for themselves, and the authors should be congratulated for including rare and humble species as well as conventional beauties.

As the final essay on princely collections explains, mineral collecting is an odd passion, involving scientific curiosity, aspirations to completeness, and the competitive urge for "bragging rights." Early mineral collections were intended for medical research, but they later became hubs of social activity and tourism for the learned leisure class. The mineral collections of counts and royal physicians were purchased by museum patrons and eventually became national treasures. Today, mineral collectors come from all socioeconomic backgrounds, all cultures, and all age groups. One can never accumulate the best collection, only the best available. All the standard *caveat emptor* principles apply: Learn from many sources, not just one; be suspicious of anything too good to be true; and take everything with a grain of salt.

Nevertheless, as shown in this beautiful volume, we can only marvel at the treasures our planet provides—and at the talents their discoverers and preparers demonstrate. Together, what masterpieces they create!

MARY L. JOHNSON
*Gemological Institute of America
Carlsbad, California*

Gemological ABSTRACTS

2005

COLORED STONES AND ORGANIC MATERIALS

Gemological and mineralogical properties of black jadeite. M. Zhang, P. Hou, and J. Wang, *Jiangsu Geology*, Vol. 28, No. 2, 2004, pp. 100–102 [in Chinese with English abstract].

Mozui, which means "black jadeite" in Chinese, is mined in Myanmar and southern China. Recently, it has become common in Asian jade markets. It is essentially monomineralic, consisting of >90% omphacite, which is a pyroxene (like jadeite). This article reports on the gemological and mineralogical properties of this blackish green to black material and provides a comparison to jadeite.

The refractive indices (1.667–1.670) and specific gravity (3.34–3.44) of "black jadeite" are almost identical to those of jadeite. It has a strong vitreous luster, and polished stones have a smooth surface. Petrographic studies show that the omphacite occurs as prisms or fibers of varying length; the grain size is usually <0.3 mm. Albite, tremolite, and some minute opaque grains with metallic luster are minor constituents. Only subtle differences are found in the infrared absorption spectra and X-ray powder diffraction patterns of the two materials. The chemical formula of the omphacite in "black jadeite" is $(Ca,Na)(Mg,Fe^{2+},Fe^{3+},Al)(Si_2O_6)$; the ratio $Na/(Na+Ca)$ is 0.45, which lies between that of jadeite (>0.8) and diopside (<0.2). The main trace elements are Sr, Cr, and Mn.

Even though there is a clear difference in the chemical compositions of the main pyroxene minerals in "black jadeite" (omphacite) and jadeite, the authors suggest that the black material should nevertheless be considered jadeite, since their physical properties are almost same. Yet, they acknowledge resistance to this suggestion; the name "omphacite jade"

was recommended by C. M. Ou Yang et al. ("Recent studies on inky black omphacite jade, a new variety of pyroxene jade," *Journal of Gemmology*, Vol. 28, No. 6, 2003, pp. 337–344). *TL*

Harvesting impacts and invasion by alien species decrease estimates of black coral yield off Maui, Hawaii. R. W. Grigg, *Pacific Science*, Vol. 58, No. 1, 2004, pp. 1–6.
After 40 years of successful management, three new developments threaten the sustainability of the black coral fishery in Hawaii. First, harvesting pressure on the colonies has increased, while the biomass of black coral off Maui has decreased 25% since 1976. Second, an alien species of coral, *Carijoa riisei* (often called "cutthroat coral"), has overgrown many of the black coral colonies. Initially detected in Pearl Harbor, Oahu, in 1972, this invasive species is believed to have been brought from the Atlantic Ocean on the hulls and/or in ballast water of ships between 1940 and 1970. During the 1990s, *C. riisei* was reported at sites in the eight major Hawaiian Islands. Third, increasing sales of black coral in recent years (about $30 million retail in Hawaii alone) is placing more demands on the resource.

A larger size (height) limit of the coral and a reduction in the amount harvested are measures that can be implemented to help conserve the resource. Divers and the coral industry must abide by stricter regulations to ensure the future of the black coral fishery in Hawaii. *MC*

Study on compositions and colouring mechanism of freshwater cultured pearls. M. Yang, S. Guo, L. Shi, and W. Wang, *Journal of Gems and Gemmology*, Vol. 6, No. 2, 2004, pp. 10–13 [in Chinese with English abstract].
Chinese freshwater cultured pearls display a large range of colors (e.g., white, pink, gray, purple, red), however, there is no reliable explanation for these variations. In this article, the authors attempt to correlate the color variations with trace-element contents and other parameters. Three color varieties (white, orange-red, and dark purple; two samples of each), representing the color range of Chinese freshwater cultured pearls, were analyzed for their inorganic mineral components by X-ray diffraction, for selected trace metals by plasma emission spectroscopy, for conchiolin by FTIR spectroscopy, and for carotenoids by Raman spectroscopy.

There were no significant differences in the inorganic mineral components of the three color varieties. However, the concentrations of the trace metals Zn, Mg, Ti, V, Ag, and Co varied significantly, being particularly high in the dark purple cultured pearls. For example, the Zn content (945 ppm) in the dark purple specimens was nearly eight times higher than in the white ones (121 ppm). The concentrations of Ti and V were higher in the

orange-red cultured pearls than in the white samples, but less than in the dark purple specimens. Cu, Fe, Cr, and Al were not detected (<0.1 ppm) in any of the samples. From these data, the authors conclude that selected trace elements are responsible, at least in part, for the coloration of Chinese freshwater cultured pearls.

Among the organic components, there were no significant differences in the conchiolin in the various samples. However, Raman spectra showed four carotenoid-related peaks in both the orange-red and the dark purple samples, but not in the white ones, suggesting that carotenoids also play a role in the coloration of these freshwater cultured pearls. *TL*

Study on star spinel. L. Tian, W. Huang, H. Liu, and Y. Chen, *Journal of Gems and Gemmology*, Vol. 6, No. 2, 2004, pp. 1–3 [in Chinese with English abstract].
Spinel occasionally displays asterism with either a six-rayed or a four-rayed star; however, multiple sets of stars in the same sample are relatively rare. This article describes three oval cabochons of bluish or grayish black Sri Lankan spinel (2.88, 3.21, and 3.31 ct) that displayed four sets of six-rayed stars and three sets of four-rayed stars, all of which were bright and sharp. An abundance of tiny needle-like inclusions parallel to several octahedral planes were observed with the microscope. Electron-microprobe imaging showed these inclusions to be <1 µm in diameter and 5–20 µm long. They were composed of two different minerals based on their cross-sectional shapes and chemical compositions: (1) a triangular Fe-containing mineral, and (2) an irregular-shaped Ca-containing mineral. The multiple sets of stars were attributed to these tiny inclusions distributed along the three edges of each octahedral (111) face in the spinel crystals. Eight sets of six-rayed stars together with 12 sets of four-rayed stars would be seen if the spinel crystals had been polished into spheres. *TL*

DIAMONDS

About signs of mechanical and chemical effects upon diamond crystals from the Urals deposits. V. N. Anfilogov, *Proceedings of the Russian Mineralogical Society*, Vol. 133, No. 3, 2004, pp. 105–108 [in Russian with English abstract].
The complex morphology of diamond crystals is reviewed for the possible application of locating their primary source. Dislocations on the surface of crystals cannot be explained by mechanical distortion; rather, the dislocations formed during crystal growth due to internal defects. The occurrence of rounded diamonds in the Urals placer deposits cannot be explained by tumbling in water. It is suggested that the primary sources of these diamonds are nearby kimberlites. *RAH*

Carbonatitic melts in cuboid diamonds from Udachnaya kimberlite pipe (Yakutia): Evidence from vibrational spectroscopy. D. A. Zedgenizov [zed@uiggn.nsc.ru], H. Kage, V. S. Shatsky, and N. V. Sobolev, *Mineralogical Magazine*, Vol. 68, No. 1, 2004, pp. 61–73.

Micro-inclusions (1–10 μm) in 55 diamonds of cubic habit from the Udachnaya kimberlite pipe in Russia were shown by IR and Raman spectroscopy to contain a multiphase assemblage that includes carbonates, olivine, apatite, graphite, water, and silicate glasses. These micro-inclusions had an elevated internal pressure that indicated the original materials were trapped during growth of the host diamond. These internal pressures—extrapolated to mantle temperatures—lie within the stability field of diamond, but the temperatures are relatively low. Such temperatures are typical for the formation of cuboid diamonds. In contrast to previous data for African diamonds, the micro-inclusions in the Udachnaya cuboids were extremely carbonatitic in composition [$H_2O/(H_2O+CO_2)$ ~5–20%], and the assemblage contained in their micro-inclusions was similar to that found in some types of carbonatites. The low water and silica contents testify that the material in the micro-inclusions of the Udachnaya diamonds was a near-solidus carbonatitic melt. *RAH*

Do Arraial do Tejuco à Diamantina: 290 anos de produção de diamantes [From the Arraial do Tejuco to Diamantina: 290 years of diamond production]. R. H. Corrêa-Silva, *Diamond News*, **Part I.** Vol. 5, No. 17, 2004, pp. 40–44; **Part II.** Vol. 5, No. 18, 2004, pp. 13–19 [in Portuguese].

Part I of this article describes the early history of the Diamantina mining district in Minas Gerais, Brazil, from the discovery of gold in the 17th century and of diamonds around 1714 to the end of the 19th century, by which time Diamantina had lost its position as the world's leading diamond producer to South Africa. It focuses on certain aspects of the industry, such as the regulation of diamond production and trade by the Portuguese Crown and the role of some prominent personalities.

Part II gives a description of the geologic setting, mineralogy, and mining at Diamantina. The diamonds are found in conglomerates, and in colluvial and alluvial deposits (the primary source rocks have not yet been identified). They are generally small and of gem quality. Diamonds from the conglomerates frequently have a green or brown coating from natural irradiation. Mining is done both by *garimpeiros* who also rework old diggings, and by mechanical operations ("dragas") mostly on the Rio Jequitinhonha. Minerals that accompany the diamonds are anatase, kyanite, lazulite, magnetite, gold, quartz, rutile, and zircon. *RT*

Prospects of diamond-bearing ability in Ukraine and trends of geological prospecting works. D. S. Gursky, V. S. Metalidi, V. L. Prykhodko, and Yu. V. Geiko, *Mineralogical Journal* (Ukraine), Vol. 26, No. 1, 2004, pp. 7–17.

This evaluation of possible diamond-bearing occurrences in the six major structural units of the Ukrainian shield takes into consideration potential secondary (placer) deposits as well as primary (i.e., kimberlite and lamproite) sources in the region. Although no deposits are currently known, there are encouraging indications that the Ukrainian shield has diamond potential. For example, (1) detrital Cr-bearing pyropes often associated with diamonds are reported from several areas, and (2) diamonds 0.2–0.3 mm in size have been recovered from sands of the Baltian Neogene region and in the beach deposits of the northern coast of the Sea of Azov. The authors recommend detailed mapping of heavy minerals, as well as the use of other prospecting methods. [*Abstracter's note:* This is one of six articles, all in English, in a thematic issue of the *Mineralogical Journal* (Ukraine) on the potential for diamond occurrences in the Ukraine. Abstracts of two additional articles follow.] *RAH*

Age correlation of endogenic processes of the Slave (Canada) and Middle-Peri-Dnieper (Ukraine) cratons in connection with the diamond-bearing ability problems. N. P. Shcherbak, G. V. Artemenko, and A. V. Grinchenko, *Mineralogical Journal* (Ukraine), Vol. 26, No. 1, 2004, pp. 18–23.

The Slave craton of the Canadian shield and the Middle-Peri-Dnieper (MPD) craton of the northwestern Ukrainian shield both stabilized in the Archean and have not been subjected to any considerable reworking in the Proterozoic or Phanerozoic. This stability is an essential condition for the diamond occurrences in the Slave craton. In the MPD craton, diamonds have been found only in Tertiary and Quaternary sedimentary formations, but, based on the occurrence of 2300–2000 and 1400–1200 million-year-old dike complexes in both cratons, the MPD craton is considered a promising prospect for diamond-bearing rocks. *RAH*

Paleotectonic, petrological and mineralogical criteria of diamond-bearing ability of the Ukrainian Shield. V. M. Kvasnytsya, Ye. B. Glevassky, and S. G. Kryvdik, *Mineralogical Journal* (Ukraine), Vol. 26, No. 1, 2004, pp. 24–40.

Regional estimates are given for the possibility of diamond discoveries in the various structural blocks of the Ukrainian shield on the basis of Clifford's rule, which states that economic diamond deposits occur only in ancient stable cratons, or "archons," with a crustal age of not less than 2,800 million years. The Middle-Peri-Dnieper craton in the Ukrainian shield has thickened crust, and the most promising region for the discovery of mantle (i.e., kimberlite or lamproite) diamond deposits is where the archon slopes adjacent to a sediment-filled linear trough called the Dnieper-Donets aulacogen. *RAH*

GEM LOCALITIES

Archaeological geology of the world's first emerald mine.
J. A. Harrell [james.harrell@utoledo.edu], *Geoscience Canada*, Vol. 31, No. 2, 2004, pp. 69–76.
An archaeological and geologic survey of the mountain valley region of Wadi Sikait in the Eastern Desert of Egypt was conducted to map the distribution of ancient mine workings, deduce ancient mining methods, and describe the geologic occurrence of emerald at this, the world's first emerald mine. Several other sites in the area also have indications of ancient emerald extraction. Mining probably began toward the end of the Ptolemaic period in the 1st century BC. Most of the activity, however, dates to the Roman and early Byzantine periods, from the late 1st century BC through the 6th century AD. Renewed small-scale mining during the first three decades of the 20th century proved unsuccessful, probably due to the poor quality of the emeralds.

The author provides a map of the mine workings, which combines topographic and geologic information. The Wadi Sikait area is divided into sections known as the North Village, Middle Village and Road, and South Village. Archaeological excavations of the South Village area have uncovered ancient temples and administration buildings, possibly from the first century AD.

The emerald deposits are characterized by the intrusion of Be-bearing quartz or pegmatite veins into Cr- or V-bearing mafic or ultramafic rocks (i.e., the source of the chromophores). Emeralds formed in the contact zone between phlogopite schist and the quartz/pegmatite veins. *JEC*

Marble-hosted ruby from Vietnam. P. V. Long [vggc@fpt.vn], H. Q. Vinh, V. Garnier, G. Giuliani, and D. Ohnenstetter, *Canadian Gemmologist*, Vol. 25, No. 3, 2004, pp. 83–95.
This article compares the gemological characteristics and geologic setting of rubies from Luc Yen and Quy Chau in northern Vietnam. At Luc Yen, rubies occur as disseminated crystals in small veinlets or fissures within marbles of Upper Proterozoic to Lower Cambrian ages. Secondary ruby deposits occur in associated alluvial gravels. At Quy Chau, the economic ruby and sapphire deposits are found only in placers.

The ruby crystals from Luc Yen examined were typically hexagonal bipyramids, whereas those from Quy Chau commonly formed short hexagonal prisms. Compared to the Luc Yen material, the color of the Quy Chau rubies was usually more saturated and showed a stronger red fluorescence to long- and short-wave UV radiation. R.I. values of rubies from both areas were 1.762–1.770 (birefringence ~0.008). S.G. values for samples from Luc Yen were 3.92–4.01, whereas those from Quy Chau were 3.94–4.05. Rubies from both areas exhibited twinning, straight and angular growth zoning, and (in

some instances) various forms of color zoning. The most common mineral inclusions in material from both localities were apatite, calcite, dolomite, rutile, diaspore, phlogopite, and zircon. Three kinds of fluid inclusions (both primary and secondary) also were found. The inclusion characteristics and geologic settings indicate that rubies from these deposits are the result of high-grade (amphibolite facies) regional metamorphism. *JES*

Nuristan–South Pamir province of Precambrian gems. A. K. Litvinenko [litvinenko78@yahoo.com], *Geology of Ore Deposits*, Vol. 46, No. 4, 2004, pp. 263–268.
A highly metamorphosed Precambrian tectonic block measuring 660 ∞ 165 km in the Afghanistan-Pakistan-Tajikistan region has a remarkable abundance of gem deposits. More than three dozen localities contain minerals suitable for use as gems or ornamental stones. A partial list of these materials includes lazurite, spinel, clinohumite, ruby, sapphire, scapolite, cordierite, emerald, and tourmaline. Many of these come from various types of metamorphic deposits, the nature of which is determined by the composition of the sedimentary protoliths (e.g., the presence of highly aluminous clay) and by the intensity and type of metamorphism. *EF*

INSTRUMENTS AND TECHNIQUES

Ein notwendiger Test in der Perlenuntersuchung [A necessary test for the pearl identification]. H. A. Hänni [gemlab@ssef.ch], *Gemmologie: Zeitschrift der Deutschen Gemmologischen Gesellschaft*, Vol. 53, No. 1, 2004, pp. 39–42 [in German with English abstract].
X-radiography is a standard method for distinguishing natural from cultured pearls by revealing their different internal characteristics. With recent progress in pearl culturing, the structures of natural and cultured pearls are becoming increasingly similar. Unlike their saltwater counterparts, freshwater pearls (natural or cultured) luminesce to X-ray excitation because of the Mn content of their nacre. As the nuclei of most cultured pearls are made of freshwater nacre, this luminescence (as viewed through the subsequent cultured overgrowth) can be used as an additional test to identify various kinds of natural and cultured pearls. The author gives a brief description of the practical application of this technique. *RT*

Impurity measurements in diamond using IR. W. Taylor [pterodia@wxc.com.au], *Rough Diamond Review*, No. 4, 2004, pp. 40–42.
IR spectroscopy provides a quantitative method for identifying nitrogen and other light-element (e.g., H, O, B) impurities and their associated defects in diamonds; these elements may substitute for carbon atoms in the diamond lattice in amounts up to several thousand parts per mil-

lion. The abundance and configuration of such impurities are of importance for determining the post-growth history of diamonds in the earth's mantle and for distinguishing diamonds from different sources. Within individual crystals, the zonation of nitrogen content and aggregation state can be mapped and correlated to growth history. Nitrogen-aggregation plots show a correlation between nitrogen population types and diamond properties, such as color and morphology.

IR spectra that are characteristic of the atomic configuration and concentration of nitrogen and the other light-element impurities, and molecular submicroscopic fluid inclusions (e.g., H_2O, CO_2), are illustrated and/or discussed in this article. Also presented are practical aspects of measuring and interpreting IR spectra of diamonds (e.g., using software that deconvolutes the spectra to isolate the contributions from various nitrogen centers).   *AI*

JEWELRY RETAILING

Are natural diamond engagement rings forever? E. H. Fram and R. Baron, *International Journal of Retail & Distribution Management*, Vol. 32, No. 7, 2004, pp. 340–345.

The authors conducted a study of the attitudes toward natural diamond engagement rings among 459 students at the Rochester Institute of Technology, New York; these young people are the prime target market for such rings. One-third of the respondents were in the 18–22 age group, while the rest were 23 and older. The male:female ratio was 55:45, with 93% of the students coming from the U.S. Of the full sample, 15% were already married or engaged, 54% said they had no expectation of becoming engaged within the next three years, and 31% believed they might become engaged in that time period.

While a majority (61%) of respondents believed that a natural diamond engagement ring was very or somewhat important, a significant number were either neutral (22%) or believed such rings were somewhat/very unimportant (16%). In addition, 45% of the women believed it was appropriate to celebrate an engagement without a natural diamond ring; only 28% of the men agreed with that statement. About one-third of the respondents would consider alternatives to natural diamond engagement rings, either jewelry or nonjewelry, while nearly one-fourth were neutral on the subject. The report concluded that the number of women predisposed to acquiring a diamond engagement ring might not be as high as believed, and this might represent a downward trend that could impact future diamond engagement ring sales.   *RS*

Diamond geezers. M. Prince [princem1@southernct.edu], *Business Strategy Review*, Vol. 16, No. 1, 2005, pp. 22–27.

The diamond engagement ring is a product that creates desire beyond reason in the eye of the beholder, especially those rings that fulfill the requirements of a prestige brand—products for which consumers will pay a premium. The characteristics of these brands are that they set themselves on a higher plane than the competition, represent high expectations of quality and value, and make a personal statement about the user/wearer.

Diamond engagement rings offer a conspicuous display of romantic emotion and social position. Diamonds from a prestige jeweler can also stimulate a feeling of attachment toward that brand, kinship with other purchasers of that brand, disdain for competing products in the same market, and an elitist mentality. Brand choices can be affected by age, gender, ethnic background, education, and sophistication levels.   *RS*

Evolution of an advertising campaign. A. DeMarco, *JCK*, Vol. 176, No. 5, 2005, pp. 149–152.

This article details the development of a new advertising campaign for Lockes Diamantaires, a boutique-type retail diamond jewelry store established by a De Beers Diamond Trading Company sightholder in Manhattan. The advertising agency, AgencySacks, began by proposing a campaign that would combine credibility and good value to a predominantly female clientele in the age range 26 to 65 and earning more than $75,000/year. The goal was to position the store as a professional, quality-oriented alternative to both "wholesale-to-the-public" operations and high-end retailers. The creative staff of the agency developed three potential advertisements that focused on image and emotions rather than product. However, some members of Lockes' staff wanted some products featured, so two different advertisements were produced. One was an image ad for magazines, while the other, for newspapers, stressed product and value.   *RS*

TREATMENTS

Doping by diffusion and implantation of V, Cr, Mn and Fe ions in uncoloured beryl crystals. J. C. R. Mittani [juan.mittani@dfn.if.usp.br], S. Watanbe, M. Matsuoka, D. L. Baptista, and F. C. Zawislak, *Nuclear Instruments and Methods in Physics Research B*, Vol. 218, 2004, pp. 255–258.

The coloration of slabs from a natural crystal of colorless beryl (from Salinas, Minas Gerais, Brazil) was carried out through doping by diffusion and ion implantation with V, Cr, Mn, and Fe. [*Editor's note:* The authors do not describe the colors produced by this treatment process.] The beryl slabs were cut to test whether treatment was easier perpendicular or parallel to the c-axis. Specimens were placed in an alumina crucible with chemical-grade compounds (VCl_3, Cr_2Cl_3, $MnCl_2$, or $FeCl_3$) and heated to 700, 725, or 750°C for periods of 7, 14, or 21 days. After treatment, they were analyzed using optical absorption, electron para-

magnetic resonance, and inductively coupled plasma–laser ablation–mass spectroscopy. The results showed that the ion species could be doped into the beryl by the diffusion procedure. However, the low dosage used during the implantation process failed to introduce any significant level of the ions. One interesting feature documented during the ion implantation process was the changing of pre-existing Mn^{2+} and Fe^{3+} into Mn^{3+} and Fe^{2+}. Diffusion parallel to the c-axis was easier than perpendicular to this axis due to the structural channels in the beryl.   *EF*

If you can't stand the heat, get out of the gem business: Part IV. G. Roskin. *JCK*, Vol. 175, No. 9, 2004, pp. 109–114.

While the vast majority of HPHT-treated diamonds can be identified, some still confound gemological laboratories. GIA has documented nearly 11,000 HPHT-annealed diamonds submitted for reports. Only a small percentage (primarily colored diamonds) were submitted without having been declared as HPHT-treated. Other laboratories have reported seeing "limited numbers" of HPHT-annealed diamonds. The range of diamonds that are treated has expanded beyond the original type IIa, most commonly to some varieties of type Ia.

The article questions the claim, made by some HPHT diamond treaters, that the process "finishes what Mother Nature started." Quite often the process of treating diamonds involves temperatures far higher than those found naturally.   *RS*

Quality enhancement of Vietnamese ruby by heat treatments. P. Winotai [scpwn@mahidol.ac.th], P. Limsuwan, I. M. Tang, and S. Limsuwan, *Australian Gemmologist*, Vol. 22, No. 2, 2004, pp. 72–77.

The heating of Vietnamese rubies in an oxygen atmosphere improves their color and clarity. Trace amounts of Fe^{3+} in these rubies causes a pale yellow coloration, whereas the intervalence charge-transfer mechanism between Fe^{2+} and Ti^{4+} gives them an undesirable bluish color. The latter can be diminished by heating the ruby in oxygen so that most of its Fe^{2+} is converted to Fe^{3+}, resulting in a more intense red. X-ray diffraction analysis showed that the cation/anion ratio of the structure was smallest after heat treatment at 1,300°C. The number of Fe^{2+} ions converted to Fe^{3+} (as detected by electron spin resonance spectrometry) was found to increase with temperature. Vietnamese ruby may acquire an intense red color (with no yellow or blue modifier) after optimal heating at 1,500°C for 12 hours.   *RAH*

Study on colorific mechanism of topaz after irradiated by positron annihilation technique. Y. Deng and Y. Zhang, *Nuclear Electronics & Detection Technology*, Vol. 24, No. 1, 2004, pp. 62–66 [in Chinese with English abstract].

Topaz can be color enhanced by irradiation with gamma rays, neutrons, and high-energy electrons; however, the mechanism(s) by which the radiation changes the color is still unclear. To gain insight into this problem, samples of untreated and irradiated topaz were studied using the positron annihilation technique. This technique yields information on crystal lattice defects, such as vacancies and micro-voids, by measuring the average lifetimes of positrons after irradiation. From such data, causes and mechanisms of color enhancement can be deduced.

Natural topaz samples from Taishan, Guangdong, China, were divided into three groups for the experiments: colorless, blue (from neutron irradiation), and light blue (from high-energy electron irradiation). The average lifetimes of the positrons were about the same in samples within each group, but there were significant differences in the average lifetimes between the three groups. The average lifetimes were proportional to color intensity (i.e., longer in darker samples). Irradiation by neutrons and/or electrons induces many point defects in the topaz lattice, and these defects are the main cause of color. Some of these induced defects and associated colors disappear with annealing. The authors suggest that all methods capable of producing vacancies and micro-voids in the topaz lattice could be used for color enhancement.   *TL*

Topical coatings on diamonds to improve their color: A long history. T. Moses, C. P. Smith, W. Wang, and M. Hall, *Rapaport Diamond Report*, Vol. 27, No. 20, 2004, pp. 91–93.

The oldest form of treatment applied to diamonds to mask or alter their color appearance involves coatings. Coatings with a colored substance were applied to the backs of diamonds as early as the 16th century in Italy. At that time, for example, greenish colors were commonly achieved by adding a green or blue coating to the back of yellow stones. Yet virtually any color can be imparted to a diamond with an appropriate coating. Such coatings, which are still occasionally seen today, are relatively unsophisticated, requiring only a steady hand and the proper coating medium. Through the years, the methods by which coatings have been applied to diamonds have changed. Since the 1950s, sputter or vapor deposition techniques have enabled metallic and fluoride coatings (originally developed for lenses during World War II) to be applied to diamonds. In these instances, typically a blue or purple coating is applied to the entire pavilion or just near the girdle to neutralize or mask a yellow bodycolor.

Coatings are best detected by microscopic examination. Two light sources, darkfield and overhead diffused light, combined with a subtle diffuser placed between the diamond and the light well of the microscope, provide the most effective viewing conditions. The coatings may appear as blotches or uneven areas of color and frequently have a blue or purplish tint in those cases where metallic or fluoride coatings have been applied; gas bubbles are observed in rare instances. Indications of the presence of a

coating may be encountered during color grading, from the different colors seen when the diamond is viewed face-up and table-down; in addition, the color may be concentrated along the girdle. In the future, coatings of synthetic diamond on natural diamond, applied by chemical vapor deposition (CVD) techniques, have the potential not only to modify the less desirable color of a diamond, but also to add weight to the original stone. Such CVD-coated diamonds may be difficult to detect.   *JEC*

Yellow and brown coloration in beryllium-treated sapphires.
V. Pisutha-Arnond [pvisut@geo.sc.chula.ac.th], T. Häger, P. Wathanakul, and W. Atichat, *Journal of Gemmology*, Vol. 29, No. 2, 2004, pp. 77–103.
Elevated levels of Be (up to ~11 ppm) have been discovered in both natural and synthetic sapphires heat treated in Thailand. This article investigates the causes of yellow and brown coloration in such Be-treated sapphires. Using a series of irradiation and Be-heating experiments on both synthetic and natural colorless sapphires, the authors show that the geochemical behavior of Be mimics that previously proposed for Mg. Stable yellow or brown colors can be produced or removed depending on the (Be+Mg)/Ti ratio of the sapphires, the presence or absence of Fe, and whether heating is done in an oxidizing or reducing environment.   *WMM*

MISCELLANEOUS

Diamonds and civil conflicts in Africa—The conflicts in central Africa and west Africa. M. K. Kachikwu, *Journal of Energy & Natural Resources Law*, Vol. 22, No. 2, 2004, pp. 171–193.
This article reiterates the belief that the most serious and prolonged civil conflicts within African states are the result of rebel groups and governments battling to control resources, especially diamonds. Because of their easy transport across borders and conversion to cash, diamonds are particularly susceptible to illicit purposes.

The author recounts the histories of civil conflicts in diamond-producing countries, specifically Angola, Sierra Leone, and the Democratic Republic of the Congo. Patterns are cited of colonial plunder and superpower interference, followed by world neglect, as background for the recent conflicts. In two of the cases (Sierra Leone and Angola), revolutions borne out of political or social unrest were eventually subverted into grabs for diamond wealth. In the Congo, the author maintains, diamonds were the prize for outside invasion forces seeking influence within that vast nation. The case of Liberia is also cited. That country has essentially no indigenous diamond production, but illicit diamond trade running through its borders supported the corrupt regime of Charles Taylor. The article also describes the efforts of the Kimberley Process to stop trade in conflict diamonds. It notes, however, that

without massive intervention from the United Nations and the superpowers, African nations may again fall into the same patterns of commodity-driven civil strife.   *RS*

The diamond frontier. From bleak and barren to bling-bling: How a growing industry is changing Canada's northern communities. D. McDonald, *Time* (Canadian edition), Vol. 163, No. 14, 2004, pp. 48–55.
The 1991 discovery of diamonds in Canada, and the subsequent opening of the Ekati and Diavik diamond mines, have transformed economic prospects for the 20,000 aboriginal people of the Northwest Territories (NWT). Native communities are experiencing increased self-esteem and a better quality of life than a decade ago, yet they have still found ways to maintain their traditional values. Much of the credit for these achievements can be attributed to the mining companies' acknowledgment that they are operating on lands traditionally used for hunting and trapping, and their negotiating agreements favorable to the native people. These agreements include such matters as hiring (a target of 40% in the mines), training (to overcome a lack of education leading to skilled jobs), and business opportunities (such as service contracts). Never before have the aboriginal people participated to such an extent in resource development on their traditional lands even though, by legal statute, royalties from mines in the NWT go to the federal government.

The results have been spectacular. For example, unemployment among native people has been greatly reduced, and when mines under construction (e.g., Snap Lake) come into production, there may even be a shortage of aboriginal workers to fill the target quotas. Nevertheless, diamonds also present problems for the NWT aboriginal communities. For example, increased wealth has brought pressures on communities that have a tradition of sharing. Native people now distinguish between goods that have been shared historically (e.g., harpoons and rifles) and those that have not (e.g., snowmobiles). In addition, the increased salaries have not solved—and in some cases, have contributed to—familiar social problems such as alcohol and substance abuse.   *AAL*

The Great Diamond Hoax of 1872. R. Wilson, *Smithsonian*, Vol. 35, No. 3, 2004, pp. 70–79.
In 1871–1872, Philip Arnold and his partner, John Slack, played on people's greed and conned millionaires and politicians into buying stock in a company that supposedly had found a diamond field in Colorado. Mr. Arnold had acquired knowledge of diamonds from his previous employer, Diamond Drill Co. With a bag of rough diamonds (presumably taken from the drill maker) mixed with rubies and garnets, the two con men approached businessmen and bankers in early 1871 telling of their diamond find and looking for investors. After getting an initial payment of $50,000, the two went to England in July 1871 to buy $20,000 of uncut diamonds and rubies for use

in obtaining more investment capital. Seeing actual diamonds in hand (and, later, "salted" at the supposed deposit), the speculators were easily duped. In fact, when some of the investors sent 10% of the uncut stones to Charles Lewis Tiffany in New York (in October 1871) for appraisal, he unwittingly supported the scam by reporting their value as $150,000. (After the hoax was exposed, it was revealed that Mr. Tiffany did not have much experience with uncut stones.)

The hoax unraveled in October 1872, when Clarence King, a geologist conducting a survey for the U.S. government, and his men overheard a few people talking about a diamond find that happened to be in the survey's purview. If diamonds actually occurred on land he was surveying, King feared, he would have to explain to Congress why he and his men had not found them. When they inspected the so-called diamond field, King noticed that everywhere there was a diamond there were rubies surrounding it, which was too perfect a coincidence to be natural. Also, anthills containing gems were always surrounded by footprints, which was quite suspicious. King concluded that the diamond field was a hoax and published a letter exposing it in November 1872. Although a grand jury did indict Arnold and Slack for fraud, it seems the investors, out of embarrassment, let the case drop.   *JS*

In the wake of things: Speculating in and about sapphires in northern Madagascar. A. Walsh, *American Anthropologist*, Vol. 106, No. 2, 2004, pp. 225–237.
Sapphires were "discovered" in the area around Ambondromifehy in the northern part of Madagascar in 1996; before then, the locals held them in such low esteem that children used them as slingshot pellets. The fact that "foreigners" place so much value on these stones, which have no local use, is a source of great speculation and suspicion among local inhabitants—even the Malagasy traders who make their livings by buying and selling these stones.

This article describes the complex trading culture that has grown up around the mining areas. Local miners, traders, and *demarchers* (brokers) have developed a trading ethic divided between *businessy* for legitimate deals and *katramo* for deceptive practices. *Businessy* encompasses many practices—some unquestionably ethical, and others that require a great deal of awareness on the part of both parties. *Katramo* is pure deception. Local traders, however sharp, consider themselves at a disadvantage to foreigners because of their ultimate "secret," that sapphires have no use or value within their country. Thus, because the Malagasy do not understand why foreigners value sapphires, they believe that foreign traders are constantly getting the better of them. Nor do the locals believe that sapphires are used primarily for jewelry. Common suspicions hold that the stones are used in armaments for the Iraq War, electronic gear, watches, and even to construct impenetrable walls for the houses of foreign "billionaires."   *RS*

Injuries and injury care among child labourers in gem polishing industries in Jaipur, India. R. R. Tiwari [rajtiwari2810@yahoo.co.in], A. Saha, J. R. Paikh, and H. N. Saiyed, *Journal of Occupational Health*, Vol. 46, No. 3, 2004, pp. 216–219.
The gem polishing industry in Jaipur, India, employs about 200,000 people who process colored stones imported mostly from various African sources. About 20,000 of these workers are children (<18 years old). For this study, researchers at India's National Institute of Occupational Health interviewed 588 child workers randomly selected from various cutting operations. Most (78% in this study) were in the 10–14 year age range. They found that these workers were frequently exposed to minor injuries associated with the cutting, faceting, and drilling of gem materials and were not covered by any type of health plan. The prevalence of injuries within this age group could indicate they are too immature to understand safety practices. Their injuries were often complicated by problems with hygiene and lack of knowledge regarding wound care and first aid. Chemicals such as chromium oxide were often absorbed into their wounds, contaminating those injuries.

They also found that children working longer shifts (>6 hours) were more likely to injure themselves than those working a few hours a day, as fatigue negatively affects concentration. Those employed less than two years tended to sustain more injuries because of their lack of experience.   *MC*

The next African revolution. S. Benson, *New York Diamonds*, Vol. 86, January 2005, pp. 40–46.
The South African government is considering legislation that could radically transform the diamond industry in that country. Its aim is to increase "beneficiation" (i.e., deriving greater added value from diamond resources in the form of employment, majority ownership, and government revenues). Proposed amendments to the South African Diamond Act of 1986 would allow the country's Diamond Board to require De Beers's Diamond Trading Company (DTC) and other miners to supply local manufacturing operations directly. Currently, De Beers exports all of its rough diamonds to its DTC office in London and supplies South African manufacturers from sights with a mix containing rough diamonds from mines in Africa and Russia. In addition, the proposed new Mining Charter would require that 26% of equity in the country's existing mines be held by "historically disadvantaged" people within 10 years.

DTC managing director Gareth Penny said he agreed with the basic goals of beneficiation but believed the proposed legislation ultimately would make the mining and cutting industries smaller and less competitive. Neighboring governments of Namibia and Botswana are watching results of South Africa's beneficiation laws as a potential model for their countries.   *RS*

The
Other Side
of the Lens

Photo by Karen Myers

With 81 *G&G* cover shots to their credit—and counting—it's time we introduced you to Harold and Erica Van Pelt, the husband-and-wife team whose gem and jewelry photos have appeared in every issue of *Gems & Gemology* since 1981.

Kansas native Harold, known to his friends as "Van," studied at the famed Brooks Institute of Photography in Santa Barbara, California. Erica was born and raised in Germany, where she trained as a photographer. The two met in 1962, at a Los Angeles museum exhibit of Harold's photos, and have worked together since then.

The Van Pelts originally specialized in the photography of high-end furniture, but their focus began to shift in the late 1960s, when a private collector commissioned them to photograph a group of tourmalines (still their favorite gem to shoot). They were entering largely uncharted waters. With the exception of Lee Boltin, whose work appeared in 1965's *Gems in the Smithsonian Institution*, there were no true artists working in gem and mineral photography. Free to follow their own vision, the Van Pelts developed innovative compositions and lighting techniques that revolutionized the way we look at these treasures.

In addition to *G&G*, their photographs have been featured in *Lapidary Journal*, *Mineralogical Record*, *JCK*, and countless other publications, as well as dozens of books, including their own popular *Birthday Book of Gems* and *Birthday Book*

of Diamonds. Though they are quick to downplay the accolades they have received, the Van Pelts are honorary life members of the American Gem Trade Association, as well as honorary fellows of the Bowers Museum of Cultural Art in Santa Ana, California.

One vital ingredient to their success is teamwork. "The most interesting part of our relationship is that we both have our departments, even though we're always treading on each other's territory," Erica explains. "The layout, the designs for the photos, and the props are my department; Van's is the technical lighting and operating the camera." A single shot, like the yellow diamonds cover for this issue of *G&G*, can require hours of meticulous work to set up the stones, the background, the lights, and the best camera angle.

The Van Pelts have taken that same complementary approach in becoming world-class lapidaries. Since the 1970s, they have carved objects such as candlesticks, vases, containers, and eggs from rock crystal quartz and other materials. They have even designed or modified much of the machinery they use for rock carving. Their creations have been exhibited at a number of international gem and mineral shows, though none have ever been offered for sale (see J. Sinkankas, "Artistry in rock crystal: The Van Pelt collection," Winter 1982 *G&G*, pp. 214–220, for several notable examples).

In between photo shoots and their travels, Harold is putting the finishing touches on a full-sized agate chair, eight years in the making. Erica is involved in setting up a gem exhibit for a collector that will open in Shanghai this October. Another ongoing project at their Hollywood home/studio is cataloguing the thousands of shots they have taken over the years. Most of the information on these images resides only in the Van Pelts' collective memories. Once they have compiled all the data and had the photos digitally scanned, their photo library will be a valuable resource for the gem and mineral world.

In the meantime, each photo still offers a new challenge. "We always start from the beginning," Erica says. "We always strive to build on our last shot, so we have to find a different approach every time."

Stuart Overlin
Associate Editor